



<https://theses.gla.ac.uk/>

Theses Digitisation:

<https://www.gla.ac.uk/myglasgow/research/enlighten/theses/digitisation/>

This is a digitised version of the original print thesis.

Copyright and moral rights for this work are retained by the author

A copy can be downloaded for personal non-commercial research or study,  
without prior permission or charge

This work cannot be reproduced or quoted extensively from without first  
obtaining permission in writing from the author

The content must not be changed in any way or sold commercially in any  
format or medium without the formal permission of the author

When referring to this work, full bibliographic details including the author,  
title, awarding institution and date of the thesis must be given

Enlighten: Theses

<https://theses.gla.ac.uk/>  
[research-enlighten@glasgow.ac.uk](mailto:research-enlighten@glasgow.ac.uk)

# **FUNCTIONAL ANALYSIS OF THE CHEMOKINE RECEPTOR, CCX-CKR**

**Iain Comerford**

**August 2005**

This thesis is submitted to the University of Glasgow  
in accordance with the requirements for the degree of  
Doctor of Philosophy in the Faculty of Medicine

Cancer Research UK Beatson Laboratories  
Switchback Road  
Glasgow  
G61 1BD

Department of Immunology, Infection and Inflammation  
University of Glasgow  
University Avenue  
Glasgow  
G12 8QQ

© **Iain Comerford**

ProQuest Number: 10800573

All rights reserved

INFORMATION TO ALL USERS

The quality of this reproduction is dependent upon the quality of the copy submitted.

In the unlikely event that the author did not send a complete manuscript and there are missing pages, these will be noted. Also, if material had to be removed, a note will indicate the deletion.



ProQuest 10800573

Published by ProQuest LLC (2018). Copyright of the Dissertation is held by the Author.

All rights reserved.

This work is protected against unauthorized copying under Title 17, United States Code  
Microform Edition © ProQuest LLC.

ProQuest LLC.  
789 East Eisenhower Parkway  
P.O. Box 1346  
Ann Arbor, MI 48106 – 1346

**GLASGOW  
UNIVERSITY  
LIBRARY:**

# ACKNOWLEDGEMENTS

First of all, I would like to thank my supervisor, Rob Nibbs, for all of his hard work, patience, encouragement, and support during the past three and a bit years (although the less said about his ‘banter’, the better...). Thanks also to Gerry Graham for his support, time, and useful advice and my advisor, Dave Gillespie, for all of his time and interest during my studentship. Thanks to all past and present members of R6 and R2 (now the Chemokine Research Group). I’d have been at a loss on many occasions if I hadn’t been able to steal your reagents, pens, protocols etc. over the last 3 years. Some of you were also fun to work with (at times!). They were, in no particular order, and hopefully not missing anyone out, Tam, Val, Jane, Tim, Derek, Clare Simpson, Emma, Jan, Jemma, Rhona, Pauline, Maureen, Paul, Kenny, Clare Shepherd, Chris, Paz, Wendy, Michele Weber, and Michelle Bryson. Thanks to various members of the Immunology department for their help, especially Yvonne Bordon for her time, advice, and smiles. I’d also like to thank Dr. Gracie at Glasgow Royal Infirmary and Colin Nixon at Glasgow Vet school for their assistance. Huge thanks also to Steve Forrow and his transgenic team for all their hard work and persistence with my project. I would also like to thank all the members of the Beatson animal facility, especially Steven Bell, Maria Hendry, Tom Hamilton, Tom Byars, and Derek Millar, and all the support staff at the Beatson for the sequencing, IT support etc. Billy Clark, Shaeron Wylie, Peter McHardy and Iain White to name but a few. Finally, I would like to thank my Mum and Dad and the rest of my family for all of their encouragement and support. Lastly, I would like to give a special thank you to the beautiful, and long suffering, Yvonne.

# TABLE OF CONTENTS

Acknowledgements.....	ii
List of Tables .....	ix
List of Figures .....	x
Publications Arising From This Work .....	xiii
Abbreviations .....	xiv
Abstract .....	xx
<b>Chapter I: Introduction .....</b>	<b>1</b>
<b>1.1 The Immune System.....</b>	<b>1</b>
1.1.1 The Systemic Organisation of the Immune System .....	5
1.1.2 The Multi-step Paradigm of Leukocyte Extravasation.....	11
<b>1.2 The Chemokines.....</b>	<b>13</b>
1.2.1 Historical Perspectives .....	13
1.2.2 Nomenclature.....	16
1.2.3 Chemokine Structure and Subclassifications .....	18
1.2.4 Genetic Organisation and Phylogenic Origin .....	22
1.2.5 Redundancy and Promiscuity.....	24
<b>1.3 Chemokine Receptors .....</b>	<b>26</b>
1.3.1 The Structure of Chemokine Receptors.....	26
1.3.2 Chemokine Receptor Expression .....	27
1.3.3 The Chemokine/Chemokine Receptor Interaction .....	29
1.3.4 Signal Transduction.....	31
1.3.5 Desensitisation, Endocytosis, and Recycling of Chemokine Receptors.....	37
<b>1.4 Post-Translational Control of Chemokines.....</b>	<b>42</b>
1.4.1 Chemokine Storage and Release.....	42
1.4.2 Chemokine Presentation.....	44
1.4.3 Proteolytic Control of Chemokines.....	45
1.4.4 Microbial Regulation of Chemokines .....	50
1.4.5 Chemokine Decoy and Transport Receptors .....	52
1.4.5.1 Duffy Antigen/Receptor for Chemokines (DARC) .....	54
1.4.5.2 D6: A Pro-inflammatory Chemokine Scavenger .....	56

1.4.6 CCX-CKR, a Chemokine Receptor of Unknown Function .....	60
<b>1.5 Immunological Function of CCX-CKR Ligands .....</b>	<b>62</b>
1.5.1 The Primary Lymphoid Organs .....	62
1.5.1.1 The Bone Marrow.....	62
1.5.1.2 The Thymus .....	63
1.5.2 The Secondary Lymphoid Organs .....	66
1.5.2.1 Chemokines and the Organogenesis of Secondary Lymphoid Organs.....	67
1.5.2.2 Ectopic Secondary Lymphoid Formation.....	69
1.5.2.3 Lymphocyte Entry via High Endothelial Venules.....	70
1.5.2.4 'Remote Control' and Chemokine Transcytosis .....	73
1.5.2.5 Chemokines and Lymphocyte Compartmentalisation .....	74
1.5.2.6 Lymphocyte Egress .....	76
1.5.2.7 Dendritic Cell Traffic to Secondary Lymphoid Organs.....	77
1.5.2.8 Lymphocyte Activation.....	80
1.5.3 Tissue Specific Homing of Antigen Activated Cells.....	81
1.5.4 Immune Responses in <i>Null</i> Mice .....	83
<b>1.6 Aims of Study .....</b>	<b>85</b>
<b>Chapter II: Materials and Methods .....</b>	<b>86</b>
<b>2.1 Materials .....</b>	<b>86</b>
2.1.1 Antibodies and Secondary Detection Reagents.....	86
2.1.2 Bacteriology.....	86
2.1.3 Cell Culture.....	87
2.1.4 Chemicals.....	88
2.1.5 Chemokines .....	89
2.1.6 Enzymes and Kits .....	89
2.1.7 Miscellaneous .....	90
2.1.8 Oligonucleotides .....	91
2.1.8.1 Tagged Expression Construct Oligos.....	91
2.1.8.2 Sequencing Oligos.....	91
2.1.8.3 Genotyping Oligos.....	92
2.1.8.4 Screening Oligos.....	92
2.1.8.5 cDNA Amplification Oligos .....	92
2.1.9 Plasmids .....	93

<b>2.2 Methods</b> .....	94
2.2.1 Molecular Biology.....	94
2.2.1.1 Oligonucleotide Synthesis.....	94
2.2.1.2 Nucleic Acid Preparation.....	94
2.2.1.2.1 Genomic DNA extraction with Phenol.....	94
2.2.1.2.2 Genomic DNA extraction on 96 well plates.....	95
2.2.1.2.3 Preparation of Genomic DNA from Tailtips for Genotyping.....	95
2.2.1.2.4 Preparation of Genomic DNA from Tailtips for Southern blots.....	96
2.2.1.2.5 Plasmid DNA preparation (Minipreps/Maxipreps).....	96
2.2.1.2.6 Plasmid DNA Precipitations.....	96
2.2.1.2.7 RNA extraction with Trizol™.....	97
2.2.1.2.8 cDNA synthesis from RNA.....	98
2.2.1.3 Polymerase Chain Reaction (PCR).....	98
2.2.1.4 Agarose Gel Electrophoresis.....	99
2.2.1.5 Restriction Enzyme Digests.....	100
2.2.1.6 Gel purification of DNA fragments.....	100
2.2.1.7 DNA Ligation.....	100
2.2.1.8 Transformation of DH5α Competent Bacterial Cells.....	101
2.2.1.9 Cloning of DNA Fragments into TOPO® Plasmids.....	101
2.2.1.10 Southern Blotting.....	102
2.2.1.11 DNA Sequencing.....	104
2.2.1.12 Plasmid Construction.....	105
2.2.1.12.1 FLAG-hCCR7.....	105
2.2.1.12.2.HA-hCCR7-GFP.....	105
2.2.1.12.3 HA-hCCX-CKR-GFP.....	106
2.2.1.12.4 CCX-CKR GFP KIKO.....	106
2.2.1.13 SDS-PAGE and Western blotting.....	107
2.2.2 Cell Culture.....	107
2.2.2.1 Harvesting Cells.....	108
2.2.2.2 Freezing Cells.....	108
2.2.2.3 Defrosting Cells.....	108
2.2.2.4 Cell Counts.....	109
2.2.2.5 Transfection of HEK293 Cells.....	109
2.2.2.5.1 Transient Transfections.....	109

2.2.2.5.2 Stable Transfections .....	110
2.2.3 Analysis of Cell Fluorescence .....	110
2.2.3.1 Confocal Microscopy .....	110
2.2.3.2 Flow Cytometry .....	111
2.2.4 <i>In Vitro</i> Assays.....	115
2.2.4.1 Radioligand Internalisation Assays.....	115
2.2.4.2 Radioligand Degradation Assays .....	115
2.2.4.3 Radioligand Uptake Assay .....	116
2.2.4.4 Radioligand Binding Assays .....	116
2.2.4.5 Radioligand Dissociation Assay .....	117
2.2.4.6 Chemotaxis Assay .....	117
2.2.4.7 Biotinylated Chemokine Uptake Assays .....	117
2.2.4.8 Antibody Staining for Surface CCX-CKR or CCR7 .....	118
2.2.5 Gene Targeting .....	119
2.2.6 Animals and <i>In vivo</i> Assays .....	119
2.2.6.1 Maintenance of Mice.....	119
2.2.6.2 Genotyping of Mice.....	119
2.2.6.3 Sacrifice of Mice .....	120
2.2.6.4 Dissection of Mice.....	120
2.2.6.5 Weighing Inguinal Lymph Nodes.....	120
2.2.6.6 Harvesting of Leukocytes.....	120
2.2.6.7 Immunostaining of Mouse Leukocytes for Flow Cytometry.....	120
2.2.6.8 Histology of Mouse Tissue .....	121
2.2.6.9 Cutaneous PMA Paint .....	121
2.2.6.10 Subcutaneous Immunisation with OVA/CFA .....	121
2.2.6.11 Measuring OVA-Specific Total Serum IgG Antibody by ELISA.....	122
2.2.6.12 Measuring Antigen Specific Cell Proliferation .....	122
2.2.6.13 Measuring Antigen Specific Cytokine Production.....	123
2.2.6.14 Induction of Contact Sensitivity with the Hapten DNFB .....	124
2.2.7 Statistical Analysis.....	124
<b>Chapter III: Results.....</b>	<b>125</b>
<b>3.1 Biochemical Analysis of human CCX-CKR and CCR7 .....</b>	<b>125</b>
3.1.1 Constructs and Cell Lines.....	125

3.1.1.1	FLAG tagged hCCR7 .....	127
3.1.1.2	GFP fusion HA tagged receptors .....	128
3.1.2	Internalisation and Degradation of CCL19 by its Receptors .....	130
3.1.2.1	CCL19 Internalisation .....	130
3.1.2.1.1	Optimisation of Radioligand Internalisation Assay .....	130
3.1.2.1.2	CCX-CKR and CCR7 Internalise Bound <sup>125</sup> I-CCL19 .....	131
3.1.2.1.3	Internalisation of Biotinylated CCL19/ Streptavidin-Cy3 .....	133
3.1.2.2	Fate of Internalised CCL19 .....	134
3.1.2.2.1	Degradation of Preloaded <sup>125</sup> I-CCL19 by CCX-CKR and CCR7 .....	135
3.1.2.2.2	Dissociation of CCL19 from CCX-CKR and CCR7 .....	137
3.1.2.2.3	Effect of Cold Competitor and Endosomal Neutralisation .....	139
3.1.2.2.4	CCL19 Degradation in Continuous Culture .....	142
3.1.2.2.5	Inhibition of Splenocyte Chemotactic Responses .....	146
3.1.3	Receptor Behaviour after Chemokine Exposure .....	148
3.1.3.1	Biotinylated CCL19 Uptake .....	148
3.1.3.2	Radiolabelled CCL19 Uptake .....	155
3.1.3.3	Surface Receptor Levels following Ligand Exposure .....	156
3.1.4	Molecular Mechanisms of CCL19 Uptake .....	161
3.1.4.1	Dynamin .....	161
3.1.4.2	β-arrestins .....	163
3.1.4.3	EPS15 .....	166
3.1.4.4	RabGTPases .....	168
3.1.4.5	Caveolae and Lipid Rafts .....	172
<b>3.2</b>	<b>Generation of CCX-CKR Knock-out mice .....</b>	<b>179</b>
3.2.1	Strategy .....	179
3.2.2	Construction of CCX-CKR Targeting Vectors .....	181
3.2.3	Targeting of CCX-CKR .....	183
3.2.4	<i>In Vitro</i> Cre-Mediated Excision of Neomycin Resistance Cassette .....	186
3.2.5	Blastocyst Injections, Chimeras, and Test Breeds .....	189
3.2.6	<i>In vivo</i> Cre-Mediated Excision of Neomycin Resistance Cassette .....	190
3.2.7	Other CCX-CKR KIKO Strains .....	192
3.2.8	Targeting of D6 .....	194
<b>3.3</b>	<b>Analysis of CCX-CKR Knock-out mice .....</b>	<b>195</b>
3.3.1	Fertility and Viability .....	195

3.3.2 Histological Analysis.....	195
3.3.3 Secondary Lymphoid Organs.....	196
3.3.3.1 The Spleen .....	196
3.3.3.2 Inguinal Lymph Nodes.....	199
3.3.4 Inguinal Lymph Node and Skin Responses to Topical Application of the Phorbol Ester Irritant PMA.....	205
3.3.5 Primary Immune Responses to Subcutaneous Antigen.....	211
3.3.6 Contact Hypersensitivity Responses to the Hapten DNFB.....	219
<b>3.4 Reporter Expression in CCX-CKR KIKO Animals .....</b>	<b>223</b>
<b>Chapter IV: Discussion .....</b>	<b>226</b>
<b>4.1 Comparative Biochemistry of CCX-CKR and CCR7 .....</b>	<b>226</b>
<b>4.2 The <i>In Vivo</i> Expression of CCX-CKR .....</b>	<b>237</b>
<b>4.3 The <i>In Vivo</i> Function of CCX-CKR .....</b>	<b>239</b>
4.3.1 Steady-State Analysis.....	241
4.3.2 Function of CCX-CKR in Immunity and Inflammation .....	245
<b>4.4 Overall Conclusions and Future Perspectives .....</b>	<b>248</b>
<b>Chapter V: References .....</b>	<b>250</b>
<b>Chapter VI: Appendices .....</b>	<b>279</b>
6.1 The Genetic Code .....	279
6.2 The Amino Acids.....	280
6.3 The Greek Alphabet.....	281
6.4 Primary Sequence Line-up of CCX-CKR Across Species.....	282

SV40	simian virus 40
TCA	trichloroacetic acid
TCR	T cell receptor
Th1	T helper cell type 1
Th2	T helper cell type 2
T <sub>REG</sub>	regulatory T cell
TM	transmembrane
TNF $\alpha$	tumour necrosis factor- $\alpha$
Tween-20	polyoxyethylene-sorbitan monolaurate
VCAM-1	vascular cellular adhesion molecule-1
vCKBP	viral chemokine binding protein
WT	wild-type
w/v	weight per unit volume

# LIST OF FIGURES

<i>Number</i>	<i>Page</i>
1.1.1 Cells of The Immune System .....	2
1.1.2 Structure of a Lymph Node .....	9
1.1.3 Structure of the Spleen .....	11
1.1.4 The Multistep Paradigm of Leukocyte Extravasation .....	12
1.2.1 The Chemokine Subfamilies .....	19
1.2.2 Chemokines: Primary, Secondary and Tertiary Structure .....	20
1.2.3 Genetic Organisation of Chemokines .....	24
1.3.1 General Structural Features of a Chemokine Receptor .....	27
1.3.2 Chemokine Receptor Ligation .....	30
1.3.3 G-protein Activation .....	32
1.3.4 Signaling Pathways Downstream of Chemokine Receptor Ligation .....	33
1.3.5 Signal Transduction Leading to Rapid Integrin Activation .....	36
1.3.6 Molecular Control of Endocytosis and Vesicular Traffic .....	39
1.4.1 Proteolytic Control of Chemokines .....	46
1.4.2 Regulation of Chemokine Function by Chemokine Decoy or Transport Receptors .....	54
1.4.3 D6 and Cutaneous Inflammation .....	59
1.4.4 CCX-CKR Ligands .....	61
1.5.1 The Role of CCR7 in Thymocyte Development .....	66
1.5.2 Organogenesis of Secondary Lymphoid Organs .....	68
1.5.3 The Multi-step Adhesion Cascade for Naïve T cell Entry into LN from the Blood .....	72
1.5.4 The Splenic Architecture in CXCR5 <sup>-/-</sup> , CCR7 <sup>-/-</sup> and CXCR5 <sup>-/-</sup> CCR7 <sup>-/-</sup> Mice .....	75
2.2.1 A Southern Blot by Capillary Transfer .....	102
2.2.2 Setting up the Flow Cytometer for Single Colour Analysis .....	112
2.2.3 Setting up the Flow Cytometer for 2 Colour Analysis .....	113
2.2.4 FACS Analysis of Mouse Leukocytes .....	114
3.1.1 <sup>125</sup> I-CCL19 Binding and CCX-CKR Surface Expression by HEK-hCCX-CKR Cells .....	126
3.1.2 Plasmids and Tagged Receptors used in Study .....	127
3.1.3 <sup>125</sup> I-CCL19 Binding and CCR7 Surface Expression by HEK-hCCR7 Cells .....	129

3.1.4 Optimisation of Acid Wash.....	131
3.1.5 Internalisation of <sup>125</sup> I-CCL19 by HEK-hCCX-CKR and HEK-hCCR7 .....	132
3.1.6 Kinetics of <sup>125</sup> I-CCL19 Internalisation by HEK-hCCX-CKR and HEK-hCCR7 .....	133
3.1.7 Internalisation of BioCCL19/Cy3 by HEK-hCCX-CKR and HEK-hCCR7.....	134
3.1.8 Degradation of <sup>125</sup> I-CCL19 by HEK-hCCX-CKR and HEK-hCCR7 Cells.....	136
3.1.9 Effect of Alterations in pH on <sup>125</sup> I-CCL19 Binding to CCX-CKR and CCR7 .....	138
3.1.10 Effect of Cold Competitor and Endosomal Neutralisation .....	140-41
3.1.11 Degradation of CCL19 by HEK-hCCX-CKR Cells in Continuous Culture .....	143
3.1.12 SDS-PAGE Analysis of Supernatants from Continuous Culture with CCL19 .....	144
3.1.13 Activity of HEK-hCCX-CKR Supernatants on <sup>125</sup> I-CCL19 Degradation.....	145
3.1.14 Inhibition of Splenocyte Chemotaxis by Pre-incubation of CCL19 with CCX-CKR.....	146
3.1.15 Uptake of BioCCL19/PE is Dependent on the Expression of a CCL19 Receptor...149	
3.1.16 Continued Chemokine Accumulation by HEK-hCCX-CKR Cells .....	150
3.1.17 BioCCL19/PE Uptake Assay Measures Total Chemokine Accumulation.....	151
3.1.18 Priming and Desensitisation of HEK-hCCX-CKR and HEK-hCCR7 Cells.....	152
3.1.19 Dose and Time Dependent Priming of CCX-CKR by CCL19, CCL21 and CCL25 .....	153
3.1.20 Chemokine Priming of CCX-CKR Increases the Rate of BioCCL19/PE Uptake ...154	
3.1.21 Radioligand Uptake by CCX-CKR and CCR7 Following Chemokine Stimulation .....	156
3.1.22 CCL19 Causes CCX-CKR Internalisation in a Dose Dependent Manner .....	157
3.1.23 CCL21 and CCL25 Induce Similar CCX-CKR Internalisation as CCL19 .....	158
3.1.24 Internalisation of CCR7 Following Ligand Stimulation .....	158
3.1.25 Effect of Dynamin (K44A) on BioCCL19/PE Uptake by CCX-CKR .....	162
3.1.26 Effect of $\beta$ -arrestin-1 (V53D) on BioCCL19/PE Uptake by CCX-CKR .....	163-64
3.1.27 Uptake of BioCCL19/Cy3 by MEFs (-/- or +/- for $\beta$ -arrestins) .....	165
3.1.28 Mutants of EPS15 .....	167
3.1.29 Effect of Genetic Inhibition of EPS15 on BioCCL19/PE Uptake .....	169
3.1.30 Effect of Genetic Inhibition of RabGTPases on BioCCL19/PE Uptake .....	170-71
3.1.31 Effect of Cholesterol Depletion on BioCCL19/PE Uptake.....	173
3.1.32 Effect of Genetic Inhibition and Overexpression of Caveolin-1 CCL19 Uptake.....	175
3.1.33 Effect of Over-expression of Caveolin-1 on CCX-CKR Surface Receptor Levels .....	176

3.2.1 Targeting constructs for CCX-CKR containing <i>lacZ</i> or GFP .....	181
3.2.2 Restriction Maps of the Mouse CCX-CKR Genomic Clone and Targeting Constructs.....	182
3.2.3 PCR Screen for Targeted Integration of CCX-CKR KIKO Constucts.....	184
3.2.4 Southern Blot Analysis of Targeted CCX-CKR KIKO ES Cell Clones .....	185
3.2.5 PCR and Southern Blot Screen for <i>in vitro</i> Cre Recombination.....	187
3.2.6 Genotyping of Pups at CCX-CKR Locus .....	190
3.2.7 Southern Blots of CCX-CKR GFP KIKO neo Recombination After ZP3/Cre Cross.....	191
3.2.8 Screening of Genomic DNA from CCX-CKR GFP KIKO Founder Mouse .....	192
3.2.9 Overall Strategy for Generation of CCX-CKR KIKO Mice.....	193
3.3.1 Effect of CCX-CKR Ablation on Mouse Fertility.....	195
3.3.2 Analysis of Leukocyte Populations in Spleens of CCX-CKR <i>+/+</i> and <i>-/-</i> . Part1 .....	197
Analysis of Leukocyte Populations in Spleens of CCX-CKR <i>+/+</i> and <i>-/-</i> . Part2 .....	198
3.3.3 Analysis of H+E Sections of ILNs from CCX-CKR <i>+/+</i> and <i>-/-</i> .....	200
3.3.4 Weight and Cell Number from ILNs of CCX-CKR <i>+/+</i> and <i>-/-</i> .....	201
3.3.5 Analysis of Leukocytes in ILNs from CCX-CKR <i>+/+</i> and <i>-/-</i> .....	202-03
3.3.6 Expression of CCX-CKR in Normal Mouse Skin.....	206
3.3.7 Histoligical Analysis of Mouse Skin Following 3xPMA Paint .....	207
3.3.8 Analysis of Inguinal Lymph Node Weight Following 3xPMA Paint.....	207
3.3.9 Analysis of Cellularity of ILNs 3 Days After 3xPMA Paint .....	208
3.3.10 Analysis of Leukocytes in ILNs 3 Days After 3xPMA Paint .....	209
3.3.11 Analysis of ILN Weight and Cellularity 3 Days After OVA/CFA.....	212
3.3.12 Analysis of Leukocytes in ILNs on Day 3 After OVA/CFA .....	213
3.3.13 Cellularity of ILNs Following OVA/CFA Immunisation .....	214
3.3.14 Analysis of OVA-Specific IgG in Mouse Serum After OVA/CFA .....	214
3.3.15 Analysis of OVA-Specific Proliferation in ILN Cell Culture.....	215
3.3.16 Analysis of Cytokine Levels in Supernatants from ILN Cell Culture .....	217
3.3.17 Analysis of ILN Weight and Cellularity on Day 3 After DNFB Paint.....	220
3.3.18 Measurements of Ear Thickness in Mice Following DNFB Challenge .....	221
3.3.19 Analysis of H+E Sections of Ears Either Painted or Unpainted with DNFB .....	222
3.4.1 Analysis of CCX-CKR and GFP Expression in <i>+/+</i> and <i>+/-</i> CCX-CKR GFP KIKO Mice ..	224
4.1.1 Proposed Model of CCL19 Uptake by CCX-CKR and CCR7 .....	234

## **PUBLICATIONS ARISING FROM THIS WORK**

Comerford, I., and Nibbs, R. J. (2005). **Post-translational control of chemokines: a role for decoy receptors?** *Immunol Lett* 96, 163-174.

Comerford, I., Milasta, S., Morrow, V., Milligan, G., Nibbs, R.J (2005) **Non-desensitised, caveolin-regulated, sequestration of the chemokine CCL19 by its receptor, CCX-CKR.** (*J Biol Chem*, submitted)

Morrow, V., Simpson, C.V., Milasta, S., Comerford, I., Battle, J., Milligan, G., Nibbs, R.J (2005) **The D6 chemokine receptor is localised to lipid rafts and requires beta-arrestins for continuous but not transient chemokine uptake.** Manuscript in preparation.

# ABBREVIATIONS

°C	degrees celcius
µg	microgram
µl	microlitre
-/-	knock-out
+/-	heterozygote
+/+	wild type
-RT	without reverse transcriptase
Ab	antibody
ADAM	a disintegrin and metalloproteinase
Ag	antigen
AIDS	acquired immunodeficiency syndrome
APC	antigen presenting cell
BAL	bronchoalveolar lavage
bioCCL19	biotinylated CCL19
bioCCL19/cy3	biotinylated CCL19 conjugated to streptavidin-cy3
bioCCL19/PE	biotinylated CCL19 conjugated to streptavidin-PE
BITS	Beatson Institute Technology Services
BITU	Beaston Institute Transgenics Unit
BM	bone marrow
bp	base pair
Ca <sup>2+</sup>	calcium ion
CCL	CC chemokine ligand
CCPs	clathrin-coated pits
CCR	CC chemokine receptor
CCVs	clathrin-coated vesicles
CD	cluster of differentiation
CFA	complete Freund's adjuvant
CLA	cutaneous lymphocyte antigen
CMV	cytomegalovirus
CNS	central nervous system
CO <sub>2</sub>	carbon dioxide
ConA	Concanavalin-A

cpm	counts per minute
CX3CL	CX3C chemokine ligand
CX3CR	CX3C chemokine receptor
CXCL	CXC chemokine ligand
CXCR	CXC chemokine receptor
DAG	diacyl-glycerol
DARC	Duffy antigen/receptor for chemokines
DC	dendritic cell
ddH <sub>2</sub> O	distilled water
DEPC	diethylpyrocarbonate
DMEM	Dulbecco's modified Eagle's medium
DMSO	dimethyl sulphoxide
DNA	deoxyribonucleic acid
DNFB	di-Nitro-Fluoro-Benzene
dsRNA	double stranded RNA
DTH	delayed-type hypersensitivity
EC	endothelial cell
ECM	extracellular matrix
<i>E.coli</i>	Escherichia coli
EDTA	ethylenediaminetetraacetic acid
EH	EPS15 homology
ELISA	enzyme linked immunosorbent assay
EPS15	epidermal growth factor receptor substrate 15
ER	endoplasmic reticulum
ES cell	embryonic stem cell
EST	expressed sequence tag
EtOH	ethanol
FACS	fluorescence activated cell sort
FAK	focal adhesion kinase
FITC	fluorescein isothiocyanate
FCS	foetal calf serum
FDC	follicular DC
fMLP	formyl-methionyl-leucyl-phenylalanine
g	gram

G418	geneticin
GAG	glycosaminoglycan
GAP	GTPase activating protein
GC	germinal centre
G-CSF	granulocyte colony stimulating factor
GDP	guanine biphosphate
GEF	GDP exchange factors
GFP	green fluorescent protein
GPCR	G protein coupled receptor
GRK	G protein coupled receptor kinase
GTP	guanine triphosphate
h	hour(s)
H+E	haematoxylin and eosin
HA	haemagglutinin
HEK	human embryonic kidney cells
Het	heterozygote
HEV	high endothelial venule
HHV	human herpes virus
HIV	human immunodeficiency virus
HRP	horseradish peroxidase
HSC	haematopoietic stem cell
HSV	herpes simplex virus
ICAM-1	intracellular adhesion molecule-1
IFN $\gamma$	interferon- $\gamma$
Ig	immunoglobulin
IL	interleukin
ILN	inguinal lymph node
i.v	intravenous
IP3	inositol 1,4,5 triphosphate
IRES	internal ribosomal entry site
JAK	Janus-family tyrosine kinase
kb	kilobase pairs
kDa	kiloDalton
kg	kilogram

KIKO	knock in knock out
KO	knock out
l	litre
LC	Langerhans cell
LEC	lymphatic endothelial cell
LN	lymph node
LPS	lipopolysaccharide
LT	lymphotoxin
M	molar
M $\beta$ CD	methyl- $\beta$ -cyclodextrin
M cell	microfold cell
MadCAM-1	mucosal addressin cellular adhesion molecule-1
MAPK	mitogen activated protein kinase
MEF	mouse embryonic fibroblast
MFI	mean fluorescence intensity
mg	milligram
MHC	major histocompatibility complex
min	minute(s)
ml	millilitre
mM	millimolar
MMP	matrix metalloproteinase
mRNA	messenger RNA
MZ	marginal zone
neo	neomycin resistance gene
nm	nanometre
nM	nanomolar
NK	natural killer
OD	optical density
ORF	open reading frame
OVA	ovalbumin
PALS	periarteriolar lymphoid sheath
PBS	phosphate buffered saline
PCR	polymerase chain reaction
PE	phycoerythrin

PFA	paraformaldehyde
pg	picogram
PGK	phosphoglycerine kinase promoter
PH	pleckstrin homology
PI3K	phosphatidylinositol 3-kinase
PIP <sub>2</sub>	phosphatidylinositol 4,5-biphosphate
PIP <sub>3</sub>	phosphatidylinositol 3,4,5-triphosphate
PKA	protein kinase A
PKB	protein kinase B
PKC	protein kinase C
PLC	phospholipase C
PLD	phospholipase D
<i>plt</i>	paucity of lymph node T cells
PMA	12-O-tetradecanoylphorbol-13-acetate
PNAd	peripheral node addressin
PP	Peyer's patch
PTEN	phosphatase and tensin homologue deleted on chromosome ten
PTX	pertussis toxin
RA	rheumatoid arthritis
RBC	red blood cell
rcf	gravitational force
RGS	regulator of G-protein signaling
RNA	ribonucleic acid
rpm	revolutions per minute
RPMI	Roswell Park Memorial Institute medium
RT	room temperature
RT-PCR	reverse-transcription PCR
S1P	sphingosine 1-phosphate
S1PR1	sphingosine 1-phosphate receptor 1
SCZ	subcapsular zone
SDS	sodium dodecyl sulphate
sec	second(s)
SS	Sjögrens syndrome
STAT	signal transducer and activator of transcription

SV40	simian virus 40
TCA	trichloroacetic acid
TCR	T cell receptor
Th1	T helper cell type 1
Th2	T helper cell type 2
T <sub>REG</sub>	regulatory T cell
TM	transmembrane
TNF $\alpha$	tumour necrosis factor- $\alpha$
Tween-20	polyoxyethylene-sorbitan monolaurate
VCAM-1	vascular cellular adhesion molecule-1
vCKBP	viral chemokine binding protein
WT	wild-type
w/v	weight per unit volume

# ABSTRACT

Chemokines comprise a large family of low molecular weight, mainly secreted proteins, well known for their role in directing leukocyte traffic, a vital component of immune and inflammatory responses. However, chemokines also regulate a broad range of other biological functions, including cell survival, growth, and differentiation. All these responses are mediated through cognate interactions with chemokine receptors, seven transmembrane (T/M) spanning G-protein coupled receptors. Importantly, the role of chemokines and their receptors in an enormous range of pathologies is apparent from a large number of studies in the last two decades, and these molecules have become popular targets for the pharmaceutical industry.

Despite the explosion in our understanding of chemokine networks, much less is known about regulatory mechanisms which must be in place to control and facilitate the biological effects of chemokines *in vivo*. Recent work has suggested the existence of a subset of atypical chemokine receptors that sequester their ligands to help remove or transport chemokines. This focus of this thesis regards the function of one of these molecules, CCX-CKR. This acts as a receptor for CCL19, CCL21 and CCL25, chemokines involved in constitutive and inflammatory trafficking of key leukocytic subsets in lymphoid tissue and small intestine. However, CCX-CKR does not appear to directly mediate these migratory events and, despite displaying high affinity binding, this receptor does not activate downstream signaling pathways typically involved in chemokine receptor function. Instead, roles for CCX-CKR in regulating chemokine levels or localisation have been proposed. The studies described in this thesis have examined the biochemistry of CCX-CKR *in vitro* with a view to determining what this receptor is capable of. These studies form a molecular

framework for the interpretation of phenotypes emerging from CCX-CKR *null* mice generated as part of this study.

The results from *in vitro* assays demonstrate that, in heterologous transfectants, human CCX-CKR mediates the internalisation and intracellular degradation of the chemokine CCL19. Importantly, unlike CCR7, CCX-CKR is primed, not desensitised, by previous exposure to ligand, allowing continuous CCL19 sequestration. This endows CCX-CKR with an impressive ability to sequester and destroy its ligands in continuous culture and therefore modify adjacent CCR7-driven responses. Mechanistically, CCL19 uptake by CCX-CKR is dependent on dynamin but, unlike CCR7, not reliant on  $\beta$ -arrestins. Genetic inhibition of both clathrin mediated endocytosis and early endosome function had no apparent effect upon CCL19 uptake by CCX-CKR, but inhibited uptake by CCR7. In contrast, over-expression of caveolin-1 dramatically inhibited CCX-CKR mediated CCL19 uptake while leaving CCR7 function unaffected, implicating caveolae in CCX-CKR endocytosis. The significance of these alternative pathways of receptor internalisation is discussed.

In parallel, the *in vivo* significance of CCX-CKR function was examined by generating CCX-CKR knock-out mice. These mice did not display any gross phenotypic abnormalities, yet detailed analysis revealed a significant reduction in the cellularity of inguinal lymph nodes compared with wild-type mice. In addition, the phenotype of splenic macrophages appeared altered in CCX-CKR *null* mice. Moreover, the topical application of irritant or hapten, to these mice, did not cause the subsequent inguinal lymph node hypertrophy observed in wild-type counterparts. However, CCX-CKR *null* mice were capable of mounting relatively normal immune responses although proliferative responses to antigen appeared to persist longer in the lymph nodes of *null* animals.

Taken together, the results from this study suggest that CCX-CKR contributes to the organisation and regulation of the immune system during homeostasis and immune response. This may be achieved through the control of chemokine availability such that the responses through the receptors CCR7 and CCR9 are modified. Importantly, the work described in this thesis represents the first attempt to dissect the function of CCX-CKR and provides the foundation for future studies aimed at more precisely defining the function of this atypical chemokine receptor.

# CHAPTER ONE

## INTRODUCTION

### 1.1 The Immune System

Throughout life, we are continually exposed to a diverse spectrum of potentially pathogenic microorganisms. In order to survive, a wide variety of protective mechanisms have evolved, known collectively as the immune system. When working effectively, our immune system can distinguish, at the molecular level, not only self from non-self, but also harmless from dangerous. This is achieved through a highly complex system of specific molecular recognition events executed mainly by motile cells. Immunology, the study of the immune system, is of great importance to biology and medicine for many reasons. For example, induction of immunity through vaccination has largely controlled many previously deadly infections, and has led to the near eradication of a major human pathogen: smallpox. However, other communicable diseases have not been contained as effectively, especially in the third world. The successful control and treatment of infectious diseases, such as HIV/AIDS, malaria, and tuberculosis, remain key goals of modern medical research. In addition, while the immune system has the capacity to protect us from pathogens, it can also cause us great harm. Pathological consequences of immunity, such as autoimmune diseases and allergies are an increasing cause of death, ill health, and distress in the modern world. Similarly, immune rejection of transplanted organs remains a significant obstacle to the successful treatment of many patients. An increased knowledge of the molecular workings of the immune system is leading to a greater understanding of these phenomena, and should lead to improvements in the treatment of numerous pathologies. Furthermore,

understanding how to control and harness the power of the immune system should enable us to use it as a more effective tool in the fight against many diseases, including cancer.

Generally, features of the immune system can be described as being either innate or adaptive. These are two distinct, but co-operating, arms of immunity. Characteristically, innate immunity describes those mechanisms which display a limited range of pathogen recognition, and which do not alter upon repeated exposure to the same pathogen. In contrast, adaptive immunity is highly specific in nature, and displays 'memory': subsequent responses to the same stimulus are enhanced. Both innate and adaptive immune responses depend largely on leukocytes, the nucleated cells of the blood. These cells are detailed in figure 1.1.1

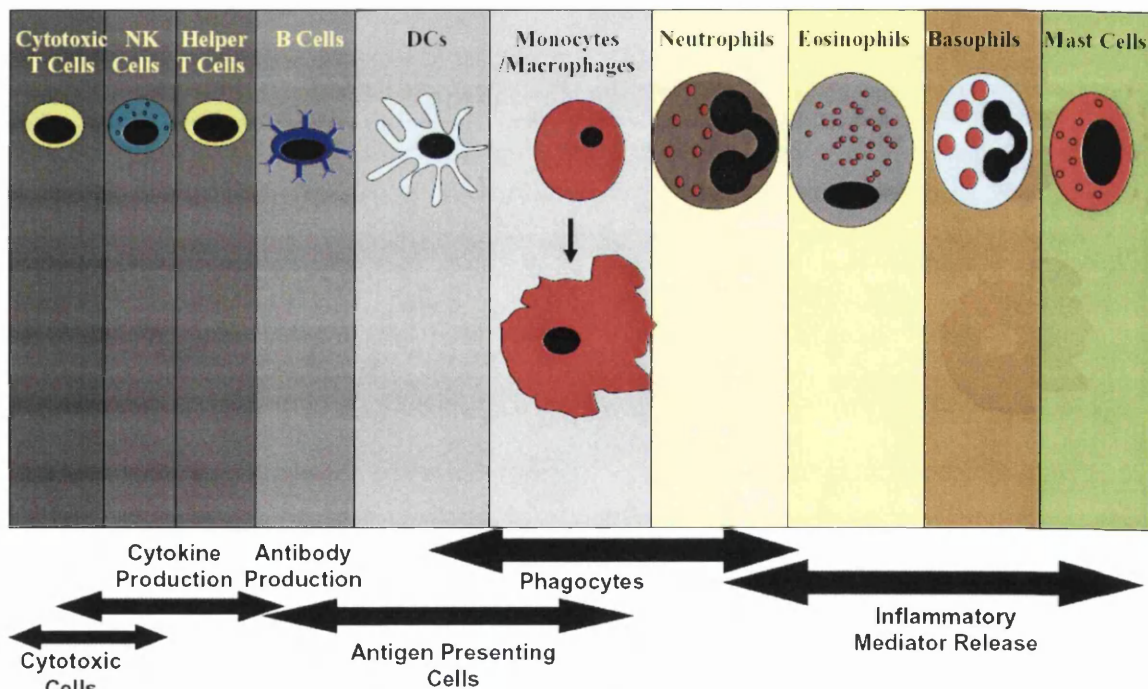


**Figure 1.1.1: Cells of the Immune System:** A schematic of the principal leukocytic cell types which comprise the mammalian immune system. The most commonly prescribed function of each of the cell types is indicated at the bottom of the figure.

The innate immune system comprises several different types of defensive mechanism: physical and chemical barriers, serum proteins, natural killer (NK) cells and phagocytic

cells. Anatomical barriers, such as the skin and mucous membranes, protect us from infection by preventing entry and attachment of pathogenic microbes. The acidic pH of the stomach, reflexes such as sneezing and coughing, and the genito-urinary flush, all contribute to host defence. Proteins present in blood plasma, such as members of the complement system, provide protection against a wide range of foreign pathogens. These directly lyse certain types of bacteria, or bind to them allowing more effective recognition by other immune mechanisms. NK cells, using innate immune mechanisms, can detect and destroy cells infected with viruses. The ingestion of extracellular material such as bacteria, a process known as phagocytosis, is another important feature of innate immunity. Conserved molecules on the surface of many invading microbes are recognized by receptors on the surface of phagocytic leukocytes (eg. neutrophils and macrophages) which can then internalise and digest the pathogen.

Tissue damage by wounding, infection with a pathogen, or autoimmune attack, causes the induction of a cascade of events known collectively as the inflammatory response. The local release of inflammatory mediators causes blood vessel dilation and an increase in vascular permeability at the site of damage/infection. Significantly, this is accompanied by an influx of phagocytic and cytotoxic cells from the bloodstream to tissue. This generally results in clearance and resolution of the infection after which the response subsides and the tissue heals, returning to normal. These relatively non-specific mechanisms of innate immunity effectively protect us against infection from the vast majority of potential pathogens.

Specific immune responses, i.e targeted immune reactions to particular pathogens, are termed adaptive immunity. These responses are shaped by previous exposure to pathogens. The adaptive immune system can provide effective life-long protective immunity to re-

infection by a pathogen that has previously been experienced by the host. The essential cells for adaptive immunity are a specialized subset of leukocytes termed lymphocytes. Lymphocytes are able to specifically recognize pathogens through their expression of antigen (Ag) specific receptors, whose diversity and specificity is generated by a complex system of genetic recombination and clonal selection. As a result of these phenomena, the Ag receptor repertoire of any one individual should be capable of recognizing any potential pathogen. Lymphocytes can be functionally segregated into those which leave the bone marrow (BM) and mature in the thymus (T cells), and those which complete their maturation in the BM (B cells). Upon exposure to their specific Ag, lymphocytes direct and regulate immunity. T cells can be directly cytotoxic and kill cells infected with a particular pathogen (CD8<sup>+</sup> T cells) or produce soluble factors such as cytokines (CD4<sup>+</sup> T cells) which control the activity of other lymphocytes or innate effector cells. In addition, a subset of T cells, termed regulatory T cells (T<sub>REGS</sub>), have specificity for self or harmless non-self Ag and produce cytokines that ensure tolerance is maintained to these Ags (O'Garra and Vieira, 2004). B cells, when activated, produce specific antibody which can neutralize and lead to pathogen clearance. Generally, B cells are reliant upon CD4<sup>+</sup> T cell help to produce antibody, but can also act as Ag presenting cells (APCs) for T cells, stimulating their activation. Upon activation, a certain number of Ag specific lymphocytes differentiate into long-lived 'memory' cells which are capable of mounting rapid and enhanced specific responses to subsequent challenge from the same Ag.

There is significant interaction and cross-talk between the innate and adaptive immune systems and indeed the distinction between the two is increasingly blurred. For example, T cells are reliant upon innate phagocytic APCs to display Ag to them and allow them to become activated. APCs, such as dendritic cells (DCs) or macrophages, non-specifically ingest microbes or their products and process antigenic peptides for presentation on major

histocompatibility complex (MHC) molecules. Depending upon the activation state of the APC and the nature of the Ag presented, T cells can be stimulated in different ways. For example, T cells can either become activated to respond to the Ag or become anergic (incapable of further activation). Therefore, non-adaptive mechanisms of danger recognition by APCs can determine whether tolerance or immunity is acquired to a particular Ag. Similarly, the adaptive immune system can influence innate immune cells. For instance, T cells produce cytokines which in turn activate macrophages, enabling them to more effectively destroy the intracellular pathogens they have phagocytosed; B cells produce antibodies which bind specifically to Ag, and these antibodies are then recognized either by complement proteins in the serum or receptors on phagocytes, enabling more efficient pathogen destruction. Clearly, both innate and acquired immunity are involved in the fine tuning and regulation of one another and co-operate to ensure effective responses are initiated, maintained and resolved (general textbooks with information about the immune system are Abbas and Lichtman, 2005; Goldsby, 2003; Janeway and Travers, 1997).

### **1.1.1 The Systemic Organisation of the Immune System**

Frequent and co-ordinated interactions between cells of the immune system are essential for its proper function. To this end, various organs of the body are specialized to concentrate and contain these cells, facilitating these contacts. Generally, the organs of the immune system can be classified as either primary or secondary lymphoid organs, depending upon their major function in immunity. Primary lymphoid organs are sites of lymphocyte maturation and selection, while secondary lymphoid organs are the sites of immune response initiation. A description of these organs and the cells which populate them is necessary for this introduction.

There are two major primary lymphoid organs in humans and mice. These are the BM and the thymus. After birth, the BM is the major site for haematopoiesis and is the location of B lymphocyte maturation. Haematopoietic stem cells (HSCs), which are capable of differentiation into all the different cell types of the blood, colonise the BM, and grow and mature on a meshwork of stromal cells. The stroma provides support for growth and differentiation of HSCs by providing essential cell-cell contacts and secreting diffusible growth factors. Throughout life, continuous production of haematopoietic cells from the BM is maintained. B lymphocyte maturation is also reliant upon interactions with stromal cells in the BM. Both membrane-bound and soluble growth factors from the stroma are required for the survival, immunoglobulin (Ig) gene-rearrangement, and proliferation of B cell precursors. In addition, self-reactive B cells are either deleted or 'edited' following specific encounter with Ags expressed by stromal cells within the BM. Mature, non-autoreactive B lymphocytes then leave the BM into the circulation (reviewed in Hardy and Hayakawa, 2001).

T cell precursors emigrate from the BM and complete their maturation in the thymus, an encapsulated, bilobed organ situated above the heart. The lobes of the thymus are divided into lobules by connective tissue, and each lobule is divided into two compartments, the cortex (outer compartment) and the medulla (inner compartment). T-cell precursors enter the thymus at the cortico-medullary junction and migrate outwards, through the cortex, towards the sub-capsular zone. Following T cell receptor (TCR) gene rearrangements, developing thymocytes interact with cortical epithelial cells. Only thymocytes that recognize self-MHC molecules on cortical epithelial cells are positively selected (not deleted) and these cells then migrate to the medulla. Here, positively selected thymocytes interact with haematopoietic APCs (DCs and macrophages) and are negatively selected (deleted) if they recognize self Ags presented via MHC molecules on these cells.

Thymocytes that survive positive and negative selection leave the thymus, forming the peripheral T cell pool (reviewed in von Boehmer et al., 2003).

After their development in the thymus or BM, mature naïve lymphocytes circulate through the bloodstream, into the secondary lymphoid organs in search of their specific Ag. Although the number of lymphocytes specific for any one Ag may be very few in number, and the total number of lymphocytes in the human body ranges from  $10^{10}$  -  $10^{12}$ , APCs are still able to efficiently come into contact with, and activate, lymphocytes specific for the Ags they carry. This is due to the exquisite organisation of the secondary lymphoid organs and the complex system of cell trafficking that occurs in these tissues. These organs include the spleen, lymph nodes (LNs), and gut associated lymphoid tissues (GALT) such as the Peyer's patches (PPs), tonsils and adenoids. These organs are strategically positioned in order to capture Ag from all the organs of the body. The spleen samples Ag from the blood, and the PPs sample directly from the intestine. The LNs filter the skin, mucosal surfaces and other organs, with Ags delivered by the lymphatic vasculature. Once lymphocytes are activated within secondary lymphoid organs, they undergo intense proliferation and differentiate into either effector or memory cells with distinct homing capabilities. Effector lymphocytes infiltrate sites of inflammation while memory cells recirculate through tissues and secondary lymphoid organs, primed for rapid subsequent responses upon repeat exposure to their specific Ag. A brief description of the general structure of the secondary lymphoid organs and cellular flow through these tissues will now follow, focussing on LNs, PPs and spleen.

LNs are a series of encapsulated structures which are dispersed strategically throughout the body and which contain a densely packed network of lymphocytes, macrophages and DCs. Structural features of a LN and routes of cellular entry and exit are represented

schematically in figure 1.1.2. There are two distinct vascular systems which allow entry into the LN. First, Ags, APCs and memory lymphocytes can enter through the afferent lymphatic vessels which drain tissue fluid, to the LN. Alternatively, circulating lymphocytes (and certain other cell types eg. monocytes and NK cells during inflammation) can enter LNs from the bloodstream through specialized high endothelial venules (HEVs). Once inside LNs, Ag and cells percolate via a conduit system, interacting with cells and matrix components of the LN (Gretz et al., 1997; Sixt et al., 2005). Structurally, LNs can be segregated into three separate compartments, each supporting distinct microenvironments. The outermost layer contains mainly follicular DCs (FDCs) and B cells arranged into follicles, which can develop into germinal centres (GCs) during immune responses. Beneath this lies the paracortex, sometimes called the T cell area. As the names suggests, this area consists mainly of T cells but also contains interdigitating DCs which present Ag to the T cells. The innermost area of the LN is known as the medulla. This area is much more sparsely populated than other regions of the LN and contains lymphoid cells, such as antibody secreting plasma cells. Cells leave LNs via efferent lymphatics, which empty back into the bloodstream via the thoracic duct (reviewed in von Andrian and Mempel, 2003).

APCs continuously drain from the periphery to LN, bringing Ag and information of tissue health status. Inflammation in the tissue augments this APC exodus to speed up information flow and prepare the LN for initiation of immune responses. To do this, cellular entry to the LN is enhanced and egress is slowed down. This causes LN enlargement (independently of cell proliferation) and aids the cognate interactions between APCs and T cells required for many immune responses. DCs play an important role in causing the induction of this LN hypertrophy. Indeed, recent studies have shown that the more DCs migrate to a LN, the more expansion takes place (Martín-Fontecha et al., 2003). This change in LN cellularity is

also induced by inflammatory cytokines draining from the periphery, such as mast cell derived tumour necrosis factor- $\alpha$  (TNF $\alpha$ ) (McLachlan et al., 2003).

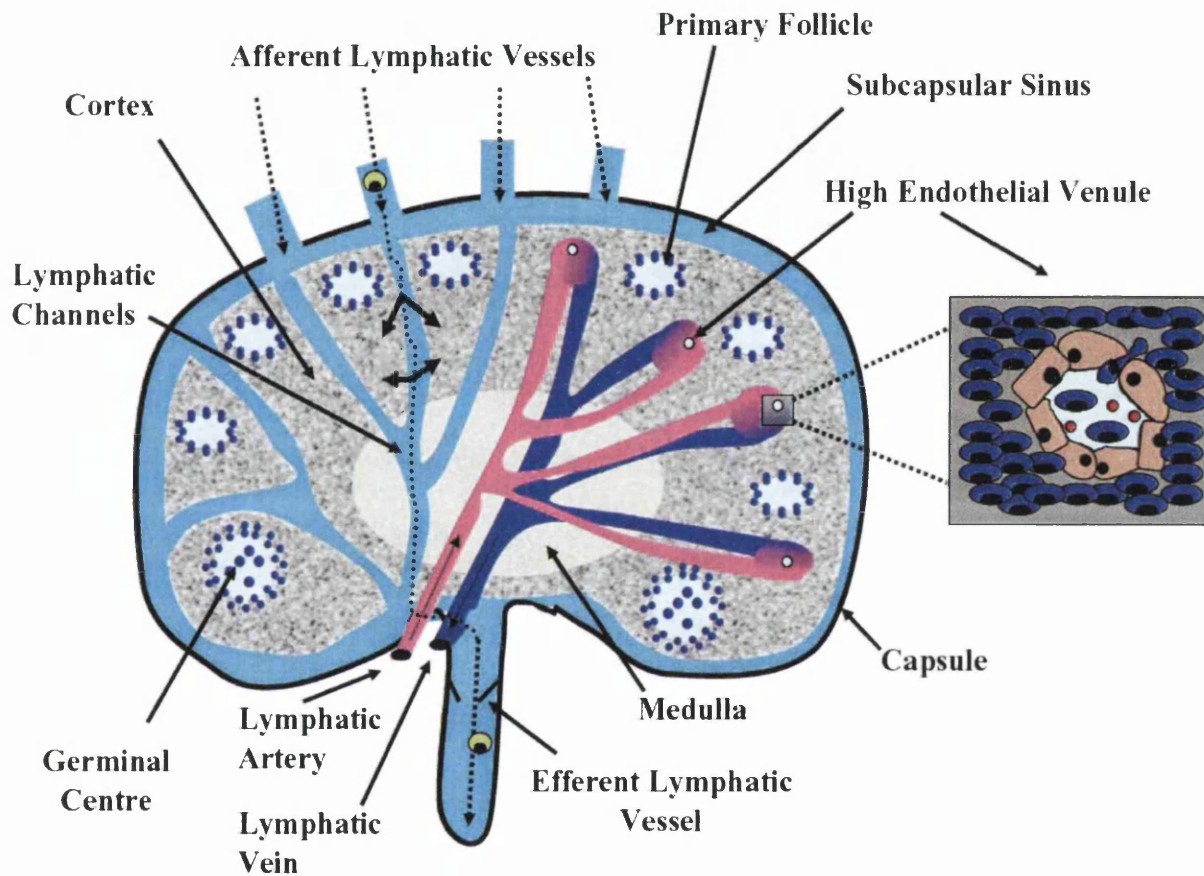


**Figure 1.1.2: Structure of a Lymph Node.** A schematic representation of the major structural features of a LN. The indent shows a close up of lymphocytes emigrating across a high endothelial venule into the LN. Blue cells = lymphocytes, light coloured cells = endothelial venules, red circles = red blood cells. A cell (in green) is shown entering via the afferent lymphatic vessel and its route through the lymphatic channels, LN conduits, and exit via the efferent lymphatics is depicted with arrows. The main features of the LN (described in the text) are highlighted by solid arrows.

Peyer's patches are largely similar structures to peripheral LNs but differ in several key aspects. Located along the length of the submucosa of the small intestine, PPs are specialized to sample Ag directly from the gut lumen. Therefore, the entry of an Ag to the PP is quite distinct from that found in the LN, being transported through specialized cells

called microfold cells (M cells) which effectively form pores in the gut epithelial wall. In the layer below the M cells and epithelium, lies the subepithelial dome, an area rich in APCs. Beneath this is a layer of lymphoid cells, segregated into T cell areas and B cell follicles. Lymphocyte entry into PPs occurs through HEVs which open into either the T cell area or, unlike peripheral LNs, open directly into B cell follicles. Cellular exit from PPs is distinct from peripheral LNs, with cells leaving through the afferent lymphatics which drain from the gut to the mesenteric LNs (the structure and function of PPs is covered in Mowat, 2003).

The spleen, located in the upper abdominal cavity, is the largest secondary lymphoid organ and is specialized both for the disposal of senescent erythrocytes, and for detecting blood borne Ags leading to the initiation of systemic immune responses. The organization of the spleen is shown schematically in figure 1.1.3. The splenic red pulp is the site of red blood cell (RBC) phagocytosis by macrophages. The white pulp surrounds the splenic artery and consists of the T cell rich periarteriolar lymphoid sheath (PALS) and the B cell rich follicles. The marginal zone (MZ), which is peripheral to the PALS, is populated mainly by MZ B cells and macrophages. Macrophages within the MZ are essential for the capture of blood-borne Ags (Aichele et al., 2003). In contrast to LNs and PPs, where lymphocytes enter through HEVs, leukocyte entry into the spleen comes through terminal arterioles of the splenic artery which open into either the MZ or the red pulp. Most blood cells then pass through the the red pulp and rejoin the circulation through venous sinuses. However, lymphocytes migrate from the red pulp to the white pulp and organize into the T and B cell areas described above.

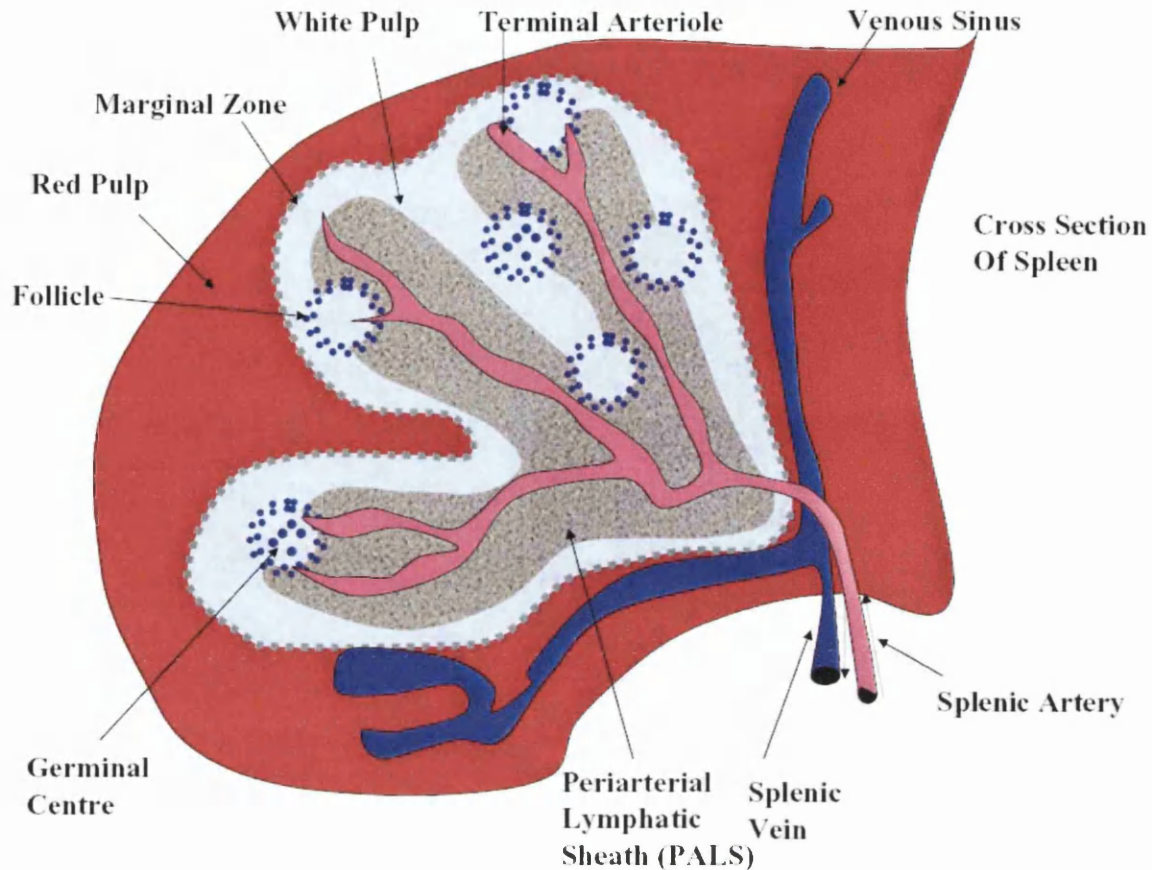


**Figure 1.1.3: Structure of the Spleen:** The general structural features of the spleen relevant to this discussion are shown in a cross section schematic. Features described in the text are highlighted by arrows.

### 1.1.2 The Multistep Paradigm of Leukocyte Extravasation

From the discussion above, it is clear that central to effective immunity and inflammation are mechanisms controlling the temporal and spatial positioning of leukocytes. From their emigration from the BM, circulation through tissues, blood and lymph, tissue infiltration during inflammation, and egress during wound healing – leukocyte homing is an extremely important and exquisitely orchestrated process involving a diverse range of molecular mechanisms. A key feature is the ability of leukocytes to migrate out of the bloodstream, across endothelial barriers and into either peripheral tissues (across inflamed endothelium) or secondary lymphoid organs (across HEVs). When the extremely high shear pressure encountered by leukocytes within blood vessels is considered, this extravasation cannot be

regarded as anything other than an impressive feat. Quite how leukocytes are able to do this is still to be completely resolved. However, a multistep paradigm of leukocyte extravasation has emerged over the past thirty or so years. This is summarized in figure 1.1.4. Normally, leukocytes coursing through the circulation will randomly collide with blood vessel walls and immediately rebound to be carried on with the flow of blood. However, low affinity interactions mediated by selectins and their ligands causes some leukocytes to adhere to the endothelial cells (ECs) of the vessel wall for a fraction of a second, causing them to ‘roll’ along, sampling the endothelial surface. During this time, and given the appropriate signals from the EC, a proportion of these leukocytes are able to increase the strength of the interaction via activation of integrins, and firmly adhere to the vessel wall. Further signals between adhered leukocytes and the endothelium allow the leukocyte to undergo cytoskeletal changes and squeeze through gaps between ECs, out of the circulation and into tissues.

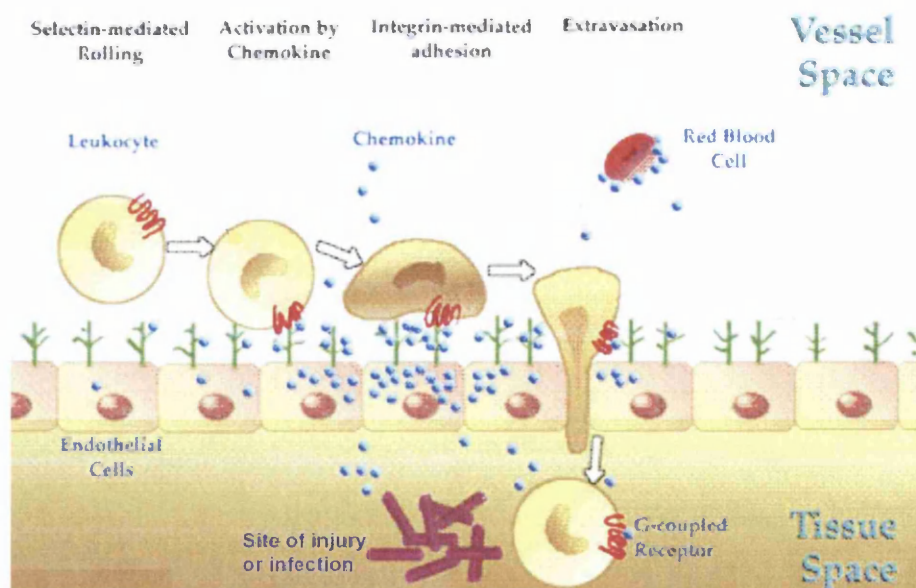


**Figure 1.1.4: The Multistep Paradigm of Leukocyte Extravasation.** A diagram showing the different steps involved in leukocyte extravasation from the circulation into tissues. Leukocytes within the bloodstream ‘roll’ on ECs. Cells become activated following a specific signaling event allowing firm adhesion. Finally cells can cross the endothelial barrier and enter the inflamed tissue. See text for more details. Chemokines depicted as blue spheres, receptors are red and purple rods represent bacteria. Figure modified from a diagram downloaded from the website of Chemocentryx Inc.

Once a leukocyte has left the blood, its correct homing within a tissue is critical to enable that leukocyte to exert its function, and ensure appropriate leukocyte compartmentalisation, exquisitely demonstrated in tissues like LNs and spleen. Among the molecules known to play important roles in these complex migratory events are cell surface adhesion molecules such as selectins and integrins, soluble proteins such as leukotrienes, prostaglandins, sphingosine-phosphates, and chemotactic factors such as the complement component C5a and the formyl peptide fMLP. However, in the field of leukocyte migration, perhaps the most important and now best understood molecules are a class of cytokine known as the chemokine superfamily. It is these molecules, their function in immunity and inflammation, and their regulation which form the basis of this thesis.

## **1.2 The Chemokines**

### **1.2.1 Historical Perspectives**

The importance of directed cell migration in the immune system has long been recognized. Indeed, studies as far back as the 1950's established that leukocyte migration was a dynamic process which could be influenced by bacteria or their products (Martin and Chaudhuri, 1952). Subsequent investigations characterized lymphocyte trafficking patterns (Cannon and Wissler, 1965; Elves, 1970; Gowans, 1959) and demonstrated that subsets of lymphocytes could be segregated based upon their differential migration properties (Lance and Taub, 1969). However, the molecular mechanisms controlling these processes remained largely elusive until relatively recently. The field of chemokine biology has emerged within the last 18 years. Although a molecule now recognized as a chemokine, Platelet-Factor 4 (PF4), was identified as far back as 1977 (Walz et al., 1977; Wu et al., 1977), specific chemotactic properties of this molecule have still not been established. It

was not until 1987 and the discovery of the secreted neutrophil-attracting cytokine Interleukin-8 (IL-8) (Walz et al., 1987; Yoshimura et al., 1987) that a true CHEMOtactic cytoKINE (Chemokine) had been recognised. This was quickly followed up with the discovery of many other similar molecules such as Macrophage Inflammatory Protein 1 α (MIP-1 $\alpha$ ) (Davatelis et al., 1988; Wolpe et al., 1988), Regulated upon Activation, Normal T cell Expressed and Secreted (RANTES) (Schall et al., 1988), Monocyte Chemottractant Protein-1 (MCP-1) (Yoshimura et al., 1989), and Interferon inducible Protein-10 (IP-10) (Ohmori and Hamilton, 1990; Vanguri and Farber, 1990). Investigators identified these molecules while attempting to characterise proteins secreted by leukocytes upon activation, or after the addition of an inflammatory stimulus. Subsequently, through the increased use of bioinformatics and mining of expressed sequence tag (EST) databases, many other chemokines have now been recognized. Due to their relatively short coding sequences and conserved motifs, chemokines can be encompassed by a single EST and are particularly easily identified by these methods (Wells and Peitsch, 1997). This allowed the cloning and identification of chemokines which are not highly or inducibly expressed, or those which are restricted to particular tissues. Consequently, in the last 10 years there has been an explosion of the discovery of these molecules. Today, the known chemokine superfamily in humans comprises 44 proteins (37 in mice), and the rate of identification of novel molecules within this superfamily has slowed significantly. Indeed, the most recent chemokine to be identified was CXCL16 in 2000 (Matloubian et al., 2000) and it is now thought likely that most, if not all, human and murine chemokines have been discovered.

Shortly after the discovery of IL-8, it was demonstrated that the neutrophil chemotactic properties of this molecule could be prevented by pharmacological inhibition of a class of intracellular signaling molecules called G-proteins (Bacon and Camp, 1990). This suggested that the secreted chemokine was exerting its biological effects through a cell

surface G-protein coupled receptor (GPCR). Indeed, it was subsequently shown (Holmes et al., 1991; Murphy and Tiffany, 1991) that the IL-8 receptor was a GPCR, which are a large family of seven T/M spanning receptors with a wide range of biological functions. The cloning and characterization of other chemokine receptors quickly followed (Birkenbach et al., 1993; Combadiere et al., 1995; Gao et al., 1993; Nomura et al., 1993; Schweickart et al., 1994; Yamagami et al., 1994) and these were categorized into four subfamilies based on their chemokine ligand specificities. At present, 18 true human chemokine receptors have been described. A more detailed description of chemokine receptors follows in section 1.3.

Combined with the explosion in chemokine identification, the demonstration in 1996 that two chemokine receptors, termed CCR5 and CXCR4, were essential co-receptors for the entry of human immunodeficiency virus (HIV) into host cells, and that the chemokine ligands of these receptors could block viral infection, stimulated great interest in the field of chemokine and chemokine receptor biology (reviewed in Simmons et al., 2000). An enormous amount of research into these molecules has taken place in the last decade and chemokines are now recognized as important regulators in virtually all immune-mediated pathologies. Furthermore, chemokines and chemokine receptors are now also known to play roles in processes as divergent as central nervous system (CNS) function, embryonic development, wound healing, and cancer, and control the biology of many non-leukocytic cell types. A detailed summary of all these functions is beyond the scope of this thesis. Instead, I intend to introduce the field of chemokine/chemokine receptor biology, focussing on its role in immunity. In particular, the biology of three chemokine receptors called CCR7, CXCR5, and CCR9, and their ligands shall be discussed as these have most relevance to this study. I also intend to discuss the regulation of chemokine activity and introduce the emerging concept of decoy receptors in this system. I shall go on to describe

CCX-CKR, a recently cloned receptor that binds to the same chemokines bound by CCR7, CXCR5, and CCR9, and whose function is the main subject of investigation in this thesis.

### 1.2.2 Nomenclature

As chemokines were rapidly and independently identified, many existed in the literature under different names. For example, Epstein-Barr Virus Induced Molecule-1 Ligand Chemokine (ELC) is also known as MIP-3 $\beta$  and exodus-3 (Kim et al., 1998; Yoshida et al., 1997; Yoshie et al., 1997). Additional confusion was created by the fact that the genes which coded for the chemokine proteins also had unique names. These were designated Small secreted Cytokine (SCY), followed by a letter designating which chemokine subfamily the protein they coded for belonged to (SCYa, SCYb, SCYc, and SCYd), and a number indicating the chronological order in which the genomic sequence was identified. To eliminate any ambiguity, a new systematic nomenclature was introduced in 2000 based around the important amino-terminal cysteine motif (described in detail below) and the number assigned to the gene which coded the protein (Zlotnik and Yoshie, 2000). Thereby, ELC is now known as CC chemokine ligand 19 (CCL19), with CC indicating the subfamily, L indicating that it is a ligand, and 19 corresponding to the gene SCYb19 (the 19<sup>th</sup> SCYb gene cloned). From here-on, the new systematic name for each chemokine will be used exclusively. The chemokine superfamily with traditional and new systematic nomenclature is summarised in table 1.1.

The nomenclature for the 18 chemokine receptors has not had the complications which have surrounded the ligands. Ever since it was recognized that chemokine receptors were generally restricted to responding to chemokines of a particular subclass (see section 1.2.3), they were named with that subfamily prefix, followed by an R for receptor, and a number designated chronologically to their discovery. Hence the first CXC chemokine receptor was

named CXCR1 and so on. It is important to note that to be officially designated as a chemokine receptor, and to be included in the systemic nomenclature, a given receptor must be demonstrably able to transduce intracellular signals upon chemokine binding (Murphy, 2002; Murphy et al., 2000). On this basis, three receptors which display high affinity binding but apparently do not couple to downstream signaling pathways have been excluded from the nomenclature. These receptors, which are of particular relevance to this study, are the Duffy antigen / receptor for chemokines (DARC), D6, and CCX-CKR (and are discussed in more detail later). The ligands bound by these molecules are indicated in Table 1.1.

### 1.2.3 Chemokine Structure and Subclassifications

Chemokines share a number of key structural and functional similarities. Although they often display only a limited amount of primary amino acid sequence homology, it is the primary sequence which defines them as chemokines. This is because of a conserved motif which confers a well-defined secondary structure on these molecules (see figures 1.2.1 and 1.2.2). Generally ranging between approximately 6-11kDa in size, these mainly secreted molecules characteristically display a three stranded anti-parallel  $\beta$ -pleated sheet (the so called 'Greek Key' motif) with a C-terminal  $\alpha$ -helix laid across (Baldwin et al., 1991; Chung et al., 1995; Hoover et al., 2000; Lubkowski et al., 1997). This distinctive three-dimensional structure of chemokines is the result of disulphide bonds between a defining tetra-cysteine motif. The chemokine superfamily can be subdivided by the exact configuration of this motif at the amino terminus. The two major subfamilies of chemokines are the  $\alpha$  (or CXC) chemokines, and the  $\beta$  (or CC) chemokines. The CXC chemokines have a single, non-conserved, amino acid between the first two cysteine residues of this motif, while in the CC chemokines these residues are directly juxtaposed.

Systemic Name	Other names	Human Chromosome	Chemokine Subtype	Receptor(s) Bound
<b>CC family (<math>\beta</math> Chemokines)</b>				
<i>CCL1</i>	I-309	17q11.2	4 cysteines	CCR8
<i>CCL2</i>	MCP-1	17q11.2	4 cysteines	CCR2, D6, DARC
<i>CCL3</i>	MIP-1 $\alpha$ , LD780	17q12	4 cysteines	CCR1, CCR5
<i>hCCL3L1</i>	MIP-1 $\alpha$ P, LD783	17q12	4 cysteines	CCR1, CCR3, CCR5, D6
<i>CCL4</i>	MIP-1 $\beta$	17q12	4 cysteines	CCR5, D6
<i>hCCL4L1</i>	MIP-1 $\beta$ 2	17q12	4 cysteines	CCR5
<i>CCL5</i>	RANTES	17q12	4 cysteines	CCR1, CCR2, CCR5, D6, DARC
<i>mCCL6</i>	C10	n/a	4 cysteines	CCR1
<i>CCL7</i>	MCP-3	17q11.2	6 cysteines	CCR1, CCR2, CCR3, D6
<i>CCL8</i>	MCP-2	17q11.2	4 cysteines	CCR3, D6
<i>mCCL9</i>	MIP-1 $\gamma$	n/a	6 cysteines	CCR1
<i>mCCL10</i>	MIP-1 $\gamma$	n/a	4 cysteines	CCR1
<i>CCL11</i>	Eotaxin	17q11.2	4 cysteines	CCR3, D6, DARC
<i>mCCL12</i>	MCP-5	n/a	4 cysteines	CCR2, D6
<i>hCCL13</i>	MCP-4	17q11.2	4 cysteines	CCR2, CCR3, D6, DARC
<i>hCCL14</i>	HCC-1	17q12	4 cysteines	CCR1, D6, DARC
<i>hCCL15</i>	HCC-2	17q12	6 cysteines	CCR1, CCR3
<i>CCL16</i>	HCC-4	17q12	4 cysteines	CCR1, CCR2, CCR5
<i>CCL17</i>	TARC	16q13	4 cysteines	CCR4, DARC
<i>hCCL18</i>	PARC	17q11.2	4 cysteines	Unknown
<i>CCL19</i>	ELC, MIP3 $\beta$ , exodus-3	9p13.3	4 cysteines	CCR7, CCX-CKR
<i>CCL20</i>	LARC, MIP3 $\alpha$ , exodus-1	2q36.3	4 cysteines	CCR6
<i>CCL21</i>	SLC, 6CKine, exodus-2	9p13.3	6 cysteines	CCR7, CCX-CKR
<i>CCL22</i>	MDC	16q13	4 cysteines	CCR4, D6
<i>hCCL23</i>	MIP1-1	17q12	6 cysteines	CCR1
<i>hCCL24</i>	Eotaxin-2	7q11.23	4 cysteines	CCR3
<i>CCL25</i>	TECK	19p13.3	4 cysteines	CCR9, CCX-CKR
<i>hCCL26</i>	Eotaxin-3	7q11.23	4 cysteines	CCR3
<i>CCL27</i>	CTACK, Eskine, PESKY	9p13.3	4 cysteines	CCR10
<i>CCL28</i>	MEK	5p12	6 cysteines	CCR3, CCR10
<b>CXC family (<math>\alpha</math> Chemokines)</b>				
<i>CXCL1</i>	GRO $\alpha$	4q21.1	ELR+	CXCR1, CXCR2, DARC
<i>CXCL2</i>	GRO $\beta$ , MIP-2	4q21.1	ELR+	CXCR2, DARC
<i>CXCL3</i>	GRO $\gamma$	4q21.1	ELR+	CXCR2, DARC
<i>CXCL4</i>	PF4	4q21.1	ELR-	CXCR3B, DARC
<i>CXCL5</i>	ENA-78	4q21.1	ELR+	CXCR2
<i>CXCL6</i>	GCP-2	4q21.1	ELR+	CXCR1, CXCR2
<i>hCXCL7</i>	NAP-2	4q21.1	ELR+	CXCR2, DARC
<i>hCXCL8</i>	IL-8	4q21.1	ELR+	CXCR1, CXCR2, DARC
<i>CXCL9</i>	Mig	4q21.1	ELR-	CXCR3A/B
<i>CXCL10</i>	IP-10	4q21.1	ELR-	CXCR3A/B
<i>CXCL11</i>	I-TAC	4q21.1	ELR-	CXCR3A/B
<i>CXCL12</i>	SDF-1	10q11.21	ELR-	CXCR4
<i>CXCL13</i>	BLC, BCA-1	4q21.1	ELR-	CXCR5, CCX-CKR
<i>CXCL14</i>	BRAK, bolekine	5q31.1	ELR-	Unknown
<i>mCXCL15</i>	Lungkine, WECHÉ	n/a	ELR-	Unknown
<i>CXCL16</i>	SR-PSOX	17p13	ELR-/TM	CXCR6
<b>C family (<math>\gamma</math> Chemokines)</b>				
<i>XCL1</i>	Lymphotactin- $\alpha$ , SCM-1 $\alpha$	1q24.2		XCR1
<i>hXCL2</i>	SCM-1 $\beta$	1q24.2		XCR2
<b>CX3C family (<math>\delta</math> Chemokines)</b>				
<i>CX3CL1</i>	Fractalkine/neurotactin	16q13	TM	CX3CR1

**Table 1.1: The Chemokine Superfamily.** Systematic nomenclature for each chemokine is given along with common old name or names. CCX-CKR ligands are highlighted in green. The human chromosomal location and structural subdivision of the chemokines is also included where relevant. Those chemokines only present in humans or mice are prefixed with 'h' or 'm' respectively. Italicized chemokines are generally classified as 'constitutive'. Receptors which the full length unmodified chemokine acts as an agonist are shown, along with potential decoy receptor, D6, DARC or CCX-CKR. Abbreviations: ELR+/-, the presence or absence respectively of Glu-Leu-Arg motif in CXC chemokines (see text for details); T/M, chemokine with transmembrane domain. (Adapted from a table in Comerford and Nibbs, 2005).

There are two other minor chemokine subfamilies which have different variations of this motif. The CX3C chemokines, of which there is only one identified member, CX3CL1, have three amino acids between the first two cysteines, while in the C chemokine subfamily one of these residues is lacking. As already eluded to, this structural subdivision is also a functional division as members of a particular subfamily are generally restricted to binding only chemokine receptors specific for that subclass of chemokine (there are some notable exceptions to this, of which more later). However, within each subfamily there is a degree of redundancy and promiscuity. Many chemokines are able to bind to multiple different receptors of that subtype and many receptors are able to bind several different chemokines. The significance of this will be discussed in more detail later.

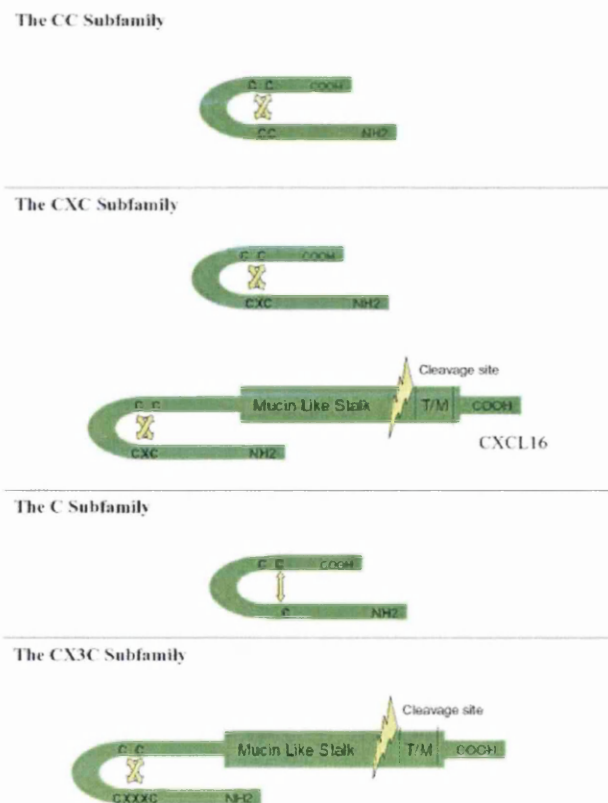


**Figure 1.2.1: The Chemokine Subfamilies.** The structural subdivisions which segregate the 4 chemokine subfamilies are shown. These are described in detail in the text. Cysteine residues are marked with a 'C'. Disulphide bonds which give the 'chemokine fold' are shown in yellow arrows. Amino and carboxy termini are marked NH<sub>2</sub> and COOH respectively. Mucin like stalk and T/M domains are also shown where appropriate. Proteolytic cleavage site shown in yellow.

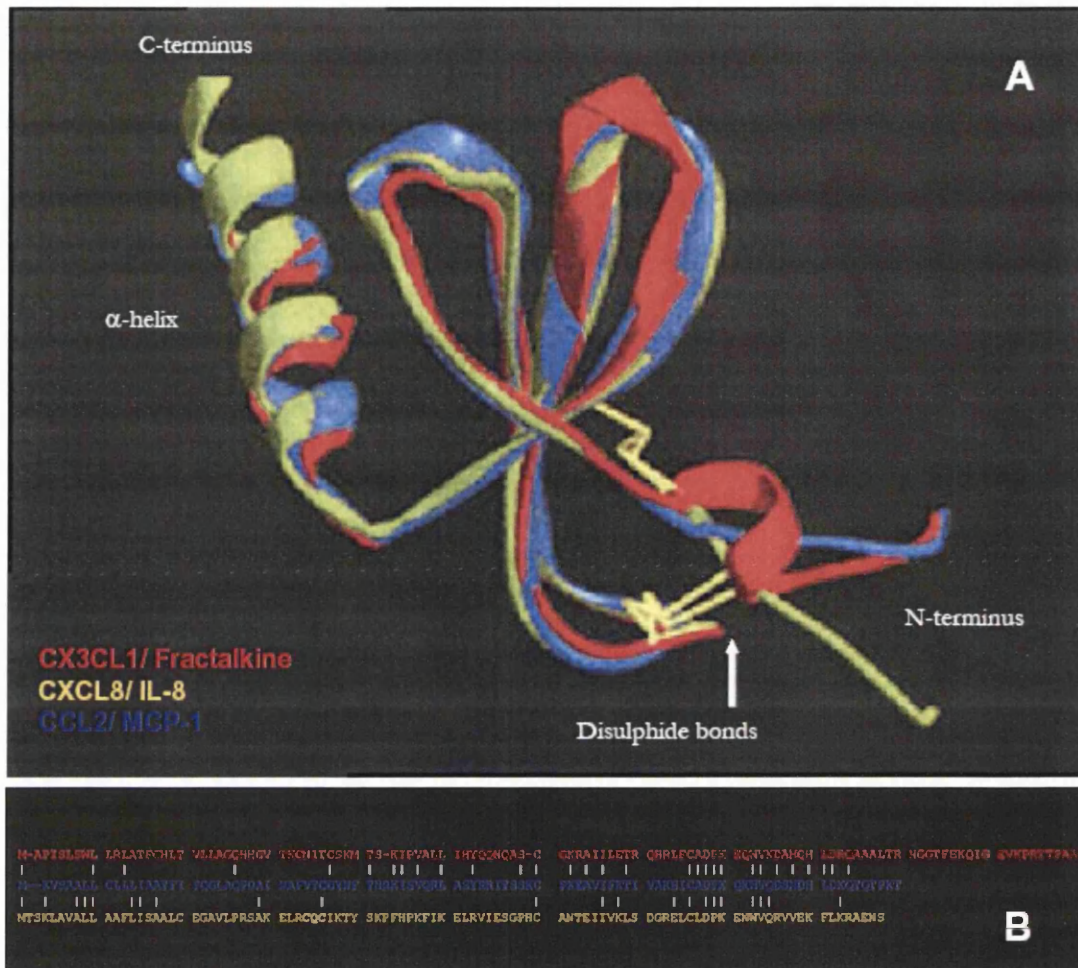


**Figure 1.2.2: Chemokines: Primary, Secondary, and Tertiary Structure.** (A) When secondary and tertiary structure is examined between 3 chemokines from different subfamilies (in red CX3CL3, in blue CCL2, in yellow CXCL8) there are clear structural similarities. However, a line up of the primary amino acid sequence (B) shows that there is limited homology between chemokines at this level. The defining cysteine residues are marked in bold. Conserved residues linked with a ( ). Part (A) of this figure is modified from a diagram downloaded from the website of Chemokine Therapeutics Corp.

CC chemokines, which make up the largest chemokine subfamily, are potent chemoattractants for a wide range of leukocytes including monocytes, DCs, eosinophils, basophils, NK cells and lymphocytes. Chemokines of the CXC class were initially thought to exert their functions primarily on neutrophils. However, the discovery of CXCLs9-16 showed that some members of this family have specificity for lymphocytes and other cell

types also. In the past, the CXC subfamily has been further subdivided based upon the presence or absence of a glutamic acid-leucine-arginine (ELR) motif directly preceding the first amino terminal cysteine residue. ELR+ CXC chemokines have specificity for the receptors CXCR1 and/or CXCR2 (and were thought to exclusively attract neutrophils), while ELR- chemokines use other CXC chemokine receptors (and were thought to only attract lymphocytes). This subdivision was also thought to divide CXC chemokines into those that are angiogenic (promote blood vessel growth, ELR+), and those which are angiostatic (inhibit blood vessel growth, ELR-) (Koch et al., 2001; Strieter et al., 1995). However, this functional subdivision is less clear now with evidence that ELR+ chemokines can also attract cells other than neutrophils (Hess et al., 2004; Ramjeesingh et al., 2003; Salcedo et al., 2000; Takata et al., 2004) and that ELR- chemokines can also be angiogenic (Kryczek et al., 2005; Salcedo and Oppenheim, 2003). The most recently identified CXC chemokine, CXCL16, differs from all the other members of this subfamily, in that it is expressed with a mucin-like stalk and a T/M domain and therefore is primarily expressed at the cell surface, rather than being secreted (see figure 1.2.1). The only member of the CX3C chemokine family, CXCL1, also displays these T/M features. Both CXCL16 and CX3CL1 are able to be released as soluble proteins following proteolytic cleavage and this has functional relevance for their biology (discussed in more detail in section 1.4.1).

Most chemokines are expressed in one of two characteristic patterns and have been subdivided on this basis. Generally, chemokines can be described as being either inflammatory (inducible) or constitutive (homeostatic) (see table 1.1). Inducible chemokines are expressed following an inflammatory stimulus. Leukocytes, including neutrophils, macrophages, immature DCs and lymphocytes, express chemokine receptors for inducible chemokines. This allows them to infiltrate damaged tissues in order to orchestrate and effect inflammatory and immune responses. Due to their inducible and high

level expression, these chemokines tended to be among the earliest identified. As such they include CXCLs1-11, (perhaps excluding CXCL4), CCLs2-16, XCL's1-2 and CX3CL1 (see table1.1). In contrast, constitutive chemokines are continuously expressed in the absence of danger signals, and control a wide range of homeostatic functions such as cell homing during embryonic development, lymphorganogenesis and immune surveillance. They are also of fundamental importance in co-ordinating cell movements during immune responses. Of particular relevance to this thesis are the constitutive chemokines CCL19, CCL21 and CXCL13 which are intimately involved in the homing of cells to, and their compartmentalisation within, secondary lymphoid organs. These chemokines facilitate the homing of T and B cells, along with DCs, into the appropriate areas of these organs where they undergo interactions essential for lymphocyte activation and immunity, and will be discussed in more detail in section 1.5. Other constitutive chemokines are tissue restricted and control traffic to those sites. For example, CCL25 (again of relevance to this thesis) is expressed in the thymus and by epithelial cells of the small intestine (Campbell and Butcher, 2002), while CCL27 directs migration to the skin (Homey et al., 2002). Whilst this functional division of chemokines has general use, the difficulty with the inducible/constitutive classification of chemokines is that most constitutive chemokines are subject to some degree of induction during inflammation, which blurs the distinction between these groups (Bonacchi et al., 2003; Christopherson et al., 2003; Columba-Cabezas et al., 2003; Nakayama et al., 2001; Serra et al., 2004).

#### **1.2.4 Genetic Organisation and Phylogenic Origin**

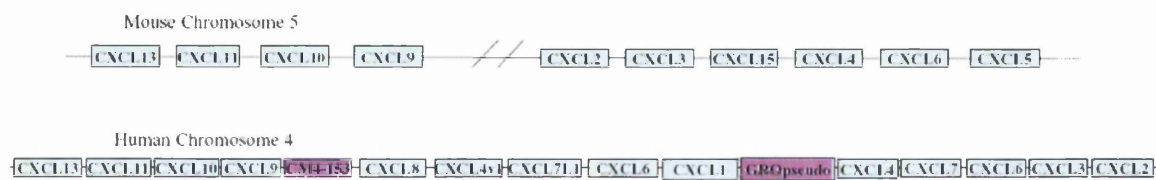
Similar to other gene families with pivotal roles in the immune system, such as the MHC genes, the chemokine gene family has evolved rapidly, probably through a series of duplication events followed by divergence. Phylogenic analysis suggests that the chemokine CXCL12 is the modern representative of an ancestral chemokine. Functional

CXCL12 orthologs are conserved from higher mammals through other vertebrates, such as birds and fish (Huisling et al., 2004) and to lower vertebrates, such as *Xenopus laevis* (Braun et al., 2002). It should be noted that this means chemokines must have evolved before the development of complex immune systems, probably with the development of the CNS. Indeed, chemokines such as CXCL12 (and its receptor CXCR4) are essential for successful embryogenesis, with CXCR4 or CXCL12 *null* mice displaying a wide variety of defects in such things as cerebellar and cardiac development, and vascularisation of the gastrointestinal tract (Tachibana et al., 1998; Zou et al., 1998). The rapid expansion of chemokine genes in higher mammals coincides with the development of more sophisticated immune systems. It is likely that the intricate cell homing that is required for the development of complex primary and secondary lymphoid microenvironments, and for robust immune and inflammatory responses, has driven the selective pressure which has forced the dramatic adaptive radiation of mammalian chemokine genes (Huisling et al., 2003). The adaptive nature of the chemokine system means that these genes have evolved so recently that functional chemokine orthologs do not always exist even between relatively closely related species. For example, there is no mouse ortholog of human CXCL8 and no human equivalent of murine CXCL15. It is likely that the human chemokine system is still evolving relatively rapidly, as the selective pressure exerted by the HIV pandemic is likely to favour the survival of individuals with high copy number of CCL3-L1 or who have the CCR5 $\Delta$ 32 mutation (Gonzalez et al., 2005; Mummidi et al., 1998).

In humans, the major chemokine clusters are on chromosomes 14 and 17 (the CXC cluster and the CC cluster, respectively) and in mice these clusters are located on chromosomes 5 and 11 (see figure 1.2.3) (Nomiya et al., 2001). Structurally and functionally related chemokine genes tend to be closely linked, reflecting their probable origin from recent (in evolutionary terms) genetic duplication events. This is especially true of 'inducible'

chemokines, which have the highest tendency to be clustered. Not all chemokines lie within these clusters. Indeed, CXCL12 is the only chemokine gene on the human chromosome 10 (Shirozu et al., 1995) and other smaller minor clusters exist, such as on human chromosome 9 where CCL19 and CCL21 reside (Nakano and Gunn, 2001; Yoshida et al., 1998) and human chromosome 16 which is home to CCL17 and CCL22 (Imai et al., 1998). In mice, CCL19 and CCL21 are found on chromosome 4 but have undergone considerable duplication events. Significantly, this has generated two forms of CCL21, termed CCL21*ser* and CCL21*leu*, expressed in different arms of the vasculature. Thus, CCL21*leu* is expressed by lymphatic endothelial cells (LECs), whilst CCL21*ser* is produced by HEVs.

#### The Major CXC chemokine gene cluster in humans and mice



#### The Major CC chemokine gene cluster in humans and mice

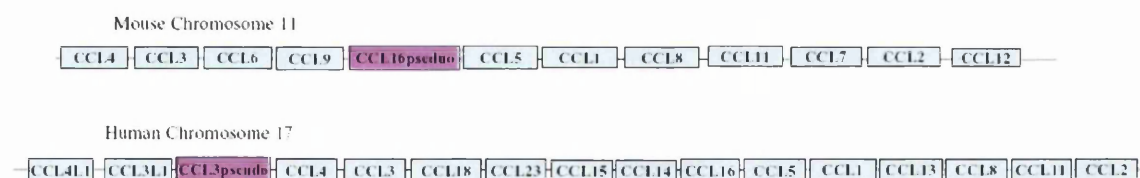


**Figure 1.2.3: Genetic Organisation of Chemokines.** The major chemokine gene clusters in humans and mice are shown. Filled blue boxes represent chemokine genes while purple boxes represent pseudogenes. The protein that is coded by the gene is indicated.

### 1.2.5 Redundancy and Promiscuity

As has been touched on briefly earlier, a degree of redundancy and promiscuity exists within the chemokine system with some receptors able to bind multiple ligands and some chemokines able to bind several different receptors. For example, CCR7 is a receptor for

both CCL19 and CCL21 while the chemokine CCL5 can bind to CCR1, CCR3, CCR5, D6 and DARC (see table 1.1). There are many probable reasons for these phenomena. First, this provides a level of robustness to the chemokine system. Thus, natural polymorphisms in an outbred population which affect the chemokine system can be compensated for by the redundancy of the system. Because multiple chemokines can, for example, attract macrophages through CCR5, the loss of production of one of these chemokines will not necessarily have functional consequences (reviewed in Mantovani, 1999). Second, the redundancy of the chemokine system may help prevent pathogen subversion of the system. As shall be discussed in more detail later, as a strategy to manipulate host immune responses and favour their survival, many viruses produce chemokine binding proteins, chemokine decoy receptors, and receptor antagonists (reviewed in Liston and McColl, 2003). By having multiple chemokines capable of producing the same or similar functional outcomes, our immune systems are often relatively resistant to these forms of microbial subversion. Third, different chemokines are produced in response to different types of stimulus. Therefore, to ensure robust responses, a single chemokine receptor may need to be able to recognise several different chemokines which are differentially produced. Furthermore, different chemokines are produced in different anatomical locations. For example, CCL19 is expressed by stromal cells and DCs within secondary lymphoid organs, while the alternative CCR7 ligand, CCL21 is produced by LECs and HEVs. This may be important in allowing the step-wise navigation of cells expressing a single receptor to specific anatomical compartments. Moreover, although different chemokines may be able to bind to the same receptor, different signals and functional responses may be induced. Indeed, recent studies have shown this to be the case. For example the two CCR7 ligands, CCL19 and CCL21, differentially activate signaling pathways (Kohout et al., 2004) and the different CCR1 ligands also lead to different types of signals from this receptor (Tian et al.,

2004). In fact, gene knock-out (KO) studies have demonstrated that chemokines which bind to the same receptor are not always redundant. The loss of one ligand is not always replaced by another. Examples of this are the CCL2 and the CCL3 KO mice. Although both of these chemokines are ligands for receptors which bind several different chemokines, mice deficient in either CCL2 or CCL3 still exhibit significant functional defects (Chintalacheruvu et al., 2005; Cook, 1996; Huang et al., 2001).

## **1.3 Chemokine Receptors**

### **1.3.1 Structure of Chemokine Receptors**

Chemokines exert their biological functions at nanomolar (nM) concentrations through their interactions with cell surface-expressed chemokine receptors that belong to the large family of type-V GPCRs. Although chemokine receptors, unlike their ligands, lack a single structural signature, the general structure of these receptors is largely conserved. This structural homology is evident at the level of primary sequence with chemokine receptors displaying between 25 to 80% identity. It should be noted that other non-chemokine receptor GPCRs, such as the dopamine or  $\beta$ -adrenergic receptors, are also largely similar to chemokine receptors at this level. Characteristically, chemokine receptors are about 40kDa in size and between 340-370 amino acids in length. They feature seven hydrophobic T/M domains, an acidic extracellular amino terminus, an intracellular tail at the carboxy terminus, and three intracellular and extracellular loops. The second intracellular loop contains the motif DRYLAIVHA, or a variation of it, which is involved in G-protein coupling, and the third intracellular loop tends to be short and basic. Each of the extracellular loops contains a cysteine residue, between which form disulphide bridges

important for maintaining the 3 dimensional structures of these molecules (see figure 1.3.1) (reviewed in Horuk, 1994).

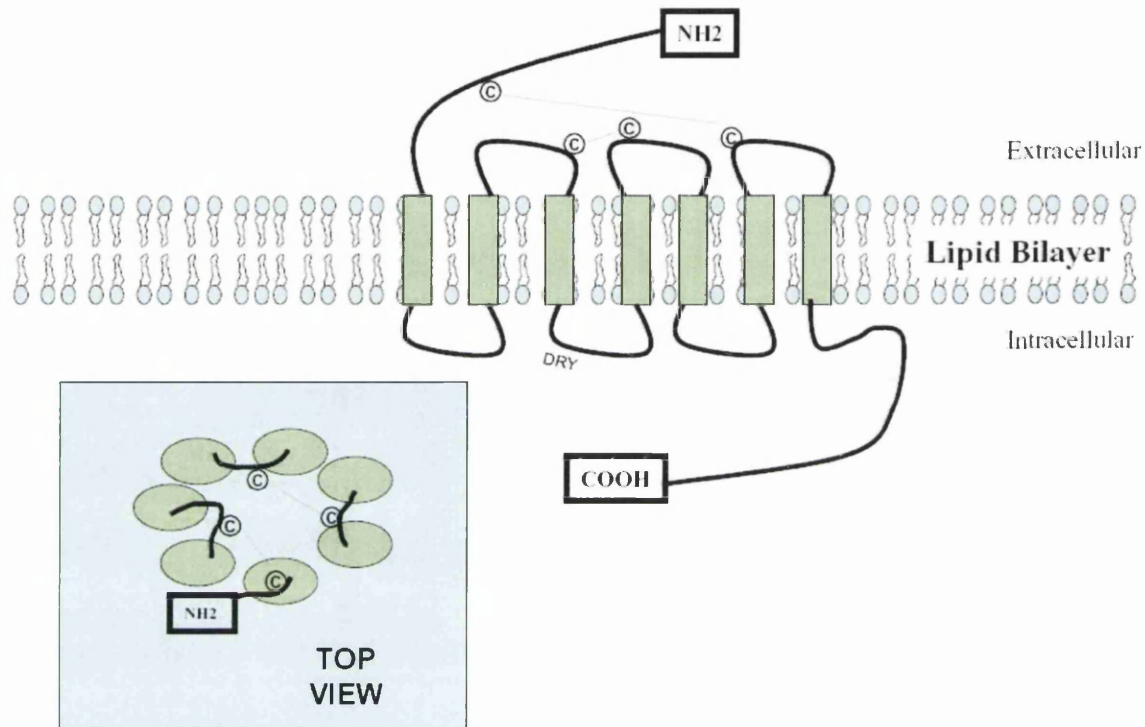


**Figure 1.3.1: General Structural Features of a Chemokine Receptor.** A schematic representation of a chemokine receptor in the plasma membrane, from two different perspectives. **TOP:** A chemokine receptor showing the seven T/M spanning domains (green rectangles), the extra- and intracellular loops and amino (NH<sub>2</sub>) and carboxy (COOH) termini are shown by solid black lines. Extracellular cysteine residues and the disulphide bonds between them shown by © and dotted lines, respectively. The conserved DRY motif on the second intracellular loop is shown. **INDENT:** A top view of a chemokine receptor looking down onto a cell. Green ellipses represent T/M domains.

### 1.3.2 Chemokine Receptor Expression

The expression of chemokine receptors, and hence the diversity of cells which respond to particular chemokines, is highly restricted and tightly regulated. Although it is now recognized that some chemokine receptors are expressed on a wide range of cell types, it is receptor expression on leukocytes which has been studied in greatest detail. Different leukocytic subsets display different chemokine receptor preferences. Importantly, the

expression of chemokine receptors is also modified in certain cell types upon activation or differentiation. This not only allows the immune system to differentially attract functionally distinct subsets of cells depending upon the type of receptors which are expressed, but also permits cells to modify their responses in concert with functional differentiation requiring relocalisation. A brief outline of the chemokine receptor expression profiles of the various leukocytic cell types and the functional significance of this follows.

Generally, innate effector cells express receptors allowing homing to sites of peripheral inflammation. Different types of innate effector cells express a different array of chemokine receptors allowing specificity of attraction depending on the type of response required. Neutrophils, for example, express CXCR1 and CXCR2 allowing their infiltration to sites of acute inflammation, where production of chemokines such as CXCL8 tends to be an early event. Eosinophils express CCR3 which favours their recruitment to sites of Th2 type immune responses, such as airway allergy or schistosome granulomas. Macrophages express CCR1 and CCR5 which favours their migration to Th1 effector sites (reviewed in Baggiolini, 1998).

DCs have two distinct functional phases in their life, designated immature and mature. Immature DCs express receptors such as CCR1 and CCR5 allowing their localisation in peripheral tissues where they can pick up Ag. Upon activation, these cells must present this Ag to lymphocytes within LNs and their chemokine receptor expression profile is altered accordingly. A loss of CCR1 and CCR5 is therefore accompanied by an acquisition of CCR7 expression, facilitating emigration of DCs to the LN via the afferent lymphatics (reviewed in Sallusto and Lanzavecchia, 2000).

Similarly, expression of chemokine receptors by lymphocytes is a dynamic process, changing as cells develop and differentiate. Naïve lymphocytes express chemokine

receptors such as CCR7 which enable their efficient trafficking to secondary lymphoid organs. Upon activation however, the chemokine receptor expression profile of lymphocytes is reprogrammed. T cells destined for follicles upregulate CXCR5, and activated Th1 or Th2 effector cells differentially express CXCR3 or CCR3 and CCR8, respectively. This allows the immune system to differentially attract functionally distinct subtypes of leukocytes depending upon the type of response required. In other scenarios, lymphocytes activated by DCs which picked up Ag the mucosa of the small intestine are programmed by these DCs to express CCR9, facilitating lymphocyte migration to the intestine. Conversely, lymphocytes activated by skin derived DCs are induced to express CCR4 and CCR10, enabling their migration to the skin. These alterations in chemokine receptor expression are normally in concert with changes in adhesion molecule expression, further assisting in the tissue specific migration of these cells (Moser and Loetscher, 2001; Sallusto et al., 2000).

The biological significance of CCR7 and CCR9 and their ligands will be discussed in greater depth in section 1.5. However, there first follows a discussion of the biochemical properties of chemokine receptors, a key introductory section to set the scene for *in vitro* studies performed in this thesis on CCX-CKR.

### **1.3.3 The Chemokine/Chemokine Receptor Interaction**

The molecular interactions between chemokines and chemokine receptors have been studied in detail and reveal many interesting aspects of chemokine biology. Although in concentrated solution, or in crystals, chemokines have a tendency to oligomerise (Baldwin et al., 1991; Clore et al., 1990), it is clear that chemokines interact with their receptors as monomers (Clark-Lewis et al., 1995). Structural studies of various chemokines have revealed the critical importance of the amino terminus for receptor binding and activation.

For example, the aforementioned amino terminal ELR motif found in a subset of CXC chemokines is essential for their activation of either CXCR1 or CXCR2 (Baggiolini et al., 1997). Discrete motifs have been identified which differentially affect receptor binding and activation. The extreme amino terminus of CXCL12 (residues 1 and 2) have been demonstrated to be critical for activation (but not binding) of CXCR4, while another motif, designated RFFESH, in the loop region of CXCL12 has been shown to be crucial for receptor binding but not activation (Crump et al., 1997). Collectively, structure-activation studies have revealed a two step model for a chemokine agonizing its cognate receptor. First, the receptor recognizes the binding site within the loop region of the chemokine (so called ‘docking’). This immobilizes the chemokine and allows its extreme amino terminus to interact with and activate the receptor, inducing a conformational change in the receptor (so called ‘triggering’) (Crump et al., 1997). This two step model of receptor activation is illustrated in figure 1.3.2. As shall be discussed in section 1.4.3, this has great relevance to the regulation of the chemokine system as some N-terminally modified chemokines retain receptor binding, but lose activation capabilities, creating effective receptor antagonists.

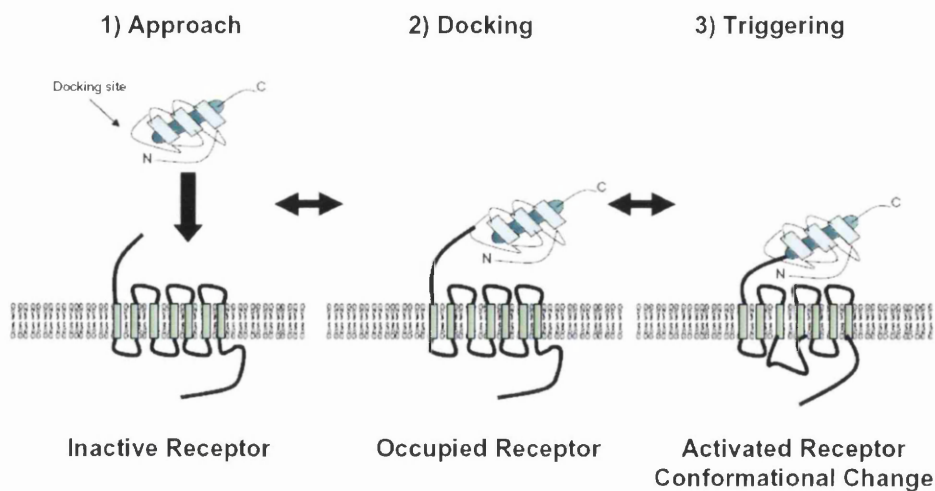


**Figure 1.3.2: Chemokine Receptor Ligation.** Chemokines interact with chemokine receptors with their docking site, shown in (1). Docked chemokines (2) bring their N-terminal triggering domain into close proximity with the extracellular helices of the receptor, leading to a conformational change and receptor activation (3).

### 1.3.4 Signal Transduction

The molecular events in the responding cell following chemokine/chemokine receptor ligation determine the downstream biological effects of this interaction. These responses can be highly diverse depending on the specific chemokine/chemokine receptor interaction, which cell type is responding to the chemokine, and the context of the signal. Directed leukocyte motion, the most commonly associated downstream effect of chemokine receptor signaling, involves many phenomena including cytoskeletal rearrangements, cell polarization and changes in integrin affinities. A great deal is known about various signaling pathways which are activated downstream of chemokine receptors, however it is less well understood how these signals result in effective polarized chemotactic responses. A full summary of these diverse pathways is beyond the scope of this thesis, however, I shall briefly summarise the most well-characterized signaling pathways downstream of chemokine receptors and outline the current thinking on how chemotaxis and integrin activation can take place.

Chemokine receptors are known to couple to several well-characterised intracellular signaling cascades upon agonist stimulation. All of the best understood of these signals originate from the exchange of GDP for GTP between the activated receptor and its associated G-proteins (see figure 1.3.3). Chemokine receptors are coupled to heterotrimeric G-proteins, and act as a GDP exchange factors (GEF) for these proteins upon receptor activation. This leads to dissociation of heterotrimeric complex, with the GTP bound  $G_{\alpha}$  subunit splitting from the  $G_{\beta\gamma}$  subunit, both of which go on to initiate the activation of a range of signaling cascades. This response is subsequently terminated by the hydrolysis of GTP on the  $G_{\alpha}$  subunit which, now in its GDP bound form, reassociates with the  $G_{\beta\gamma}$  subunit. The rate of this hydrolysis can be enhanced by regulators of G-protein signaling (RGS proteins) which provides both a means of negative feedback to this system and

provides a mechanism for cells to regulate responsiveness to chemokine induced signals (Agenes et al., 2005; Moratz et al., 2004; Moratz et al., 2000). The exotoxin of the bacteria *Bordetella pertussis*, pertussis toxin (PTX), inhibits the interaction of heterotrimeric G proteins with receptors by catalysing the ADP-ribosylation of the  $G\alpha$  subunits, keeping them in their GDP bound inactive state (Ladant and Ullmann, 1999). PTX effectively inhibits many responses driven through chemokine receptors (Bacon and Camp, 1990; Cyster and Goodnow, 1995; Qin et al., 2005).

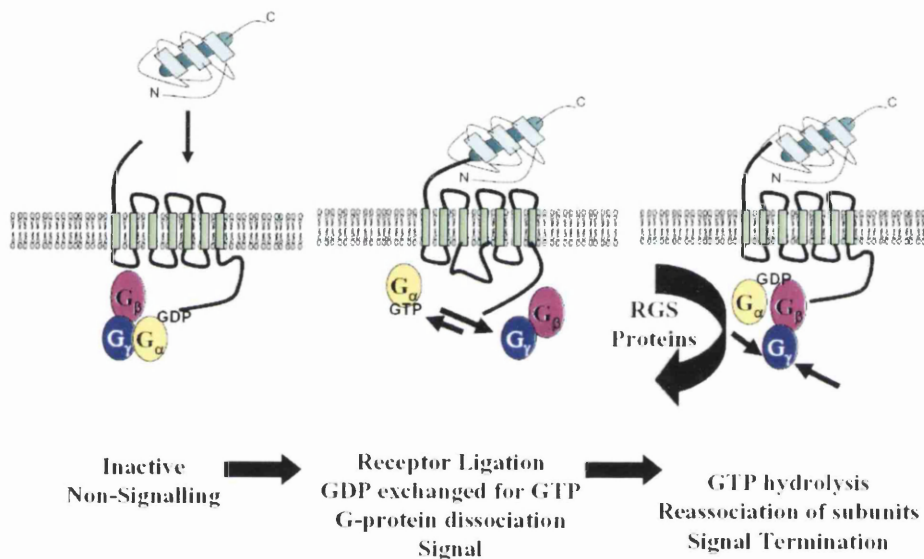


**Figure 1.3.3: G-Protein Activation.** Unoccupied receptors associate with the heterotrimeric G-protein complex in which the  $G\alpha$  subunit is bound to GDP. Receptor activation following ligand binding causes a conformational change in the receptor which allows the receptor to act as a guanine nucleotide exchange factor for the associated G-proteins. The now GTP bound  $G\alpha$  subunit dissociates from the  $G\beta\gamma$  subunits. Both of these subunits go on to activate downstream signaling cascades. Following GTP hydrolysis, G-protein subunits reassociate, terminating signaling. The rate of this hydrolysis can be enhanced by RGS proteins. (See text for more details).

Various cascades of downstream second messengers are activated by the G-protein subunits. The principal subunit required for chemotactic responses is the  $G\beta\gamma$  subunit. When released from the heterotrimeric complex,  $G\beta\gamma$  rapidly activates various downstream effectors. For example,  $G\beta\gamma$  activates the phosphoinositide specific phospholipase C (PLC) which catalyses the cleavage of phosphoinositide inositol diphosphate ( $PIP_2$ ) into

diacylglycerol (DAG) and inositol-1,4,5-triphosphate (IP<sub>3</sub>) (see figure 1.3.4). IP<sub>3</sub> binds to a specific receptor on the endoplasmic reticulum (ER) which subsequently causes mobilisation of intracellular calcium stores causing a transient rise in calcium ion (Ca<sup>2+</sup>) concentration within the cell. DAG, along with the released Ca<sup>2+</sup>, activates various isoforms of protein kinase C (PKC), a family of serine/threonine kinases. Activation of PKC is a common event downstream from various membrane receptor induced signals and is not unique to chemokine receptors. As shall be discussed in more detail later, signals activated downstream of PKC are important for receptor desensitisation and internalisation, and are required for responses mediated through chemokine receptors such as integrin activation, through activation of the GTPase RhoA. However, PKC signaling does not seem to be particularly important for gradient sensing and directed cell chemotaxis (chemokine receptor signalling is reviewed in Thelen, 2001).

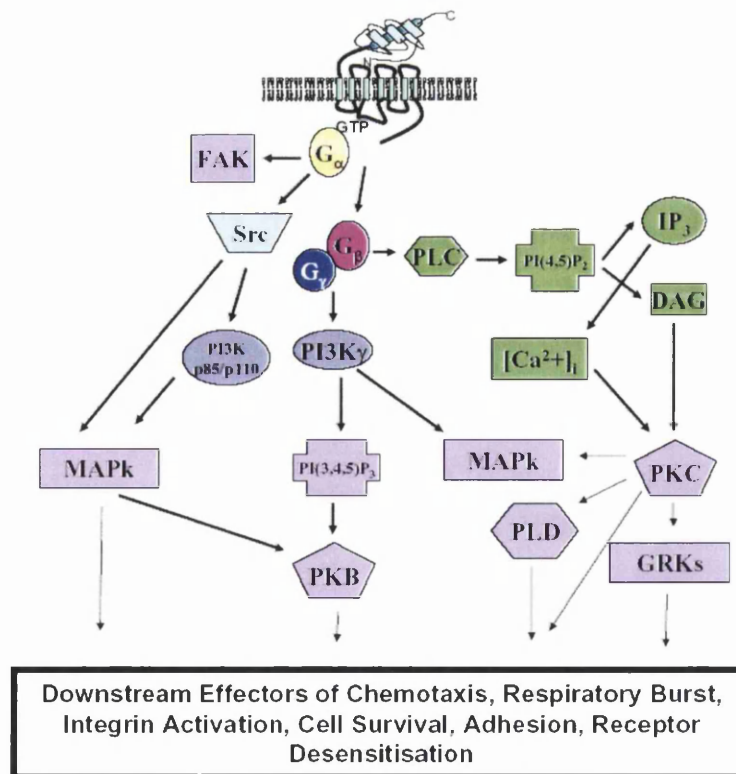


**Figure 1.3.4: Signaling Pathways Downstream of Chemokine Receptor Ligation.** Some of the major signaling players involved in various pathways activated by chemokine receptors and the effects of signaling are shown (see text for more details). Arrows indicate 'activated downstream'.

One of the major players in directing cell chemotaxis is phosphoinositide 3-kinase- $\gamma$  (PI3K $\gamma$ ). The importance of PI3K $\gamma$  activation in directing leukocyte chemotaxis has been demonstrated in numerous studies with cells lacking this enzyme (Del Prete et al., 2004; Reif et al., 2004; Sasaki et al., 2000). However, this seems to depend upon the cell type studied and the receptor being activated, with T cells in particular seemingly able to utilise PI3K $\gamma$  independent mechanisms (Cronshaw et al., 2004; Ward, 2004).

Like PLC, activation of PI3K $\gamma$  is also mediated by the G $\beta\gamma$  subunit following its release from the heterotrimeric complex. PI3K $\gamma$  rapidly phosphorylates the membrane lipid phosphatidylinositol leading to the formation of the second messenger phosphatidylinositol 3,4,5-triphosphate (PIP<sub>3</sub>). Interestingly, this occurs principally at the leading edge of the chemotaxing cell. PIP<sub>3</sub> provides high affinity docking sites in the cell membrane for proteins containing pleckstrin homology (PH) domains. One of the best characterised PH domain containing proteins, and one which is recruited to the membrane by PIP<sub>3</sub>, is the serine/threonine protein kinase B (PKB). Here, PKB is activated by another PH domain containing protein, PIP<sub>3</sub>-dependent protein kinase 1. Activated PKB then phosphorylates various downstream effectors of chemokine receptor signaling. Proteins which have been shown to be critical for chemotaxis are the Rho family of GTPases, such as RhoA, Rac, and cdc42, whose activity is regulated by guanine nucleotide exchange factors (GEFs) and GTPase activating proteins (GAPs), which are recruited to the leading edge of the cell via PH domains. Therefore, activation of PI3K $\gamma$  leads to rapid accumulation at the leading edge of the cell, activated factors critical for the actin polymerisation and cytoskeletal rearrangements required for chemotaxis. In addition, the PIP<sub>3</sub>-specific phosphatase, PTEN, is excluded from the leading edge and accumulates at the trailing edge, preventing PTEN from dephosphorylating PIP<sub>3</sub> which would inhibit the accumulation of positive regulators of chemotaxis at the leading edge (reviewed in Procko and McColl, 2005).

Activation of membrane lipids are not the only types of signals directly transduced through chemokine receptors. Protein kinase pathways are also directly activated, though in many instances the functional importance of these kinases in mediating chemokine responses remains unclear. The  $G_{\alpha}$  subunits, when released from the heterotrimeric complex, can activate Src family kinases leading to activation of proteins such as focal adhesion kinase (FAK), an important regulator of cytoskeletal adhesion to the extracellular matrix (ECM) (Le et al., 2005). Mitogen-activated protein kinase (MAPK) cascades are also activated in response to chemokine receptor signaling, although the direct role of G-protein subunits in their activation is not clear. In addition, other diverse signaling pathways may also be activated by chemokine ligation of receptor. For example, there are reports that chemokine receptors oligomerise following ligation and that this can lead to G-protein independent activation of janus-family tyrosine kinases and signal transducers and activators of transcription (JAKs and STATs) (Mueller and Strange, 2004; Soldevila et al., 2004; Vila-Coro et al., 1999; Zhang et al., 2001) However, this remains a controversial issue, with recent studies disputing the importance of this signaling pathway, at least for some receptors (Moriguchi et al., 2005).

Despite the many advances in understanding chemokine receptor signaling, the precise program of molecular events involved in transducing signals from chemokine receptors leading to chemotaxis are not yet fully understood. Moreover, it should be noted that the signaling requirements clearly vary depending upon the cell type studied, the activation state of that cell, and the chemokine receptor which has been ligated. Most detailed studies of the complex signaling required for chemotaxis have used the model organism *Dictyostelium amoebae*, or have studied neutrophils (reviewed in Parent, 2004). However, extension of these findings to other cell types such as lymphocytes has revealed that homologous mechanisms do not always apply.

Chemotaxis requires a complex series of molecular events occurring over minutes or hours as the cell finds its home. However, another important outcome of chemokine receptor signaling, crucial for leukocyte extravasation, is integrin activation that mediates chemokine induced firm adhesion. This needs to be extremely rapid, and gradient sensing is unlikely to be of importance. It is increasingly well-understood which pathways are used downstream of chemokine receptors to induce conformational changes in integrins (placing them in a high affinity state) and causing integrin clustering (figure 1.3.5). Ligation of CCR7 or CXCR4 causes LFA-1 integrin affinity changes independently of PI3K but dependent on the rapid activation of RhoA (Giagulli et al., 2004). Clustering of integrins is however dependent on PI3K (Constantin et al., 2000) and RhoA and PKC $\zeta$  (Giagulli et al., 2004). Supporting this model, a recent study showed that RhoA was required for integrin activation and firm adhesion to vascular cell adhesion molecule-1 (VCAM-1) using mouse thymocytes (Vielkind et al., 2005).

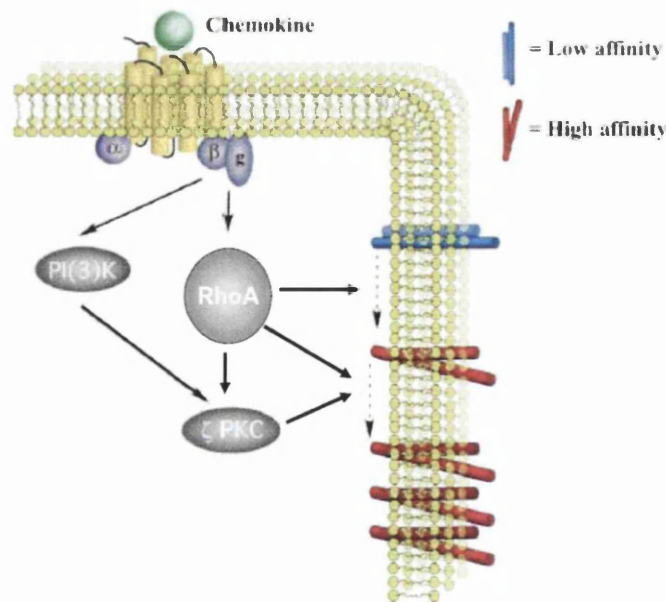


**Figure 1.3.5: Signal Transduction Leading to Rapid Integrin Activation.** Induction of LFA-1 high-affinity state by chemokines is controlled by the signaling activity of RhoA. Induction of LFA-1 lateral mobility is controlled by PKC and by further signals generated by RhoA. The capability of PKC to control LFA-1 lateral mobility depends on translocation to the plasma membrane, which is controlled by the RhoA, as well as by PKC kinase activity. PKC appears to be an effector of both PI3K and RhoA mediating LFA-1 lateral mobility induced by chemokines. (reproduced from Giagulli et al., 2004)

### **1.3.5 Desensitisation, Endocytosis, and Recycling of Chemokine Receptors**

Of particular relevance to this study are the molecular mechanisms which control chemokine receptor internalisation, intracellular trafficking, and recycling. Typically, GPCRs including chemokine receptors, following agonist ligation, transiently activate the various signaling pathways described above and are then subject to desensitisation and internalisation. Once internalised, the receptor can become resensitised and recycle back to the cell surface, or be targeted to lysosomes where it is degraded (Grady et al., 1997). This behaviour is of fundamental importance in determining GPCR signal magnitude and duration, and is an essential component of chemokine receptor function. Indeed, as discussed in section 1.4.5.2, the manner whereby D6 engages the endocytic machinery has proven instrumental in defining the function of this 'silent' receptor.

Signaling induced by chemokine receptor ligation leads to the activation of second messenger protein kinases (eg. PKB, PKC see above). These kinases, in addition to phosphorylating effector proteins enabling chemotaxis etc. also lead to the phosphorylation of serine and threonine residues on the C-terminus of chemokine receptors (figure 1.3.6). These events are insensitive to PTX and are therefore independent of  $G_{\alpha i}$ -protein mediated signals. Receptor phosphorylation leads to steric inhibition of G-protein coupling, leading to receptor desensitisation. In particular, protein kinases with specific activity for GPCRs, G-protein coupled receptor kinases (GRKs), are activated by the kinase activity of second messengers (such as PKC), and specifically phosphorylate residues in the C-terminus of agonist-occupied GPCRs. This receptor phosphorylation by GRKs provides a binding site for multifunctional intracellular adaptor and scaffold proteins called  $\beta$ -arrestins. There are various consequences for the receptor once arrestins have bound. First,  $\beta$ -arrestins provide further steric blockade to the interaction of the receptor with G-proteins, contributing to

desensitisation of subsequent signaling through the receptor. Thus,  $\beta$ -arrestins provide a negative feedback mechanism regulating GPCR activity. Second,  $\beta$ -arrestins act as adaptor proteins linking the receptor complex to the endocytic machinery via interactions with the polyhedral lattice-forming molecule clathrin (Goodman et al., 1996), and the  $\beta$ 2-adaptin subunit of the key clathrin adaptor protein AP-2 (Laporte et al., 1999). This generally leads to internalisation of the receptor complex via clathrin-coated pits (CCPs). Finally, recent work has shown that  $\beta$ -arrestins also act as a scaffold which actually transduce certain signals, such as MAPK activation (reviewed in Lefkowitz and Shenoy, 2005).

Endocytosis via CCPs is a complex process dependent upon interactions between an array of molecules. The extensive effort to understand this process has revealed novel genetic approaches to inhibit this pathway. Of particular relevance to this thesis are epidermal growth factor receptor substrate 15 (EPS15), and dynamin. EPS15 interacts via a C-terminal binding domain to AP-2, and has been shown to be important in linking AP-2 to the plasma membrane. Interactions between the EPS15 homology (EH) domains at the N-terminus of EPS15 and various other proteins critically involved in endocytosis, such as synaptojanin (Haffner et al., 1997) and epsin (Salcini et al., 1999), link AP-2 and hence clathrin to the endocytic machinery. Numerous studies have shown that inhibition of EPS15 function via use of dominant negative inhibitors effectively prevents endocytosis via CCPs (Belleudi et al., 2003; Benmerah et al., 1999; Benmerah et al., 1998). The large GTPase dynamin is also recruited to endocytosing clathrin-complexes, where it self assembles into ring-like supramolecular structures, stimulating its own GTPase activity and 'pinching' the invaginating pit of clathrin-coated plasma-membrane to form an intracellular vesicle. Dynamin is thought to be essential for all forms of receptor-mediated endocytosis (reviewed in Sever, 2002).

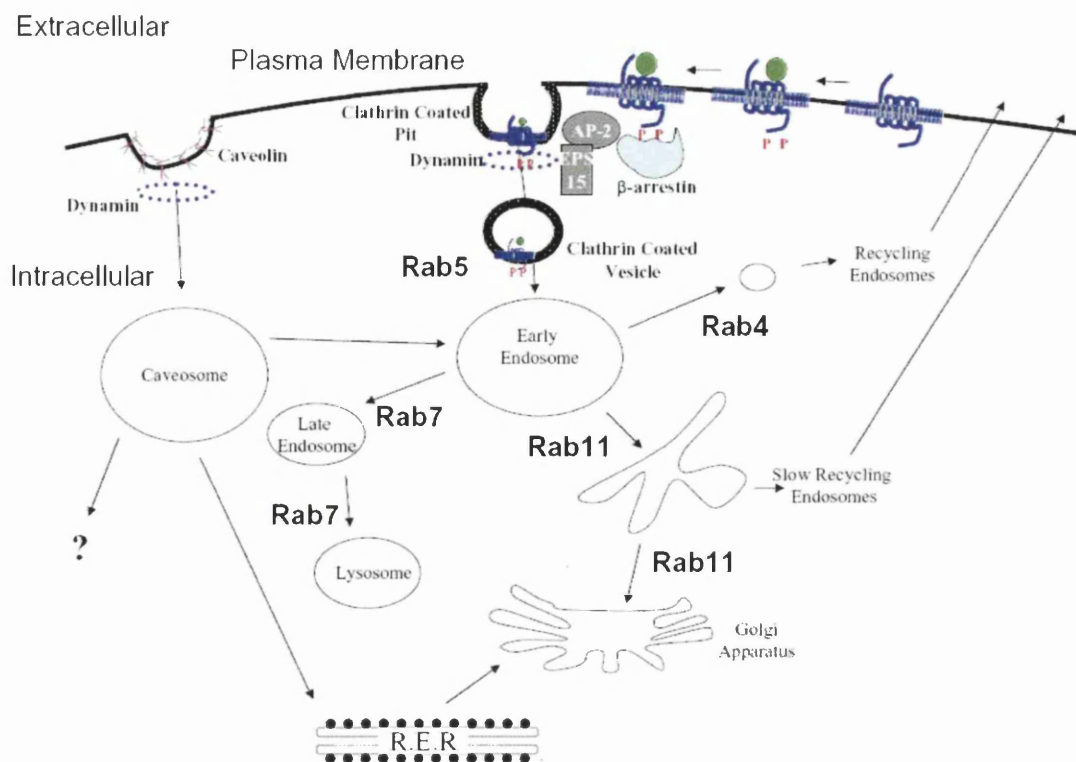


**Figure 1.3.6: Molecular Control of Endocytosis and Vesicular Traffic.** The two best understood pathways of endocytosis, CCPs and caveolae are shown. Selected molecules known to play crucial roles in these pathways are shown and the routes of intracellular trafficking and recycling are shown with arrows. GPCR internalisation following ligand binding is shown. For more details see the text.

Alternative means of endocytosis are utilised by some GPCRs. The best understood clathrin-independent endocytic compartment are caveolae, a subset of cholesterol-enriched lipid rafts which characteristically contain the dimeric cholesterol-binding membrane proteins, the caveolins. These structures are present in many cell types, but are particularly abundant in ECs, where they are proposed to play a role in transendothelial transport of various macro-molecules. Caveolins are 21-24kDa proteins which function to stabilise caveolae at the plasma membrane (Thomsen et al., 2002). However, signaling resulting in tyrosine phosphorylation of caveolins can result in endocytosis of caveolae into an endosomal compartment termed the caveosome (Pelkmans and Helenius, 2002). Similar to clathrin-mediated endocytosis, the activity of the GTPase dynamin is critically involved in

the 'pinching' of the invaginating caveosome from the plasma membrane (Henley et al., 1998). Certain GPCRs are known to localise to caveolae, where many diverse signaling molecules often cluster, and some have been shown to internalise via these structures, such as the  $\beta$ -adrenergic and A1 adenosine receptors (Escriche et al., 2003; Gines et al., 2001; Rapacciuolo et al., 2003). However, reports of chemokine receptors undergoing caveolar endocytosis are patchy. CCR5 has been shown to localise to lipid rafts and this is important for ligand binding and receptor activation. However, endocytosis of CCR5 has, like almost every other chemokine receptor studied, been shown to be dependent on CCPs (Signoret et al., 2005). The only chemokine receptor which so far, to my knowledge, has been shown to internalise via caveolae is CCR2 when stimulated with CCL2, at least in ECs from the blood-brain barrier and astrocytes (Andjelkovic et al., 2002; Dzenko et al., 2001; Ge and Pachter, 2004). However, the possibility, that in this context, CCR2 is mediating chemokine transcytosis must be considered. It also of interest to note, especially in the context of the potential role in protein transcytosis mediated by caveolae, that DARC has been detected in EC structures containing caveolin (more details on the potential role of DARC in chemokine transcytosis follow in section 1.4.5.1) (Chaudhuri et al., 1997).

Once internalised, clathrin-coated-vesicles (CCVs) fuse with vesicles of the early endosomal compartment. An important regulator of this is the small GTPase, Rab5, a member of a large family of RabGTPase Ras-like G-proteins. These proteins act as a molecular 'switch' cycling between an inactive GDP bound state and active GTP bound state. This is regulated by guanine nucleotide exchange factors (GEFs) and GTPase activating proteins (GAPs). The different isoforms of the RabGTPases localise to the membranes of different intracellular compartments and organelles (reviewed in Tuvim et al., 2001). Here, Rab proteins, through their GTPase activity, regulate the transport, fusion, and budding of vesicles. Importantly, the function of Rab proteins in intracellular

trafficking has been determined by using dominant negative or constitutively active forms of a given Rab protein, which inhibit endogenous Rab functions or mimic Rab-GTP, respectively. These molecules have been employed to great effect in dissecting the trafficking tendencies of GPCRs (Seachrist and Ferguson, 2003). Rab5 is found the early endosomal compartment and regulates fusion of CCVs to this compartment and subsequent behaviour of these early endosomes. Agonist occupied GPCRs which are internalised and reach the early endosomes can have two fates. 1) The ligand dissociates from the receptor, the receptor is dephosphorylated and recycles back to the cell surface (resensitisation). 2) The receptor is targeted to lysosomes for degradation (long-term downregulation). RabGTPases also play an important role in regulating these processes. Some Rab5+ early endosomes fuse with Rab4+ endosomes, and recycle rapidly back to the cell surface. This route is employed by some GPCRs following their dephosphorylation (Seachrist et al., 2000). Alternatively, receptors can recycle back to the plasma membrane via the slower Rab11+ recycling endosomal compartment. The chemokine receptor CXCR2 has been shown to employ this route of recycling (Fan et al., 2003). Receptors which are targeted for degradation upon long term agonist stimulation traffic there via a Rab7+ compartment which fuses to the lysosomes.

The molecular mechanisms which control the fate of cargo internalised via caveolae are not yet well-characterised. However, simian virus 40 (SV40) and cholera toxin, both internalised via caveolae can enter the Rab5+ early endosomes, and are directed to the Golgi apparatus or ER, respectively (Pelkmans et al., 2004). Similarly, the autocrine motility factor receptor is also internalised via caveolae and traffics to the ER (Benlimame et al., 1998; Le et al., 2002). Trafficking of cargo endocytosed via caveolae is not yet well-understood and is an active area of current research.

## **1.4 Post-Translational Control of Chemokines** (parts of this section have previously been published in a modified form (Comerford and Nibbs, 2005)).

Chemokines and their receptors play critical roles in many aspects of a fully functional immune system. Much research has focussed upon chemokine production and receptor activation, but comparatively less attention has fallen upon the regulation of chemokines after they have been produced. Indeed, such processes may act to limit or modify the responsiveness of these systems or control the localisation or presentation of chemokines. It is now clear that post-translational control of the chemokine network is of fundamental importance in regulating immune cell function. Importantly, as will be discussed later, the properties of CCX-CKR, the focus of this thesis, have led to the hypothesis that this molecule plays a role in chemokine regulation. Thus, in this next section, I consider mechanisms that influence chemokine activity after synthesis and describe emerging evidence for the existence of a subset of chemokine receptors involved in chemokine sequestration and/or transport. Within this context, CCX-CKR is introduced.

### **1.4.1 Chemokine Storage and Release**

Excluding the nuclear-targeted form of murine CCL27 (Gortz et al., 2002), synthesized chemokines are transported into the cell's secretory apparatus. However, this does not necessarily lead to immediate chemokine release. In certain scenarios, chemokines can be directed to intracellular storage compartments, for rapid release on cell activation. For example, CCLs 3 and 5 are stored in the granules of HIV-specific CD8<sup>+</sup> T cells, alongside the cytolytic enzymes, granzyme and perforin. Upon antigenic stimulation these cells degranulate, lysing virus-infected cells, and releasing CCL3 and 5 which can help prevent free HIV from infecting neighboring cells (Wagner et al., 1998). Another recent study found that CD8<sup>+</sup> T cells release pre-stored CCL5 from a novel storage compartment upon T cell receptor engagement (Catalfamo et al., 2004). The consequences of this storage and

release may be diverse - leukocyte attraction, further T cell degranulation, or amplification of T cell activation – and by storing packages of chemokine, the response will be relatively instantaneous, bypassing the need for comparatively slow transcriptional changes.

T cells are not alone in storing chemokines. Many chemokines, are stored in platelet  $\alpha$ -granules and released on platelet activation, allowing rapid participation in thrombus formation and possibly angiostasis (through CXCL4), plus leukocyte attraction (by other chemokines CCL3, 5, 7, CXCL8) at sites of vascular injury. CCL5 and 11 are found in eosinophils and released after degranulation signals are received (Bandeira-Melo et al., 2002). In addition, at least *in vitro*, ECs can store many chemokines for rapid release, including CCL26 and CXCL8 in Weibel-Palade bodies, and CXCL1 and CCL2 in a histamine-responsive compartment (Oynebraten et al., 2004). In fact, it has been proposed that CXCL8 storage acts as an EC ‘memory’ of inflammatory stimulation based on the observation that this chemokine was stored during the first stimulation, allowing rapid release on the second stimulation (Utgaard et al., 1998; Wolff et al., 1998). The physiological significance of chemokine storage has yet to be examined *in vivo*, but it seems likely that the secretion of these stores provide for the rapid initiation of chemokine-driven responses without the delay required to initiate transcription.

In addition to storage, CXCL16 and CX3CL1, are produced attached to a mucin-like stalk and T/M domain. In this form, they act as adhesion molecules, sticking the chemokine-expressing cell to cells expressing the appropriate receptor. However, members of the ‘a disintegrin and metalloproteinase’ (ADAM) family of proteases can specifically cleave these molecules, releasing the chemokine domain (Gough et al., 2004; Hundhausen et al., 2003). This not only disrupts chemokine/receptor-mediated cell-cell adhesion, but also allows the attraction of distant cells expressing the appropriate receptor.

### 1.4.2 Chemokine Presentation

Once chemokines are secreted, their diffusion is limited by complex interactions with extracellular and cell surface constituents. High profile has been given to their binding to charged sulphated sugars of the glycosaminoglycan (GAGs) family. The *in vivo* significance of this interaction in chemokine biology has been a matter of much discussion. Undoubtedly, interactions with GAGs on ECs provides chemokine presentation to peripheral blood cells, preventing soluble chemokines from being washed away by blood flow, and allowing for the induction of firm leukocyte adhesion to the vessel wall. Interestingly, GAGs are differentially expressed on different types of ECs and different GAGs have varying binding affinities for different chemokines. It is possible that this may permit the selective display of certain chemokines, and hence for selective cellular influx into particular tissues. Interestingly, *in vivo* studies exploiting recombinant chemokine mutants suggests that oligomeric chemokine binding to GAGs is crucial for biological responses (Proudfoot et al., 2003). These mutants retained full *in vitro* activity, but their inability to oligomerise on GAGs was hypothesized to be responsible for their lack of *in vivo* activity. Beyond the blood vessels, in the interstitial space, it has long been suggested that GAG binding is required to maintain haptotactic chemokine gradients along which migrating cells traffic. It is indeed likely that chemokines are presented on GAGs to migrating cells, and that GAGs act to store, protect, or limit the distribution of chemokines. However, the existence of continuous chemokine gradients *in vivo* has, to my knowledge, received no experimental support and indeed presents significant conceptual problems concerning their establishment and maintenance in complex 3-dimensional tissues. Instead, perhaps, the idea of chemokine boundaries proposed by Pelletier and colleagues (Pelletier et al., 2000) seems more realistic, where responsive cells polarize once a chemokine/no

chemokine boundary is encountered on a suitable substratum, and this polarization and directed migration occurs in the absence of a continuous gradient.

GAGs also seem to influence the nature of the chemokine/receptor interaction. Soluble components of GAGs, such as heparin sulphate, bind chemokines and modulate their activity, although in many instances the data is inconsistent. For example, some reports present data that heparin-CXCL8 complexes do not have agonistic effects on either CXCR1 and CXCR2, and that heparin reduces the chemotactic activity of this chemokine on neutrophils (Kuschert et al., 1999). However, earlier work suggested that these complexes were in fact more active as neutrophil attractants (Webb et al., 1993). Nonetheless, the release of soluble GAGs may be a strategy to rapidly modulate local chemokine function whilst the ECM is degraded during inflammation. Such control may contribute to the resolution of the response, and encourage wound healing and tissue repair.

### **1.4.3 Proteolytic Control of Chemokines**

Including the ADAM-mediated release of membrane-bound chemokines described above, many mammalian proteases have specific regulatory effects on the bioactivity of chemokines. Some simply degrade chemokines, but others exert more subtle regulation either by modification of the chemokine itself, or through the restructuring of the ECM. The dipeptidyl peptidase CD26 and the large matrix metalloproteinase (MMP) family have come under most scrutiny and the ways these proteases control and fine tune local *in vivo* chemokine responses are discussed below and summarised in figure 1.4.1.

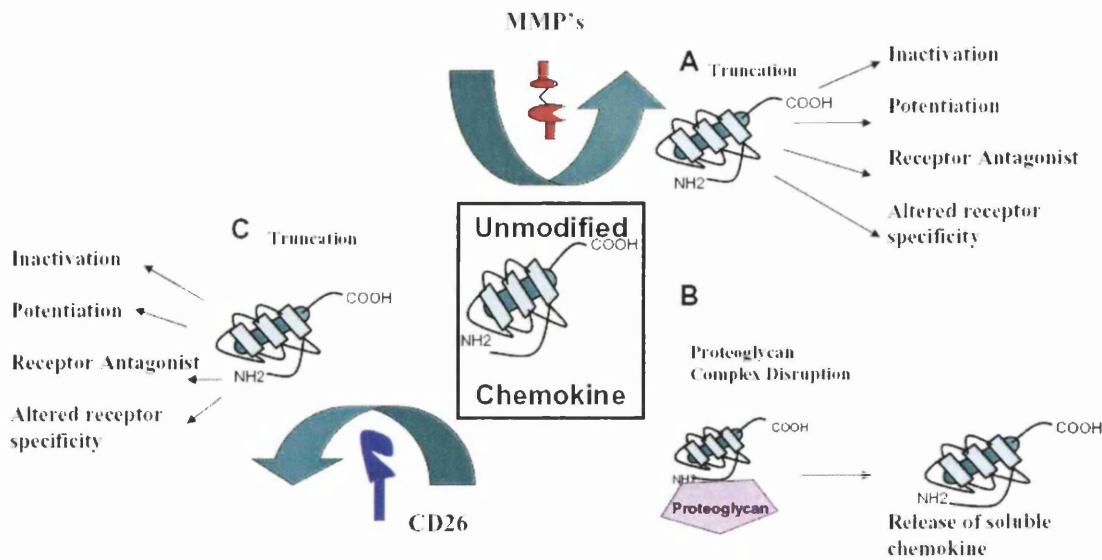


**Figure 1.4.1: Proteolytic Control of Chemokines:** Chemokine regulation by matrix metalloproteinases (MMPs) and the dipeptidyl peptidase CD26. (A+B) MMPs can cause the degradation, shedding or amino terminal clipping of select chemokines. (C) CD26 also clips the amino terminus of some chemokines. Clipping can result in inactivation or potentiation of chemokine bioactivity, alter receptor specificity, or generate antagonists. For further details, refer to the main text.

The MMPs are a family of zinc-dependent proteinases, expressed as either as membrane-anchored or secreted forms, which are critical in ECM degradation and remodelling. These proteases play an important role in the tissue degradation required for leukocyte infiltration during inflammation, and tumour cell escape during metastasis. The action of these proteases will release GAGs that, as discussed above, can alter chemokine interactions with its receptor. In addition, cleavage of ECM components may allow the release of deposits of chemokine. Compelling work from Li and colleagues (Li et al., 2002) has suggested that MMP-7 mediates the shedding of chemokines associated with the proteoglycan, syndecan-1, into alveolar fluid from the surface of damaged lung epithelial cells. Pro-inflammatory CXC chemokines associate with syndecan-1 after their production in response to injury, and also help attract neutrophils from the blood vessels. However, these neutrophils will only move into the alveolar space if MMP-7 releases syndecan/chemokine complexes. As

a consequence, MMP-7 *null* mice are protected from the neutrophil-mediated lung injury seen in wild type (WT) mice in response to bleomycin, with neutrophils accumulating in the interstitial space rather than traversing the epithelium. In a similar manner, mice lacking MMP-2 showed reduced bronchoalveolar lavage (BAL) chemotactic activity, including lower levels of CCL11, in a model of asthma. This was accompanied by reduced leukocyte egress across the epithelium with these cells appearing to be retained in the lung parenchyma, which in this model, lead to a significantly increased risk of asphyxiation (Corry et al., 2002). On the other hand, MMP-9 *null* mice have exaggerated allergic inflammation and higher BAL chemokine levels, suggesting this MMP may regulate chemokine destruction (McMillan et al., 2004). Indeed, MMP-9 does degrade several CXC chemokines *in vitro*, but it can also clip the amino terminus of CXCL8 and CXCL12 either potentiating or inactivating, respectively, their activity on their known receptors (McQuibban et al., 2001; Opdenakker et al., 2001). Interestingly, MMP-9 is released from neutrophils after CXCL8 stimulation, enhancing neutrophil infiltration by ECM degradation, and through the cleavage of CXCL8 to make it a more potent CXCR1 agonist. Thus, regulation of CXCL8 by MMP-9 may create an amplification loop promoting neutrophil chemotaxis and tissue invasion during inflammation.

It is now clear that many MMPs can regulate chemokine bioactivity by taking amino acids (typically the first four) off the critical receptor interaction/activation domain in the amino terminus. Truncated forms of CCL2, 7, 8, and 13 created by MMP cleavage *in vitro* lose their ability to activate their receptors, CCR2 or 3, but binding is retained (McQuibban et al., 2000; McQuibban et al., 2002). Thus, these molecules are transformed into effective antagonists, blocking migration mediated by the uncleaved chemokine, both *in vitro* and *in vivo*. A similar MMP-2-mediated four amino acid truncation of CXCL12 had been viewed as being inactivating, as interaction with its receptor CXCR4 is lost (McQuibban et al.,

2001). However, recent intriguing work has shown that truncated CXCL12, possibly generated during HIV-associated dementia, is able to bind to a currently unidentified G-protein coupled receptor on neurons, through which it mediates cell death (Zhang et al., 2003). Proteases again impinge on the biology of CXCL12 during haemopoietic stem cell (HSC) mobilization from the BM by granulocyte-colony stimulating factor (G-CSF) treatment (Petit et al., 2002). CXCL12/CXCR4 interactions play a crucial role in HSC homing and retention in the BM: G-CSF stimulates the release of elastase from neutrophils which degrades CXCL12, releasing HSCs into the blood. Contrary to these general views of chemokine inactivation by proteases, has come the recent demonstration that unusual 'long' chemokines CCL6, CCL9 and CCL15 and CCL23 are cleaved by proteases to generate extremely potent CCR1 agonists (Berahovich et al., 2005). Together, these observations suggest that the specific MMP milieu found in an inflamed site will have a profound impact on chemokine bioactivity and subsequent immune cell recruitment.

CD26 is a T/M serine protease which can clip two amino acids from the amino termini of proteins carrying a proline or alanine at the second position (Van Damme et al., 1999). This includes the chemokines CXCLs 6, 9-12, and CCLs 3L1, 4, 5, 11 and 22 (Guan et al., 2004; Lambeir et al., 2001; Proost et al., 1998), which can be trimmed to -2 variants *in vitro*, with a further two amino acids removed in some instances. Notably, -2 forms of several chemokines are detectable in biological samples. N-terminal truncation of chemokines by CD26 results in different functional alterations depending on the chemokine, and the receptor interaction studied. For example, CD26-processed CXCL12 is inactive on CXCR4, and its HIV entry inhibitory properties are abolished. Similarly, CD26-truncated forms of CXCLs 9-11, and CCLs 5, 11 and 22 all have reduced ability to attract target cells through their cognate receptors (Lambeir et al., 2001; Proost et al., 2001). In addition, whilst truncated CCL5 loses its ability to agonise CCR1 and CCR3, it retains

CCR5 binding, and hence its HIV-1 suppressive properties (Proost et al., 1998). CD26-truncated CCL3L1 bioactivity is also dramatically different from its intact form, losing the ability to signal through CCR3, but showing increased activity through CCR1 and 5. This converts CCL3L1 into a potent monocyte chemoattractant and HIV entry inhibitor, that lacks the ability to attract CCR3+ cells, such as Th2 lymphocytes, eosinophils and basophils (Proost et al., 2000). Removal of the first two amino acids from CCL4 has little impact on CCR5 binding, but now allows this chemokine to interact with CCR1 and 2 (Guan et al., 2002). Thus, by regulating chemokine function by subtly clipping the amino terminus, CD26 may be able to alter local recruitment of leukocytes.

The *in vivo* significance of CD26-mediated chemokine trimming has yet to be fully explored, and experimental analysis is likely to be confused by the other substrates and functions of CD26. Also, target chemokines show dramatic variation in their readiness to be clipped by CD26 (Lambeir et al., 2001), with CXCL12 and CCL22 being particularly sensitive. It is possible that these molecules are the principal chemokine targets for this protease. CD26 is expressed by a variety of cell types, and is present as a soluble form in normal plasma. It is also up-regulated by T cells upon activation (Fleischer, 1994), maintained on CXCR3+ Th1 cells (Ludwig et al., 2002), and is particularly abundant on anergic T cells (James et al., 2003). It is tempting to speculate that this gives T cells the option of modifying their local chemokine milieu to alter the composition and behaviour of their leukocytic neighbours. Alternatively, it may allow T cells to extinguish the signals that attracted them in the first place, and it is perhaps no coincidence that CXCL12 and CCL22, excellent CD26 substrates, are potent T cell attractants. This may be of particular significance for anergic T cells, where the clipping of T cell chemokines on EC surfaces or emanating from an APC could help suppress the attraction of non-anergic, Ag-specific cells, and thus prevent their activation (James et al., 2003).

### 1.4.4 Microbial Regulation of Chemokines

During millions of years of co-evolution with their hosts, microbes have developed numerous adaptations to combat the host immune response (reviewed in Alcami, 2003). Many viruses have developed ways of manipulating the chemokine system, presumably to promote their own survival. The existence of these strategies not only emphasises the importance of the chemokine system in host defense: but also highlights potential mechanisms of chemokine regulation that could exist in the mammalian host, or that could be exploited therapeutically. This is achieved by viral genes encoding soluble chemokine-binding proteins, chemokine receptor antagonists, or receptor homologues with chemokine sequestration activity.

Viral chemokine binding proteins (vCKBPs) fall into three groups. vCKBP1, from myxoma virus, interacts weakly with chemokines via their GAG binding domains, although homologous proteins from related viruses show no chemokine affinity. This may dislodge chemokines from their GAGs, disrupting presentation to leukocytes (Lalani et al., 1997). vCKBP2, encoded by myxoma and vaccinia viruses, interacts with most CC chemokines through their receptor-binding domain, blocking receptor interaction (Alcami et al., 1998). Similarly, herpesvirus vCKBP3 blocks host chemokine activity, but has even broader specificity binding members from all four chemokine subfamilies, and also disrupting chemokine-GAG binding like vCKBP1 (Parry et al., 2000). Viruses have also evolved soluble proteins to neutralize inflammatory cytokines, a regulatory mechanism mimicked in mammals with soluble versions of cytokine receptors created by protease cleavage or alternative splicing (Alcami, 2003). However, despite vCKBPs representing an effective mechanism for modulation and tuning of chemokine responses, mammalian homologues have not been described. This may be due to the fact that such molecules cannot be readily generated by cleavage or alternative splicing of heptahelical chemokine receptors.

Viruses can also encode chemokine homologues that are able to exhibit two significant properties. First, they can mimic the activity of host chemokines, attracting select leukocyte subsets through host chemokine receptors, most likely to create an environment conducive to viral survival at the site of infection. For example, human herpesvirus-8 (HHV-8) encodes vMIP1 and III which act as specific CCR8 and CCR4 attractants, respectively (Endres et al., 1999; Stine et al., 2000). These receptors are preferentially expressed on Th2 cells, and the attraction of these cells to sites of virus infection could feasibly create an environment low in anti-viral Th1 activity. Second, some viral chemokines can act as chemokine receptor antagonists. Most notably, vMIP2, again from HHV-8, interferes with chemokines from all four subfamilies by binding to their receptors without activating them (Kledal et al., 1997). In this case, there are parallels within mammalian chemokine biology, as an increasing number of chemokines have been shown to have antagonistic activity. This includes MMP-truncated forms described above, but unmodified chemokines also show antagonistic activity e.g. CCL18 and CXCLs 9-11 on CCR3, CCL26 on CCR2, and CCL11 on CXCR3 (Loetscher et al., 2001; Nibbs et al., 2000; Ogilvie et al., 2003; Ogilvie et al., 2004; Xanthou et al., 2003). It is notable that agonists for CCR3 antagonise CXCR3, and vice versa. CXCR3 is predominantly found on Th1 cells, whilst CCR3 is involved in homing in Th2 responses. In this way, there exists the possibility that inflammation can be regulated by the balance of positive and negative chemokines present at the inflamed site. Indeed, CXCL9 and 10 are produced at sites of lung inflammation during a typical eosinophilic Th2 allergic response: experimental neutralization of CXCL9 enhances eosinophilia, whilst i.v. administration of low doses of the same chemokine reduces this response (Fulkerson et al., 2004).

Viruses can also carry functional homologues of chemokine receptors able to bind host chemokines and fulfill a variety of functions, presumably to the advantage of the virus.

They can behave like typical host receptors allowing infected cells to migrate in response to endogenous host chemokines, perhaps enabling them to seek out new infectible cells (Billstrom et al., 1998). Alternatively, as these receptors can often exhibit constitutive, ligand-independent signaling, they have the potential to reprogram infected cells. The best example of this is the HHV-8 encoded receptor ORF-74 which promotes angiogenesis, oncogenesis, and cellular activation through constitutive signaling resulting in excessive activation of various signaling pathways (Bais et al., 1998; Bais et al., 2003). Finally, and of most relevance here, is the proposal that viral chemokine receptors may regulate the chemokine system by acting as decoy receptors. Even in the absence of ligands, the cytomegalovirus (CMV) encoded receptor, US28 undergoes constitutive internalisation from the cell surface and recycles through late endocytic vesicles and lysosomes (Bodaghi et al., 1998; Fraile-Ramos et al., 2001). Ligands that bind US28 are consequently internalised and destroyed, preventing them from activating endogenous host receptors. In addition, as US28 resembles a constitutively activated receptor, cross desensitisation of other GPCRs (including chemokine receptors) may also be an important aspect of its biology. The mechanisms behind these unusual behaviours of US28 could provide a useful paradigm for the function of the putative mammalian chemokine decoy receptors, discussed below. The intracellular C-terminus of US28 is constitutively phosphorylated (a modification that requires ligand binding in most chemokine receptors), and this enables internalisation and recycling of US28 without stimulation (Mokros et al., 2002; Waldhoer et al., 2003). Interestingly for a GPCR, endocytosis, while being clathrin-dependent, does not appear to require  $\beta$ -arrestins (Droese et al., 2004; Fraile-Ramos et al., 2003).

### **1.4.5 Chemokine Decoy and Transport Receptors**

Within cytokine biology, particularly in the interleukin-1 and tumour necrosis factor families, numerous mechanisms of interference have evolved to regulate responses

(reviewed in Mantovani et al., 2001). True decoy receptors are present, defined as cell surface ligand-binding proteins with high affinity and specificity, but which are unable to induce downstream signaling, or present ligand to a signaling receptor. Soluble receptor forms exist, as do specific receptor antagonists. Recently, receptor-like molecules, that deplete signaling molecules away from active receptors, have also been described (Brint et al., 2004; Mantovani et al., 2004). Together, these molecules serve not only to emphasise the importance of tight regulation of these systems, but also represent potential therapeutics in a wide variety of pathologies. As discussed above, the nature of host chemokine receptors, precludes the production of soluble extracellular forms by simple proteolytic cleavage or alternative splicing. However, the existence of three, apparently 'silent', chemokine receptors in mammals has led to proposals that they are specialized decoys scavenging extracellular chemokines, or alternatively, that they mediate transcellular chemokine transport. These proteins, DARC (Chaudhuri et al., 1993; Lee et al., 2003b), D6 (Nibbs et al., 2001; Nibbs et al., 1997) and CCX-CKR (Gosling et al., 2000; Townson and Nibbs, 2002) bind subsets of chemokines, but exhibit unusual properties compared to typical leukocytic chemokine receptors. Despite structural homology to other chemokine receptors, and showing high affinity interactions with chemokines, these molecules do not couple to the major signaling pathways activated by other chemokine receptors upon ligand stimulation (described in 1.3.4), and thus do not mediate cell migration. In fact, no alternative signals have been described from these receptors, leading to them often being referred to as 'silent'. Furthermore, they exhibit unusual expression patterns and, unlike typical chemokine receptors, are difficult to find on peripheral blood leukocytes. Moreover, recent exciting data have provided further support that these molecules neutralise or transport chemokines. These concepts are discussed below and summarised in figure 1.4.2.

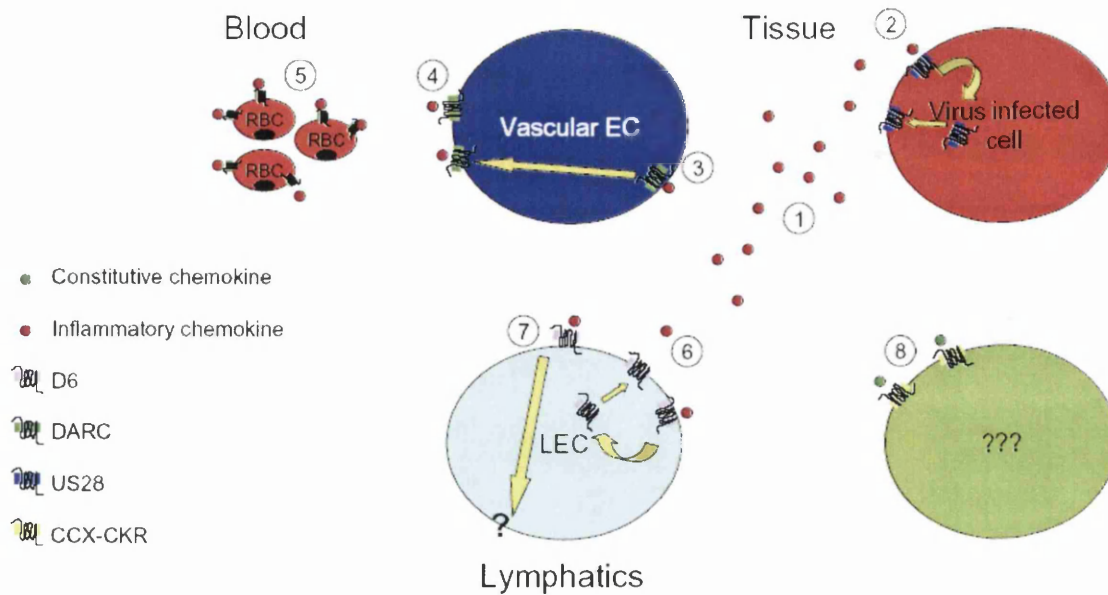


**Figure 1.4.2: Regulation of Chemokine Function by Chemokine Decoy and Transport Receptors.** Pro-inflammatory chemokines (1) (represented as red circles) may be sequestered by virus-infected cells (2) using receptors like CMV US28. On blood vessel ECs, DARC transports pro-inflammatory CC and CXC chemokines (3) from the interstitial space to the luminal surface for presentation on GAGs to blood leukocytes. DARC may also mediate chemokine degradation on ECs (4). On RBCs, DARC appears to buffer serum chemokine levels (5). D6, found on LECs, internalizes and destroys its CC chemokine ligands (6). A role for chemokine transport (7) by D6 is not yet clear. CCX-CKR, the third atypical mammalian chemokine receptor, may possibly act as a decoy receptor for its ‘constitutive’ CC ligands, CCLs 19, 21 and 25 (represented as green circles), from a currently unknown cellular home (8). See main body of the text for further details.

### 1.4.5.1 The Duffy Antigen Receptor for Chemokines (DARC)

The Duffy blood group Ag was first described in 1950. The same protein acts as an entry receptor on erythrocytes for some malarial parasites (Miller et al., 1975), and interestingly, its absence, caused by promoter mutation in Duffy negative individuals, provides erythrocyte resistance to malarial infection (Horuk et al., 1993). It later transpired that Duffy Ag is a receptor for various pro-inflammatory chemokines of both CC and CXC subclasses (Neote et al., 1993) (Table 1.1), leading to its renaming as DARC, Duffy antigen/Receptor for Chemokines. Along with erythrocytes, DARC is also expressed on vascular ECs, where it is up-regulated during inflammation (Lee et al., 2003a; Patterson et

al., 2002). It is particularly prominent at sites of leukocyte extravasation, including the HEVs of LNs and post-capillary venules (Girard et al., 1999; Hadley et al., 1994). Importantly, DARC lacks canonical intracellular signaling motifs (Chaudhuri et al., 1993), and does not support any detectable ligand-induced signaling or migration (Neote et al., 1994). Furthermore, as mentioned earlier, DARC is associated with caveolae vesicles in ECs, and these structures are commonly associated with transcellular transport of their cargo (Chaudhuri et al., 1997). These features have led to hypotheses that DARC is involved in the transcytosis, or neutralization, of chemokines at EC barriers (Lee et al., 2003b) and, on erythrocytes, that it may act to regulate plasma chemokine concentrations (Darbonne et al., 1991).

*In situ* binding assays have revealed that radiolabelled chemokines selectively bind to vein and venule ECs and that the specificity of this binding matched the ligand specificity for DARC (Hub and Rot, 1998). Indeed, unpublished studies using DARC *null* mice have shown that this EC chemokine binding is DARC dependent (see review by Nibbs et al., 2003). More refined immunoelectron microscopy studies in skin have demonstrated that chemokines can be internalized by ECs, transported across the cell, and presented on the tips of luminal microvilli, presumably associated with GAGs (Middleton et al., 1997). Although GAGs may play a significant permissive role in transcellular chemokine transport, DARC has been put forward as the key mediator. In keeping with this, recent *in vitro* data have shown that CXCL8 can be transported across EC monolayers in a DARC-dependent fashion (Lee et al., 2003b). Moreover, neutrophil recruitment to tissues, after intratracheal CXCL8 administration or bacterial lipopolysaccharide (LPS) injection, is diminished in DARC *null* mice (Lee et al., 2003b; Luo et al., 2000). However, a separate report suggested an anti-inflammatory role for DARC, observing increased neutrophil infiltration in response to higher doses of LPS in DARC *null* mice (Dawson et al., 2000).

One possible explanation for this apparent discrepancy is that at low doses of LPS, DARC-mediated chemokine transcytosis is required for optimal neutrophil homing, while increasing the amount of LPS induces more chemokine production, dampened through a decoy receptor function of DARC. Additional evidence for a decoy function of DARC has emerged from studies on mice engineered to over-express DARC in ECs. These mice show reduced angiogenic responses to certain CXC chemokines. In this instance, DARC may sequester these chemokines, preventing them agonizing EC CXCR2, thus blocking angiogenic signals from this receptor (Du et al., 2002). The combined data from these *in vivo* studies are an interesting start, but it is clear that further careful investigations are required to dissect the function of DARC on ECs.

What of the role of erythrocyte DARC? A serum chemokine sink, or decoy, function has been proposed, but it is now emerging that DARC may also function as a chemokine reservoir, maintaining plasma concentrations of certain chemokines. DARC negative humans display reduced plasma levels of CCL2 compared with DARC positive individuals (Jilma-Stohlawetz et al., 2001) and injected chemokines more rapidly disappear from the circulation in DARC *null* mice (Fukuma et al., 2003). Thus, erythrocyte DARC may act as a chemokine buffer, sequestering chemokines present at high levels in the serum, but maintaining a homeostatic level as their presence subsides. Because plasma chemokines desensitize circulating leukocytes, careful buffering by DARC may control leukocyte sensitivity to pro-inflammatory chemokines, limiting under- or over-responsiveness.

#### **1.4.5.2 D6: A Pro-inflammatory Chemokine Scavenger**

D6 binds to almost all pro-inflammatory CC chemokines (CCLs 2, 3L1, 4, 5, 7, 8, 11-14, and 22, and weakly to CCL17 (Bonecchi et al., 2004; Nibbs et al., 2001; Nibbs et al., 1997) but is unable to couple to the major signaling pathways typically activated by chemokine

receptors, or mediate chemotaxis. This may in part be due to D6 lacking a canonical DRYLAIV motif in the second intracellular loop, carrying DKYLEIV instead. Interestingly, when this sequence is introduced in place of DRYLAIV in CCR5, signaling is blocked, whilst mutation to DRYLAIV in D6 introduces weak signaling capability into D6 (Nibbs, unpublished). In humans, D6 is abundant on the LECs of the vessels draining the skin, the gut, and the lungs (Nibbs et al., 2001). It can also be found on tissue mast cells, macrophages, and DCs in some contexts. In addition, D6 is also expressed by trophoblasts at the foetal-maternal interface (Nibbs, unpublished). From these observations, it has been hypothesised that D6 is involved in the clearance of inflammatory chemokines from these sites, by acting as decoy receptor. Indeed, subsequent *in vitro* biochemical investigations revealed several key properties of D6 that appear to make it ideally suited for a role as a functional decoy receptor. First, D6 can rapidly internalise its ligands (Bonocchi et al., 2004; Fra et al., 2003; Weber et al., 2004). How does D6 achieve this in the absence of signaling? As detailed in section 1.3.5, chemokine receptors normally require ligand-induced signals to induce their endocytotic internalisation. However, D6 undergoes ligand-independent constitutive internalisation, rapidly cycling to and from the cell surface through the early and recycling endosomal compartments (Weber et al., 2004). One consequence of this is that the majority (>95%) of cellular D6 is found inside cells at any one time. Second, unlike CCR5, the affinity of D6 for its ligands is reduced at the low pH conditions found in endosomes, facilitating the dissociation of internalised chemokine from D6, and ensuring intracellular retention (Weber et al., 2004). These internalised chemokines are then degraded, whilst the receptor recycles. In this way, D6 ligands can hitch their way into cells for degradation, without requiring signalling and without desensitising the cell to subsequent exposure to D6 ligands. The molecular mechanisms controlling the behaviour of D6 in these systems have not yet been fully resolved. However, investigations have

shown that D6, similar to CMV US28, is constitutively phosphorylated, and that exposure to ligand does not increase the extent of phosphorylation (Blackburn et al., 2004). Thus, the possibility arises that constitutive phosphorylation facilitates ligand-independent endocytosis of D6 in a manner akin to US28. Notably, endocytosis of D6 appears to be via CCPs, since genetic inhibition of EPS15, clathrin, and dynamin all inhibit chemokine uptake via this receptor. The role of  $\beta$ -arrestins in D6 endocytosis remain unresolved however, with two independent studies coming to conflicting conclusions (Galliera et al., 2004; Weber et al., 2004).

Despite questions remaining over the precise mechanisms at work, the *in vitro* data strongly suggest that D6 has the biochemical hallmarks of a chemokine-sequestering decoy receptor. Importantly, this has recently received support from the analysis of D6 *null* mice. These animals display an exaggerated inflammatory response to the repeated application of a topical phorbol ester irritant, PMA (Jamieson et al., 2005). In this model of cutaneous inflammation, local production of TNF $\alpha$  induces production of inflammatory chemokines in the skin which drives leukocyte infiltration (see figure 1.4.3). In WT animals, inflammation resolves several days after the cessation of PMA painting. However, in D6 *null* mice inflammation is dramatically enhanced leading to a pathology which resembles human psoriasis. This phenotype was characterised by a hyper-proliferative epidermal compartment containing CD3+ T cells and enhanced dermal mast cell numbers. Blocking studies clearly demonstrated the importance of TNF $\alpha$ , and T cells in the development of the pathology. Moreover, inflammation was associated with higher levels of inflammatory D6 binding CC chemokines in skin of the D6 knock-outs. Therefore, it appears that in this model D6 acts as a decoy receptor, removing inflammatory CC chemokines from the skin, inhibiting further leukocyte infiltration and dampening the inflammatory response.

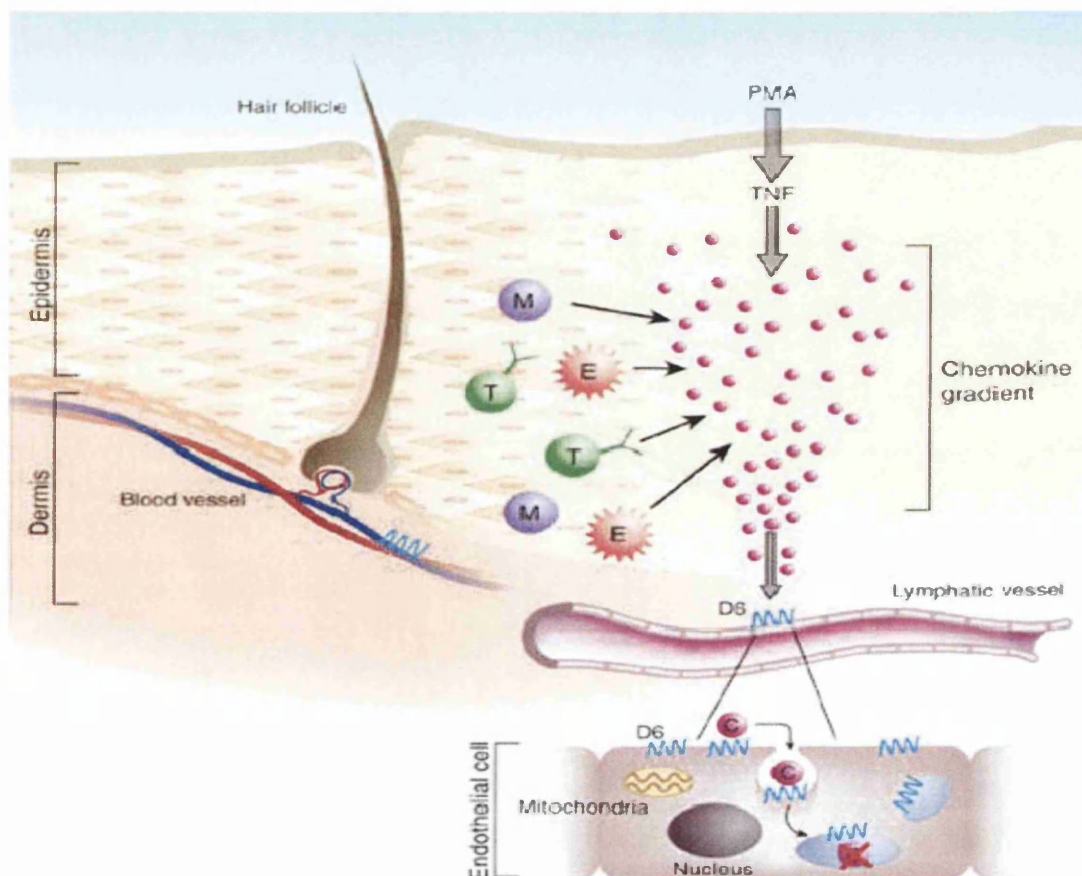


**Figure 1.4.3: D6 and Cutaneous Inflammation:** PMA initiates an acute and self-limiting inflammation in WT mice, the initiation of which is dependent on the generation of TNF. Later, genes encoding many CC chemokines, in addition to the CXC chemokine CXCL2 (which uniquely recognizes CXCR2), are induced and transcribed, forming a chemotactic gradient that attracts CD4 and CD8 T lymphocytes (T), polymononuclear neutrophils (E) and mast cells (M). In D6 *null* mice, the inflammatory response is intense and prolonged, as the chemokine half-life is extended. As a result, the pathological picture resembles human psoriasis. D6 is found in the lymphatic endothelium, where it acts as a 'conveyor belt' to 'mop up' and deliver the chemokines to degradative endosomes. (reproduced from Gerard, 2005).

This data is strengthened by a recent report demonstrating that D6 *null* mice, receiving a subcutaneous injection of complete Freund's adjuvant (CFA), develop a more severe cutaneous lesion than WT mice. Furthermore, this study also showed that, when compared to WT mice, the draining LNs of D6 *null* mice contained higher levels of inflammatory chemokines and had increased cellularity following CFA injection (de la Torre et al., 2005). This suggests that D6 restricts the transport of these chemokines from the tissue to the

draining LN. The broader role of D6 in the resolution of inflammatory disease is now an active area of investigation. Preliminary experiments indicate that D6 may be important in successful pregnancy (at least after cross-strain embryo transfer and presumably due to its placental expression) and also acts as a tumour suppressor gene (Nibbs, unpublished observations). The *in vivo* function of D6 in other tissues merits further investigation, and the potential therapeutic manipulation of this molecule remains an untested, but important, avenue of research.

#### **1.4.6 CCX-CKR, A Chemokine Receptor of Unknown Function**

Our emerging understanding of DARC and D6 clearly broadens the potential roles played by chemokine receptors. In 2000, a novel human chemokine receptor was identified by various groups of investigators. This was originally designated CCR11 based upon apparent induction of chemotaxis through this receptor by CCL2, CCL8 and CCL13 (Schweickart et al., 2000). However, this was later revised following the demonstration that the high affinity ligands for the receptor were, in fact, CCL19, CCL21, CCL25, and (more weakly) human CXCL13 (Gosling et al., 2000; Townson and Nibbs, 2002), chemokines that were already known to interact with one of the receptors CCR7, CCR9 or CXCR5 (Figure 1.4.4). Importantly, like D6 and DARC, mobilisation of intracellular  $Ca^{2+}$  and cellular chemotaxis are not detected following ligation of CCX-CKR with any of its ligands (Gosling et al., 2000; Townson and Nibbs, 2002). Structurally, CCX-CKR most closely resembles CCR7, CCR9 and CCR6. However, the canonical DRYLAIVHA motif in the second intracellular loop of CCX-CKR is changed to DRYVAVTKV (in humans) and DRYWAVTKA (in mice) (see Appendix 6.4) which may explain the lack of typical signaling through this receptor. However, this has yet to be addressed experimentally. In the absence of signaling, the use of CCR nomenclature was inappropriate and the name CCX-CKR has become accepted (Chemocentryx chemokine receptor) after the name of the company that first

described this molecule. More importantly, these properties place CCX-CKR firmly in a group of 'atypical' chemokine receptors, along with D6 and DARC. Perhaps it too plays a role in chemokine removal or transport.

Little else is known about this receptor. Receptor expression is detected in a wide range of tissues and cell types by RT-PCR (Dorf et al., 2000; Gosling et al., 2000; Townson and Nibbs, 2002), with strongest Northern blot signals from the heart, small intestine, and lung (Khoja et al., 2000; Schweickart et al., 2000; Townson and Nibbs, 2002). In humans, two copies of CCX-CKR exist. These encode proteins which differ by one amino acid and their expression is differentially regulated (Townson and Nibbs, 2002). However, in both humans and mice, the specific cell types expressing CCX-CKR remain unclear.

The presence of an additional receptor for these chemokines is intriguing bearing in mind their key importance in regulating leukocyte migration, lymphorganogenesis, secondary lymphoid tissue compartmentalisation, immune responses and tissue specific lymphocyte homing (all discussed in detail in the section 1.5). It is clear that our understanding of CCX-CKR is seriously limited and the function of this receptor is the main focus of this study. To begin to understand this molecule, we first need to understand what its ligands can do.

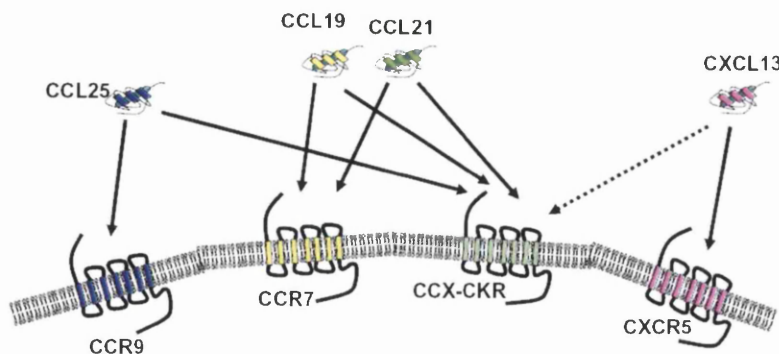


**Figure 1.4.4: CCX-CKR Ligands:** The chemokines which bind to CCX-CKR are shown alongside the other chemokine receptors which they also bind to. Binding in both humans and mice are shown by solid arrows, binding in humans only is shown by a dotted arrow. See text for more details.

## **1.5 Immunological Function of CCX-CKR Ligands**

A complete and detailed summary of the diverse biological functions of all aspects of the chemokine system in immunology is clearly beyond the scope of this introduction. Thus, instead, there follows a detailed discussion of key components of the chemokine network of direct relevance to CCX-CKR, the ligands for which are constitutive chemokines which play a major role in primary and secondary lymphoid microenvironments. These effects appear to be exclusively mediated through the receptors CCR7 (for CCL19/21), CCR9 (for CCL25), and CXCR5 (for CXCL13). Understanding the biology of these chemokines is clearly of paramount importance if we are to form hypotheses of CCX-CKR function. With this in mind, there follows a discussion of the function of these chemokines and their receptors in lymphoid organ development, leukocyte traffic, and the induction of immunity, focussing on primary and secondary lymphoid organs, and covering tissue-specific leukocyte homing. In addition, the role of CXCR4/CXCL12 and the lysophospholipid sphingosine 1-phosphate (S1P) and its receptor shall be discussed where appropriate, as these are also important factors in understanding the biology of these organs.

### **1.5.1 Chemokines and Primary Lymphoid Organs**

#### **1.5.1.1 The Bone Marrow**

In humans and mice, the BM is the site of haematopoiesis and B cell maturation (see section 1.1.1). CXCL12/CXCR4 appears to be the principal chemokine/receptor pair involved in this B cell development. BM stromal cells produce the chemokine CXCL12, which attracts B cell progenitors through their expression of CXCR4. Stromal cells produce growth factors and provide cell-cell contacts essential for B cell maturation. In fact, CXCL12 itself has been shown to be a growth factor for these cells (D'Apuzzo et al., 1997). The essential role of this chemokine/chemokine receptor pairing for B cell development is

demonstrated by the severe impairment of B cell lymphopoiesis in mice which lack either CXCL12 or CXCR4 (Ma et al., 1998; Nagasawa et al., 1996). These mice die perinatally with numerous developmental defects and display elevated numbers of B cell precursors in the blood and reduced BM numbers (Ma et al., 1999).

The role in BM of CCX-CKR ligands is not particularly well-established, and they are likely to play a peripheral role in this organ. A recent study reported that both CXCR5 and CCR7 are expressed during B cell ontogeny and it is known that the responsiveness to CXCL13 and CCL19/21 changes as maturation progresses (Bowman et al., 2000). Further evidence exists suggesting that CCX-CKR ligands may play additional roles in BM. Lymphocyte, NK cell, and macrophage precursors have been reported to express CCR7 and to be attracted by CCL21 *in vitro* (Kim et al., 1999; Kim et al., 1998). In addition, BM stromal cells have been shown to inducibly express CCL19 in response to inflammatory stimulus (Kim et al., 1998). Therefore, it has been suggested that CCR7 ligands play a role in increasing macrophage production in the BM during inflammation, although to my knowledge, this has not yet received experimental support. Regarding CCL25 in BM, knock-out mice lacking expression of CCR9 have been reported to have fewer BM pre-pro B cells (a population of cells responsive to CCL25). However, no differences in the resulting mature B cell populations are evident in these mice, making interpretation of this observation difficult (Wurbel et al., 2001).

### **1.5.1.2 The Thymus**

As mentioned in section 1.1.1, T cell precursors enter the thymus at the cortico-medullary junction as so-called double negative (DN) thymocytes, as they express neither CD4 nor CD8. These cells migrate outwards toward the subcapsular zone (SCZ) where they undergo proliferation and T-cell receptor (TCR) gene rearrangement. Later, once TCR

rearrangement has taken place, thymocytes mature into CD4+, CD8+ double positive (DP) cells, as they undergo positive selection in the thymic cortex. Following positive selection, DP thymocytes migrate inwards to the medulla where they are negatively selected. Thymocytes surviving negative selection leave the thymus as single positive (either CD4+ or CD8+) cells which form the mature T cell pool. Thus, T cell maturation occurs in a spatially-defined manner and chemokines are now known to provide crucial migratory cues controlling thymocyte entry, localisation, and exit from the thymus (Annunziato et al., 2001). Pivotal CXCR4/CXCL12 interactions have been shown to play an important role in the thymus. Initially, this receptor ligand pairing was thought to be of peripheral importance in the thymus as CXCR4 deficient mice were observed to be capable of supporting entry of thymic precursors into the fetal thymus, and thymi engrafted from CXCR4 deficient embryos into T cell deficient mice still support emigration of mature T cells. However, CXCL12 has been shown to play a role in maintaining a proliferative thymocyte pool (Hernandez-Lopez et al., 2002), and a role for CXCR4 in directing thymic emigration by chemotaxis has been proposed (Poznansky et al., 2002). Egress of departing thymocytes has also been shown to be critically dependent upon interactions between S1P and the sphingosine 1-phosphate receptor 1 (S1PR1) (Matloubian et al., 2004).

CCX-CKR ligands CCL19, CCL21 and CCL25 play significant roles in the thymus. These chemokines are expressed in the thymus and thymocyte precursors have been shown to express CCR7 and CCR9 (Campbell et al., 2003). Their importance has been demonstrated by using neutralising antibodies to these chemokines, or genetically-modified mice. This includes the *plt* (paucity of lymph node T cells) mouse strain, that lacks expression of CCL19 and a LN expressed isoform of CCL21 (CCL21<sub>ser</sub>), though the LEC-specific CCL21<sub>leu</sub> remains intact. Specifically, the migration of thymic precursors into the fetal thymus has been shown to be impaired in the *plt* mouse and neutralising antibody against

CCL25 further blocked this (Liu et al., 2005). Although analysis of CCR7 deficient mice did not initially reveal any abnormalities in the thymus (Forster et al., 1999), more recent investigations have revealed the essential role of this chemokine receptor and its ligands in several aspects of thymocyte homing (Figure 1.5.1). Thymocyte migration from the cortico-medullary junction to the subcapsular zone has been shown to be dependent upon CCR7 and its ligands (Misslitz et al., 2004) and migration of positively selected thymocytes towards the medulla is also impaired in these mice (Ueno et al., 2004). In addition, emigration of mature SP thymocytes from the thymus has also been proposed to be partially controlled by CCL19/CCR7 (Ueno et al., 2002). Quite how CCR7 can be involved in trafficking cells both inwardly and outwardly in the thymus remains to be resolved, although the possibility that the high CCR7 ligand density in the medulla initially exerts a chemorepulsive effect on DN thymocytes and then later chemoattracts positively selected DP cells is intriguing.

Analysis of CCR9 deficient mice revealed that this receptor is not essential for thymocyte development. However, a transient delay in the arrival of DP thymocytes to the thymi of these animals was observed (Wurbel et al., 2001). In addition, BM cells from CCR9 *null* mice were less efficient at reconstituting the thymus of irradiated recipient mice than BM from WT littermates. Furthermore the total number of  $\alpha\beta$ -T cells (which mature in thymus) were reduced in CCR9 knock-out mice (Uehara et al., 2002a). CCR9 expression is detectable on DP thymocytes but seems to be downregulated following positive selection (Uehara et al., 2002b). More recent work has demonstrated that CCR9/CCL25 interactions are essential for thymocyte migration from the cortex to the SCZ. However, surprisingly, this was not essential for T cell development (Benz et al., 2004). Overall, these data suggest that the CCR9/CCL25 axis plays a partially redundant role in directing thymocyte migration and development, which overlaps with CXCR4 and CCR7. To fully understand

the role of these chemokines and their receptors in the thymus, careful analysis of double deficient mice will be required.

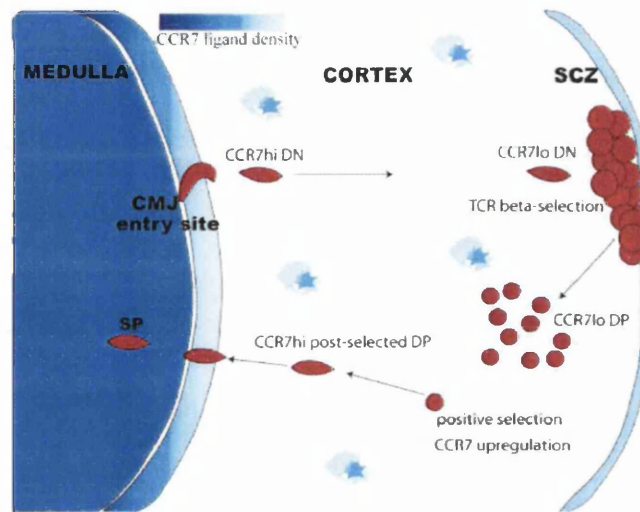


**Figure 1.5.1: The Role of CCR7 in Thymocyte Development.** Thymocyte migration and the role of CCR7 and its ligands in the adult thymus. The migratory paths taken by developing thymocytes and the proposed roles for CCR7 in these migrations is shown. The density of CCR7 ligands, CCL19 and CCL21, is represented by blue shading, with highest levels in the medullary region, and additional sites of expression in the SCZ and scattered cells throughout the cortex. (reproduced from Witt and Robey, 2004)

## 1.5.2 The Secondary Lymphoid Organs

As discussed in section 1.1.1, secondary lymphoid organs are structures specialized for the initiation of immune responses. Experiments with animals lacking these organs have demonstrated their essential role in adaptive immunity (Lakkis et al., 2000; Miyawaki et al., 1994; Rennert et al., 2001), and a great deal of evidence now demonstrates a key role for the chemokine system in almost all aspects of their biology. In particular, the chemokines CCL19, CCL21 and CXCL13 are of central importance, first for secondary lymphoid organogenesis during development, and also subsequently for cell homing to, and compartmentalisation within, these organs during homeostasis and responses. In addition, these chemokines play a role in the ectopic formation of secondary lymphoid like structures

seen in some chronically inflamed sites, such as the inflamed synovium in Rheumatoid arthritis (RA).

### **1.5.2.1 Chemokines and the Organogenesis of Secondary Lymphoid Organs**

The development of the secondary lymphoid organs is a highly complex process, involving the appropriate temporal and spatial expression of a variety of molecules. Generally, a common developmental pathway is followed by LNs and PPs but entirely different signals are required for the development of the spleen. Genetic studies have highlighted the role of chemokines in secondary lymphoid organogenesis, with various KO and mutant mice strains unable to support the correct development of different LNs and PPs. However, because overall splenic development is not impaired in these animals, the subsequent role of chemokines in compartmentalisation within secondary lymphoid organs can be studied in this organ (see section 1.5.2.4).

In LN and PP development, current paradigms highlight the importance of clustering of so called 'inducer' cells with stromal 'organiser' cells to initiate the development of these organs (figure 1.5.2). The inducers are haematopoietic cells which originate from the fetal liver and are phenotypically characterised as being IL-7 $\alpha$ R+, CD3-, CD4+, CD45+. They also express the chemokine receptors CXCR5 (Honda et al., 2001; Mebius et al., 1997) and CCR7 (Luther et al., 2003; Ohl et al., 2003) which play an important role in the attraction of these cells to the sites of lymphoid organogenesis, and subsequent inducer cell behaviour. The ligands for these receptors have been shown to be expressed by mesenchymal cells in proximity to the stromal organiser cells (Ohl et al., 2003), where they presumably mediate the recruitment of inducers. Once inducers and organisers come together, clustering is maintained by interactions between adhesion molecules, such as VCAM-1 on the stromal cells and the  $\beta$ 1 or  $\beta$ 7 integrins on the inducers. CXCR5 triggering activates the  $\beta$ -integrins,

encouraging tight adhesion between the cells. This allows members of the TNF superfamily, such as lymphotoxin- $\alpha\beta 2$  (LT $\alpha\beta 2$ ) on the inducers and LT $\beta$  receptor (LT $\beta$ R) on the stroma, to interact, activating various signaling pathways leading to gene transcription. In fact, there is evidence that CXCR5 activation directly upregulates further LT $\alpha\beta 2$  expression (Ansel et al., 2000). Prominent amongst newly transcribed proteins downstream of LT $\beta$ R signaling are various chemokines. Additional CXCL13 is produced by the stromal cells, creating a positive feedback loop attracting in more inducer cells (Ansel et al., 2000). CCL19 and CCL21 are also switched on and contribute to the recruitment of inducer cells through CCR7. CXCL12 is also induced and may contribute to inducer responses through CXCR4 activation. Thus, through the concerted action of cytokines and chemokines, the inducer/organiser clusters subsequently grow in size and complexity creating the secondary lymphoid anlagen. Notably, inducer cells cannot differentiate into lymphocytes but instead develop into FDCs, NK cells or APCs within the secondary lymphoid organ (Mebius et al., 1997). Once sufficient clustering has taken place, ECs differentiate into HEVs and the chemokine milieu in the structure effectively promotes the colonisation of the organ by attraction of lymphocytes from the circulation.

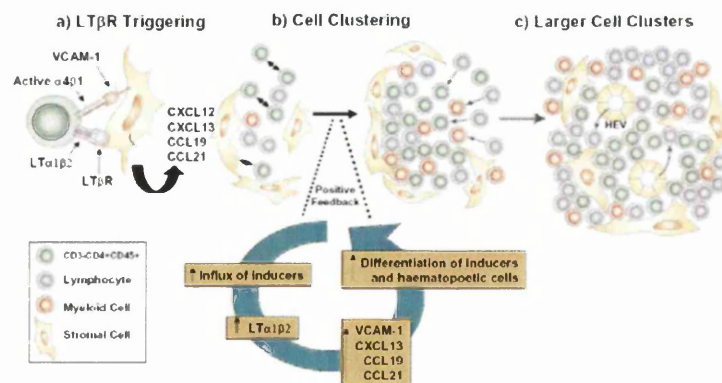


**Figure 1.5.2: Organogenesis of Secondary Lymphoid Organs.** a) LT $\alpha\beta 2$  expressing inducer cells bind to stromal organiser cells which express the LT $\beta$ R via interactions between adhesion molecules. Chemokines are produced as a result of LT $\beta$ R signaling. b) Chemokine production leads to further accumulation of inducer cells causing clustering and setting up a positive feedback loop leading to enhanced LT $\alpha\beta 2$  production and enhanced chemokine production. c) Large cell clusters form and blood vessels develop into HEVs. See text for more details.(reproduced from Mebius, 2003)

The relative importance of CXCR5, CCR7 and their respective ligands in secondary lymphoid development varies between different secondary lymphoid structures and has been revealed by gene KO experiments. For example, mesenteric LNs are still present in CXCR5<sup>-/-</sup> and CXCL13<sup>-/-</sup> mice despite these mice having severely reduced numbers of PPs and almost no development of other peripheral LNs (Ansel et al., 2000). In *plt* and CCR7<sup>-/-</sup> mice, LN and PP development still takes place (Forster et al., 1999; Nakano et al., 1997). However, anecdotal evidence suggested that there was occasional absence of some LN in these mice (Luther et al., 2003). Indeed, when CXCL13<sup>-/-</sup> mice were crossed with *plt* mice, they displayed a greater disruption to secondary lymphoid organ development than CXCL13<sup>-/-</sup> mice alone, although mesenteric nodes remained (Luther et al., 2003). The possibility that mesenteric LNs are able to develop in these mice under the control of the CCR7 ligand CCL21*leu*, the LEC-specific CCL21 isoform, not affected by the *plt* mutation, was ruled out by a subsequent study which observed a similar phenotype in mice double-deficient for CXCR5 and CCR7 (Luther et al., 2003; Ohl et al., 2003). Together, these experiments demonstrate an overlapping role for CCR7 and its ligands with the more important CXCR5/CXCL13 interaction for the development of PP and most LNs. Mesenteric LN development is an interesting anomaly and it is tempting to speculate that the CXCL12/CXCR4 axis represents the dominant chemokine requirement in this organ.

### 1.5.2.2 Ectopic Secondary Lymphoid Formation

During the course of certain types of chronic inflammation, such as the autoimmune diseases RA and Sjögrens syndrome (SS), a common feature in the diseased tissue is the formation of structures resembling secondary lymphoid organs (Hjelmstrom, 2001). These structures probably potentiate local self-antigen presentation, perpetuating autoimmunity. The chemokines CCL19, CCL21, and CXCL13 have been shown to play differing but important roles in the formation of these structures (Luther et al., 2002). Similarly to

organogenesis of secondary lymphoid organs during development, the induction of  $LT\alpha1\beta2$  signaling leads to chemokine production and infiltration of lymphocytes and DCs. The expression of CXCL13 drives the development of lymphoid follicles, while CCL21 and CCL19 define the T cell areas. Furthermore, production of these chemokines establishes a positive feedback loop which promotes further  $LT\alpha1\beta2$  production, which itself promotes further chemokine production. Thus, once initiated, this process promotes its self continuation until sufficient cell infiltration and organisation has occurred.

It has been shown using transgenic models that ectopic expression of CCL21 is sufficient to drive the formation of secondary lymphoid-like structures in the pancreas (Chen et al., 2002). However, tissue specific factors are clearly involved as these phenomena were not seen after transgenic expression of CCL21 in the skin (Chen et al., 2002). Furthermore, CCL21 expression has also been shown to be associated with lymphoid neogenesis in human chronic liver disease (Grant et al., 2002), and expression of CXCL13 and CCL21 is associated with lymphoid neogenesis in SS (Barone et al., 2005). The precise mechanisms by which initiation and regulation of these processes takes place have not yet been fully elucidated, and this remains an important area of research in the potential treatment of autoimmune diseases.

### **1.5.2.3 Lymphocyte Entry via High Endothelial Venules**

Once lymphoid tissues have developed, they recruit lymphocytes, a process that occurs continuously throughout life with an estimated  $2.5 \times 10^{10}$  lymphocytes passing through a LN each day. Naïve lymphocyte entry to LNs and PPs is dependent upon entry through HEVs found in the cortex of LNs and PPs and additionally in PP follicles. Lymphocytes roll along on HEVs of LNs via interactions between L-Selectin on lymphocytes and its ligand, peripheral node addressin (PNAd), on the endothelium. In PPs,  $\alpha4\beta7$  integrin expressing

lymphocytes roll on HEVs which express the mucosal addressin cell adhesion molecule 1 (MadCAM-1). In both PPs and LNs, these rolling lymphocytes express chemokine receptors, principally CCR7, CXCR5 and CXCR4. The ligands for these receptors are presented on the luminal surface of the HEV (see figure 1.5.3). The chemokine receptor signals induced by ligand activation cause integrin activation, firm adhesion and subsequent extravasation into the LN or PP (see sections 1.1.2 and 1.3.4). The relative importance of the different chemokine receptor ligands in mediating HEV extravasation into LNs and PPs is not yet clear, although it is well-characterized that different cell types have distinct chemokine entry requirements. T cells are mainly dependent upon CCR7 and its ligands for entry (Stein et al., 2000). The secondary lymphoid organs of *plt* mice show severe reductions in the number of T cells which enter the secondary lymphoid organs, demonstrating the crucial role of HEV presentation of CCR7 ligands for T cell entry (Nakano and Gunn, 2001). The importance of CCR7 in T cell entry across HEVs has also been demonstrated by analysis of CCR7<sup>-/-</sup> mice. These animals have markedly reduced number of T cells in LNs and PPs and elevated numbers in peripheral blood (Forster et al., 1999). It should also be added that CXCL12 and CXCR4 interactions may also be important for T cell entry across HEVs. However, although this receptor ligand pairing can induce integrin activation of T cells *in vitro* (Campbell et al., 1998), this is less pronounced *in vivo* (Weninger et al., 2003). However, other genetic factors may be involved, as there seems to be strain dependence on the importance of CXCL12/CXCR4, with C57Bl/6 mice able to support some T cell entry through this interaction, while mice on a DDD/1 background are less able to do so (Okada et al., 2002; Warnock et al., 2000).

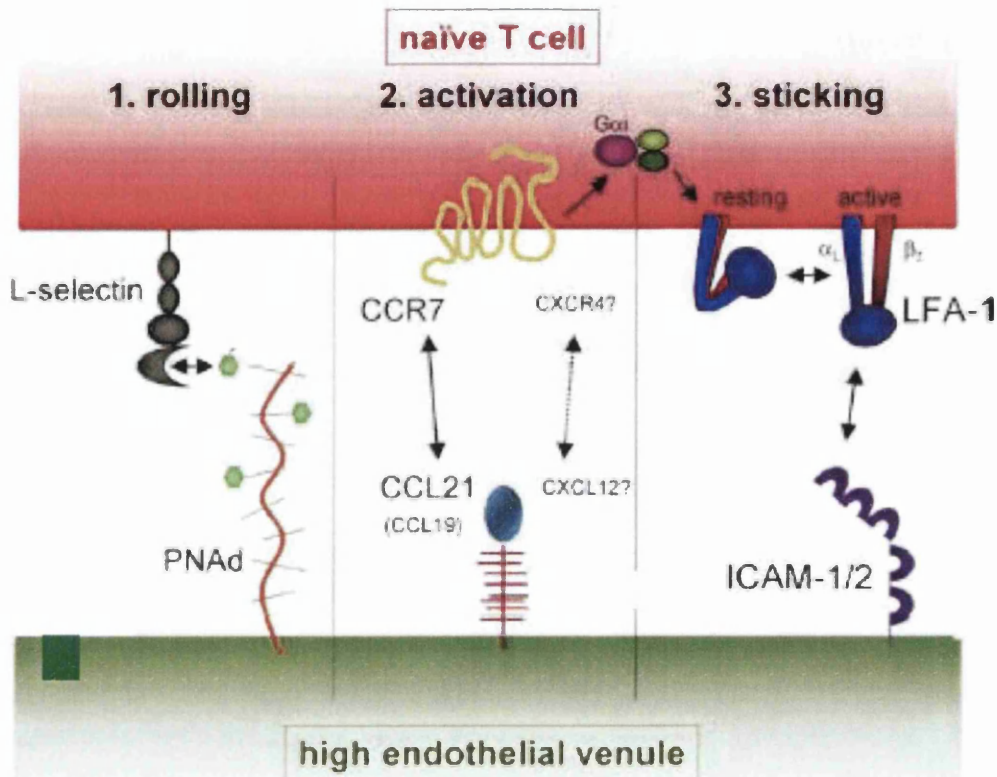


**Figure 1.5.3: The Multi-step Adhesion Cascade for Naïve T cell Entry into LN from the Blood.** T cell rolling on HEVs is mediated by binding of T cell-expressed L-selectin to PNAd displayed on HEV. In the second step, CCL21, and perhaps CCL19, which are presented on the HEV surface, bind to CCR7 on rolling T cells. CXCR4/CXCL12 interactions have also been proposed to play an accessory role. Chemokine binding to their respective receptors elicits intracellular G protein-linked signals, which induce a rapid conformational change in LFA-1 on T cells. LFA-1 in its active form then binds to endothelial ICAM-1 and/or ICAM-2, which mediates firm arrest of rolling T cells (reproduced from Weninger and von Andrian, 2003).

B cells also use CCR7 to gain entry across HEVs, although they are less reliant upon it than T cells. In *plt* mice, CXCR4/CXCL12 interactions are sufficient to support extravasation of B cells (Okada et al., 2002). In PPs, B cells can directly enter the follicular regions through HEVs which traverse them via interactions between CXCR5 on the B cell and CXCL13 presented on the HEV (Okada et al., 2002). However, the role of CXCL13/CXCR5 in B cell trafficking entry into LNs is a matter of debate. One study could not detect CXCL13 expression on HEVs of peripheral LNs, and saw no reduction in B cell entry to these nodes in CXCR5<sup>-/-</sup> mice (Okada et al., 2002). However, a separate investigation detected CXCL13 on approximately 50% of peripheral LN HEVs, and measured a quantifiable

reduction in B cell accumulation in peripheral LNs in CXCR13<sup>-/-</sup> compared with WT animals (Ebisuno et al., 2003). The reasons for these discrepancies are not clear and require future resolution. The fact that HEVs in peripheral LNs generally do not enter the follicular regions, suggests that functional CXCR5 will still be required for B cell accumulation in these areas. Some desensitisation of CXCR5 is likely to occur if it is activated during HEV passage, which would perhaps limit the ability of B cells to enter the follicles. It seems more likely therefore, that in LNs at least, B cell entry is mainly dependent upon CXCR4 and CCR7.

#### **1.5.2.4 “Remote Control” and Chemokine Transcytosis**

To draw cells from blood into LNs requires the presentation of appropriate chemokines on HEV surfaces. In mice, mRNA encoding CCL21 and CXCL13 can be expressed by HEVs, while CCL19 mRNA is produced only in the T cell area in non-ECs. However, in humans CCL21 is not detectably produced by HEVs, and is instead expressed with CCL19 by cells in the T cell area, including perivascular cells (Carlsen et al., 2005). So how do chemokines produced on the wrong side of ECs induce the firm adhesion of blood lymphocytes? One attractive hypothesis is that chemokines are actively transported, or transcytosed, across ECs for presentation, a process discussed in section 1.4.5.1. Indeed, two studies have demonstrated that CCL19 and CCL21 can be transcytosed across HEVs and thereby influence lymphocyte recruitment (Baekkevold et al., 2001; Stein et al., 2000). In fact, CCL19 injected intradermally is able to drain to the LN, cross HEVs, and recruit lymphocytes. This intriguing observation suggests that peripheral tissues exert chemokine mediated “remote control” over LN cell recruitment. This is not limited to CCL19. CCL2 is able to drain from inflamed sites to HEV surfaces where it recruits monocytes into LNs (Palframan et al., 2001). As DARC is expressed on HEVs, it is tempting to speculate that it

facilitates the transport of chemokines across these cells, and that perhaps D6 aids transcytosis across LECs into lymphatics. These ideas await investigation.

### 1.5.2.5 Chemokines and Lymphocyte Compartmentalisation

Once naïve lymphocytes have entered secondary lymphoid organs, they segregate into distinct T cell and B cell areas. This is controlled to a large extent by chemokines and is largely similar in all secondary lymphoid organs. Differential expression of CXCR5 and CCR7 between naïve B and T cells generally dictates whether they locate to the follicles or to the T cell areas, respectively. Gene KO studies have revealed the relative importance of chemokines in the organization of the T and B cell areas in the spleen and mesenteric LNs (secondary lymphoid organs which develop in the absence of these chemokine/receptor pairs). Deficiency in CXCR5 results in a reduction in numbers of splenic white pulp B cells (Forster et al., 1996) (Figure 1.5.4). In contrast, CCR7<sup>-/-</sup> and *plt* mice show reduced T cell migration into the PALS (Forster et al., 1996; Forster et al., 1999; Gunn et al., 1999). Analysis of mice deficient in both CXCR5 and CCR7 further reveals the critical role of these receptors in the development and organization of splenic architecture. In these animals, both the T and B cell areas are sparsely populated and highly disorganised, follicles do not develop, and there is no discernible MZ (Figure 1.5.4). Similar phenotypes to those seen in CXCR5<sup>-/-</sup>, CCR7<sup>-/-</sup> and double CXCR5<sup>-/-</sup> CCR7<sup>-/-</sup> are observed in mice lacking the ligands of these chemokine receptors, confirming the importance of these chemokine/receptor pairings in splenic architecture. Importantly, these results suggest that the biological effects of CCL19, CCL21 and CXCL13 on LN development and lymphocyte homing and compartmentalisation are mediated exclusively through CCR7 and CXCR5. KO studies have not provided any indication of additional receptors to mediate the biological effects of these chemokines. This is important when the potential functions of CCX-CKR are considered.

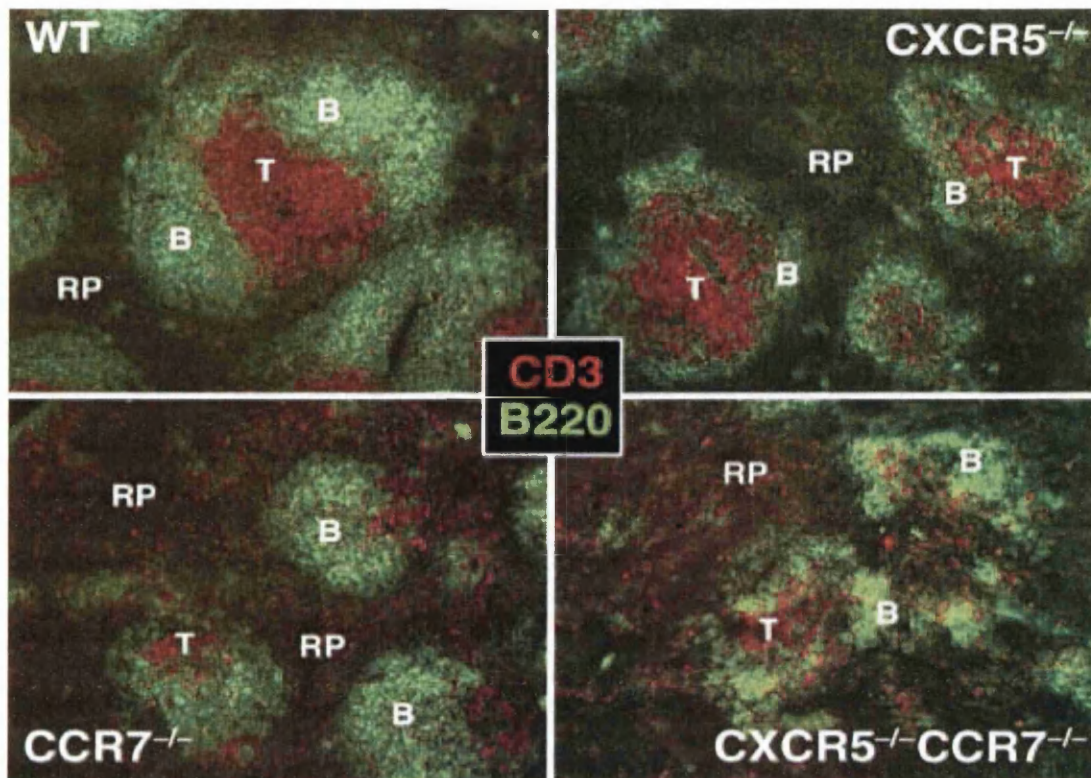


**Figure 1.5.4: The Splenic Architecture in  $CXCR5^{-/-}$ ,  $CCR7^{-/-}$  and  $CXCR5^{-/-}CCR7^{-/-}$  Mice.** Sections of spleen stained with green-labeled anti-B220 and red-labeled anti-CD3 to visualize the arrangement of B-cells and T-cells within the white pulp. In WT mice, the T-cell zone is situated around a central arteriole with B-cell-rich areas peripheral to these. T-cell areas of the  $CXCR5^{-/-}$  mice are encircled by a small ring of B cells. In  $CCR7^{-/-}$  mice, few T cells can be detected next to the central arteriole; however, B-cell-rich areas are still present. T cells are mainly excluded from the white pulp and can be found scattered throughout the red pulp. T-cell-rich and B-cell-rich areas are largely disintegrated in mice double deficient for  $CXCR5$  and  $CCR7$ . Small clusters of B cells are intermixed with the red pulp. T cells are randomly distributed throughout the red pulp (B, B-cell zone; RP, red pulp; T, T-cell zone). (reproduced from Muller et al., 2003).

Although direct experimental evidence is lacking, it is assumed that after  $CCR7$ -mediated extravasation  $CCR7$  also contributes to the navigation of T cells to the appropriate areas within LNs and PPs. However, for this to be the case,  $CCR7$  would have to not be subject to desensitisation following its activation at HEVs. Differences in the behaviour of  $CCR7$  in response to its two ligands  $CCL19$  and  $CCL21$  may help to explain this. Studies have demonstrated that  $CCL19$  and  $CCL21$  differentially stimulate  $CCR7$  (Bardi et al., 2001; Kohout et al., 2004).  $CCL21$  does not induce  $\beta$ -arrestin recruitment and subsequent

receptor desensitisation and internalisation, while CCL19 does. This has led to a two-step model of receptor activation and trafficking being proposed, whereby CCR7 regulates HEV extravasation through interactions with CCL21, but retains its activity allowing subsequent migration towards CCL19 in LN T cell areas.

In addition to follicular B cells, the spleen also contains a population of B cells which reside in the MZ (MZ B cells), an area also rich in macrophages (section 1.1.1). Localisation of B cells within the MZ depends upon the  $\alpha$ L $\beta$ 2 and  $\alpha$ 4 $\beta$ 1 integrins (Lu and Cyster, 2002), and S1P overcoming the follicular attraction of CXCL13 (Cinamon et al., 2004). In addition, it has been demonstrated that macrophage localisation in the splenic MZ depends upon CCL19 and CCL21 acting through CCR7 on these cells (Ato et al., 2004) and that macrophages also control the retention of B cells within the MZ via direct interactions via the macrophage scavenger receptor (Karlsson et al., 2003). Therefore, CCL19 and CCL21, perhaps indirectly, may contribute to B cell compartmentalisation within the spleen.

### 1.5.2.6 Lymphocyte Egress

As discussed above, many of the molecular mechanisms governing cell entry and localisation within secondary lymphoid organs are broadly understood. In contrast, the molecular requirements for cellular egress from these tissues, either during homeostasis or during immune responses, are only now becoming clear. In this regard, S1P and its receptor S1P1 have recently gained much prominence. As in cellular egress from the thymus, the exit of cells from LNs is dependent upon signaling by the receptor S1P1 (Matloubian et al., 2004). The immunosuppressant drug FTY720 mimics S1P and causes downregulation of S1P1 resulting in cellular retention in secondary lymphoid organs (Mandala et al., 2002). Chemokines are also likely to be involved to some extent in egress from secondary lymphoid organs. CXCL12 expression in the spleen and LNs is highest in the red pulp and

medullary cords respectively. Here it is likely that it is involved in attracting CXCR4 expressing cells, which have downregulated CXCR5 and CCR7, out of the follicles and T cell areas, encouraging their exodus (Ellyard et al., 2005; Hargreaves et al., 2001).

### **1.5.2.7 Dendritic Cell Trafficking and Antigen Presentation**

Most populations of DCs, similar to other non-lymphocyte leukocytes, do not normally express the appropriate chemokine receptors and adhesion molecules to allow direct entry into secondary lymphoid organs via blood HEVs. However, DC entry into LNs is a crucial aspect of their biology, as lymphocyte activation and hence immunity is largely dependent upon cognate interactions between professional APCs and lymphocytes. It is now clear that CCR7 and its ligands play crucial roles in steady state and inflammatory DC migration and function.

In the absence of infection or inflammatory stimulus, most DCs are tissue resident cells found in virtually all anatomical surfaces and compartments (reviewed in Banchereau and Steinman, 1998). Here, DCs have an 'immature' phenotype and they are very potent at Ag uptake and processing. DCs are dynamic cells even in the absence of inflammatory stimulus. DC precursors circulate through the bloodstream and express chemokine receptors and adhesion molecules which allow their extravasation into peripheral tissues, especially inflamed tissues (Randolph et al., 1998; Sozzani et al., 1995). This is facilitated, at least to some extent, by chemokine receptors such as CXCR1, CCR1, CCR2 and CCR5. Furthermore, there is a basal rate of DC traffic from tissues to the draining LNs. These semi-mature DCs, which have presumably sampled self-Ag in the periphery, have a slow rate of traffic to LNs where they present these Ags to T cells, a process postulated to be important in the maintenance of self-tolerance (Wilson et al., 2003). In the skin, using *CCR7 null* mice, this steady state traffic has recently been shown to be dependent upon

transient expression of CCR7 by Langerhans cells (LC), the specialised epidermal DC (Ohl et al., 2004). Steady-state trafficking of LCs into afferent lymphatics is not impaired in the *plt* mouse, indicating that expression of CCL21 $_{leu}$  by LECs, not abrogated in the *plt* mutant, is the likely ligand attracting LCs out of the dermis (Gunn et al., 1999). However, DC accumulation in the T cell areas of LNs of both CCR7 *null* and *plt* mice is severely reduced when compared with WT mice. These observations indicate that CCR7 and its ligands within the LN are required for the precise localisation of migrating DCs under steady state conditions (Forster et al., 1999; Gunn et al., 1999; Martín-Fontecha et al., 2003; Ohl et al., 2004). Thus, rather like the extravasation across HEVs (section 1.5.2.3) there appears to be a two-step process of DC homing to LN T cell areas, where the differential CCR7 internalisation properties of CCL21 and CCL19 may be significant to maintain responsiveness.

Although there is a relatively slow rate of DC migration from peripheral tissues to LNs during homeostasis, a dramatic change in DC behaviour and trafficking is evident following exposure to an inflammatory stimulus, eg. LPS, dsRNA, and pro-inflammatory cytokines, which induce a process referred to as DC maturation. The changes in DC phenotype are manifold, including reduction in Ag uptake, expression of MHC-II molecules, and upregulation of co-stimulatory molecules. Importantly, these changes are accompanied by alterations in DC migratory capacity that are critically dependent upon chemokine receptor switching. Chemokine receptors (e.g. CCR1 and CCR5) and adhesion molecules which promote retention in inflamed sites are downregulated, and this is concomitant with an upregulation of CCR7 and expression of adhesion molecules for entry to the secondary lymphoid organs. CCR7 $^{-/-}$  or *plt* mice, do not accumulate mature DCs in LN T cell areas in response to antigenic stimulus though it is notable that in *plt* mice, DCs accumulate in the

subcapsular sinuses suggesting LEC CCL21*leu* drives DCs into lymphatic vessels (Forster et al., 1999; Gunn et al., 1999; Ohl et al., 2004).

Interestingly, interactions between CCR7 and CCL19/21 are not only crucial for regulating DC traffic to and within secondary lymphoid organs, but also impact upon the maturation and morphology of DCs. CCL19 stimulation of mature DCs has been shown to induce the rapid formation of dendrites, extensions of the cytoskeleton which may greatly enhance the availability of contacts for T cell interaction during Ag presentation. CCL21 stimulation had an antagonistic effect on this phenomenon (Yanagawa and Onoe, 2002). This further suggests that CCL21 mainly controls DC migration into the secondary lymphoid organ (where a motile morphology would be advantageous) and that CCL19 production by DCs acts in an autocrine manner further activating the DC for Ag presentation. Furthermore, recent data suggests that both CCL19 and CCL21 act upon DCs to induce terminal maturation of these cells. Mature LN DCs which express high levels of CCR7 have been shown to produce pro-inflammatory cytokines and upregulate MHC-II molecules upon stimulation with either CCL19 or CCL21 (Marsland et al., 2005).

The arrival of mature activated DCs in the LN has further implications for the phenotype of the node. In order to facilitate Ag presentation between cognate APCs and T cells, cellular exodus from LN is inhibited, and cell entrance enhanced following the arrival of mature DCs. The extent of LN hypertrophy caused by these phenomena has been shown to be directly proportional to the number of DCs which reach the LN, and is (at least initially) independent of lymphocyte proliferation (Martín-Fontecha et al., 2003). Interestingly, the arriving DCs produce CCL19. After transcytosis across HEVs, this chemokine may contribute to enhanced lymphocyte recruitment into activated LNs. Alternatively, DC-derived CCL19 may encourage T cells to interact directly with arriving DCs to initiate key

events of Ag recognition. However, it must be emphasised that studies using the *plt* mouse have shown that this is not essential in facilitating these contacts (Mori et al., 2001). In the *plt* mouse, DC and T cells seem to co-localise in the subcapsular regions of LNs rather than in the T cell areas, but interactions still occur. Instead other chemokines may be important in initiating DC/T cell interactions. Indeed, there is some evidence that CCL22 may be involved in drawing recently activated T cells towards mature DCs (Tang and Cyster, 1999). However, CCL19 may be required for the priming of CD8<sup>+</sup> T cells within the LN. A recent study, using a truncated form of CCL19 which acts as a CCR7 receptor antagonist blocking CCL19, but not CCL21 interactions, led to inhibition of CD8<sup>+</sup> T cell responses in an allogeneic immune response without globally preventing cell migration to the LN (Pilkington et al., 2004).

### **1.5.2.8 Lymphocyte Activation**

The activation of naïve T cells within secondary lymphoid organs, via interactions with APCs expressing antigenic peptides on MHC molecules with appropriate co-stimulatory molecules, leads to T cell activation, proliferation and differentiation. Chemokines play major roles in influencing and executing these differentiation decisions. First, it is becoming increasingly evident that chemokines influence whether CD4<sup>+</sup> T cells develop with a Th1 or a Th2 cytokine secretion profile (reviewed in Luther and Cyster, 2001). Indeed, CCR7 ligands are now known to be involved, as recent evidence suggests that CCL19, acting on DCs, can induce IL-12 production and thereby indirectly promote CD4<sup>+</sup> T cell Th1 differentiation (Marsland et al., 2005). In addition, CCL21 has been shown to directly induce proliferation and Th1 polarisation of naïve T cells (Flanagan et al., 2004).

Second, once primed, chemokines direct the subsequent behaviour of T cells. Most CD4<sup>+</sup> T cells activated by DCs in the T cell area, transiently increase responsiveness to CXCL13

(perhaps through upregulation of CXCR5), and migrate to the edge of the follicles where they interact with B cells (Ansel et al., 1999; Garside et al., 1998; Schaerli et al., 2001). Likewise, Ag-activated B cells upregulate CCR7 (while keeping expression of CXCR5) and migrate to the edge of the follicles at the boundary of the T cell area (Reif et al., 2002). Cognate interactions between T and B cells lead to the formation of GCs, areas of rapid proliferation where somatic hypermutation and high affinity antibody maturation take place (reviewed in Berek and Ziegner, 1993). GCs can be histologically divided into dark and light zones. Dark zones are areas of intense proliferation and are the site of somatic mutation of B cell receptors, whereas the light zone is the area where selection of B cells, based upon the affinity of their receptors for Ag, takes place. The chemokine receptors CXCR4 and CXCR5 differentially direct B cells into the dark and light zones, respectively, and the ligands for these receptors are differentially expressed in these zones (Allen et al., 2004). B cells which survive this selection and express high affinity immunoglobulin can differentiate to become tissue homing plasma cells or memory B cells, cells with their own distinct homing properties determined by their chemokine receptor repertoire.

### **1.5.3 Tissue Specific Homing of Antigen Activated Cells**

Chemokines are critical mediators of lymphocyte homing to peripheral sites following activation. Activated proliferating T cells downregulate CXCR5 (Schaerli et al., 2001) and develop down one of two major developmental pathways. Most become effector T cells, and express chemokine receptors, such as CCR1, CCR2, CCR5, and CXCR3, which facilitate homing to sites of inflammation. Alternatively, some T cells become memory cells, primed for their next exposure to the same Ag.

Activated effector Th1 lymphocytes express receptors such as CXCR3 and CCR5, while Th2 lymphocytes express CCR3 and CCR8. This allows effective recruitment of different T

cell subsets based upon the chemokine ligands produced in different types of inflammatory situations. T cells which home to the skin express CCR10 and CCR4 which facilitate homing to epithelial sites which produce CCL27 and CCL17, respectively (reviewed in Kunkel and Butcher, 2002). IgA secreting plasma cells have been also been shown to use CCR10 for tissue specific homing. However, these cell migrate primarily towards CCL28 produced in mucosal tissues (Kunkel et al., 2003). An interesting role for CCR9 and CCL25 in the specific homing of cells to the small intestine has emerged in recent years. In addition to being expressed in thymus, CCL25 is highly expressed by epithelial cells of the small intestine, especially those most closely associated with vessels expressing the mucosal addressin cell adhesion molecule, MAdCAM-1 (Kunkel et al., 2000). Here, CCL25 is displayed on the endothelium (perhaps following transcytosis) and attracts CCR9+ cells (which also express the  $\alpha 4\beta 7$  integrin) out of the circulation, into the gut mucosa during both inflammation and homeostasis (Hosoe et al., 2004; Marsal et al., 2002). The importance of this is highlighted by the fact that the majority of T cells in the small intestine are CCR9+ (Kunkel et al., 2000). Interestingly, DCs which pick up Ag in the gut mucosa can specifically program the T cells which they prime in regional LN to migrate to the small intestine. This is achieved by the DC inducing the expression of CCR9 (and the  $\alpha 4\beta 7$  integrin) on the T cell (Johansson-Lindbom et al., 2003). CCR9/CCL25 is also involved in the homing of precursor cells to cryptopatches (sites of extrathymic T cell maturation) (Wurbel et al., 2001), and also in the homing of IgA secreting plasma cells to the small intestinal epithelium (Bowman et al., 2002).

CCR7 expression on mature T lymphocytes helps define a population of memory T cells based upon their migratory capacity. Long-lived Ag experienced T cells can be segregated into central memory or effector memory T cells (Sallusto et al., 1999). Central memory cells express CCR7 and L-selectin, enabling their recirculation through the secondary

lymphoid organs. Effector memory cells on the other hand do not express CCR7 and instead home to inflamed peripheral tissues via expression of receptors such as CXCR3. However, it has been suggested that upon activation, effector memory cells can regain CCR7 expression and subsequently traffic to secondary lymphoid organs (Ebert et al., 2005).

#### **1.5.4 Immune Responses in *Null* Mice**

It is clear from the above discussion that CXCR5 and CCR7 are of fundamental importance in controlling lymphocyte and DC localisation. Thus, it would be anticipated that the absence of these molecules would impact upon immune responses. Indeed, mice lacking expression of CCR7 display no contact or delayed-type hypersensitivity (DTH), processes dependent upon T cell activation. In addition, these animals have delayed development of antibody responses compared with WT animals (Forster et al., 1999). Furthermore, immune responses leading to the rejection of allografts is also partially impaired in these mice (Beckmann et al., 2004). CD8<sup>+</sup> T cell responses against viral infections still develop, but priming is less efficient and the response is delayed (Junt et al., 2004). These defects in CCR7 *null* mice are more severe than those seen in *plt* mice, where some CCL21 expression is maintained. *plt* mice exhibit delayed, but enhanced, T cell responses to subcutaneous Ag and are capable of contact sensitisation immune responses (Mori et al., 2001). This surprising result suggests that, although DC migration is impaired to some degree in these mice, lymphatic CCL21 still allows their migration to the LN. Furthermore DC-T cell interactions may not be regulated in the same way when they occur outside the T cell area, leading to the exaggerated response seen in these animals. Alternatively, this phenomenon could reflect a failure of CCR7<sup>+</sup> T<sub>REGS</sub> to become activated, which may be necessary for response resolution.

CXCR5 *null* mice are still capable of GC formation in the spleen, although these are severely disrupted (Voigt et al., 2000). Other studies have shown that although follicular migration is dependent upon CXCR5 and CXCL13, GC formation once it is initiated in the T cell zone is independent of CXCL13 (Ansel et al., 2000). However, it is perhaps surprising that major defects in the induction of immune responses have not been reported in mice lacking CXCR5 or CXCL13.

## 1.6 Aims of Study

The chemokine ligands for CCX-CKR are of central importance in controlling lymphocyte and DC localisation and thereby regulating immune responses. However, the functions of these chemokines appear to be mediated by CCR7 and CCR9, and from the outset of the project, it was completely unknown how CCX-CKR influenced or mediated the biology of these chemokines. In the absence of ligand-induced signals from CCX-CKR, chemokine decoy and transport functions had been proposed, but no evidence existed to support these hypotheses. Thus, to examine these ideas, a two-pronged approach was planned. First, investigations designed to characterise the biochemical properties in heterologous transfectants were undertaken. Initial focus lay on determining whether CCX-CKR could mediate ligand internalisation, and if so, to define the fate of the internalised ligand and the molecular mechanisms underpinning this internalisation. It was hoped that these experiments would provide the molecular basis for ideas about *in vivo* functions which could be tested. However, the *in vivo* characterisation of this ‘silent’ chemokine receptor was in its infancy at the outset of this study. Nothing was known of the cell types expressing CCX-CKR *in vivo*, reliable anti-mouse CCX-CKR antibodies were not available, and CCX-CKR *null* mice had not been described. Therefore, to simultaneously define expression profiles and assess indispensable *in vivo* function, ‘knock-in knock-out’ (KIKO) mice were planned, replacing the CCX-CKR gene with a readily detectable reporter surrogate. Combined, it was anticipated that these studies would provide new insight into the function of this unusual chemokine receptor, and expand understanding of chemokine networks *in vivo*.

## CHAPTER TWO

### MATERIALS AND METHODS

#### 2.1 Materials

##### 2.1.1 Antibodies and Secondary Detection Reagents

ANTIBODY/REAGENT	SPECIES	CONJUGATE	SUPPLIER
Anti-FLAG M1	mouse	n/a	Sigma
Anti-human CCR7	mouse	n/a	R+D Systems
Anti-KLH (isotype control)	rat	FITC	BD Pharmingen
Anti-mouse B220	rat	FITC	BD Pharmingen
Anti-mouse CD11c	hamster	PE	BD Pharmingen
Anti-mouse CD19	rat	PE	BD Pharmingen
Anti-mouse CD3	rat	PE	BD Pharmingen
Anti-mouse CD4	rat	PE	BD Pharmingen
Anti-mouse CD8 $\alpha$	rat	FITC	BD Pharmingen
Anti-mouse F4/80	rat	PE	Serotec
Anti-mouse I-A/I-E	rat	FITC	BD Pharmingen
Anti-mouse IgG	sheep	PE	Sigma
Anti-mouse IgG	goat	HRP	Amersham Biosciences
Anti-mouse IgG	goat	Peroxidase	Sigma
Anti-rat $\beta$ -arrestin I	mouse	n/a	BD Biosciences
Anti-rat dynamin I	mouse	n/a	BD Biosciences
Anti-TNP (isotype control)	hamster	PE	BD Pharmingen
ExtrAvidin	n/a	cy3	Sigma
Streptavidin	n/a	PE	Molecular Probes

##### 2.1.2 Bacteriology

Item/Reagent	Supplier
90mm bactriological petri dishes	Bibby Sterilin Ltd
Ampicillan	Sigma Chemicals
<i>Escherichia Coli</i> DH5 $\alpha$ competent cells	Invitrogen
Falcon 2059 polypropelene tubes	Becton Dickinson Labware
Kanamycin	Sigma Chemicals
LB (Luria Bertani) liquid Medium	Beatson Institute Central Services
SOC medium	Invitrogen

### 2.1.3 Cell Culture

#### Cell lines:

Human embryonic kidney cells (HEK-293)

Mouse embryonic fibroblasts (MEF)

129/1 W4 mouse embryonic stem cells

129/1 RW4 mouse embryonic stem cells

Item/Reagent	Supplier
10ml plastic pipettes	Becton Dickinson Labware
1ml plastic pipettes	Becton Dickinson Labware
2.5% Trypsin	Invitrogen
200mM L-Glutamine	Invitrogen
25ml plastic pipettes	Becton Dickinson Labware
2ml plastic pipettes	Becton Dickinson Labware
50ml plastic pipettes	Becton Dickinson Labware
5ml plastic pipettes	Becton Dickinson Labware
6 well tissue culture plates	Nunc
90mm tissue culture dishes	Becton Dickinson Labware
Cryotubes	Nunc
Dulbeccos Modified Eagle Medium (DMEM)	Invitrogen
Effectene Transfection Reagent	QIAGEN
Foetal Bovine Serum	Perbio
FuGene Transfection Reagent	Roche
Fungizone	Invitrogen
Geneticin (G418)	Invitrogen
Penicillin/Streptomycin	Invitrogen
Puromycin	AutoGen Bioclear
RPMI 1640	Invitrogen
Sterile 1xTE	Ambion
Sterile distilled water	Beatson Institute Central Services
Sterile phosphate buffered saline + EDTA (PE)	Beatson Institute Central Services
Sterile phosphate buffered saline (PBS)	Beatson Institute Central Services
Sterile plastic bijoux and universal containers	Bibby Sterilin Ltd
T25, T75, T175 cm <sup>2</sup> tissue culture flasks	Nunc
Fibronectin	Sigma
HEPES 1M Solution	Invitrogen
Concanavalin A	Worthington
96 well tissue culture plates	Corning

## 2.1.4 Chemicals

Chemical	Supplier
10M Ammonium Acetate Solution	Sigma
12-O-tetradecanoylphorbol-13-acetate	Sigma
Acetic Acid	Fisons Scientific Equipment
Acetone	Fisons Scientific Equipment
Agarose (electrophoresis grade)	Sigma
Bovine Serum Albumin	Sigma
Bromophenol Blue	Sigma
Butan-2-ol	Fisons Scientific Equipment
CellLytic-M Mammalian cell lysis buffer	Sigma
Choloroform	Fisons Scientific Equipment
Dimethyl sulfoxide	Fisons Scientific Equipment
Di-Nitro Fluro Benzene (DNFB)	Sigma
Dithiothretiol	Promega
EGTA	Fisons Scientific Equipment
Ethanol	James Burrough Ltd
Ethidium Bromide	Sigma
Ethylene diamine tetra acetate disodium salt	Fisons Scientific Equipment
Glycerol	Beatson Institute Central Services
Hydrochloric Acid	Fisons Scientific Equipment
Methanol	Fisons Scientific Equipment
Mouse Serum	Sigma
Ovalbumin (from chicken egg)	Sigma
Paraformaldehyde	Sigma
Phenol	Sigma
Propan-2-ol	Fisons Scientific Equipment
Propidium Iodide	Sigma
Sodium Acetate	Fisons Scientific Equipment
Sodium Azide	Sigma
Sodium Chloride	Fisons Scientific Equipment
Sodium Citrate	Fisons Scientific Equipment
Sodium dodecyl sulphate	Fisons Scientific Equipment
Sodium Hydroxide	BDH, UK
The RNA storage solution	Ambion
Tris-base	Fisons Scientific Equipment
TRIZOL Reagent	Invitrogen
Tween-20	Sigma
Urea	Sigma

### 2.1.5 Chemokines

Chemokine	Labelled with	Supplier
hCCL19	Biotin	Albachim
hCCL19	[ <sup>125</sup> I]	Amersham Biosciences
hCCL19	n/a	Peprotech
hCCL21	n/a	Peprotech
hCCL25	n/a	Peprotech

### 2.1.6 Enzymes and Kits

Reagent	Supplier
1.1x Pre-Aliquoted ReddyMix PCR Master Mix in Thermo-Tubes	ABgene
Alkaline Phosphatase	Kramel Biotech
BamH1	Roche
Chemiluminescent WestPico Kit	Pierce Chemical
CT-GFP-TOPO <sup>®</sup> TA Expression Kit	Invitrogen
DNAase free RNAaseA	QIAGEN
DNA-free <sup>™</sup> kit	Ambion
ECoR1	Roche
ECoRV	Invitrogen
HindIII	Invitrogen
Mouse IL-13 Antibody Beads for Luminex <sup>™</sup>	Biosource
NotI	Invitrogen
pCR2.1 TOPO <sup>®</sup> TA Cloning Kit	Invitrogen
Proteinase K	Roche
QIAprep Plasmid Maxi Kit	QIAGEN
QIAprep Spin Miniprep Kit	QIAGEN
QIAquick Gel Extraction Kit	QIAGEN
QIAquick PCR Purification Kit	QIAGEN
Rapid DNA Ligation Kit	Roche
Ready-To-Go <sup>™</sup> DNA Labelling Beads	Amersham Biosciences
Six Plex Mouse TH1/Th2 Antibody Bead Kit for Luminex <sup>™</sup>	Biosource
SstI	Invitrogen
Superscript <sup>™</sup> First-Strand Synthesis System for RT-PCR	Invitrogen
XbaI	Invitrogen

### 2.1.7 Miscellaneous

Reagent	Supplier
[ <sup>3</sup> H]-thymidine	West of Scotland Nucleotide Dispensary
[ <sup>32</sup> P]dCTP	Amersham Biosciences
0.2ml Microcentrifuge Tubes	Eppendorf
0.5ml Microcentrifuge Tubes	Eppendorf
1.5ml Microcentrifuge Tubes	Eppendorf
15ml centrifuge tubes	Becton Dickinson
24 well chemotaxis plate (5µM pore)	Corning
50ml centrifuge tubes	Becton Dickinson
Complete Freund's Adjuvant	Sigma
Decon 75	Decon Laboratories
DEPC treated water	Ambion
Gilson Pipette Tips (10,200,1000µl)	Fisher Scientific Ltd
Glass coverslips	Fisher Scientific Ltd
Glass fibre filter mats	Wallac Oy
Glass slides	Fisher Scientific Ltd
Haemocytometer	Fisher Scientific Ltd
Hybond-N+	Amersham Biosciences
Hyperladder I DNA ladder	Bioline Ltd
Hyperladder IV DNA ladder	Bioline Ltd
Marvel (dried skimmed milk)	Premier Beverages
Multimark protein molecular weight markers	Invitrogen
Polypropylene FACS tubes	Becton Dickinson
Sterile 0.2µM acrodisc filters	Gelman Sciences Ltd
Ultraspeed	Ambion
Vectashield with DAPI	Vector Labs
Whatman 3mm filter paper	Whatman International Ltd
X-Ray Film	Kodak

## 2.1.8 Oligonucleotides

With the exceptions of the M13 forward, M13 reverse, and T7 oligonucleotides (all supplied by Invitrogen), all primers were supplied by the Beatson Institute Technology Services (BITS) and synthesised by the methods outlined in section 2.2.1.1.

### 2.1.8.1 Tagged Expression Construct Oligos

Oligo Name	Oligonucleotide Sequence 5' to 3'
H3FLAGhCCR7	AGAGAGAAGCTTCCAACATGGACTACAAAGGACGACGACGACAAGGACCTGGGGAAACCAATGAAAAG
H3HAhCCR7	AGAGAGAAGCTTCCAACATGTACCCCTACGACGTGCCCGACTACGCCGGGCCGGGGACCTGGGGAAACCAATGAAAAG
H3HAhCCX	AGAGAGAAGCTTCCAACATGTACCCCTACGACGTGCCCGACTACGCCGCTTTGGGAACAGAACCAGTCAACAGATTATT
hCCR7-B-GFP	GAG AGA GGA TCC GTA TGG GGA GAA GGT GGT GGT G
hCCR7-Not1	GAG AGA GCG GCC GCC TAT GGG GAG AAG GTG GTG GTG
hCCX-B-GFP	CTC TCT GAA GCT TGA AAT GCT AAA AGT ACT GGT TGG CT
hCCX-B-GFP(2)	GGT AAA TGC TAA AAG TAC TGG TGG G

### 2.1.8.2 Sequencing Oligos

Oligo Name	Oligonucleotide Sequence 5' to 3'
GFPD1	GTG CTG CTT CAT GTG GTC G
GFPD2	GGC GGA TCT TGA AGT TCA CC
GFPD3	CTC AGG AGA GCA CAC ACT TGC
GFPU1	GCT GAC CCT GAA GTT CAT CTG
GFPU2	GCA TCG ACT TCA AGG AGG AC
GFPU3	CCG ACA ACC ACT ACC TGA GC
hCCR7D1	GTG GGC ATC TGG ATA CTA GCC
hCCR7D2	GGA CGT GCG GAA CTT TAA AG
hCCR7D3	GTC ATC ATC CGC ACC CTG C
hCCR7D4	CGA TCT CTT CAA GCT CTT CAA G
hCCR7U1	CAG CTT GCT GAT GAG AAG GAC
hCCR7U2	TGA GAG AGC ATC GCA TCG C
hCCR7U3	GGT AGG TAT CGG TCA TGG TC
hCCR7U4	GAG AAG GTG GTG GTG GTC TC
hCCXD1	AGC ATC ATT CAT ATG TAT CCA AGC
hCCXD2	TTA AAT GCT AAA AGT ACT GGT TGG C
hCCXD3	CTT GAC AAT GTT ATA AGG CAG TTG
hCCXD4	GGG TAT GCT CAG CAA GAT GG
hCCXD5	CCA TGA ACT GCA TTA ACA GCC
hCCXU1	ATG GCT TTG GAA CAG AAC CAG
hCCXU2	CAA TTC CAT GGT AGT GGC AAT
hCCXU3	GGA AAA CCA TGC TTG ATC ATC
hCCXU4	CTA CTT TAT CAC AGC AAG GAC ACT C
hCCXU5	TAC TCC CTG ATC ACC AGC TGC
M13 forward	GTA AAA CGA CGG CCA G
M13 reverse	CAG GAA ACA GCT ATG AC
T7	TAA TAC GAC TCA CTA TAG GG

### 2.1.8.3 Genotyping Oligos

Oligo Name	Oligonucleotide Sequence 5' to 3'
3IRES	CCC TAG ATG CAT GCT CGA CG
CommonScreen	CCC CTT CCA CGT TCT GTC TCT G
Cre1	ATT TGC CTG CAT TAC CGG TC
Cre2	ATC AAC GTT TTC TTT TCG G
CreTester	TTT GGC AAA GAA TTC ACT CCT C
mCCXCKRwt	GCT CAT CAA GAT GCC CAA CA
mCCXoom5	TGC TGG TGA GCT CTG GGT TC
mCCXwt5	AAT CGC CAC AAC TAC GGA GTT C
target.neo	CCG TGA TAT TGC TGA AGA GC

### 2.1.8.4 Screening Oligos

Oligo Name	Oligonucleotide Sequence 5' to 3'
mCCXout	TTG CTG TGC CTT GAT AGT CAC
mCCXoutB	AAA AAC AGA GCT CAG ACC TGT G
mCCXoutC	GTT GTT TCT GCA GTT GCT GTG
neoA	CCG TTA CTA GTG GAT CCT GGA G
neoB	CTA AAG CCA CAG TGT GGA ACA G
neoC	CAC GCT TGT GCT CTG GAA A

### 2.1.8.5 cDNA Amplification Oligos

Oligo Name	Oligonucleotide Sequence 5' to 3'
5'IRES	CAC GAT GAT AAG CTT GCC AC
$\beta$ -ActinD	TAC TCC TGC TTG CTG ATC CAC
$\beta$ -ActinU	TCC ATC ATG AAG TGT GAC GT
GFPD1	GTG CTG CTT CAT GTG GTC G
mCCXD	TGC TCT CTG TGA GTT GGA TGG
mCCXU	GCC ATC TTG CTG AGC ATA CC

## 2.1.9 Plasmids

Plasmid Name	Description	Source
$\beta$ -arrestin (V53D)	Encodes a dominant negative $\beta$ -arrestin-1	S.Ferguson, London, Canada
Caveolin-1-GFP	Encodes a C terminal GFP tagged caveolin-1	A.Helenius, Zurich, Switzerland
CCX-CKR lacZ KIKO	Targeting construct replacing mCCX-CKR gene with lacZ	Dr Nibbs
D6 lacZ KIKO	Targeting construct replacing mD6 gene with lacZ	Dr Nibbs
dynamain (K44A)	Encodes a dominant negativedynamain-1	S.Ferguson, London, Canada
EPS15 (DIII) GFP	Encodes a GFP tagged EPS15 mutant (see fig 3.1.28)	A.Benmerah, Paris, France
EPS15 (DIII $\Delta$ 2) GFP	Encodes a GFP tagged EPS15 mutant (see fig 3.1.28)	A.Benmerah, Paris, France
EPS15 (E $\Delta$ 95/295) GFP	Encodes a GFP tagged EPS15 mutant (see fig 3.1.28)	A.Benmerah, Paris, France
GFP-Caveolin-1	Encodes a dominant negative N terminal GFP tagged caveolin-1	A.Helenius, Zurich, Switzerland
GFPneolox	Encodes Farnesylated GFP with PGKneo cassette	Dr Nibbs
mCCX-CKR genomic clone	Plasmid with mCCX-CKR ORF+ genomic flanking sequences	Dr Nibbs
pcDNA3.1	Empty expression vector	Invitrogen
pcDNA3.1.hCCR7	Encodes human CCR7	Dr Nibbs
pcDNA3.1.h-CCX-CKR	Encodes human CCX-CKR	Dr Nibbs
peGFPN2	Plasmid encoding EGFP	Clontech
peGFPN3	Plasmid encoding EGFP	Clontech
Rab11 (S25N) GFP	Encodes a dominant negative GFP tagged Rab11	S.Ferguson, London, Canada
Rab4 (N121I) GFP	Encodes a dominant negative GFP tagged Rab4	S.Ferguson, London, Canada
Rab5 (S34N) GFP	Encodes a dominant negative GFP tagged Rab5	S.Ferguson, London, Canada

## **2.2 Methods**

### **2.2.1 Molecular Biology**

#### **2.2.1.1 Oligonucleotide Synthesis**

Oligonucleotides were synthesized by the BITS using an Applied Biosystems Model381A DNA synthesiser using Cruachem reagents and following the manufacturer's instructions. Oligos were synthesised without trityl group protection, obtained as pellet, and resuspended in 600µl sterile distilled water. The optical absorbance at 260nm and 280nm was measured using a Beckman DU 650 spectrophotometer and used to determine the oligonucleotide concentration. DNA purity was estimated from the  $OD_{260}/OD_{280}$ .

#### **2.2.1.2 Nucleic Acid Preparation**

##### **2.2.1.2.1 Genomic DNA Extraction with Phenol**

Confluent T75 flasks of mouse ES cell clones were harvested by brief trypsinisation (see 2.2.2.1) and pelleted by brief centrifugation (5min, 700 rcf) in 50ml falcon tubes. Cells were then resuspended in 10ml of extraction buffer (10mM TrisCl pH8, 0.1M EDTA, 0.5%SDS, 20µg/ml DNAase-free RNAaseA), and the mixture incubated at 37°C for 1h with shaking. A final concentration of 0.1mg/ml ProteinaseK was then added, and the samples incubated at 55°C for 3h with occasional swirling. 10ml of phenol was then added to each tube, which were then centrifuged briefly (5min, 700 rcf). The top layer was then carefully removed from each sample and placed in a fresh tube, to which another 10ml of phenol was added. Samples were centrifuged briefly and again the top layer carefully removed and placed in a fresh tube. 0.2 volumes of 10M ammonium acetate solution and 2 volumes of ethanol (EtOH) were added to each sample. The solution was thoroughly mixed

and incubated at  $-20^{\circ}\text{C}$  to allow DNA precipitation. The DNA precipitate was then 'hooked' out using a clean pipette tip and placed in a 1.5ml microfuge tube. Pellets were washed twice in 1ml of chilled 70% EtOH and air dried for 10-15min. DNA pellets were then resuspended in an appropriate volume of sterile 1xTE (10mM TrisHCl, 1mM EDTA). The optical absorbance at 260nm and 280nm was measured using a Beckman DU 650 spectrophotometer and used to determine the concentration, which was then adjusted to 1mg/ml.

#### **2.2.1.2.2 Genomic DNA Extraction on 96 Well Plates**

The growth medium from 96 well plates with confluent wells of mouse ES cell clones was removed by blotting onto paper towels. Wells were then washed in 200 $\mu\text{l}$  of PBS before 50 $\mu\text{l}$  of lysis buffer (10mM Tris.HCl, pH 7.5, 10mM EDTA, 10mM NaCl, 1mg/ml proteinase K, 0.5% SDS) was added to each well. The plate was then sealed with plate sealing tape and incubated at  $55^{\circ}\text{C}$  overnight. The next day, 200 $\mu\text{l}$  freshly prepared, ice cold, precipitation buffer (75mM NaCl in EtOH) was added to each well, mixed slowly, and the plate incubated at room temperature for 1h. Liquid in the wells was then blotted onto paper towels and the wells washed three times in cold 70% EtOH. The plates were then air dried for 10-15min and the precipitated DNA resuspended in 35 $\mu\text{l}$  of 1xTE.

#### **2.2.1.2.3 Preparation of Genomic DNA from Tailtips for Genotyping**

Tailtips were removed from weaned mice and incubated in 1.5ml screwcap tubes at  $55^{\circ}\text{C}$  overnight in 100 $\mu\text{l}$  lysis buffer (100mM Tris.HCl pH8.5, 5mM EDTA, 0.2% SDS, 200mM NaCl, 0.1mg/ml Proteinase K). Tubes were then heated to  $96^{\circ}\text{C}$  on a heating block for 5min before 500 $\mu\text{l}$  of ddH<sub>2</sub>O was added. Tubes were then spun in a microfuge at 13,000 rcf for 5min and then stored at  $4^{\circ}\text{C}$ .

#### **2.2.1.2.4 Preparation of Genomic DNA from Tailtips for Southern Blots**

Tailtips were removed from weaned mice and incubated in 1.5ml screwcap tubes at 55°C overnight in 100µl lysis buffer (100mM Tris.HCl pH8.5, 5mM EDTA, 0.2% SDS, 200mM NaCl, 0.1mg/ml ProteinaseK). Tubes were then spun at 13,000 rcf for 10min in a microfuge and the supernatant collected into a fresh tube to which of 1ml of propan-2-ol was added to allow DNA precipitation. The precipitate was 'hooked' out using a clean pipette tip and placed in a fresh tube. The DNA was washed twice in cold 70% EtOH, air dried for 10-15min, and resuspended in 400µl of sterile 1xTE.

#### **2.2.1.2.5 Plasmid DNA Preparation (Minipreps/Maxipreps)**

Single bacterial colonies were picked and incubated with shaking at 37°C overnight in 5ml of LB-medium containing 50µg/ml ampicillin or 50µg/ml kanamycin. 1.5ml of the overnight culture was pelleted by centrifugation (10min, 13,000 rcf). DNA was purified using the QIAprep Spin Miniprep Kit according to the manufacturer's instructions. DNA from larger volumes of overnight cultures (100-200ml) was purified using the QIAGEN Maxi kit following manufacturer's instructions.

#### **2.2.1.2.6 Plasmid DNA Precipitations**

To concentrate or sterilise plasmid DNA, precipitation was employed. Briefly, 50µg of plasmid DNA was incubated with 0.1 volume of 3M sodium acetate (pH5.5) and 2 volumes of EtOH on dry ice for 15min. Samples were then spun at 13,000 rcf for 10min and the pellet washed twice in ice cold 70% EtOH. Plasmid pellets were then air-dried (in laminar flow hood if to be used for sterile applications) and resuspended in 1xTE to give 1mg/ml.

### 2.2.1.2.7 RNA extraction with Trizol

Mouse tissues were dissected out, rinsed in PBS, snap frozen in liquid nitrogen, and stored at  $-70^{\circ}\text{C}$ . ~50mg of tissue was ground up whilst frozen using a mortar and pestle under liquid nitrogen. Ground up tissue was then collected in a sterile RNAase free microfuge tube and homogenised in 1ml of Trizol<sup>TM</sup> by pipetting vigorously up and down. RNA was then extracted according to the Trizol<sup>TM</sup> manufacturer's instructions. In brief, samples were incubated at room temperature for 5 min, spun at 12,000 rcf for 10min at  $4^{\circ}\text{C}$  and the top layer collected and placed in a fresh tube. 0.2ml of chloroform was added to samples which were then shaken vigorously for 15 sec and incubated at room temperature for 2min. Samples were then spun in a chilled microfuge for 15 min at 12,000rcf before the upper layer carefully removed and placed in a fresh tube. 0.5ml of propan-2-ol was added to each sample which were then incubated at room temperature for 10min to allow nucleic acid precipitation. Samples were then centrifuged at 8,000rcf for 10min at  $4^{\circ}\text{C}$ . RNA pellets were washed in 75% EtOH, air dried, and resuspended in The RNA Storage Solution. The optical absorbance at 260nm and 280nm was measured using a Beckman DU 650 spectrophotometer and used to determine the RNA concentration. Purity was estimated from the  $\text{OD}_{260}/\text{OD}_{280}$ .

RNA samples were DNAase treated using the DNA-free<sup>TM</sup> kit according to the manufacturer's instructions. In brief, 10 $\mu\text{g}$  of each RNA sample was diluted in 1xDNAaseI buffer containing 1 $\mu\text{l}$  of DNAaseI with the total volume made up to 50 $\mu\text{l}$  with diethylpyrocarbonate (DEPC) treated water. Samples were mixed, and incubated at  $37^{\circ}\text{C}$  for 30min. 5 $\mu\text{l}$  of DNAase Inactivation Reagent was then added and samples mixed thoroughly during incubation at room temperature for 2min. Samples were centrifuged at 10,000rcf for 1.5 min and the supernatant, containing the DNAase treated RNA, placed in a fresh tube.

### 2.2.1.2.8 cDNA Synthesis from RNA

cDNA was reverse transcribed from DNAase-treated RNA using the Superscript™ First-Strand Synthesis System for RT-PCR according to manufacturer's instructions. Briefly, 5µg of each RNA sample was mixed with 10µg/ml Oligo(dT)<sub>12-18</sub>, 200nM dNTP mix, and the volume made up to 10µl with DEPC treated water. Samples were incubated at 65°C for 5 min and then placed on ice for ~1min. To each sample, 9µl of a mixture containing the following components (final concentrations) was added: 1xRT-buffer, 5mM MgCl<sub>2</sub>, 10nM DTT, and 1µl of RNaseOUT™ Recombinant RNase Inhibitor. Samples were incubated at 42°C for 2min and then 1µl (50units) of Superscript™ II Reverse Transcriptase was added to each sample (except -RT controls). Reactions were incubated at 42°C for 50min before being terminated by incubation at 70°C for 15 min. Samples were collected by centrifugation and 1µl of RNAaseH added to each one. These were incubated at 37°C for 20min, and then stored at -20°C until used for PCR amplification.

### 2.2.1.3 Polymerase Chain Reaction (PCR)

PCR for all applications was performed using Reddymix™ PCR Master Mix tubes according to manufacturer's instructions. Briefly, 2µl of an oligonucleotide primer mixture (forward and reverse primers) was added to each tube such that each primer was at a final molarity of 0.2µM. Where the concentration of DNA template was known, 50-100ng of template was added to appropriate tubes and the final volume made up to 50µl with ddH<sub>2</sub>O. When the template concentration was not known (such as when screening DNA from ES cell clones or cDNA amplification), 3µl of DNA was added to the appropriate tubes. Tubes were then incubated in a thermocycler.

Thermocycler programs used varied depending upon the application, and were as follows:

**LONG SCREENING:-** 94°C 2mins, (94°C 10sec, 58°C 1min, 68°C 3min30sec) x35, 68°C 10mins, 4°C until end;

**GENOTYPING:-** 94°C 2mins, (94°C 30sec, 55°C 10sec, 68°C 1min) x35 68°C 10mins, 4°C until end;

**TAGGED EXPRESSION CONSTRUCT:-** 94°C 2mins, (94°C 30sec, 55°C 1m, 68°C 2min) x35 68°C 10mins, 4°C until end;

**cDNA AMPLIFICATION:-** 94°C 2mins, (94°C 30sec, 55°C 30sec, 68°C 1min) x35 68°C 10mins, 4°C until end.

PCR products were then analysed by agarose gel electrophoresis. Where appropriate, PCR products were purified using the technique described in 2.2.1.6

#### **2.2.1.4 Agarose Gel Electrophoresis**

Unless otherwise stated 1% agarose gels were used for all applications. Electrophoresis grade agarose was dissolved in 1xTAE (40mM Tris-acetate, 1mM EDTA) by heating. A final concentration of 0.5µg/ml ethidium bromide was added to cooled gels before pouring. The gel was then poured into horizontal gel cast apparatus and allowed to set at room temperature.

Unless using Reddy mix PCR tubes with loading buffer already included, DNA loading buffer (6x solution: 30% glycerol and bromophenol blue to colour) was added and samples were added to appropriate wells alongside DNA ladder markers. Unless otherwise stated, gels were run at 100V in 1xTAE buffer until bands clearly separated. DNA was visualised on a transilluminator and photographed.

### 2.2.1.5 Restriction Enzyme Digests

DNA was digested in a volume of 20-50µl using enzymes and the appropriate reaction buffers according to manufacturer's instructions. Between 5 and 10 units of restriction enzyme/µg of DNA was used. Generally, reactions were carried out for 1-2h at 37°C. However, for complete digestion of genomic DNA for Southern blotting, the reaction was for 4h before an extra 10% volume was added containing fresh 1x enzyme. The reaction was then incubated at 37°C for a further 16h. Digested plasmids which were to be used in ligation reactions (see 2.2.1.7) were treated with 1 unit of Alkaline Phosphatase and further incubated for 30min at 37°C to prevent re-ligation.

### 2.2.1.6 Gel Purification of DNA Fragments

DNA bands were excised from a gel using a scalpel and purified using a QIAGEN QIAquick Gel Extraction Kit according to the manufacturer's instructions. The DNA was eluted from the columns in 30-50µl of either 1xTE or distilled water and the yield determined both by spectrophotometry, and running a 5µl aliquot on an agarose gel alongside a DNA hyperladder of known fragment concentration.

### 2.2.1.7 DNA Ligation

Ligations were carried out using the Rapid DNA ligation kit according to manufacturer's instructions. Briefly, the amount of vector and insert used in these reactions was calculated using the following formula:

$$(50\text{ng of vector} \times \text{kb size of insert} / \text{kb size of vector}) \times (\text{ratio insert:vector}) = \text{ng of insert}$$

Generally, the ratio of insert to vector used was 4:1 and 1/10<sup>th</sup> of the above reaction was used to transform *E. Coli* DH5α competent cells (2.2.1.8)

### 2.2.1.8 Transformation of DH5 $\alpha$ Competent Bacterial Cells

A 50 $\mu$ l aliquot of DH5 $\alpha$  competent cells was thawed on ice in a chilled 15ml polypropylene tube (Falcon 2059). 1 $\mu$ l of plasmid DNA was added to each tube and left to incubate for 30min on ice. Cells were then incubated at 42°C for ~45 sec and then returned to ice for 2min before 400 $\mu$ l of warmed SOC medium (2% bactotryptone, 0.55% yeast extract, 10mM NaCl, 2.5mM KCl, 10mM MgCl<sub>2</sub>, 10mM MgSO<sub>4</sub>, 20 mM glucose) was added. Cells were then incubated at 37°C for 1h with vigorous shaking. Either 40 or 200 $\mu$ l of the reaction was then plated on L-agar plates containing 50 $\mu$ g/ml ampicillin or (when appropriate) 50 $\mu$ g/ml kanamycin. Plates were then inverted and incubated at 37°C for 16h to allow colony growth.

### 2.2.1.9 Cloning of DNA Fragments into TOPO<sup>®</sup> Plasmids

PCR amplification products which had been agarose gel electrophoresed and gel purified were cloned into pCR<sup>®</sup> 2.1-TOPO<sup>®</sup> (or in one case pcDNA3.1/CT-GFP-TOPO<sup>®</sup> see 2.2.1.12.3) according to manufacturer's instructions. Briefly, 4 $\mu$ l of purified PCR product, 1 $\mu$ l of salt solution, and 1 $\mu$ l of linearised TOPO<sup>®</sup> vector were mixed together and incubated at room temperature for 5 min. The reaction mixture was then stored on ice until used for transformation.

For each transformation reaction, 2 $\mu$ l of the TOPO<sup>®</sup> cloning reaction were transferred into a vial of One Shot<sup>®</sup> Chemically competent *E.coli*, and gently mixed. This was then incubated on ice for 5 min and subsequently heat-shocked for 30sec at 42°C. Tubes were then transferred to ice and 250 $\mu$ l of room temperature SOC medium added to each. Reactions were then incubated in a shaker (200rpm) for 1h at 37°C and then 50 $\mu$ l of each

transformation were spread on an agar plate containing 50µg/ml of ampicillin. Plates were inverted and incubated overnight at 37°C. Colonies were isolated the following day.

### 2.2.1.10 Southern blotting

Completely digested DNA samples were separated by electrophoresis on a 0.8% agarose gel containing 0.5µg/ml ethidium bromide for 6h at 80V. Gels were then visualised on a UV transilluminator and photographed alongside a translucent ruler as a reference. The gel was then trimmed and, when deemed necessary for transfer of fragments >10kb, placed in 0.2M HCl for 5-10min. This was followed by a brief rinse in distilled water and equilibration in alkali transfer buffer (0.4M NaOH, 1M NaCl) for 10min. The DNA was transferred from the gel to a Hybond N+ nylon membrane by alkali transfer Southern blotting overnight, detailed in figure 2.1.1. The next day, the apparatus was dismantled and the HybondN+ membrane containing the DNA fragments was briefly rinsed in neutralisation buffer (3M NaCl, 0.5M TrisHCl).

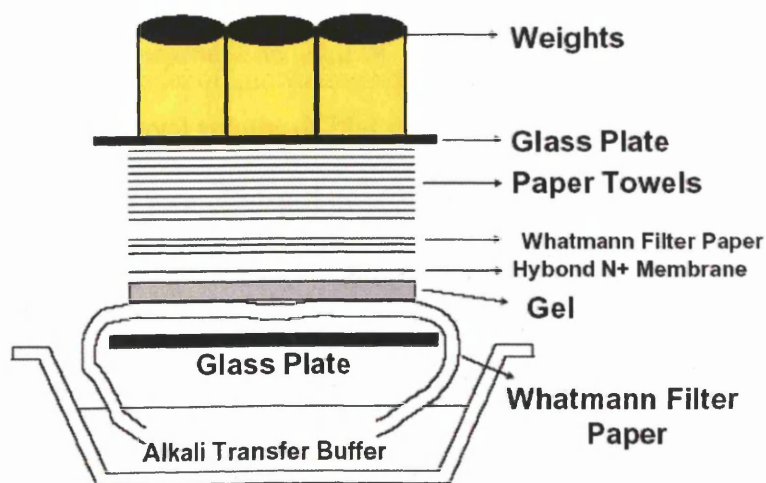


**Figure 2.2.1: A Southern Blot by Capillary Transfer.** A glass dish is half filled with alkali transfer buffer and soaked 3mm filter paper is placed upon a glass plate with both ends of the filter paper submerged in the buffer. The gel is placed upside down on the filter paper and a Hybond N+ nylon membrane (soaked in transfer buffer) carefully placed on top of the gel (taking care to remove any bubbles). Three pieces of filter paper are placed on top of this with 3-4 inches of paper towels above this. A glass plate with several weights is placed on the top. Parafilm is used to prevent short-circuiting by covering any spaces on the lower piece of filter paper not covered by the gel.

**Preparation of DNA for Probes:** The probes used for analysis of Southern blots were generated by restriction digestion of plasmid DNA with restriction enzymes (see figure 3.2.2 for details of where probes are located). Fragments were separated by agarose gel electrophoresis and bands of the indicated sizes were excised and gel purified. DNA was then resuspended at 25µg/ml. **CCX-CKR 5' probe:** Plasmid containing mCCX-CKR genomic clone was digested with *EcoRI* and *HindIII* and the ~500bp fragment purified. **CCX-CKR 3' probe:** Plasmid containing mCCX-CKR genomic clone was digested with *EcoRI* and *HindIII* and the ~1.6kbp fragment purified. **lacZ probe:** The CCX-CKR *lacZ* KIKO plasmid was digested with *XbaI* and *BamHI* and the ~3kb fragment purified. **Neo probe:** The CCX-CKR *lacZ* KIKO plasmid was digested with *XbaI* and *EcoRI* and the ~1kb fragment purified. **GFP probe:** The pEGFPN2 plasmid was digested with *EcoRI* and *NotI* and the ~800bp fragment purified.

**Labelling of Probes:** DNA fragments for probing Southern blots were labelled using Ready-To-Go™ DNA Labelling Beads according to manufacturer's instructions. In brief, labelling beads were resuspended in 20µl of 1xTE and incubated on ice. 25ng of DNA fragment was added to a total volume of 25µl of 1xTE in a separate screwcap tubes and this was boiled for 3min, and then incubated on ice. The two mixtures were then combined and 5µl of [ $\gamma^{32}\text{P}$ ]dCTP added. Reactions were mixed and then incubated at 37°C for 30min.

Unincorporated label was removed by running the samples through NICK™ columns according to manufacturer's instructions. Briefly, columns were equilibrated by running through 1xTE. The labelled probe samples were then added and an extra 350µl of 1xTE added to the column which was allowed to empty. Probes were then eluted in 500µl of 1xTE. The probe was then counted in a liquid scintillation counter, boiled for 3min, and added to hybridisation reactions at  $2 \times 10^6$  cpm/ml.

**Hybridisation of Blots:** Membranes containing blotted DNA fragments were rinsed briefly in 2xSSC (0.3M NaCl, 30mM Na Citrate) and rolled up in hybridisation bottles, taking care to remove any air bubbles. Blots were then prehybridised using Ultrahyb™ according to manufacturer's instructions. In brief, the Ultrahyb was pre-warmed to 68°C and 10ml added to each bottle. The bottles were then incubated in a rotating hybridisation oven at 42°C for 30min. Labelled, denatured, DNA probes were then added as outlined above. The hybridisation reaction continued at 42°C overnight.

**Washes and Probe Detection:** Following hybridisation, the membranes were removed from the bottles and washed twice with gentle shaking for 5 min at 42°C in low stringency wash buffer (2xSSC, 0.1% SDS). This was followed by two washes with gentle shaking for 15 min at 42°C in high stringency wash buffer (0.1xSSC, 0.1%SDS). Washed membranes were then exposed to X-ray film, which was then developed.

### 2.2.1.11 DNA Sequencing

All DNA sequencing was performed by members of the BITS using an Applied Biosystems 373A automated sequencer. Briefly, PCR amplification of the region to be sequenced was carried out with primers complimentary to domains upstream and downstream of the region of interest. PCR reactions contained 0.5µg plasmid DNA, 3.2pmoles of primer and 4µl of Big Dye Terminator Reaction premix in a final volume of 10µl (made up with distilled water).

The oligonucleotides used for sequencing the various different fragments of DNA in this study were: **i) For GFP portion of CCX-CKR GFP KIKO plasmid:** GFPU1, GFPU2, GFPU3, GFPD1, GFPD2, GFPD3. **ii) For hCCR7 constructs:** hCCR7U1, hCCR7U2, hCCR7U3, hCCR7U4, hCCR7D1, hCCR7D2, hCCR7D3, hCCR7D4. **iii) For hCCX-CKR constructs:** hCCXU1, hCCXU2, hCCXU3, hCCXU4, hCCXU5, hCCXD1,

hCCXD2, hCCXD3, hCCXD4, hCCXD5. iv) **For fragments cloned into TOPO<sup>®</sup> 2.1:** The M13 forward and M13 reverse oligos were also additionally used for sequencing PCR products v) **For inserts cloned into pcDNA3.1:** The T7 primer was additionally used.

### **2.2.1.12 Plasmid Construction**

#### **2.2.1.12.1 FLAG-tagged hCCR7**

hCCR7 was amplified by PCR using the pcDNA3.1.hCCR7 plasmid as template and priming using the oligonucleotides ‘H3FLAGhCCR7’ and ‘hCCR7-NotI’ using the ‘Tagged Expression Construct’ thermocycler conditions (detailed in section 2.2.1.3). A ~1kb fragment was resolved by agarose gel electrophoresis, gel purified, and cloned into TOPO<sup>®</sup> 2.1. This plasmid was then verified by DNA sequencing and digested with HindIII and NotI. The 1kb fragment was again resolved and purified from an agarose gel, then cloned into pcDNA3.1 which had been cut with the same restriction enzymes. This plasmid was verified by DNA sequencing to check that the N-terminal FLAG epitope (DYKDDDDK) had been correctly inserted between the first two amino acids of hCCR7.

#### **2.2.1.12.2 HA-tagged hCCR7-GFP**

hCCR7 was amplified by PCR using the pcDNA3.1.hCCR7 plasmid as template and priming using the oligonucleotides ‘H3HAhCCR7’ and ‘hCCR7-B-GFP’ using the ‘Tagged Expression Construct’ thermocycler conditions (detailed in section 2.2.1.3). A ~1kb fragment was resolved by agarose gel electrophoresis, gel purified, and cloned into TOPO<sup>®</sup> 2.1. This plasmid was then verified by DNA sequencing and digested with HindIII and BamHI. The 1kb fragment was again resolved and purified from an agarose gel, then cloned into pEGFPN3 which had been cut with the same restriction enzymes. This plasmid was verified by DNA sequencing to check for the haemagglutinin (HA) N-terminal epitope tag (YPYDVPDYA) and an in-frame hCCR7-GFP fusion.

### 2.2.1.12.3 HA-tagged hCCX-CKR-GFP

**Strategy A:** hCCX-CKR was amplified by PCR using the pcDNA3.1.hCCX-CKR plasmid as template and priming using the oligonucleotides ‘H3HAhCCX’ and ‘hCCX-B-GFP’ using the ‘Tagged Expression Construct’ thermocycler conditions (detailed in section 2.2.1.3). A ~1.1kb fragment was resolved by agarose gel electrophoresis, gel purified, and cloned into TOPO<sup>®</sup> 2.1. This plasmid was then verified by DNA sequencing and digested with *HindIII* and *BamHI*. The 1.1kb fragment was again resolved and purified from an agarose gel, then cloned into pEGFPN3 which had been cut with the same restriction enzymes. This plasmid was verified by DNA sequencing to check for the haemagglutinin (HA) N-terminal epitope tag and an in-frame hCCX-CKR-GFP fusion.

**Strategy B:** hCCX-CKR was amplified by PCR using the pcDNA3.1.hCCX-CKR plasmid as template and priming using the oligonucleotides ‘H3HAhCCX’ and ‘hCCX-B-GFP(2)’ using the ‘Tagged Expression Construct’ thermocycler conditions (detailed in section 2.2.1.3). A ~1.1kb fragment was resolved by agarose gel electrophoresis, gel purified, and cloned into pcDNA3.1/CT-GFP-TOPO<sup>®</sup>. This plasmid was then verified by DNA sequencing.

### 2.2.1.12.4 CCX-CKR-GFP-KIKO

The CCX-CKR *lacZ* KIKO plasmid was digested with *BamHI* and the large (~15kb) fragment purified following agarose gel electrophoresis. A plasmid containing farnesylated GFP cloned upstream of the PGKneo cassette (called GFPneolox) was also digested with *BamHI* and a ~5kb fragment purified from this reaction following agarose gel electrophoresis. These two DNA fragments were then ligated together, clones produced in bacteria, and plasmid orientation checked by restriction digestion. The resulting CCX-CKR GFP KIKO plasmid was further verified by sequencing of the GFP portion of the construct.

### 2.2.1.13 SDS-PAGE and Western Blotting

Cell lysates from  $1 \times 10^6$  cells were prepared in CellLytic-M Mammalian Cell Lysis Buffer according to manufacturer's instructions. An equal volume of HU buffer (8 M urea, 5% SDS, 200 mM Tris-HCl, pH 8, 0.1 mM EDTA, 100 mM dithiothreitol (DTT), 0.5% bromphenol blue) was added. Samples were incubated at room temperature for 10min, subjected to SDS-PAGE alongside Multimark protein markers, electrophoretically transferred onto polyvinylidene difluoride membrane, and blocked overnight in 10% milk/PBS. Blots were incubated with the appropriate primary antibody, washed in PBS/0.1% Tween, visualized with a  $\alpha$ -mouse IgG horseradish peroxidase-coupled secondary antibody, developed using a WestPico kit according to manufacturer's instructions, and exposed to X-ray film.

Samples from radioligand degradation experiments (2.2.4.2) were boiled for 10min, centrifuged (13,000rcf, 3min), and 25 $\mu$ l electrophoresed on a 4–12% Bis-Tris gradient acrylamide gel in 1x MES buffer. An aliquot of  $^{125}$ I-hCCL19 stock, containing an equivalent number of cpm to that found in 25 $\mu$ l of the most radioactive test sample, was prepared in 1xLB (50mM Tris-HCl, pH6.5, 2% SDS, 10mM DTT, 10% glycerol, 0.1% bromphenol blue) and loaded on the gel. Samples were run adjacent to MultiMark protein markers. After electrophoresis, gels were dried onto filter paper and exposed to X-ray film.

### 2.2.2 Cell Culture

All cell culture work was performed using strict aseptic techniques inside a Medical Air Technology Ltd Class II Microbiological Safety Cabinet laminar flow hood. Cells were incubated at 37°C in a dry atmosphere containing 5% (w/v) CO<sub>2</sub>. Human embryonic kidney (HEK)293 cells were grown in an appropriate volume of 293 medium (Dulbecco's

minimal essential medium (DMEM), 10% fetal calf serum, 4mM L-glutamine, and 100µg/ml streptomycin, and 100U/ml penicillin) in either T25, T75 or T175 tissue culture flasks. Cell culture of mouse embryonic fibroblasts (MEFs) was performed by Dr Milasta in the Department of Biochemistry at the University of Glasgow. Culture of mouse embryonic stem cells was performed by members of the Beatson Institute Transgenics Unit.

### **2.2.2.1 Harvesting Cells**

Medium was removed from cells by aspiration. Cells were then rinsed briefly in sterile PBS and then incubated with 5ml warmed 1 x trypsin solution (0.25% trypsin in PE) for ~5min. Cells were then harvested from surface of plate by pipetting up and down and placed in sterile universal container containing 5ml 293 medium. Cells were then collected by centrifugation and resuspended in 293 medium for counting, re-seeding, and experiments.

### **2.2.2.2 Freezing Cells**

Harvested cells were resuspended at  $2 \times 10^6$  cells/ml in 293 medium containing 10% DMSO and 1ml volumes were aliquoted into cryotubes. Cryotubes were then either placed into a 'Mr Frosty' (filled with 250ml propan-2-ol) or placed in a plastic beaker padded with cotton wool. The 'Mr Frosty' or the beaker was then incubated at  $-70^{\circ}\text{C}$  for 12-16h before cryotubes were removed and stored in liquid nitrogen tanks for long-term storage.

### **2.2.2.3 Defrosting Cells**

Cryotubes containing frozen cells were removed from liquid nitrogen storage and thawed in warm ( $\sim 37^{\circ}\text{C}$ ) water for several min. Cells were removed from cryotubes and diluted with 20ml 293 medium, collected by centrifugation, resuspended in 10ml 293 medium

(containing 0.8mg/ml G418 or 2µg/ml puromycin where appropriate) and seeded into T25 flasks.

#### **2.2.2.4 Cell counts**

400µl aliquots of harvested cells were diluted to a total of 20ml in PBS and the sample counted using a Casy® Technology Cell Counter. The approximate cell concentration was calculated. Alternatively, cells were counted in a haemocytometer. ~10µl of single cell suspensions were transferred to one side of a haemocytometer and the number of cells in one corner square counted under the light microscope. Cells which appeared non-viable were excluded. At least 100 cells were counted (using extra squares if necessary). The cell concentration was calculated using the following formula:

$$\text{Cells/ml} = (\text{average cell count per square}) \times 10^4$$

#### **2.2.2.5 Transfection of HEK293 Cells**

##### **2.2.2.5.1 Transient Transfections**

$2 \times 10^5$  cells in a volume of 2ml in 293 medium were plated into the wells of a six-well tissue culture dish and cultured for 48h (37°C, 5% CO<sub>2</sub>). Effectene was used for transfection according to manufacturer's instructions and using supplier's buffers. Except where indicated 1µg of plasmid DNA was mixed with 100µl of EC buffer, 3.2µl of Enhancer added, left for 5 min at room temperature, 10µl of Effectene added, and the sample mixed and incubated for a further 5–10min at room temperature. Then, 600µl of 293 medium was added, and the whole mix was added dropwise to one well of cells bathed in 2ml of warm 293 medium. Mock transfectants, omitting DNA, were done as a control. Cells were incubated (37°C, 5%CO<sub>2</sub>) overnight and harvested the next day.

### **2.2.2.5.2 Stable Transfections**

$1 \times 10^6$  cells were seeded onto a 90mm tissue culture dish in 10ml of 293 medium and incubated ( $37^\circ\text{C}$ ,  $5\%\text{CO}_2$ ) for 48h. Transfections were performed using the FuGENE 6 Reagent according to manufacturer's instructions. In brief, either 3 or  $5\mu\text{g}$  of sterile plasmid DNA was added to  $18\mu\text{l}$  of fuGENE 6 and the volume made up to  $300\mu\text{l}$  with serum free DMEM in a small sterile bijou tube. This complex was incubated at room temperature for 15-20min and then added dropwise onto the cells. Samples with no DNA added were included as mock transfected controls. Cells were incubated ( $37^\circ\text{C}$ ,  $5\%\text{CO}_2$ ) overnight, then harvested and plated out with selection medium containing  $0.8\text{mg/ml}$  geneticin (G418). Culture continued for several weeks until stable G418 resistant colonies came through.

## **2.2.3 Analysis of Cell Fluorescence**

### **2.2.3.1 Confocal Microscopy**

#### **Preparation of Slides**

Two 13mm diameter glass coverslips were put into each well of a 6 well tissue culture plate. 3ml of sterile fibronectin ( $1\mu\text{g/ml}$  in PBS) was added to each well and the plate incubated at  $37^\circ\text{C}$  in the dark for one h. The fibronectin was then aspirated off and wells washed twice with PBS.  $1 \times 10^5$  cells in 3ml of 293 medium were then added into the wells and then grown for 48h. Following experimental procedures, cells were washed gently in PBS and then incubated with 4% paraformaldehyde (PFA) for 15 min at room temperature. Cells were again rinsed with PBS and the coverslips carefully removed from the wells, air-dried, and mounted on glass slides in Vectashield containing 4,6-diamidino-2-phenylindole (DAPI). Coverslips were sealed using nail varnish, dried in the dark, and stored at  $4^\circ\text{C}$  until analysed.

## **Image Capture**

Images were captured using a Leica SP-2 confocal microscope configured with Leica software, with a 40x oil immersion objective and digital zoom. Fluorochromes were excited sequentially where appropriate with lasers at 488nm (GFP) or 543nm (Cy3), or a UV laser (DAPI), images superimposed using Leica software, and assembled using Thumbs-Plus software. Serial z-sectioning was used where necessary to confirm intracellular fluorescence localisation.

### **2.2.3.2 Flow Cytometry**

#### **a) HEK-293 Cells**

Cells from experiments were collected in 5ml polypropylene FACS tubes, resuspended in 400µl of ice cold FACS buffer (2% FCS, 0.1% sodium azide in PBS). Data acquisition was performed using a Becton Dickinson FACScan running CellQuest™ software. Cells were gated using forward and side scatter (see figure 2.2.2A). When only one colour was being detected, negative control cells were used to adjust the cytometer settings so that >95% of cells fell between  $10^0$  and  $10^1$  on the FL2-H (for phycoerythrin) or the FL1-H (for GFP) channels (see figure 2.2.2B). For two colour analysis, negative control and single stained cells were used to adjust the settings and cytometer compensation (see figure 2.2.3). Test samples were analysed with at least 10,000 gated events counted per sample. Data collected was analysed using either CellQuest™ or WinMDI software.

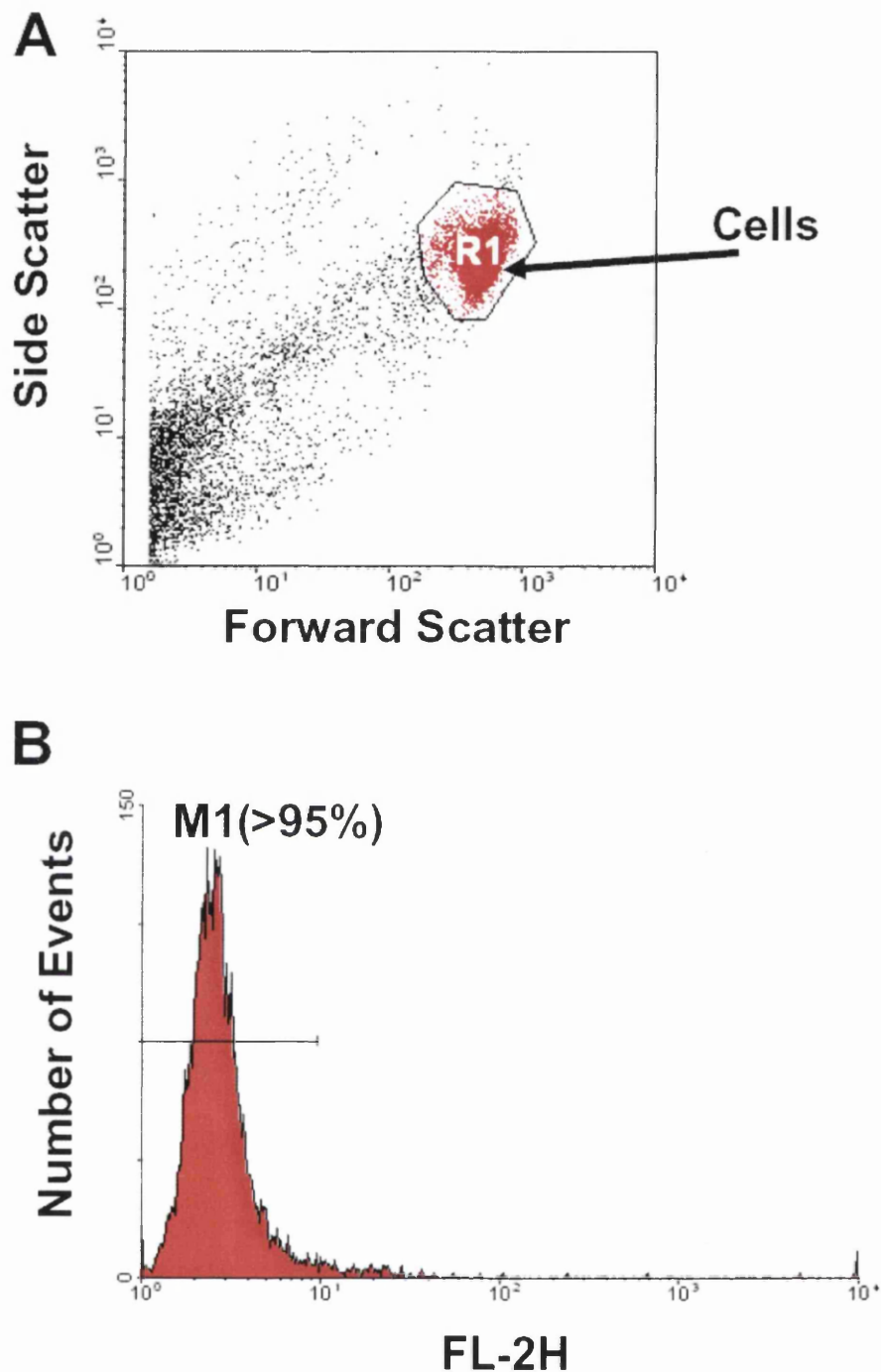


**Figure 2.2.2: Setting up the Flow Cytometer for Single Colour Analysis.** (A) Events which fall within the 'R1' gated region (coloured red) are considered viable cells and only these are subsequently analysed. (B) The cytometer is set up so that >95% of viable negative control cells fall within 'M1' (have a fluorescence intensity between 10<sup>0</sup> and 10<sup>1</sup> units).

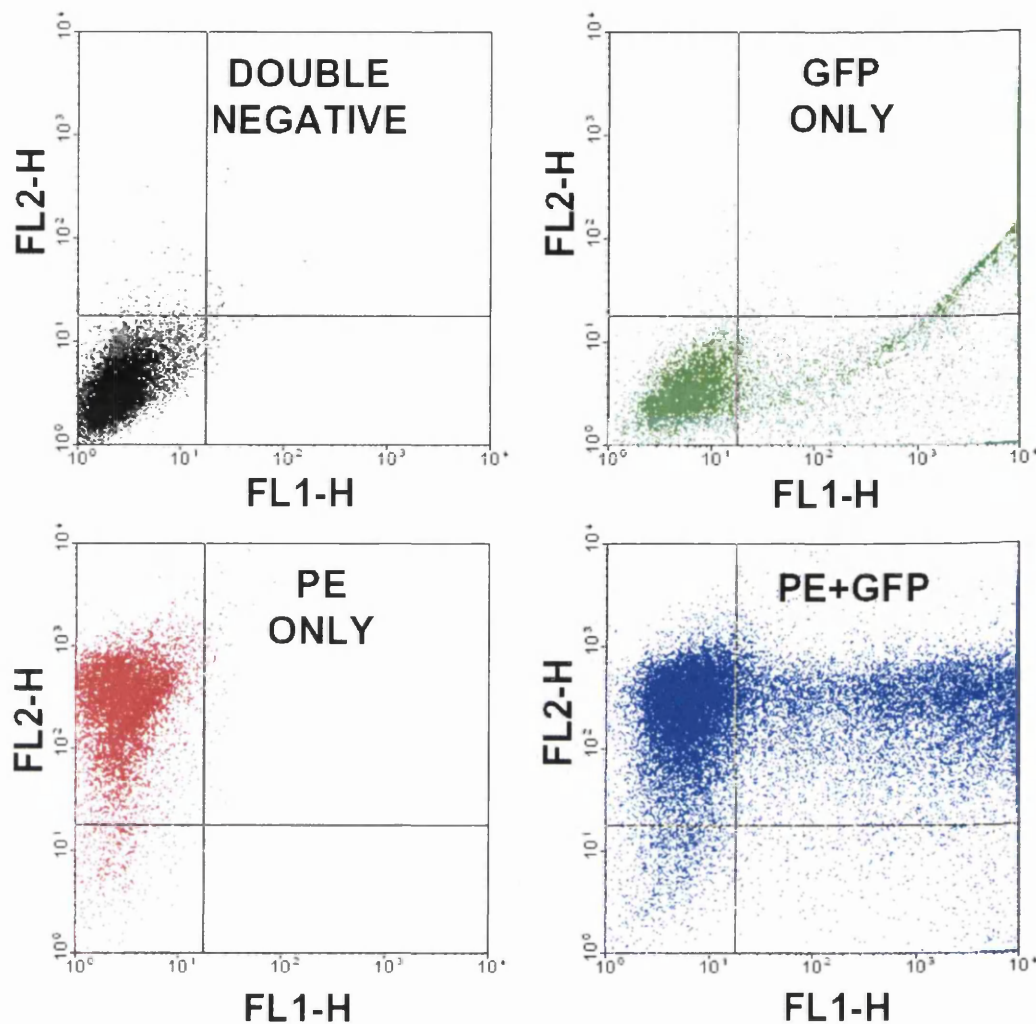


**Figure 2.2.3: Setting up the Flow Cytometer for 2 Colour Analysis.** Settings are adjusted so that unstained negative control cells (black-top left) fall within the bottom left quartile. GFP transfected cells (green-top right) are used to set the compensation so that these mostly fall under the line in the lower section of the plot. GFP-ve, PE stained cells (red-lower left) are used to set compensation so that these fall on left hand side of the vertical line. Cells both transfected with GFP and stained with PE (blue-lower right) can then be analysed.

### b) Mouse Leukocytes

Immunostained mouse leukocytes were analysed by flow cytometry using a Becton Dickinson FACSCalibur immunocytometry system. The leukocyte fraction of cells from suspensions of mouse spleen and LNs were gated based upon forward and side scatter (see figure 2.2.4A). Prior to analysis, a drop of propidium iodide was added to each sample. Dead cells were then excluded from analysis by gating on those which did not take up

propidium iodide, measured on the FL3-H channel (see figure 2.2.4B). Samples which had been stained with isotype-control fluorochrome labelled antibodies were used to adjust settings and cytometer compensation (see figure 2.2.4C). Once the cytometer had been set up, test-samples were analysed.

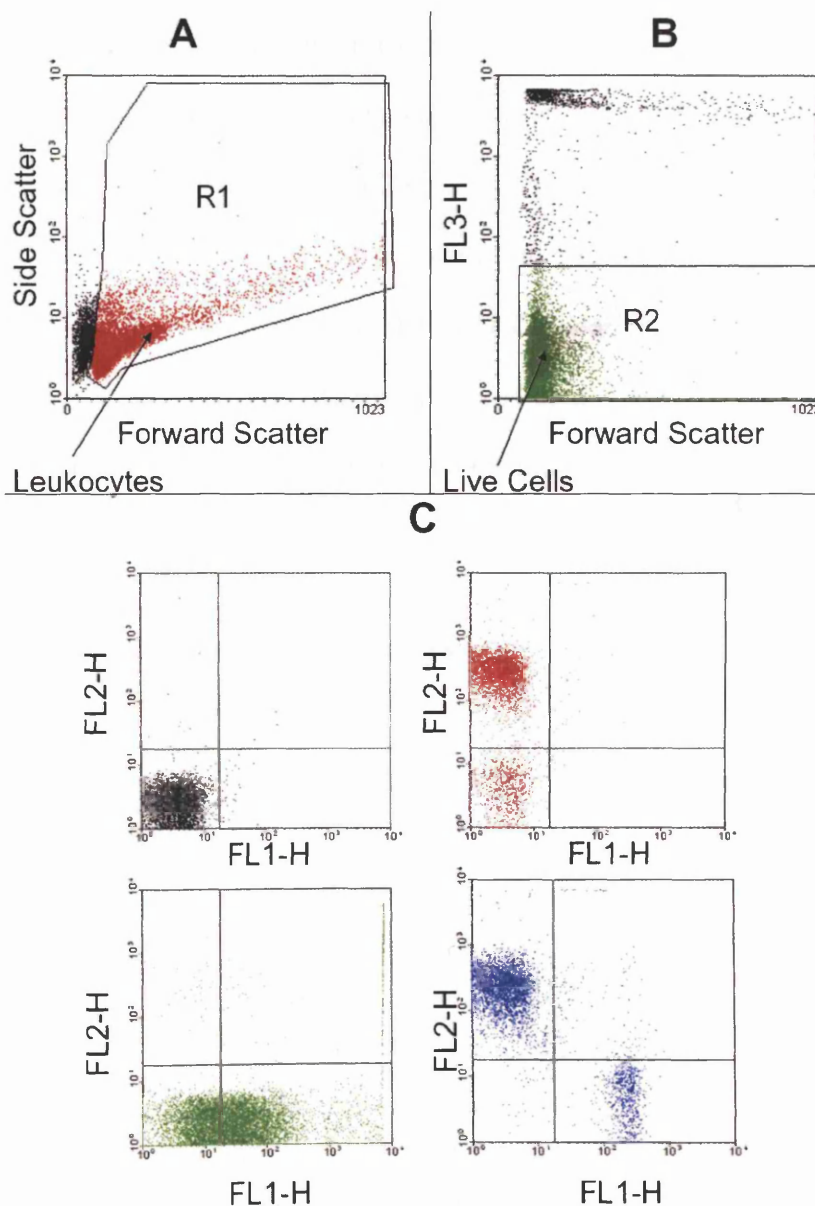


**Figure 2.2.4: FACS Analysis of Mouse Leukocytes.** (A) Leukocytes are gated upon based their forward and side side scatter. Those cells within 'R1' (labelled in red) are subsequently analysed. (B) Dead cells are excluded by propidium iodide staining. Cells within 'R2' (labelled in green) are subsequently analysed. (C) Cytometer settings and compensation are set using cells double stained with isotype control antibodies (black), cells stained with PE-conjugated antibodies and FITC conjugated isotype controls (red), and cells stained with PE-conjugated isotype controls and FITC conjugated antibodies (green). Cells stained with two labelled antibodies can then be analysed (blue).

## 2.2.4 *In Vitro* Assays

### 2.2.4.1 Radioligand Internalisation Assays

$0.5\text{--}1 \times 10^6$  harvested cells were incubated at  $4^\circ\text{C}$  for 1h in  $50\mu\text{l}$  of binding buffer (BB) (293 medium plus 20mM HEPES, pH7.4) containing  $2\text{nM}$   $^{125}\text{I}$ -CCL19. Cells were pelleted by centrifugation and washed in ice-cold phosphate-buffered saline (PBS). Cell-associated radioactivity was determined using a Beckman Gamma 5500B counter. After PBS washing, cells were resuspended in  $200\mu\text{l}$  of BB, and shifted to  $37^\circ\text{C}$  for up to 2-30min. Cells were then pelleted, the BB removed, and the cells washed with either PBS or acid wash (generally 0.2M acetic acid, 0.5 M NaCl unless indicated in the text), both ice-cold, for 5 min. Cell-associated radioactivity was determined using a Gamma 5500B counter. Ligand internalisation was calculated by the ratio of radioactivity in acid-stripped versus PBS-washed cell pellets.

### 2.2.4.2 Radioligand Degradation Assays

#### Preloaded Cells

$1 \times 10^6$  harvested cells were loaded at  $4^\circ\text{C}$  with  $2\text{nM}$   $^{125}\text{I}$ -CCL19 in BB for 1h, washed with ice-cold PBS, resuspended in  $100\mu\text{l}$  of BB, and incubated at  $37^\circ\text{C}$  for up to 2h (where indicated this incubation was in the presence of 50mM  $\text{NH}_4\text{Cl}$  and/or 200nM hCCL19). For each time point, triplicate samples were centrifuged, the supernatant taken, and the cell pellet washed in  $200\mu\text{l}$  of BB, which was subsequently combined with the first  $100\mu\text{l}$  of supernatant. Cell pellets were resuspended in  $100\mu\text{l}$  of PBS, and  $50\mu\text{l}$  was counted in a Beckman Gamma 5500B counter. To the remainder,  $50\mu\text{l}$  of 2x LB (100mM Tris-HCl, pH6.5, 4% SDS, 20mM DTT, 20% glycerol, 0.2% bromphenol blue) was added in readiness for SDS-PAGE (see 2.2.1.13).  $150\mu\text{l}$  of the supernatant was subjected to precipitation in 12.5% trichloroacetic acid (TCA). Radioactivity in the TCA pellet and non-TCA precipitable material was determined in a Beckman Gamma 5500B counter.

The percentage of retrieved radioactivity in cells, TCA pellet, and non-TCA precipitable fraction was then calculated. To the remaining 150µl of supernatant, an equivalent volume of 2xLB was added for SDS-PAGE analysis.

### **Degradation in Continuous Culture**

$7.5 \times 10^6$  cells were seeded into  $75\text{cm}^2$  tissue culture flasks and cultured for 2 days. The growth medium was then replaced with 5ml of BB containing 10nM CCL19, plus 0.1nM  $^{125}\text{I}$ -CCL19 as a tracer. Cells were then incubated at  $37^\circ\text{C}$ . At various times, 200µl aliquots of medium were removed and subjected to TCA precipitation. TCA pellets and non-TCA precipitable fractions were prepared and counted in a Beckman Gamma 5500B counter. 50µl aliquots were also taken and an equivalent volume of 2xLB was added for SDS-PAGE analysis.

#### **2.2.4.3 Radioligand Uptake Assay**

Cells in culture were incubated +/-10nM chemokine for 1h, washed, harvested, and resuspended in ice-cold BB at  $10^7$  cells/ml. 40µl aliquots were taken, 10µl of 2nM  $^{125}\text{I}$ -hCCL19 in BB added, the cells incubated at  $37^\circ\text{C}$  for 10min, retrieved by centrifugation, and then washed with ice-cold PBS. Cell-associated radioactivity was determined using a Beckman Gamma 5500B counter.

#### **2.2.4.4 Radioligand Binding Assay**

Harvested cells were used in equilibrium radioligand binding assays. These were performed at room temperature in 293 medium containing 0.5% sodium azide and 20 mM Hepes (pH 7.4), using  $10^6$  cells per point (each point performed in triplicate), 1nM  $^{125}\text{I}$ -hCCL19, and +/- 200nM unlabeled CCL19. After 90min, cells were washed with ice-cold PBS and bound  $^{125}\text{I}$ -CCL19 was detected in a Beckman Gamma 5500B counter.

### **2.2.4.5 Radioligand Dissociation Assay**

Harvested cells ( $5 \times 10^5$ ) were incubated at 4°C with 2nM  $^{125}\text{I}$ -hCCL19 in BB for at least 1h, centrifuged, and washed with regular agitation for 5 min in 1.5ml ice-cold BB adjusted to pH5–7. Control cells were washed with ice-cold PBS. Cells were retrieved by centrifugation and counted in a Beckman Gamma 5500B counter. Further acid washing (0.2M acetic acid, 0.5M NaCl) was used on some samples to confirm surface localization of radioligand.

### **2.2.4.6 Chemotaxis assay**

CCL19 was added to cultured cells, incubated at 37°C for 16h, and supernatants collected. Splenocytes were isolated from a female FVB mouse, passed through nitex membrane to form a single cell suspension, centrifuged, and resuspended at  $5 \times 10^6$  cells/ml. 400µl of supernatants from cultured cells were then put in the lower chamber of a Transwell chemotaxis plate (6.5mm diameter filter, 5µm pores) and 100µl of splenocyte suspension added to the upper chambers. Wells with no chemokine, or 200nM of fresh hCCL19, in the lower chambers were included. The plate was then incubated at 37°C for 4h. The number of cells successfully migrated to the lower chamber of each well were then counted using a haemocytometer.

### **2.2.4.7 Biotinylated Chemokine Uptake Assays**

#### **By Confocal Microscopy**

Bio-CCL19 (250ng), was mixed with 5µl of ExtrAvidin-Cy3, in a final volume of 10µl (made up with PBS), and incubated at room temperature for 45-60min to generate BioCCL19/Cy3 complexes. Control samples lacked Bio-CCL19 (i.e. ExtrAvidin-Cy3 alone). Cells (HEK293 or transfected derivatives, or MEFs) were grown on fibronectin-treated coverslips, and the premixes added where appropriate. After incubation for up to

1h, cells were washed with PBS, fixed in 4% PFA/PBS, washed again in PBS, mounted on glass slides in Vectashield mountant containing DAPI, and sealed with nail varnish (see 2.2.3.1).

### **By Flow Cytometry**

Bio-CCL19 (250ng), was mixed with 3 $\mu$ g of Streptavidin-PE (S-PE), in a final volume of 10 $\mu$ l (made up with PBS), and incubated at room temperature for 45-60min to generate BioCCL19/PE complexes. Control samples lacked Bio-CCL19 (i.e. S-PE alone). Harvested cells ( $\sim 5 \times 10^5$ ), pre-treated with or without chemokines, were resuspended in 190 $\mu$ l of BB, the 10 $\mu$ l premixed Bio-CCL19/PE complexes or S-PE alone was added, and the cells were incubated at 37°C with regular mixing for the indicated length of time. To end uptake, 1ml of ice-cold FACS buffer was added, and the cells retrieved by centrifugation, resuspended in 400 $\mu$ l of FACS buffer, and analysed by flow cytometry (see 2.2.3.2). Parental HEK293 cells, treated with Bio-CCL19/PE or S-PE alone, were used as negative controls. To assess BioCCL19/PE uptake into GFP-expressing transfected cells, untransfected parental HEK293, mock transfected HEK-hCCX-CKR cells, and GFP+ HEK-hCCX-CKR cells, treated with Bio-CCL19/PE or S-PE alone, were used as controls to set appropriate parameters on the FACScan (see figure 2.2.3).

### **2.2.4.8 Antibody Staining for Surface CCX-CKR or CCR7**

1x10<sup>6</sup> harvested cells per sample were washed with FACS buffer and resuspended in 100 $\mu$ l of ice-cold FACS buffer. After primary antibody (anti-FLAG M1 for CCX-CKR, and anti-hCCR7 for CCR7) addition, samples were incubated on ice for 30–45 min, 1ml of ice-cold FACS buffer added, and the samples centrifuged. Cells were resuspended in 100 $\mu$ l of ice cold FACS buffer containing PE-coupled anti-mouse IgG secondary antibody and placed on ice for 30–45 min. After washing with cold FACS buffer, cells

were resuspended in 400µl of FACS buffer and analysed by flow cytometry using a Becton Dickinson FACScan flow cytometer (see 2.2.3.2). Untransfected cells were used alongside test samples as negative controls.

### **2.2.5 Gene Targeting**

Transgenic mice were generated (using the constructs described in section 3.2.1) in collaboration with the Beatson Institute Transgenic Unit (BITU). Screening of DNA from ES cell clones was achieved using techniques outlined above and is detailed in section 3.2. All ES cell culture, electroporations, blastocyst injections, and microinjections were carried out by members of the BITU following standard protocols.

### **2.2.6 *In Vivo* Analysis**

#### **2.2.6.1 Maintenance of Mice**

Mice were housed in pathogen free conditions within the animal facility at the Beatson Institute and fed food and water *ad libitum*. All procedures performed on mice were in accordance with United Kingdom Home Office guidelines, and under appropriate personal and project licences.

#### **2.2.6.2 Genotyping of Mice**

Weaned mice were tail-tipped and DNA extracted from these tails (see 2.2.1.2.3). Genotype was determined by PCR. The PCR conditions are shown in section ('Genotyping' in 2.2.1.3) using the following primers for the different genotyping PCRs used in this study. **i) CCX-CKR KO/WT 5'**: mCCXwt5, mCCXcom5, 3IRES **ii) CCX-CKR KO/WT 3'**:

mCCXCKRwt, cretester, commonscreen **iii) Cre Recombinase:** Cre1, Cre2 **iv) CCX-CKR neo recombination:** mCCXCKRwt, commonscreen, target.neo

### **2.2.6.3 Sacrifice of Mice**

Mice were killed by an approved schedule one technique. This was either i) in a rising concentration of CO<sub>2</sub> or ii) severing of the spinal cord.

### **2.2.6.4 Dissection of Mice**

Killed mice were dissected using standard procedures. The carcass and dissection instruments were rinsed in 70% EtOH prior to dissection. Organs were surgically removed then rinsed in PBS. Peripheral blood was taken by cardiac puncture. Blood samples were immediately microfuged and frozen for serum analysis by ELISA.

### **2.2.6.5 Weighing Inguinal Lymph Nodes**

Inguinal LNs (ILNs) were trimmed under a dissection microscope to remove any attached connective tissue or fat, dried briefly on a paper towel, and carefully weighed on a microbalance.

### **2.2.6.6 Harvesting of Leukocytes**

ILNs or spleens were homogenised by rubbing through Nitex mesh in RPMI-1640 medium; the resulting cell suspensions were washed twice by centrifugation at 400rcf for 5 min and then resuspended in either FACS buffer or complete RPMI depending upon the downstream analysis.

### **2.2.6.7 Immunostaining of Mouse Leukocytes for Flow Cytometry**

After cell counting (see 2.2.2.4), single cell suspensions of mouse leukocytes were resuspended ( $1 \times 10^6$  cells/ml) in cold FACS buffer, and 500 $\mu$ l aliquots taken into

polypropylene FACS tubes. Samples were then incubated with fluoro-chrome-labelled antibodies against cell surface markers or fluoro-chrome-labelled isotype control antibodies, and incubated in the dark at 4°C for 45-60min. Tubes were then filled with cold FACS buffer, spun, and the cells resuspended in ~400µl cold FACS buffer. Samples were then analysed by flow cytometry (see 2.2.3.2).

### **2.2.6.8 Histology of Mouse Tissue**

Tissue for histological analysis was fixed in neutral buffered formalin and passed to Colin Nixon at University of Glasgow Veterinary School for paraffin embedding, sectioning, and staining of sections with Haematoxylin and Eosin (H+E).

### **2.2.6.9 Cutaneous PMA Paint**

Female mice between 6 and 12 weeks of age were used in all experiments. Mice were shaved, and 2 days later cutaneous inflammation was induced by the application of PMA, as a 50µM solution in acetone, to the shaved dorsal skin (this was performed by animal technicians in the Beatson animal facility). Each animal received 150µl of this solution, which is equivalent to 7.6 nmol per mouse per application. This was done on three consecutive days. Mice were then sacrificed either 3, 5, or 7 days hence. The back skin was removed from killed mice for histological analysis (see 2.2.5.7) and ILNs carefully dissected out.

### **2.2.6.10 Subcutaneous Immunisation with OVA/CFA**

Female mice between 6 and 12 weeks of age were used. 200µl of an emulsion containing 100µg of ovalbumin (OVA) in complete Freund's adjuvant (CFA) was injected subcutaneously into each flank (this was performed by trained animal technicians in the

Beatson animal facility to ensure consistent injection). Unimmunised mice were included as controls. On day 3 after immunisation, a group of mice were sacrificed to assess ILN phenotypes. 10 days after immunisation, mice were bled from the tail vein and the serum collected by centrifugation. The remainder of the mice were sacrificed either on day 17 or day 24 following immunisation. Blood was collected by cardiac puncture and ILNs harvested for analysis of cellular immune responses.

#### **2.2.6.11 Measuring OVA-Specific Total Serum IgG Antibody by ELISA**

96 well ELISA plates were coated overnight at 4°C with 120µl of a 10µg/ml solution of OVA in 0.1M carbonate buffer. Plates were then washed three times in wash buffer (0.05% Tween20 in PBS) before blocking non-specific binding sites with 200µl/well of blocking buffer (10%FCS in PBS) for 1h at room temperature. Serum samples were diluted 1/400 in blocking buffer and 100µl of diluted sample added to appropriate wells. Plates were then incubated at room temperature for ~2-3h before washing the wells three times in wash buffer. 100µl of primary antibody (anti-mouse IgG conjugated to peroxidase) was added to each well and the plate incubated for 3h at room temperature. Following three further washes, 120µl of phosphatase substrate (1mg/ml in 10% diethanolamine) was added and the plates were read at 405nm using an automatic microplate reader.

#### **2.2.6.12 Measuring Antigen Specific Cell Proliferation**

Single cell suspensions from mouse ILNs (see 2.2.6.6) taken 17 or 24 days after subcutaneous immunization were counted and resuspended at  $1 \times 10^6$  cells/ml in complete RPMI (RPMI 1640, 10% FCS, 4mM L-Glutamine, 100U/ml Penicillin, 100µg/ml Streptomycin, and 50µg/ml Fungizone) or complete RPMI supplemented with 1mg/ml OVA, or 5µg/ml Concanavalin A (ConA). Samples were culture in triplicate wells in a

volume of 200µl at 37°C in 5% CO<sub>2</sub> for 48h before a 100µl supernatant sample collected and frozen for subsequent analysis of cytokine production (see 2.2.5.9). 100µl of fresh complete RPMI (supplemented where appropriate with 1mg/ml OVA or 5µg/ml ConA) was added to cultures and the cells incubated for a further 64h at 37°C 5% CO<sub>2</sub>. Cell proliferation was assessed by the addition of 1µCi/well [<sup>3</sup>H]-thymidine for the last 18h of culture. DNA-bound radioactivity was harvested onto glass-fiber filter mats, and thymidine incorporation was measured on a Wallac Oy 1205 Betaplate scintillation counter.

### **2.2.6.13 Measuring Antigen Specific Cytokine Production**

Aliquots of supernatants removed from cultures after 48h (see 2.2.5.8) were analysed using a Mouse Th1/Th2 Six-Plex Antibody Bead Kit according to the manufacturer's instructions. In addition, Mouse IL-13 Antibody Beads were also included. Briefly, 25µl of the bead mixture was added to the wells of a pre-wetted (in 'wash buffer') 96 well plate and then a further 200µl of 'wash buffer' added to each well. This was followed by 50µl of 'incubation buffer' to each well and 100µl of standards was added to appropriate wells. Then, 50µl of assay diluent and 50µl of supernatant sample was added to each well, the plate covered in foil and incubated at room temperature with shaking for 2h. The plate was then washed and 100µl of biotinylated detector antibody added to each well. The plate was then incubated at room temperature for 1h with shaking in the dark. Following washing, 100µl of streptavidin-PE was added and the plate wrapped in foil and incubated at room temperature with shaking for 30min. The plate was then washed three times and the beads resuspended in 100µl of 'wash buffer'. The plate was then analysed in a Luminex 100™ instrument, and the concentration of each cytokine in each sample determined from standard curves generated from curve fitting software. The lower detection limits (in pg/ml) of this

assay for each cytokine were as follows: - IL-2=11.08; IL-4=15.67; IL-5=7.96; IL-10=4.01; IL-12=4.47; IL-13=29.65; IFN $\gamma$ =7.41.

#### **2.2.6.14 Induction of Contact Sensitivity with the Hapten DNFB**

Male mice aged between 12-16 weeks were used in this experiment. The back skin was shaved and 20 $\mu$ l of 0.5% DNFB in acetone/olive oil (4:1 ratio) applied to the shaved area on two consecutive days. 24h later, ILNs were removed from some mice, for analysis. 7 days later, with the remainder of the mice, ear thickness was measured using electronic callipers and then left ears were painted with 10 $\mu$ l 0.2% DNFB in acetone/olive oil, and right ears painted with 10 $\mu$ l acetone/olive oil alone. Ear thickness was then measured 24h and 48h later, and after 48h, the ears were removed for sectioning and H+E staining (2.2.6.8).

#### **2.2.7 Statistical Analysis**

All statistical analyses were made using GraphPad Prism software (GraphPad Software). Comparisons between data sets were made with Student's *t*-test. Results with *p* values <0.05 were considered to be statistically significant.

## CHAPTER THREE

### RESULTS

#### 3.1 Biochemical Analysis of human CCX-CKR and CCR7

##### 3.1.1 Constructs and Cell Lines

At the outset of this project it was planned to investigate the biochemistry of CCX-CKR, using *in vitro* transfected cell systems. As the only commercially-available radiolabelled CCX-CKR ligand was CCL19, it was decided to focus mainly upon this chemokine's interactions with CCX-CKR. In comparison, the other CCL19 receptor, CCR7 was to be used, a receptor which couples to intracellular signaling cascades and mediates chemotaxis following ligation. Before this project commenced, detailed biochemical studies of CCR7/CCL19 interactions had not, to my knowledge, been done. Thus, to compare the biochemistry of these two receptors, it was planned to generate various cell HEK293 lines expressing either human CCX-CKR or human CCR7, both with an N-terminal epitope tag and/or C-terminal GFP to allow receptor detection using antibodies and fluorescent visualisation. A HEK293 cell line expressing human CCX-CKR with an N-terminal FLAG epitope (DYKDDDD) was already available (described in Gosling et al., 2000). These cells are referred to hereafter as HEK-hCCX-CKR cells. Unlike untransfected counterparts, these cells showed displaceable binding to  $^{125}\text{I}$ -CCL19 and surface receptor could be detected using the anti-FLAG M1 antibody (Figure 3.1.1 and Gosling et al., 2000). Other cell lines generated are outlined below. A schematic of all tagged chemokine receptors planned for this study (and the plasmids generated to express them) can be found in figure 3.1.2.

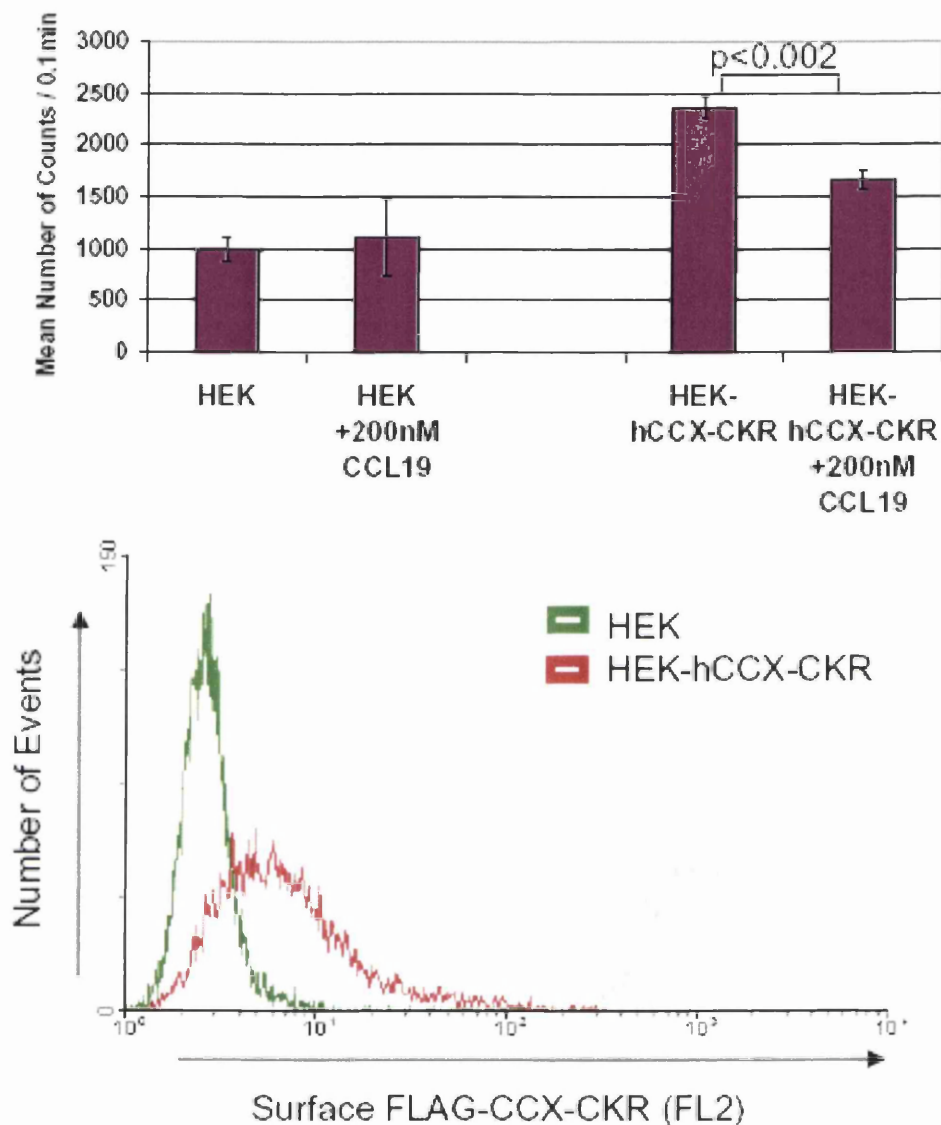


**Figure 3.1.1: <sup>125</sup>I-CCL19 Binding and CCX-CKR Surface Expression by HEK-hCCX-CKR Cells.** Top panel shows displaceable binding of <sup>125</sup>I-CCL19 by HEK-hCCX-CKR but not untransfected HEK293 cells. Inclusion of 200nM unlabelled CCL19 competes for binding of radioligand at 4°C on receptor transfectants only. Each sample was performed in triplicate and error bars shown are +/- the standard deviation. Statistical analysis was performed using a Student's t-test. Repeat experiments gave similar results (n=2). Lower panel shows detection FLAG epitope at 4°C on HEK-hCCX-CKR and untransfected HEK293 cells. Using the anti-FLAG M1 antibody and secondary detection with anti-mouse IgG -PE, surface expression can be detected on HEK-hCCX-CKR cells. Data shown is representative of that collected in 6 independent experiments.

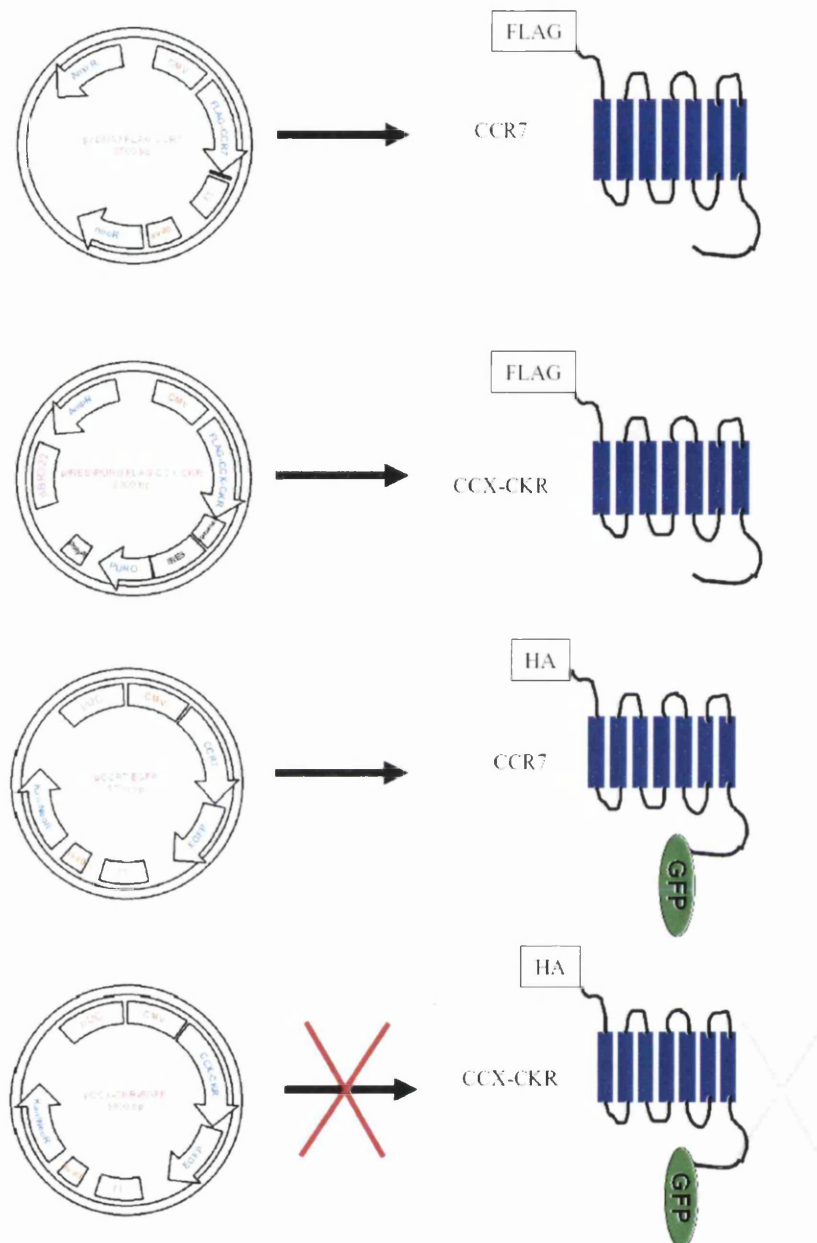


**Figure 3.1.2: Plasmids and Tagged Receptors used in Study:** Schematic representation of constructs on left hand side with resulting proteins being expressed on right hand side. Expression of the CCX-CKR-GFP protein was not detected (see text for details), illustrated by the red-cross.

### 3.1.1.1 FLAG tagged CCR7

A PCR-based strategy (see 2.2.1.12) was used to insert DNA encoding the FLAG epitope between nucleotides encoding the first 2 amino acids of hCCR7 to enable subsequent protein detection with the same antibody used to detect hCCR7. This was then cloned

into pcDNA3.1 and verified by DNA sequencing before the construct was stably transfected into HEK293 cells, a cell line which does not express any detectable endogenous chemokine receptors and has been shown to be capable of high levels of chemokine receptor surface expression following transfection with similar constructs (Blackburn et al., 2004; Weber et al., 2004). These cells are referred to hereafter as HEK-hCCR7 cells. As can be seen in figure 3.1.3, HEK-hCCR7 cells bound  $^{125}\text{I}$ -CCL19 and this could be competed by excess unlabelled CCL19. Notably, uncompeted binding was consistently significantly higher (2-3x) than that observed for HEK-hCCX-CKR cells. However, surface CCR7 could only be detected with the anti-CCR7 antibody and not with the anti-FLAG antibody. This could be due to the fact that the anti-FLAG antibody is not of high enough affinity to detect the receptor at the cell surface (although it is of high enough affinity to detect FLAG-hCCX-CKR), or alternatively the FLAG epitope may be in some way unavailable to the antibody in the context of hCCR7.

### **3.1.1.2 GFP Fusion HA Tagged Receptors**

Constructs encoding hCCX-CKR and hCCR7 with a C terminal GFP fusion were generated (2.2.1.12) and stably transfected into HEK293 cells by selection in G418. Untagged GFP was used as a control. The presence of GFP+ cells was assessed by fluorescence microscopy or flow cytometry. With hCCR7-GFP, stably transfected GFP+ cells were evident, with CCR7 causing the GFP to localise predominantly to the cell surface (data not shown). However, despite using two distinct GFP fusion vectors (see 2.2.1.12.3) and successfully generating G418 resistant cell lines, GFP+ cells were never seen after transfection with plasmids encoding CCX-CKR-GFP fusion proteins. There could be several explanations for this. First, the structure of CCX-CKR may interfere with the fluorescence of GFP when the two proteins are fused in this way. Second, this fusion protein may be highly toxic to cells which express it, preventing positive cells from being

identified. Whatever the reason for this difficulty, this inability to produce fluorescently tagged CCX-CKR unfortunately prevented future experiments where visualisation or quantification of this receptor was desirable. Thus, all subsequent experiments used HEK-hCCR7 and HEKhCCR7 cells, unless otherwise stated.

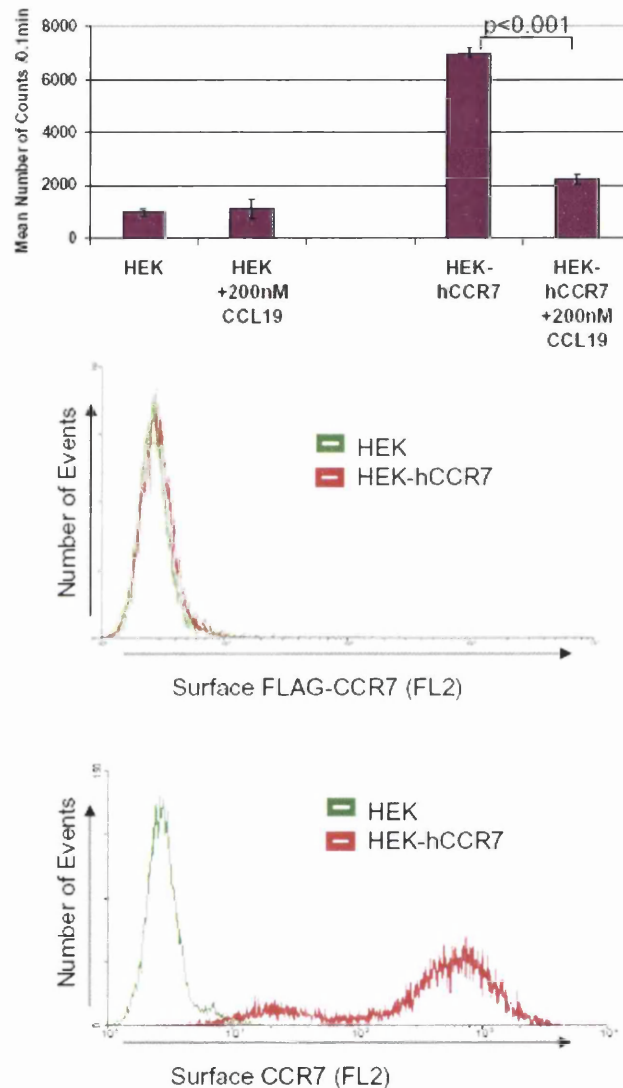


**Figure 3.1.3:**  $^{125}$ I-CCL19 Binding and Surface CCR7 expression by HEK-hCCR7 Cells. Top panel: Displaceable radioligand binding detected on HEK-hCCR7 cells. Each sample was performed in triplicate and error bars shown are  $\pm$  the standard deviation. Statistical analysis was performed using a Student's t-test. Repeat experiments gave similar results ( $n=2$ ). Middle panel: Histogram of flow cytometric analysis showing surface FLAG-CCR7 not detectable on HEK-hCCR7 cells using anti-FLAG M1 antibody. Lower panel: Histogram of flow cytometric analysis of surface CCR7 detection using an anti-CCR7 antibody and anti-mouse IgG-PE secondary. Data shown is representative of that collected in 6 independent experiments.

### **3.1.2 Internalisation and Degradation of CCL19 by its Receptors**

Both CCR7 and CCX-CKR bind CCL19, and other chemokines. In the case of CCR7, this results in the transduction of signals that orchestrate the chemotactic migration of the receptor-expressing cell. This does not occur after CCL19 binding to CCX-CKR. CCR7 activation by CCL19 also generates signals that lead to CCR7 desensitisation, and internalisation of CCL19/CCR7 complexes. Studies on one of the other atypical chemokine receptors, D6, ongoing in the lab at the start of the project, and reported recently (Weber et al., 2004), were revealing that this molecule was able to internalise and retain its chemokine ligands, which were then subsequently targeted for degradation. D6, like CCX-CKR, appears to be silent after chemokine binding, and rather than using ligand-driven signals to bring about receptor internalisation instead achieves chemokine sequestration through constitutive receptor trafficking to and from the cell surface. This internalisation is not desensitised by chemokine exposure. These biochemical properties provided support for the D6 ‘decoy’ hypothesis further validated by more recent studies on D6 *null* mice (de la Torre et al., 2005; Jamieson et al., 2005). Thus, the question arose as to whether CCX-CKR also exhibited biochemical properties consistent with a role as a chemokine-sequestering decoy or transport receptor. To address this, experiments were initiated to first investigate whether CCX-CKR could internalise CCL19, and if so determine the fate of this internalised ligand. Throughout, for comparative purposes, the typical CCL19 receptor CCR7 was studied.

#### **3.1.2.1 CCL19 Internalisation**

##### **3.1.2.1.1 Optimisation of Radioligand Internalisation Assay**

To investigate CCL19 internalisation by receptor transfectants, experiments were initiated to assess whether receptor associated <sup>125</sup>I-CCL19 could, after incubation at 37°C, become resistant to washing with acidic salt solutions (2.2.4.1). Such approaches provide an

indication of internalisation and have been used previously in work investigating D6 and other chemokine receptors (Fra et al., 2003; Weber et al., 2004). In order to do this, it was first necessary to demonstrate that the chemokine remaining at the cell surface could be effectively stripped off by specific acid wash solutions. Therefore different strength acid washes were tested for their ability to remove  $^{125}\text{I}$ -CCL19 bound to HEK-hCCX-CKR cells at  $4^{\circ}\text{C}$ . As shown in figure 3.1.4, acid wash C most effectively removed  $^{125}\text{I}$ -CCL19 reducing the total numbers of cell-associated counts to levels seen with untransfected HEK293 cells. Similar results were obtained with HEK-hCCR7 cells (data not shown). Thus, acid wash C was used in all subsequent experiments.

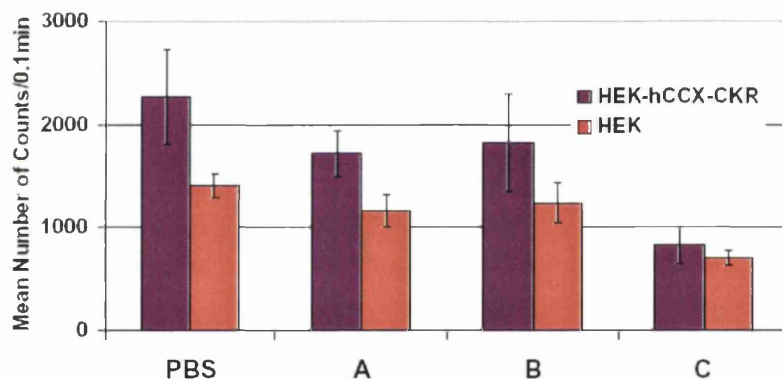


**Figure 3.1.4: Optimisation of Acid Wash.** Harvested HEK-hCCX-CKR or untransfected HEK293 cells were loaded at  $4^{\circ}\text{C}$  with  $^{125}\text{I}$ -CCL19 and then washed in either PBS, Wash A: 50nM Glycine /0.1M NaCl pH3, Wash B: 0.15M NaCl / 0.005M acetic acid or Wash C: 0.5M NaCl / 0.2M acetic acid. Cell pellets were then counted. The amount of radioactivity stripped by the wash from the cell surface was then assessed by comparison to PBS washed cells. Each sample was performed in triplicate and error bars shown are +/- the standard deviation. Statistical analysis was performed using a Student's t-test. Acid wash C effectively strips specifically bound radioligand from HEK-hCCX-CKR cells ( $p < 0.01$ ). A repeat experiment gave similar results ( $n=2$ ).

### 3.1.2.1.2 CCX-CKR and CCR7 Internalise Bound $^{125}\text{I}$ -CCL19

Next, HEK-hCCR7 and HEK-hCCX-CKR cells, loaded with  $^{125}\text{I}$ -CCL19, were incubated at  $37^{\circ}\text{C}$  prior to acid washing. As expected, acid washing then failed to remove much of the

radioactivity from HEK-hCCR7 cells, consistent with ligand internalisation, and indicating that the acid wash conditions used do not disrupt cell integrity to release internalised material (Figure 3.1.5). The majority of radioactivity associated with HEK-hCCX-CKR cells also became acid resistant after shift to 37°C. These data suggest that both CCR7 and CCX-CKR internalise  $^{125}\text{I}$ -CCL19 at 37°C. Next, more detailed analysis of the kinetics of this internalisation was undertaken by shortening the 37°C incubation time (Figure 3.1.6). Again, both cell lines internalise >95% of surface  $^{125}\text{I}$ -CCL19 within 15min of shifting to 37°C. However, differences in the precise kinetics of this internalisation were observed, with HEK-hCCX-CKR cells having internalised ~90% of surface  $^{125}\text{I}$ -CCL19 after 2min, while HEK-hCCR7 cells had internalised only ~40%.

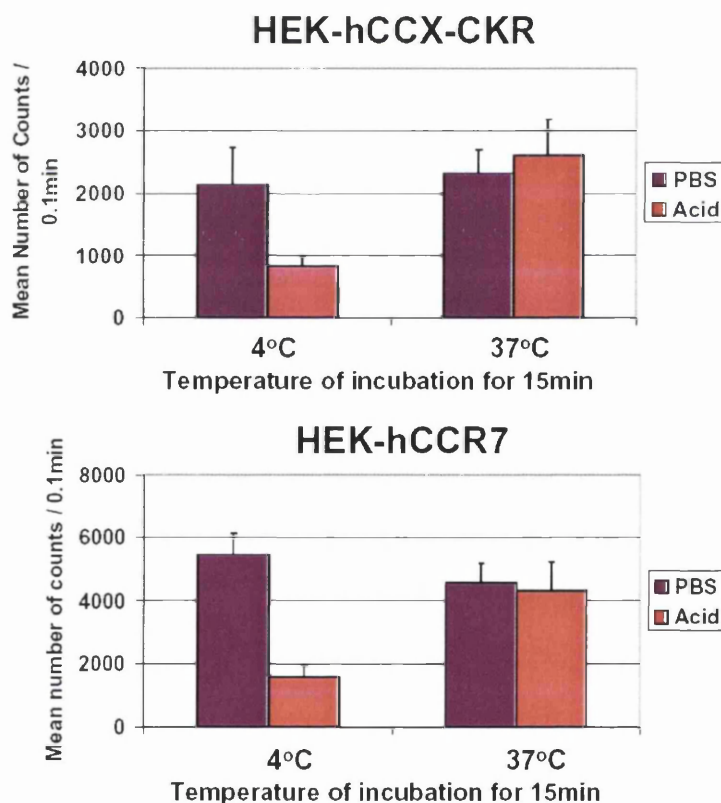


**Figure 3.1.5: Internalisation of  $^{125}\text{I}$ -CCL19 by HEK-hCCX-CKR and HEK-hCCR7.** Cells were loaded with  $^{125}\text{I}$ -CCL19 at 4°C, then incubated either at 4°C or 37°C for 15 min. Cells were then washed in either PBS or Acid wash C and the number of counts associated with cell pellets then assessed. Incubation at 37°C causes the cell associated radioactivity to become resistant to acid washing ( $p < 0.01$  for both cell lines). Each sample was performed in triplicate and error bars shown are +/- the standard deviation. Repeat experiments gave similar results ( $n=6$ ).

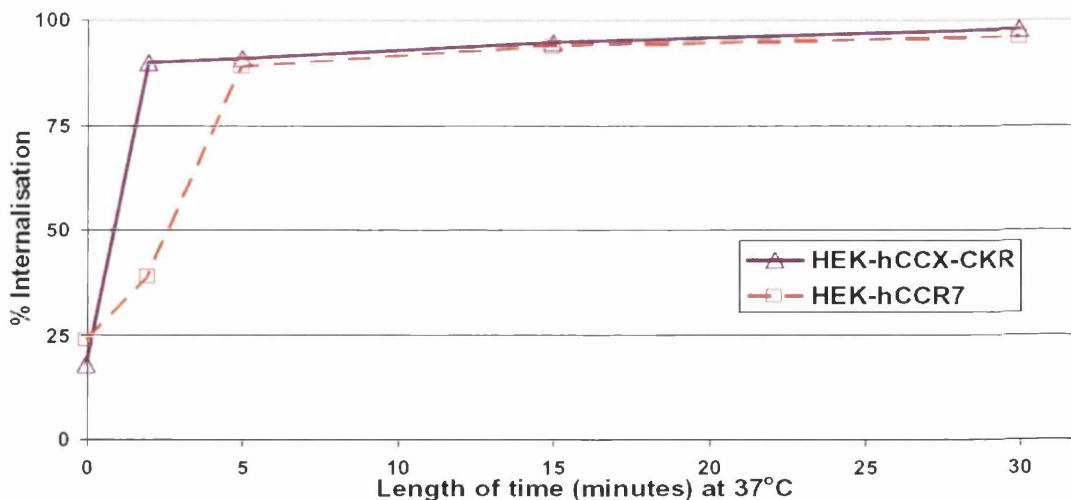


**Figure 3.1.6: Kinetics of  $^{125}\text{I}$ -CCL19 Internalisation by HEK-hCCX-CKR and HEK-hCCR7.** Cells were loaded with  $^{125}\text{I}$ -CCL19 at 4°C, then incubated either at 4°C for the duration of the assay, or 37°C for 2-30min, then back to 4°C. Cells were then washed in either PBS or Acid wash C and the number of counts associated with cell pellets then assessed. The percentage internalisation at each time-point was determined by the ratio of acid resistant- to acid-sensitive radioactivity associated with the cell pellet. Each sample was performed in triplicate and data shown is representative of 5 independent experiments.

### 3.1.2.1.3 Internalisation of Biotinylated CCL19/ Streptavidin-Cy3

To further examine CCL19 internalisation by CCX-CKR and CCR7, assays using biotinylated CCL19 (BioCCL19) were developed. This reagent contains a single biotinylated lysine residue at the C-terminus of CCL19, and retains full biological activity. Complexes of BioCCL19 associated with fluorescent streptavidin can be created by incubation of the two at room temperature (see 2.2.4.7), and these complexes can be fed to cells. This allows fluorescent detection of BioCCL19 and is an assay that has proved to be of considerable utility in quantifying CCL19 uptake, as will be outlined later. However, here it has been used simply to demonstrate CCL19 uptake by cells. Careful optical dissection of cells using confocal microscopy revealed that BioCCL19 complexed with streptavidin-Cy3 (BioCCL19/Cy3) rapidly accumulated (within 5min of incubation at 37°C) in endosomal-like structures of HEK-hCCX-CKR cells and HEK-hCCR7 cells, but

did not enter untransfected HEK293 cells (Figure 3.1.7). In addition, receptor transfectants treated with streptavidin-Cy3 alone, failed to accumulate fluorescence (not shown).

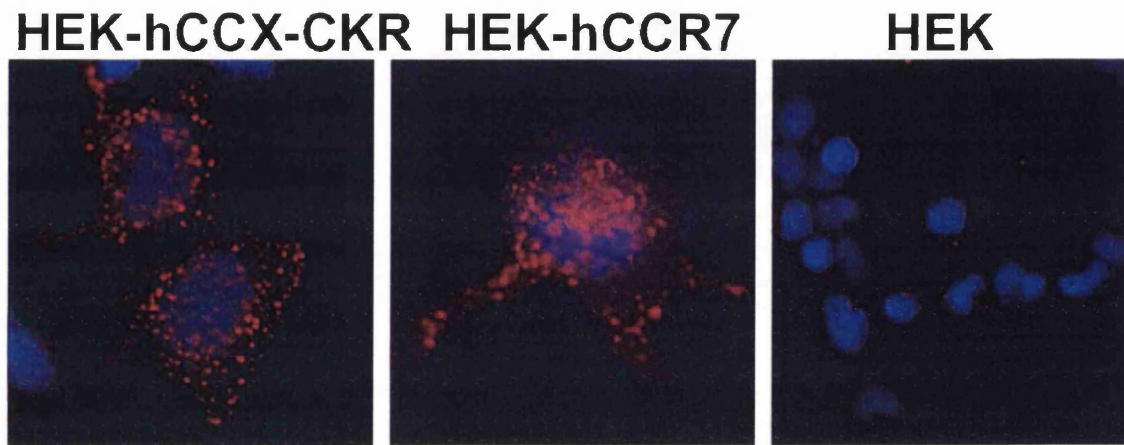


**Figure 3.1.7: Internalisation of BioCCL19/Cy3 by HEK-hCCX-CKR and HEK-hCCR7.** Cells adhered to fibronectin coverslips were incubated with complexes of BioCCL19/Cy3 at 37°C for 15min. Cells were then washed and fixed, and the coverslips mounted with Vectashield with DAPI (blue) for nuclear visualisation. Cells were then analysed by confocal microscopy. Extensive BioCCL19/Cy3 uptake could be seen in most cells from HEK-hCCX-CKR and HEK-hCCR7 slides (left hand panels) but not in untransfected HEK293 cells (right hand panel). Careful optical sections of cells were made to confirm intracellular localisation of red fluorescence. Images shown are representative of those observed in many fields of view.

### 3.1.2.2 Fate of Internalised CCL19

The data above clearly demonstrate that both CCR7 and CCX-CKR internalise CCL19. As discussed in the introduction, the chemokine receptor D6 is able to more readily retain and degrade its internalised cargo than the conventional chemokine receptor CCR5 (Weber et al., 2004), a property that may conceivably aid its *in vivo* decoy function (Jamieson et al., 2005). Thus, experiments were initiated to compare the fate of labelled CCL19 internalised through CCX-CKR or CCR7.

### 3.1.2.2.1 Degradation of Preloaded $^{125}\text{I}$ -CCL19 by CCX-CKR and CCR7

Cells were loaded with  $^{125}\text{I}$ -CCL19 at 4°C, washed, resuspended in medium, and incubated at 37°C for 15-120min (2.2.4.2). Cell pellets and supernatant fractions were then collected and the supernatants precipitated in TCA, an approach used previously to distinguish degraded from intact protein (Fra et al., 2003; Weber et al., 2004). The amount of radiolabel associated with different fractions of the cell was then determined. It should be noted however that TCA-precipitable fractions do not necessarily consist entirely of intact protein, as some partially degraded polypeptides may still precipitate under these conditions. Thus, to further examine CCL19 integrity, supernatants and cell lysates were examined by SDS-PAGE (2.2.1.13). Importantly, preliminary experiments had shown that untransfected HEK293 cells had minimal amounts of radioligand associated with them following 4°C loading, with the majority of counts associated with the TCA precipitable fraction of the supernatant (data not shown).

With HEK-hCCX-CKR cells, radiolabel was predominantly associated with the cells at early time-points, but over time began to appear in the TCA-soluble (degraded) fraction of the supernatant (Figure 3.1.8A). Indeed, after 2h at 37°C, ~90% of the recovered counts from HEK-hCCX-CKR fractions can be found in this fraction, indicating that the radioactivity is being expelled from the cells in a TCA-soluble, and presumably degraded form. No counts above background levels could be detected in the TCA-precipitable fraction, suggesting that CCL19 internalised by CCX-CKR is not subsequently released in an intact form. In contrast, radiolabel internalised by HEK-hCCR7 cells remains predominantly associated with the cell pellet throughout the time-course studied. A reduction in counts from these cell pellets was observed, but this was not as rapid as that seen for HEK-hCCX-CKR cells, with >50% of total recovered counts remaining in the cell

pellet after 120mins. Furthermore, at 120mins, a small but significant percentage (10-15%) of the radiolabel released from these cells was in the TCA-precipitable supernatant fraction, suggesting that a proportion of the ligand internalised through CCR7 is released intact.

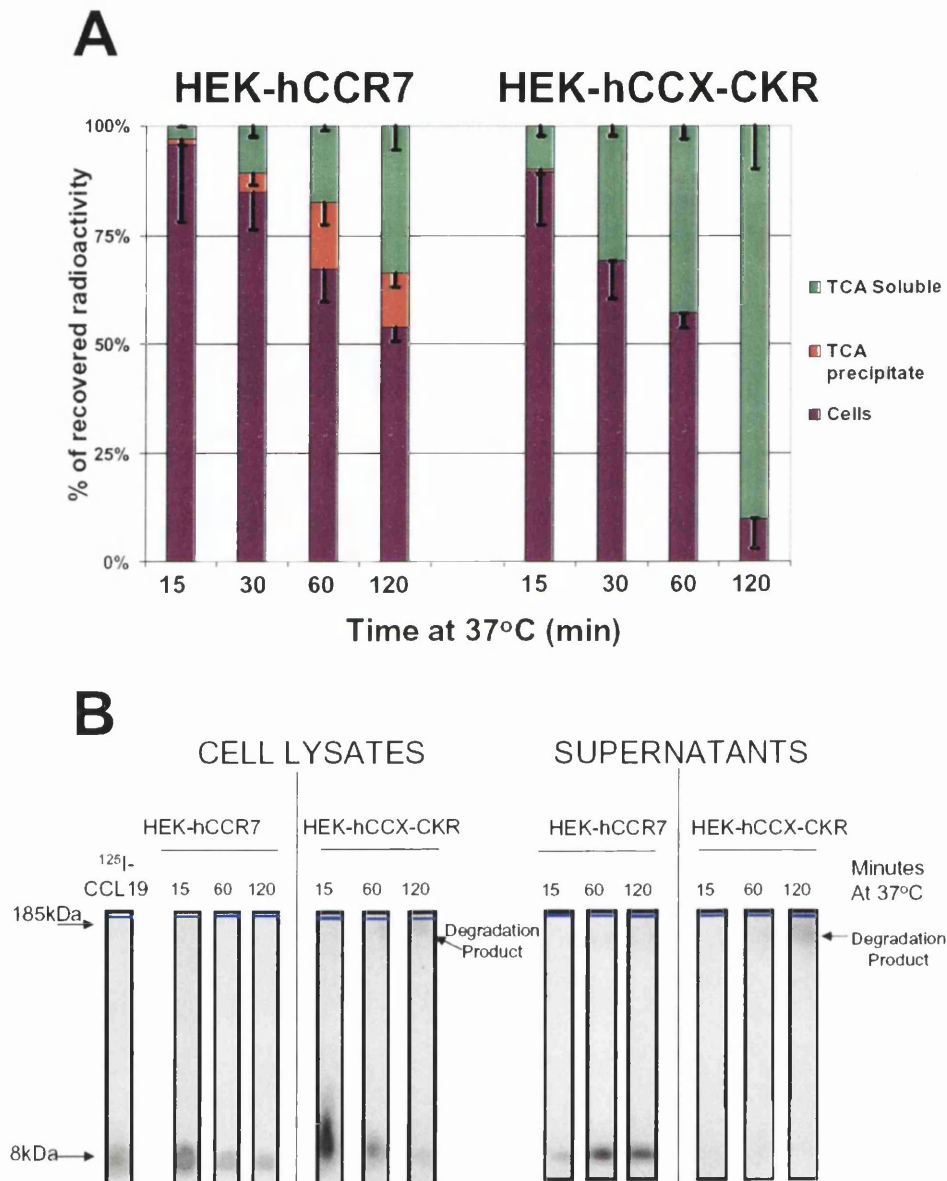


**Figure 3.1.8: Degradation of <sup>125</sup>I-CCL19 by HEK-hCCX-CKR and HEK-hCCR7 Cells.** Cells were loaded at 4°C with <sup>125</sup>I-CCL19 and then shifted to 37°C for 15 min to allow internalisation. Cells were then washed, resuspended, and incubated at 37°C for 15-120min. Cell pellets were harvested and supernatants subjected to TCA precipitation. The proportion of counts associated with each fraction is illustrated in (A). Each sample was performed in triplicate and counts in each fraction associated with untransfected HEK293 cells subtracted from those in transfected cells. Repeat experiments gave similar results. Cell lysates and supernatants from the experiment were analysed by SDS-PAGE (B). Blue lines indicate top of gel. <sup>125</sup>I-CCL19 runs at approximately 8kDa. A high mobility smear band becomes apparent in some samples, indicative of chemokine degradation.

Cell lysates and supernatants were then analysed by SDS-PAGE (see 2.2.1.13). As can be seen in figure 3.1.8B,  $^{125}\text{I}$  associated with the cells is mainly found in a band which runs coincident with  $^{125}\text{I}$ -CCL19, indicating that it has undergone little, if any, modification. As expected, the relative amount of cell-associated radioactivity reduced over time, more rapidly in HEK-hCCX-CKR than HEK-hCCR7 cells. The disappearance of intact  $^{125}\text{I}$ -CCL19 from HEK-hCCX-CKR cell lysates coincides with the emergence of radioactivity which does not enter the gel properly, running as a diffuse upper smear, perhaps indicating a degradation product. When supernatants were analysed, barely detectable intact  $^{125}\text{I}$ -CCL19 emerges from HEK-hCCX-CKR cells. The diffuse upper smear seen in the cell pellets begins to accumulate over time in the supernatants also. In HEK-hCCR7 cells, this putative degradation product also becomes evident over time in the supernatants but an increase in the intact  $^{125}\text{I}$ -CCL19 also occurs at late timepoints, in concurrence with data in figure 3.1.8A. Together, these data indicate that CCL19, internalised via CCX-CKR, is more readily retained in cells, and degraded.

### **3.1.2.2.2 Dissociation of CCL19 from CCX-CKR and CCR7**

Studies with D6 had revealed that affinity for its ligand, CCL3-L1, decreased as pH was lowered from pH7 (Weber et al., 2004). This was in contrast to CCR5 which showed increased affinity for CCL3-L1 at these mildly acidic pHs. This was hypothesized to explain the tendency for ligand internalised by D6 to be retained in cells, while CCL3-L1 internalised by CCR5 could recycle intact out of the cell, still associated with receptor (Weber et al., 2004). Therefore, the more pronounced ligand degradation and retention observed in HEK-hCCX-CKR cells, compared to HEK-hCCR7 cells, could be explained by differing abilities of these two receptors to hold on to CCL19 at the low pHs encountered in endosomes. To test this, radioligand dissociation assays were performed at low pHs (see 2.2.4.5). As can be seen in figure 3.1.9,  $^{125}\text{I}$ -CCL19 bound to hCCR7 was relatively

resistant to alterations in the pH, with no significant differences at pH7 and pH6 compared with PBS washed cells. A significant reduction in binding was observed at pH5, but ~80% of the  $^{125}\text{I}$ -CCL19 still remained bound to CCR7. In contrast, ligand bound to hCCX-CKR was much more susceptible to displacement by increasing acidity. Washing at pH7 displaced ~25% of bound  $^{125}\text{I}$ -CCL19 while cells washed at pH6 and pH5 showed a 70-80% reduction in bound ligand. These data clearly demonstrate a difference in the sensitivity of CCL19 binding to low pH between these two receptors. This presents a model, similar to that proposed for D6 and CCR5 (Weber et al., 2004), that in acidifying endosomes CCX-CKR rapidly releases its cargo into the cell while CCR7 is less-inclined to do so, leading to the observed differences in ligand fate after internalisation via these receptors.

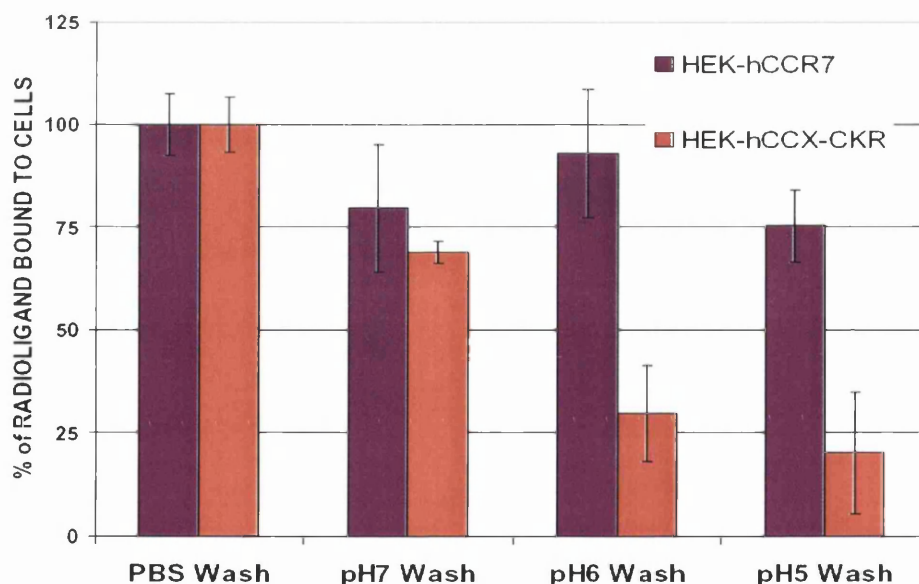


**Figure 3.1.9: Effect of Alterations in pH on  $^{125}\text{I}$ -CCL19 Binding to CCX-CKR and CCR7.** Harvested cells were loaded with radioligand at  $4^{\circ}\text{C}$  for 1h then washed for 5 min in either PBS or medium with the pH adjusted between pH7-pH5. Cell pellets were then counted to assess to percentage of radioligand remaining bound to the cells, relative to those washed in PBS alone. Each sample was performed in triplicate and error bars represent +/- the standard deviation. Statistical analysis was performed using a Student's t-test. pH adjusted washes reduced the binding of radioligand to HEK-hCCX-CKR cells compared with PBS washed cells ( $p < 0.01$ ). Repeat experiments gave similar results ( $n=3$ ).

### 3.1.2.2.3 Effect of Cold Competitor and Endosomal Neutralisation

One prediction of this model is that neutralisation of vesicle acidification, by  $\text{NH}_4\text{Cl}$  for example, should i) prevent lysosome-mediated ligand destruction, and ii) disrupt intracellular ligand retention, thus permitting enhanced intact chemokine re-emergence. Indeed, this is what is observed after D6-mediated internalisation of CCL3-L1 (Weber et al., 2004). Thus, experiments identical to those above were performed, except 50mM  $\text{NH}_4\text{Cl}$  was included in the medium (2.2.4.2). In addition, to ensure that all re-emerging radioligand was effectively displaced from the cell surface, unlabelled competitor CCL19 (present in large excess) was added during the degradation phase of the assay. This will limit re-internalisation of radioligand by competing for the re-emerging receptor. Thus, once HEK-hCCX-CKR and HEK-hCCR7 cells had been pre-loaded with  $^{125}\text{I}$ -CCL19, 200nM unlabelled CCL19 and/or 50mM  $\text{NH}_4\text{Cl}$  was added and the fate of the  $^{125}\text{I}$ -CCL19 gauged in comparison to samples free of these additives. The data from these experiments is shown in figure 3.1.10. First, it is of note that  $\text{NH}_4\text{Cl}$  inhibited the accumulation over time of counts in the TCA-soluble supernatant fraction from HEK-hCCX-CKR cells, indicating that chemokine degradation is being inhibited by endosomal neutralisation. However, surprisingly, the inclusion of unlabelled CCL19 alone to HEK-hCCX-CKR cells, loaded with internalised  $^{125}\text{I}$ -CCL19, caused a significant increase in the proportion of TCA-precipitable counts in the supernatant from these cells. Analysis of supernatants by SDS-PAGE confirmed that the extra counts released into the supernatant were electrophoretically indistinguishable from unmodified  $^{125}\text{I}$ -CCL19 (data not shown). Thus, after 30min at  $37^\circ\text{C}$ , ~30% of the counts were outside the cell in apparently non-degraded form. This proportion did not increase as the assay progressed, indicating that release of intact CCL19 only occurred early on, rather than continuously, after the addition of excess unlabelled extracellular ligand. These data suggest that a proportion of CCL19 internalised

by CCX-CKR recycles back to the cell surface in the first 30min following internalisation. When both unlabelled CCL19 and  $\text{NH}_4\text{Cl}$  were present during the assay, the release of TCA soluble radioactivity from HEK-hCCX-CKR cells was prevented as expected, and whilst TCA precipitable counts were released into the supernatant the  $\text{NH}_4\text{Cl}$  did not increase the amount of radioactivity in this fraction.

With HEK-hCCR7 cells, as seen in previous experiments, intact  $^{125}\text{I}$ -CCL19 was released in the absence of unlabelled extracellular competitor. When excess unlabelled CCL19 was included, release of intact chemokine by HEK-hCCR7 cells was marginally increased. The extra release of intact  $^{125}\text{I}$ -CCL19 caused by unlabelled competitor from HEK-hCCR7 cells did not inhibit the relatively small fraction of chemokine which was degraded by these cells.  $\text{NH}_4\text{Cl}$  reduced the release of degraded material by HEK-hCCR7 cells though the addition of unlabelled competitor CCL19 did not noticeably change the distribution of radiolabel.

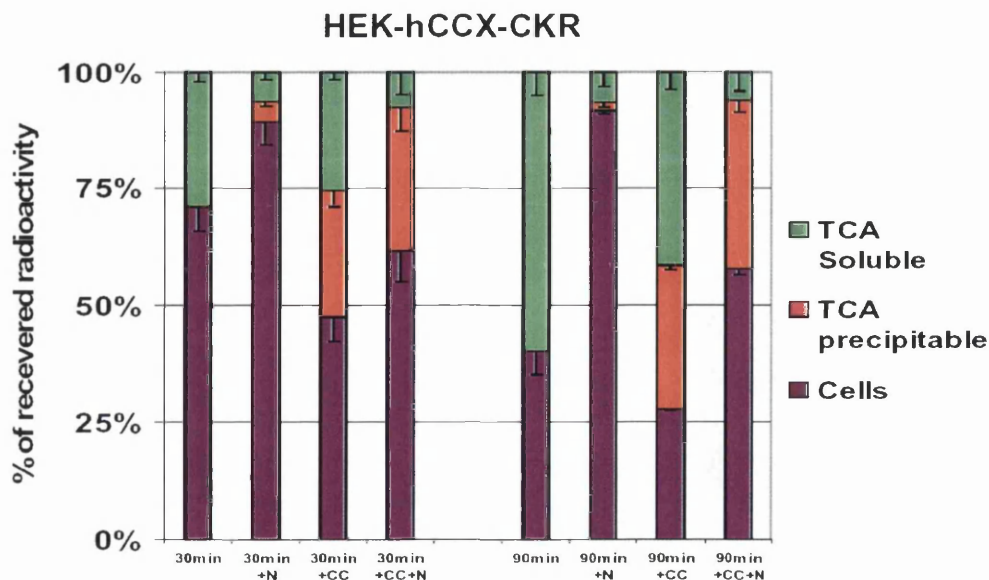


**Figure 3.1.10: Effect of Cold Competitor and Endosomal Neutralisation.** This figure is continued overleaf. Refer to the legend on next page for details.

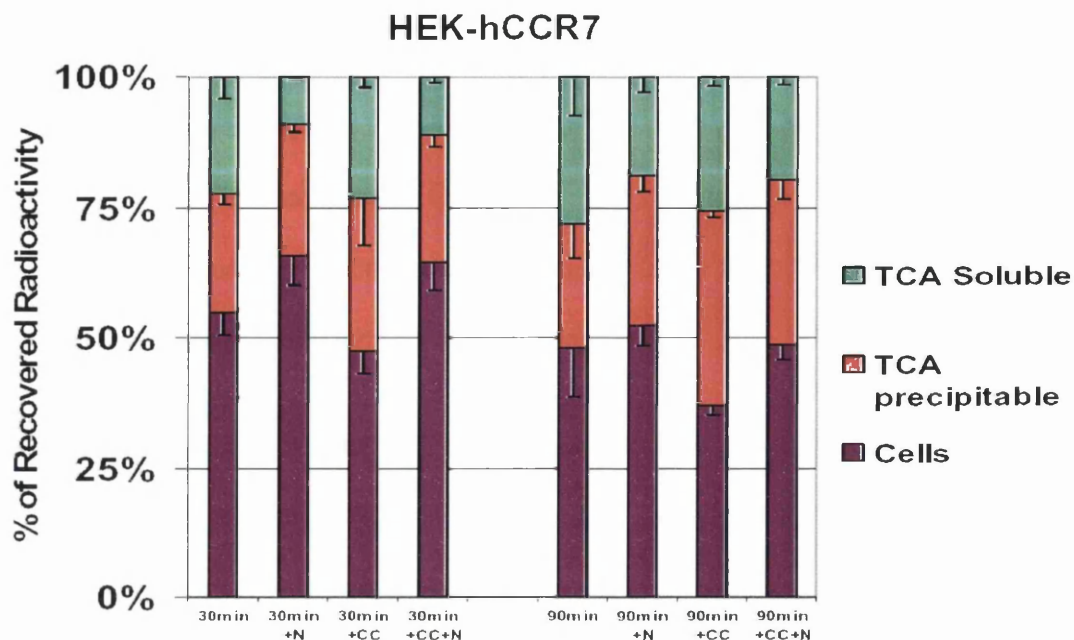


**Figure 3.1.10: Effect of Cold Competitor and Endosomal Neutralisation.** Cells were harvested and loaded with  $^{125}\text{I}$ -CCL19 at  $4^\circ\text{C}$  and then incubated at  $37^\circ\text{C}$  for 15 min to allow internalisation. Cells were then washed and resuspended in medium alone or medium which contained either 200nM CCL19 (+CC), 50mM  $\text{NH}_4\text{Cl}$  (+N), or both (+CC+N). Cells were then incubated at  $37^\circ\text{C}$  for up to 90min. Supernatants were then subjected to TCA precipitation and the radioactivity associated with cells and supernatant fractions counted. The proportion of recovered counts residing in each fraction is from HEK-hCCX-CKR and HEK-hCCR7 cell illustrated in the graphs on the previous and current page, respectively. Each sample was performed in triplicate and is shown as the mean  $\pm$  the standard deviation. Repeat experiments gave similar results.

Taken together, these data suggest the following regarding the comparative biochemistry of CCX-CKR and CCR7:

- i)  $^{125}\text{I}$ -CCL19 internalised by CCX-CKR is degraded and this degradation is dependent upon endosomal acidification (inhibited by  $\text{NH}_4\text{Cl}$ ).
- ii) A proportion of  $^{125}\text{I}$ -CCL19 internalised by CCR7 is also degraded (via a  $\text{NH}_4\text{Cl}$  sensitive pathway).

- iii) A proportion (~30%) of  $^{125}\text{I}$ -CCL19 internalised by CCX-CKR is not targeted immediately for degradation and recycles to the cell surface where its release from cells requires the presence of unlabelled competitor. A significant fraction of CCR7-internalised CCL19 is released intact from the cell, mainly independently of the presence of unlabelled extracellular competitor, and this can be increased by neutralising endosomal acidification.

These data are confusing and clearly influenced by the trafficking properties of the receptors and their affinity for CCL19. Nonetheless, what they do demonstrate is that although there are clear differences between the behaviour of CCR7 and CCX-CKR, these differences are not huge. Internalisation via CCX-CKR appears to favour CCL19 degradation compared with that mediated by CCR7, but ligand internalised by either receptor can be degraded or released intact. These data do not demonstrate a specific specialisation of CCX-CKR for ligand sequestration.

#### **3.1.2.2.4 CCL19 Degradation in Continuous Culture**

Data thus far indicate that both receptors (CCR7 and CCX-CKR) internalise ligand, and although there are some differences in the fate of the internalised CCL19, both mediate at least some CCL19 removal and destruction. However, all the above experiments were short-term, and following a single round of ligand internalisation. It is known that desensitisation and receptor degradation limit repeated stimulation of typical chemokine receptors. Thus, to examine the long-term impact of CCL19 sequestration by CCR7 and CCX-CKR, a more physiological bulk culture degradation assay was developed. For each cell line,  $7.5 \times 10^6$  cells were incubated in 6ml of binding buffer containing 10nM unlabelled CCL19. A trace amount of  $^{125}\text{I}$ -CCL19 (0.1nM) was included to allow subsequent tracking of chemokine fate. The cells were incubated for several days at 37°C, with supernatants

being periodically sampled and subjected to TCA-precipitation to assess chemokine degradation (see 2.2.4.2). Surprisingly, despite the ability of both receptors to bind, internalise, and degrade CCL19 in the short term assays described above, there were dramatic differences in the behaviour of HEK-hCCX-CKR and HEK-hCCR7 cells in this assay (Figure 3.1.11). After 12h, the majority (>60%) of counts from the culture supernatants of HEK-hCCX-CKR cells lie in the TCA-soluble (degraded) fraction, while those from HEK-hCCR7 cells precipitate with TCA (intact). By 24h, HEK-hCCX-CKR cells had degraded ~85% of the chemokine, while HEK-hCCR7 cells were no more effective at destroying intact chemokine than untransfected HEK293. When the number of degraded CCL19 molecules is considered in this assay, the differences between HEK-CCX-CKR and HEK-hCCR7 cells seems even more dramatic. Indeed, after 48h of culture, in excess of  $2 \times 10^{13}$  more CCL19 molecules have been degraded by HEK-hCCX-CKR cells (figure 3.1.11). In fact, it can be calculated that over 48h, HEK-hCCX-CKR cells degrade  $\sim 10^5$  molecules of CCL19 per cell per hour.

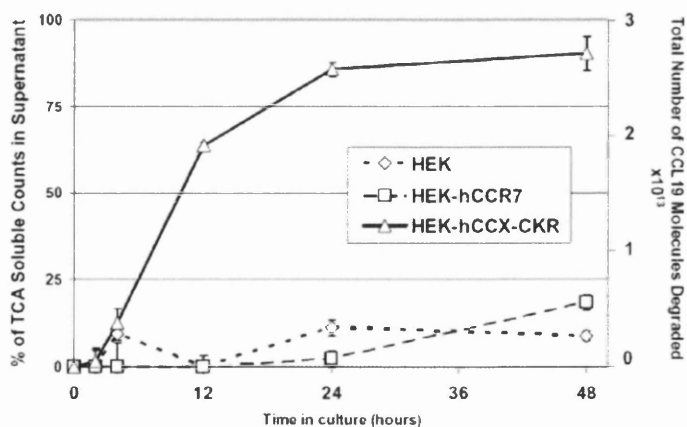


**Figure 3.1.11: Degradation of CCL19 by HEK-hCCX-CKR Cells in Continuous Culture.** Cells were cultured for 48h, before 6ml of fresh medium was added containing 10nM CCL19, of which 0.1nM was radiolabelled. Supernatants were sampled over the next 48h and subjected to TCA precipitation. CCL19 degradation was assessed by the proportion of counts in the TCA soluble and TCA precipitate fractions. Samples were performed in triplicate. Error bars are +/- the standard deviation and repeat experiments gave similar results (n=2). Statistical analysis was performed by a Student's t-test and  $p < 0.001$  at all timepoints measured after 12 hours between HEK-hCCX-CKR and other cell lines. The ~number of degraded CCL19 molecules was calculated (# of CCL19 molecules added to each flask was  $\sim 3 \times 10^{13}$ ).

To further analyse extracellular chemokine during these experiments, samples of supernatant were analysed by SDS-PAGE. As figure 3.1.12 clearly shows,  $^{125}\text{I}$ -CCL19 incubated with untransfected or HEK-hCCR7 cells remains predominantly intact throughout the course of the experiment. A slight reduction in the amount of extracellular  $^{125}\text{I}$ -CCL19 is observed in supernatants from HEK-hCCR7 cells when compared with untransfected cells. In contrast, intact chemokine becomes markedly less evident in HEK-hCCX-CKR supernatants as the experiment progresses. The disappearance of this band from these supernatants occurs concurrently with the appearance of a diffuse smear running at high molecular weight, similar to that seen in previous experiments, indicative of a  $^{125}\text{I}$ -CCL19 degradation product.

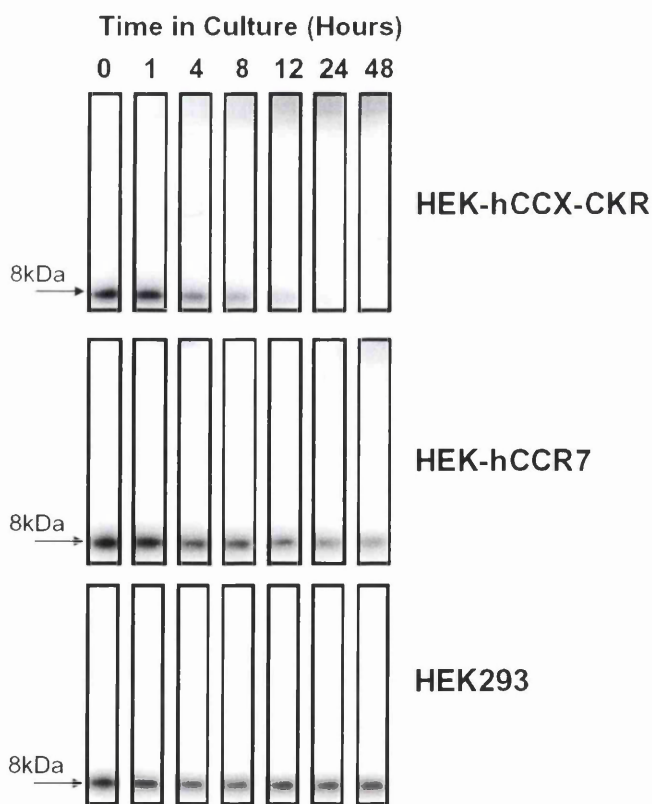


**Figure 3.1.12: SDS-PAGE Analysis of Supernatants from Continuous Culture with CCL19.** 50 $\mu\text{l}$  of supernatants from the experiment shown in figure 3.1.11 were analysed by SDS-PAGE. The gel was dried onto filter paper and exposed to X-ray film. A band of approximately 8kDa is visible, showing intact  $^{125}\text{I}$ -CCL19. High mobility smear bands are visible in supernatants from HEK-hCCX-CKR cells which have been cultured for more than 4h.

Finally, to exclude the possibility that HEK-hCCX-CKR cells release a soluble CCL19 degrading factor (possibly in response to CCL19), rather than breaking down the chemokine within the cells, supernatants were prepared from HEK-hCCX-CKR cells which had been incubated with or without 10nM unlabelled CCL19 for 9h (referred to as 'primed' or 'untreated', respectively). These supernatants were then assessed for their ability to degrade  $^{125}\text{I}$ -CCL19. It was anticipated that only 5nM CCL19 would remain in the 'primed' supernatant, as the 9h timepoint selected is the time at which ~50% of CCL19 is degraded in similar cultures (Figure 3.1.11). Thus, to ensure a comparable amount of CCL19 in the 'untreated' supernatant it was first supplemented with 5nM unlabelled CCL19. Then 0.1nM  $^{125}\text{I}$ -CCL19 was added to both supernatants, which were then incubated at 37°C for 0-120min. Supernatant samples were then subjected to TCA-precipitation. Figure 3.1.13 shows that there is no difference between the supernatants from 'primed' and 'untreated' cells. The supernatants themselves do not have any significant degradative effects of  $^{125}\text{I}$ -CCL19, with most radioactivity remaining in the TCA-precipitable fraction.

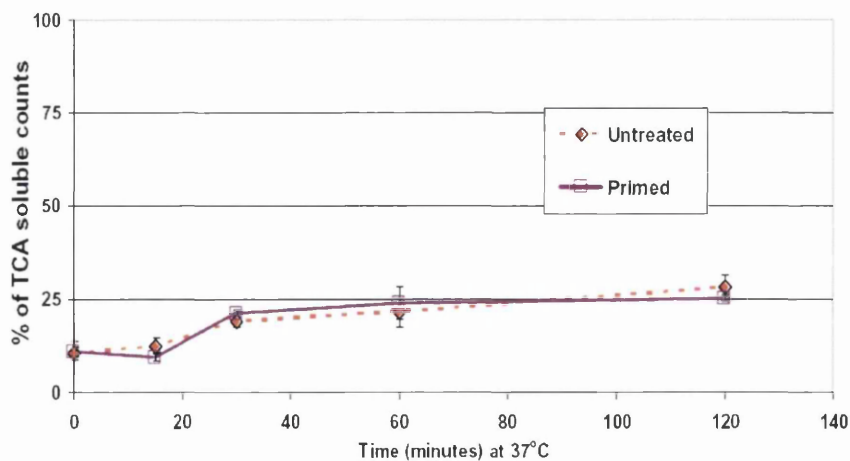


**Figure 3.1.13: Activity of HEK-hCCX-CKR Supernatants on  $^{125}\text{I}$ -CCL19 Degradation.** Supernatants from HEK-hCCX-CKR cells which had been primed in culture with 10nM CCL19 for 9h or left untreated were tested for their ability to degrade 0.1nM  $^{125}\text{I}$ -CCL19 by incubation with chemokine at 37°C for 0-120min followed by TCA precipitation. Supernatants from untreated cells were supplemented with 5nM unlabelled CCL19, as this is the estimated concentration of unlabelled CCL19 remaining in primed supernatants. Samples were done in triplicate and error bars are +/- the standard deviation.

### 3.1.2.2.5 Inhibition of Splenocyte Chemotactic Responses

To further assess whether the CCL19 degradation observed in the bulk culture experiments was functionally neutralizing this chemokine, chemotaxis assays were performed using supernatants harvested from receptor bearing cells. 10 or 200nM CCL19 was added to flasks of untransfected HEK293 or HEK-hCCX-CKR cells and incubated for 16h at 37°C. These supernatants were then collected and used in chemotaxis assays (see 2.2.4.6) using freshly-isolated mouse splenocytes, a population of cells that migrate readily to CCL19 (Pilkington et al., 2004). As can be seen in figure 3.1.14, prior incubation for 16h of 200nM CCL19 with cells which expressed CCX-CKR significantly reduced the chemotactic potential of this chemokine for mouse splenocytes when compared with chemokine similarly exposed to untransfected cells. These data indicate that expression of CCX-CKR in an environment high in CCL19 can cause the destruction of this chemokine, reducing its potential to chemoattract cells responsive to CCR7 ligands.

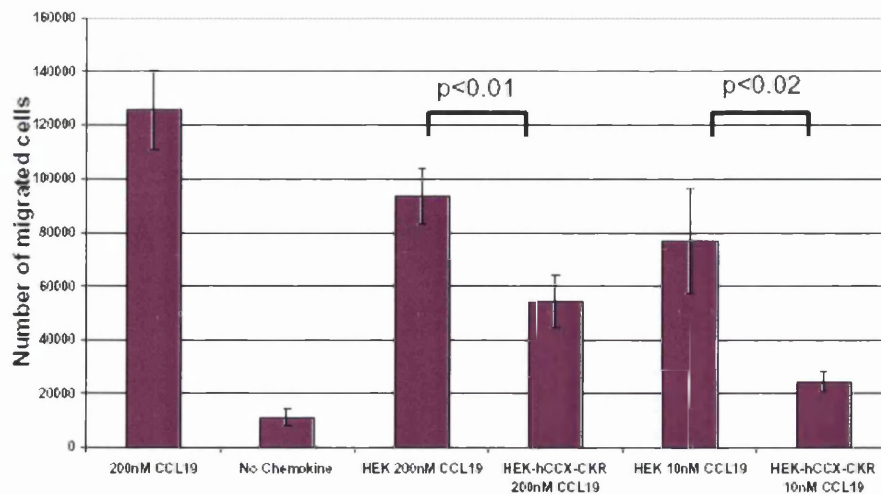


**Figure 3.1.14: Inhibition of Splenocyte Chemotaxis by Pre-incubation of CCL19 with CCX-CKR.** 10 or 200nM CCL19 was added to 2ml of medium containing either  $2 \times 10^5$  HEK293 or HEK-hCCX-CKR cells which had been growing in culture for 48h and incubated overnight. 16h later, freshly isolated mouse splenocytes were used in transwell chemotaxis assays with either medium alone, medium with 200nM CCL19 or cell cultures supernatants in the lower chamber. The plate was incubated at 37°C for 6h and the number of migrated cells in the lower chambers counted in a haemocytometer. Each sample was performed in triplicate and the error bars represent +/- the standard deviation of the mean. Statistical analysis was performed using a Student's t-test.

## Summary of CCL19 Internalisation and Degradation Studies

1. CCX-CKR and CCR7 internalise CCL19.
2. CCL19 internalised by CCX-CKR is removed from the cell in a degraded form. However, some CCL19 traffics via the cell surface prior to its degradation.
3. CCL19 internalised by CCR7 is removed less rapidly and in both degraded and unmodified forms.
4. CCL19 binding to CCX-CKR is more sensitive to acidic pH than CCL19 binding to CCR7.
5. Endosomal neutralisation with  $\text{NH}_4\text{Cl}$  inhibits degradation of CCL19 internalised by CCX-CKR.
6. A proportion of CCL19 internalised by CCX-CKR or CCR7 recycles back to the cell surface.
7. Significantly, in continuous culture, CCX-CKR mediates the effective degradation of large quantities of extracellular CCL19, while CCR7 does not.
8. CCX-CKR-mediated degradation of CCL19 can modify CCR7-mediated splenocyte responses.

### 3.1.3 Receptor Behaviour after Chemokine Exposure

The observed differences in CCL19 degradation between CCX-CKR and CCR7 in the continuous culture assays were something of a surprise. Although in preloaded radioligand degradation assays more extensive CCL19 degradation had been measured using HEK-hCCX-CKR cells rather than HEK-hCCR7 cells, this was not so pronounced that the very large differences observed between these cell lines in continuous culture could be expected. Hypothetically, this could be explained by CCR7 desensitisation following exposure to CCL19, leading to a reduction in its ability to continue to internalise and degrade this chemokine. CCX-CKR on the other hand, if it is biochemically suited to its' proposed role as a decoy receptor, may not be subject to ligand driven desensitisation. To test this, we studied the ability of these two cell lines to mediate CCL19 uptake following ligand pre-stimulation, i.e. does experiencing CCL19 alter receptor behaviour?

#### 3.1.3.1 Biotinylated CCL19 Uptake by Flow Cytometry

In order to characterise CCL19 uptake, a convenient flow cytometric assay was developed, using BioCCL19. This reagent had been used earlier in the project to assess uptake, where the BioCCL19 had been coupled to streptavidin-Cy3 (section 3.1.2.1.3). To adapt this for flow cytometry, a more suitable streptavidin linked fluorophore, phycoerythrin (PE), was used as the marker. As shown in figure 3.1.15, both HEK-CCX-CKR and HEK-hCCR7 (but not untransfected HEK293 cells) become similarly fluorescent when incubated for 10min at 37°C with BioCCL19/PE complexes. All cell lines when incubated with streptavidin-PE alone accumulated minimal fluorescence (not shown). Therefore, uptake of fluorescence in this assay is dependent upon the presence of both BioCCL19 and a CCL19 receptor.

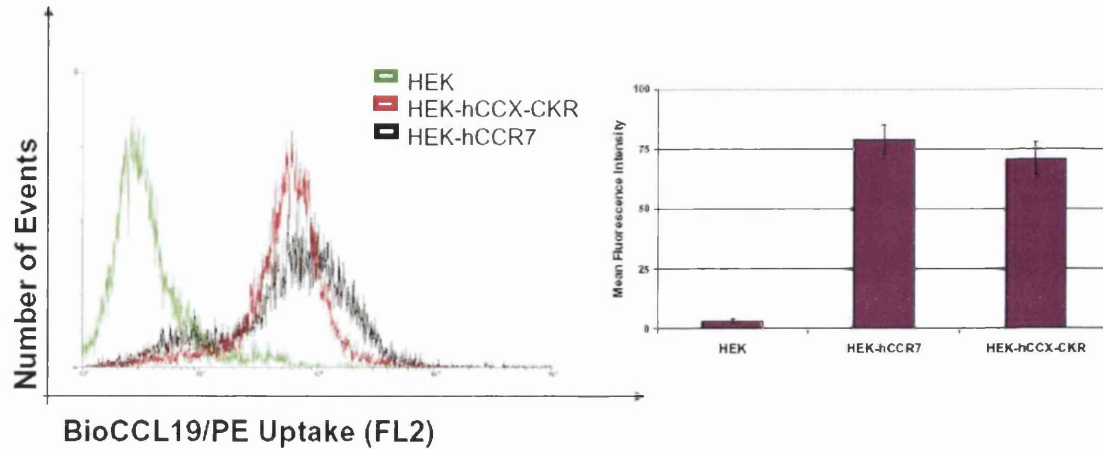


**Figure 3.1.15: Uptake of BioCCL19/PE is Dependent on the Expression of a CCL19 Receptor.** Harvested cells were incubated with BioCCL19/PE for 10min at 37°C. Cells were then washed and analysed by flow cytometry. The plot on the left hand side shows a representative histogram overlay showing accumulation of fluorescence by HEK-hCCR7 and HEK-hCCX-CKR but not untransfected HEK293 cells. This is quantified in the bar graph on the right hand side. Each sample was performed in triplicate with error bars showing +/- the standard deviation. Repeat experiments gave similar results.

From the continuous culture CCL19 degradation data (figure 3.1.11), it may be expected that HEK-hCCX-CKR cells would continue to accumulate BioCCL19/PE, the longer they were incubated with this complex. To test this, cells were incubated with BioCCL19/PE for 2 min to 1h. HEK-hCCX-CKR continued to accumulate fluorescence during the course of this experiment (see figure 3.1.16). HEK-hCCR7 cells behaved quite differently however. The internalisation of fluorescence by these cells mainly took place within the first few minutes and did not increase to any great extent with longer incubation times. These data show that CCX-CKR continues to internalise CCL19 while CCR7 becomes desensitised, thus providing an explanation for the ability of HEK-hCCX-CKR cells to degrade such significant quantities of CCL19 in continuous culture.

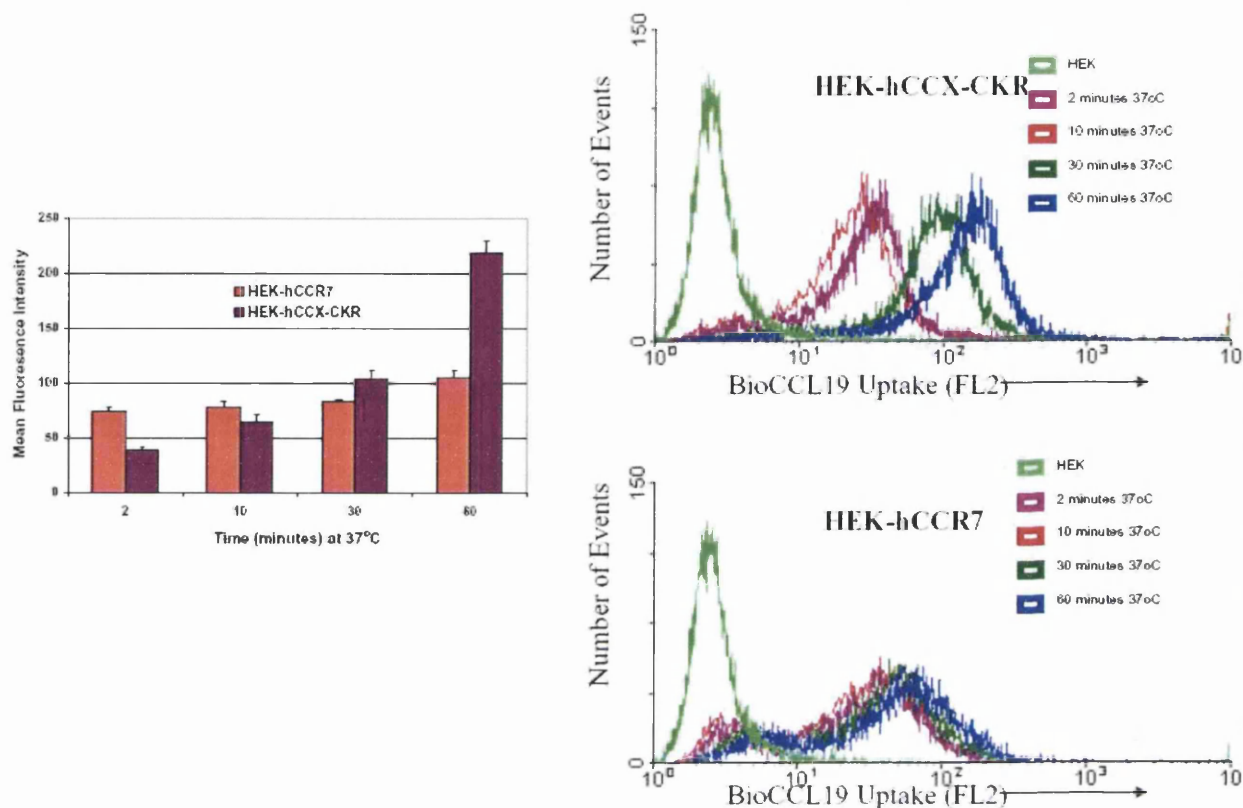


**Figure 3.1.16: Continued Chemokine Accumulation by HEK-hCCX-CKR Cells.** Harvested cells were incubated at 37°C for 2-60min with BioCCL19/PE then washed and analysed by flow cytometry. The MFI of untransfected HEK293 cells was subtracted from the MFI of receptor transfectants at each timepoint. The top right histogram overlay shows representative plots of HEK-hCCX-CKR cells and the lower right hand histogram shows the same for HEK-hCCR7 cells. The bar graph on the left shows the MFI (minus background uptake from untransfected cells). Each sample was performed in triplicate and error bars represent +/- the standard deviation. Repeat experiments gave similar results.

Importantly, in this assay, the extent of fluorescence is indicative of the amount of CCL19 that has been internalised during the incubation time, rather than the amount of CCL19 present at the end of the incubation. Thus, HEK-hCCX-CKR cells retain their fluorescence following uptake of BioCCL19/PE, for at least 3h at 37°C. Previous experiments had shown that practically all internalised CCL19 had been degraded over this time frame (Figure 3.1.8). This can be explained by the fact that although chemokine internalised by CCX-CKR is degraded, the PE remains. Therefore, this assay allows quantification of the total

amount of chemokine taken up by individual cells over time without having to pharmacologically interfere with intracellular degradation (Figure 3.1.17).

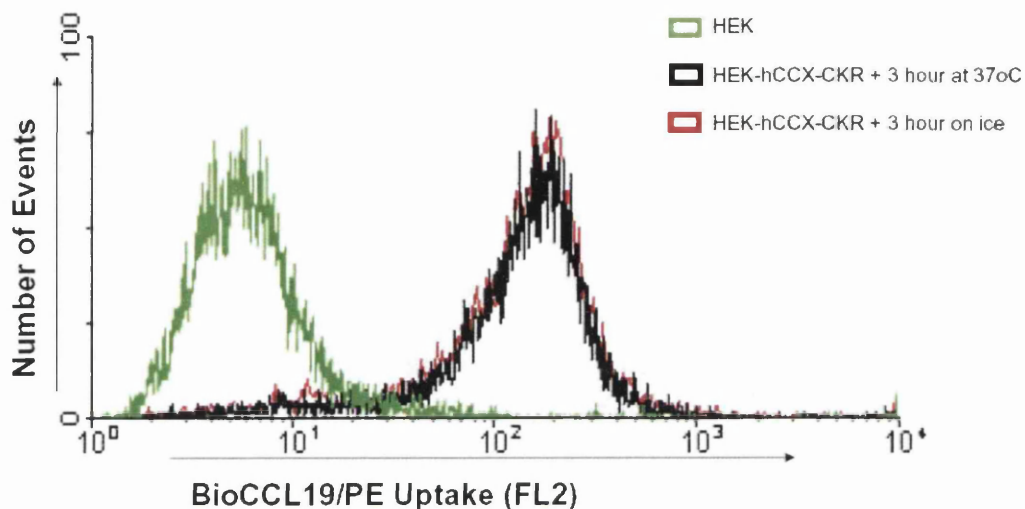


**Figure 3.1.17: BioCCL19/PE Uptake Assay Measures Total Chemokine Accumulation.** Harvested cells were incubated with BioCCL19 for 1h at 37°C. Cells were then washed and either incubated on ice or at 37°C for 3h. Cells were then analysed by flow cytometry. The histogram above shows a representative plot from 2 independent experiments.

Next, to further assess CCX-CKR and CCR7 desensitisation, transfected cells were stimulated in culture for 1h with 10nM CCL19 or CCL21. Harvested cells were thoroughly washed then used in BioCCL19/PE uptake assays. From these data it emerged that the hypothesis that CCX-CKR may be resistant to desensitisation (and therefore more able to degrade CCL19 in continuous culture) does not go far enough. In fact, it appeared that CCX-CKR, rather than being subject to ligand induced desensitisation, was actually being primed to more efficiently accumulate CCL19 following ligand exposure. As shown in figure 3.1.18, HEK-hCCX-CKR cells were primed by both CCL19 and CCL21 stimulation such that they were able to accumulate more BioCCL19/PE than untreated cells over the same time-frame. Furthermore, and as expected, pre-exposure of HEK-hCCR7 cells to

ligand reduced their capacity to subsequently take up BioCCL19/PE. These data also show that CCL19 was a more efficient ligand at desensitising CCR7 for subsequent BioCCL19/PE uptake than CCL21. This is consistent with published data which demonstrated that CCR7 is internalised and desensitised more effectively by CCL19 than by CCL21 (Kohout et al., 2004).

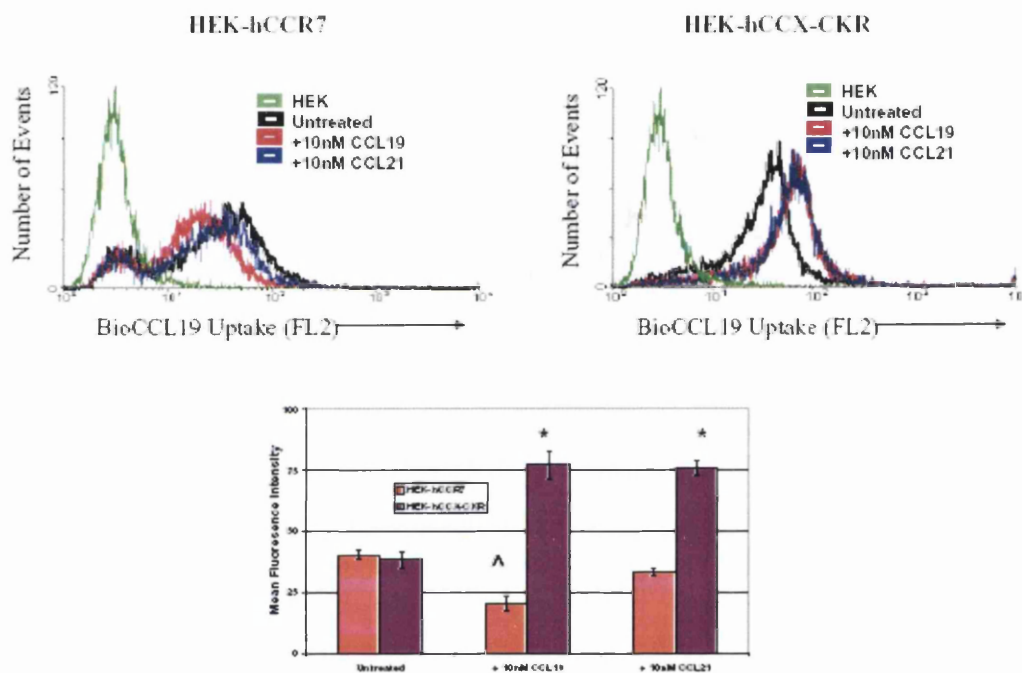


**Figure 3.1.18: Priming and Desensitisation of HEK-hCCX-CKR and HEK-hCCR7 Cells.** Cells in culture were treated with either 10nM CCL19, 10nM CCL21 for 1h or left untreated. The cells were then washed, harvested, and incubated with BioCCL19/PE for 15min at 37°C. Cells were then washed and analysed by flow cytometry. The top left histogram shows a representative overlay of the results obtained for HEK-hCCR7 cells, and the top right histogram shows the same for HEK-hCCX-CKR cells. Each sample was included in triplicate and the results shown in the lower bar graph are the MFI +/- the standard deviation. Statistical analysis was performed using a Student's t-test (\* indicates  $p < 0.001$  compared with untreated cells; ^ indicates  $p < 0.05$  compared with untreated cells). Repeat experiments gave very similar results ( $n=4$ ).

Next, the dose-response kinetics of CCX-CKR priming by all three of its ligands was studied in more detail. HEK-hCCX-CKR cells were primed in culture with 0.1nM to 100nM of CCL19, CCL21, or CCL25 for 1-16h. Cells were then washed, harvested and fed

BioCCL19/PE at 37°C for 1h. As can be seen in figure 3.1.19, all of the ligands effectively and similarly primed subsequent BioCCL19/PE uptake through CCX-CKR. Maximal priming was observed from the longest incubations (16h) with the maximum amount of chemokine (100nM). For practical purposes however, 10nM chemokine prestimulations for 2h induces an effective level of receptor priming and therefore, these conditions were used in all subsequent investigations of receptor priming. It is notable from these data that the 10nM concentration induces a priming effect that goes up, then down over time, whilst the higher (100nM) concentration does not. These data suggest that the continued presence of CCL19 may help maintain the priming effect, but as the chemokine gets degraded, this effect is reduced.

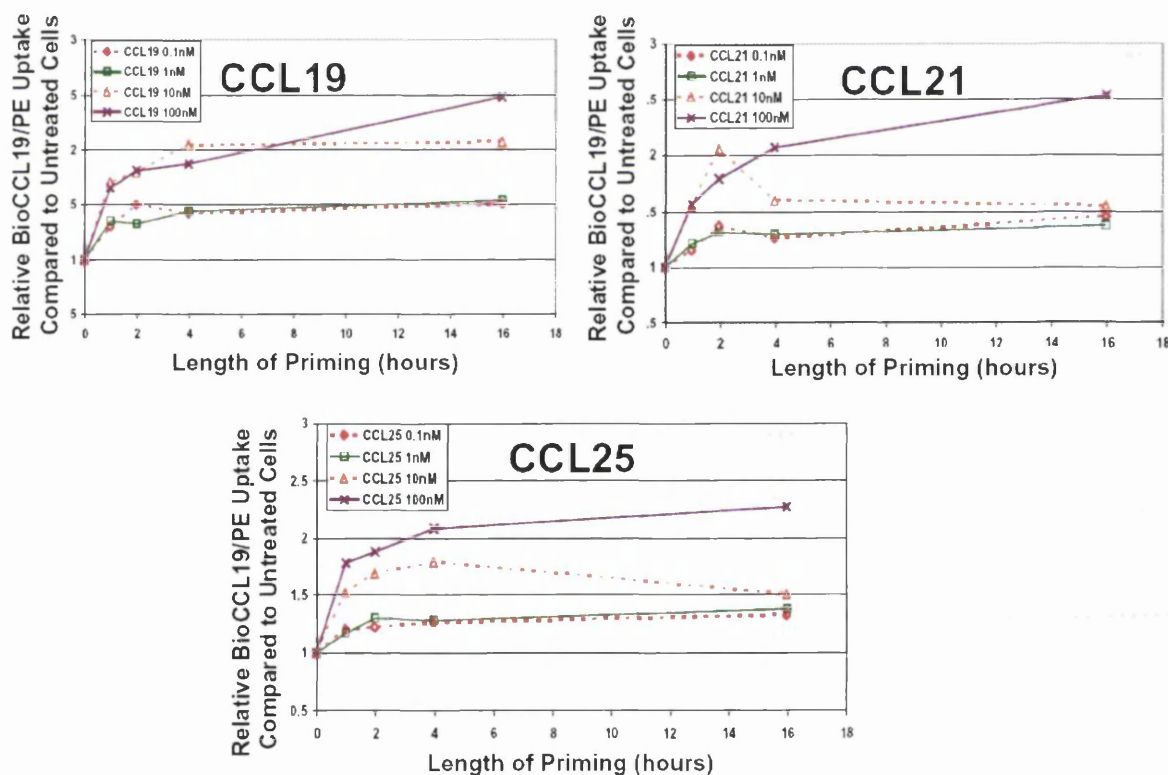


**Figure 3.1.19: Dose and Time Dependent Priming of CCX-CKR by CCL19, CCL21 and CCL25.** Cells in culture were treated with 0.1nM-100nM of CCL19, CCL21, CCL25 for 1-16h or left untreated. Cells were then washed, harvested and incubated with BioCCL19/PE for 1h. Cells were analysed by flow cytometry. The graphs above plot the relative MFI of each sample compared with HEK-hCCK-CKR cells which were not primed with chemokine. Repeat experiments gave similar results (n=2).

Next, the effect of prior chemokine exposure on the rate of BioCCL19/PE uptake by HEK-hCCX-CKR cells was examined. Cells were incubated with 10nM CCL19 or CCL21 in culture for 2h then harvested and used in BioCCL19/PE uptake assays for 2-60min. The results clearly show that prior exposure to either CCL19 or CCL21 causes not only an increase in uptake of BioCCL19/PE by HEK-hCCX-CKR cells, but also causes an increase in the rate of accumulation of this complex, indicated by the slope of the graph (Figure 3.1.20). Indeed, the rate more than doubles from ~2.4 fluorescent units/min in untreated cells to ~5 units/min in chemokine-primed cells.

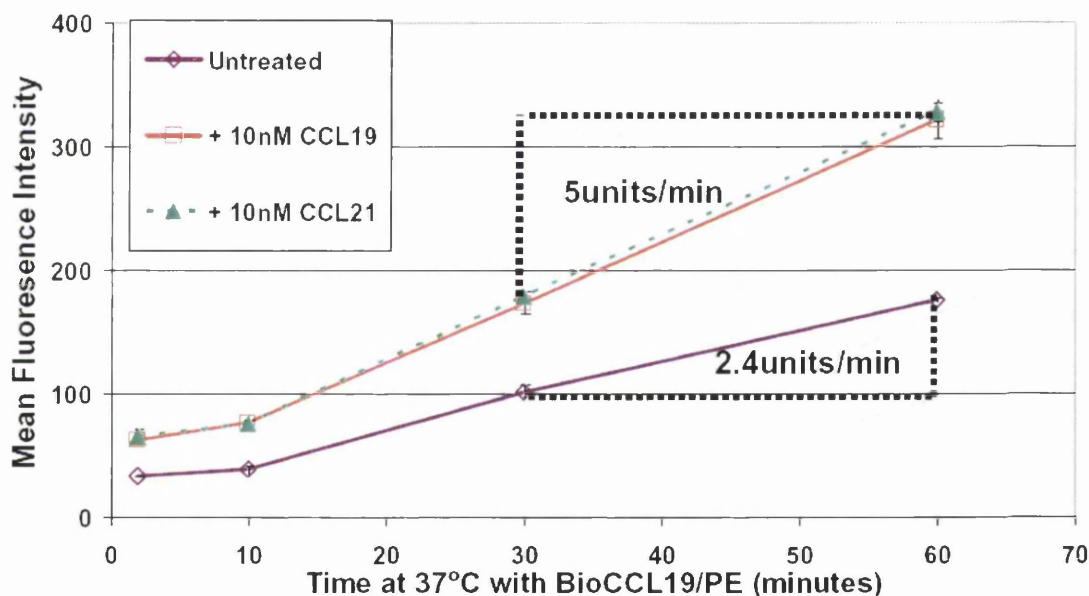


**Figure 3.1.20: Chemokine Priming of CCX-CKR Increases the Rate of BioCCL19/PE Uptake.** Cells were treated in culture for 2h with either 10nM CCL19, 10nM CCL21 or left untreated. Cells were then washed, harvested, and incubated at 37°C for 2-60min with BioCCL19/PE. Analysis of cells by flow cytometry followed. The graph above shows the MFI of each sample over the length of time of the incubation at 37°C. The rate of uptake is calculated as the slope of the line between 30 and 60mins. Dotted lines show the triangulation used to calculate the number of fluorescent units taken up by the cells per min. Each sample was included in triplicate and error bars are +/- the standard deviation. Repeat experiments gave similar results (n=2).

### 3.1.3.1 Radiolabelled CCL19 Uptake

Next, to confirm that these phenomena were not limited to the BioCCL19/PE assay,  $^{125}\text{I}$ -CCL19 uptake was assessed (see 2.2.4.3). Prior to harvesting cells, 10nM of CCL19 or CCL21 was added to cells in culture for 0.5-12h. Cells were then incubated with 2nM  $^{125}\text{I}$ -CCL19 for 10min at 37°C. This short incubation time was chosen as it should allow cell lines to accumulate radiolabelled chemokine but significant quantities should not be degraded and released from the cells. As can be seen in figure 3.1.21, preincubation of HEK-hCCX-CKR cells with either CCL19 or CCL21 led to a ~2-fold increase in the ability of this receptor to subsequently mediate the accumulation of  $^{125}\text{I}$ -CCL19. This effect was observed with chemokine pre-incubation times as short as 30min and was maintained at the longest chemokine incubation of 12h. In contrast, the amount of  $^{125}\text{I}$ -CCL19 uptake mediated by HEK-hCCR7 cells was reduced by preincubation with its ligands. This effect was not evident until these cells had been incubated for 1h in CCL19 and was not observed with CCL21 incubations until the chemokine had been present for 12h. These data were consistent with the hypothesis that CCX-CKR becomes primed, while CCR7 becomes desensitised, following agonist stimulation, and confirm the BioCCL19/PE uptake data. Together, these results demonstrate fundamentally different behaviour of CCX-CKR and CCR7 following ligand exposure, and provide a rational explanation for the remarkably different propensities of these two receptors to degrade CCL19 in continuous culture.

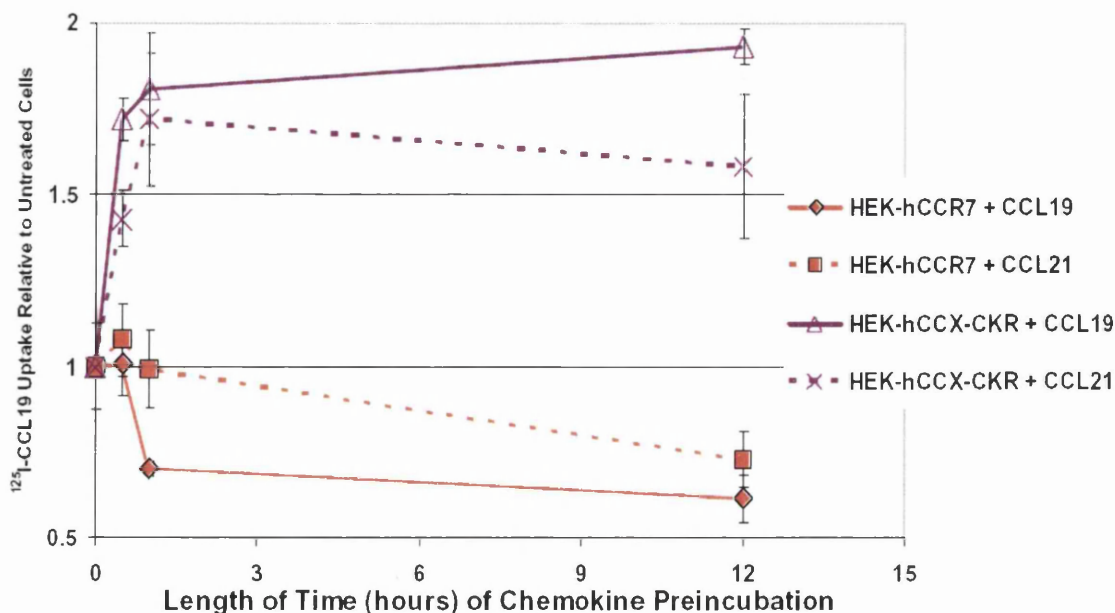


**Figure 3.1.21: Radioligand Uptake by CCX-CKR and CCR7 Following Chemokine Stimulation.** Cells were treated in culture for 1-12h with either 10nM CCL19, 10nM CCL21 or left untreated. Cells were then harvested and incubated with 2nM  $^{125}\text{I}$ -CCL19 for 30min. Cells were then washed and the amount of radioactivity associated with the cell pellet quantified. The relative number of counts compared to untreated cells was then plotted for each sample at each length of treatment. Each sample was included in triplicate and error bars represent  $\pm$  the standard deviation. Repeat experiments gave similar results ( $n=2$ ).

### 3.1.3.2 Surface Receptor Levels following Ligand Exposure

Most chemokine receptors are internalised and sequestered from the cell surface following exposure to ligand. Conversely, the increased amount of ligand uptake by HEK-hCCX-CKR cells following priming could be explained by the maintenance or increase in the amount of cell surface receptor after ligand exposure. To examine this, surface CCX-CKR levels were assessed exploiting the N-terminal FLAG epitope engineered into CCX-CKR. HEK-hCCX-CKR cells were given hCCL19 (1-100nM) for 5-60min at 37°C, before harvesting, washing, and detection of surface receptor using an anti-FLAG antibody (see 2.2.4.8). Although detection of surface CCX-CKR using this antibody was variable, and typically relatively poor, carefully controlled experiments revealed that surface CCX-CKR

levels surprisingly go down in a dose-dependent manner after incubation with CCL19 (Figure 3.1.22). All three CCX-CKR ligands were tested for their ability to induce this response and were all found to cause loss of surface receptor expression (figure 3.1.23). CCR7 surface receptor levels in HEK-hCCR7 cells were also assessed using an anti-hCCR7 antibody (as discussed in section 3.1.1, the FLAG tag was not detectable on these cells). Similar to CCX-CKR, the amount of CCR7 at the cell surface goes down following incubation with CCL19. However, unlike CCX-CKR, but in agreement with a previous report (Bardi et al., 2001), CCL21 does not cause internalisation of CCR7 (Figure 3.1.24).

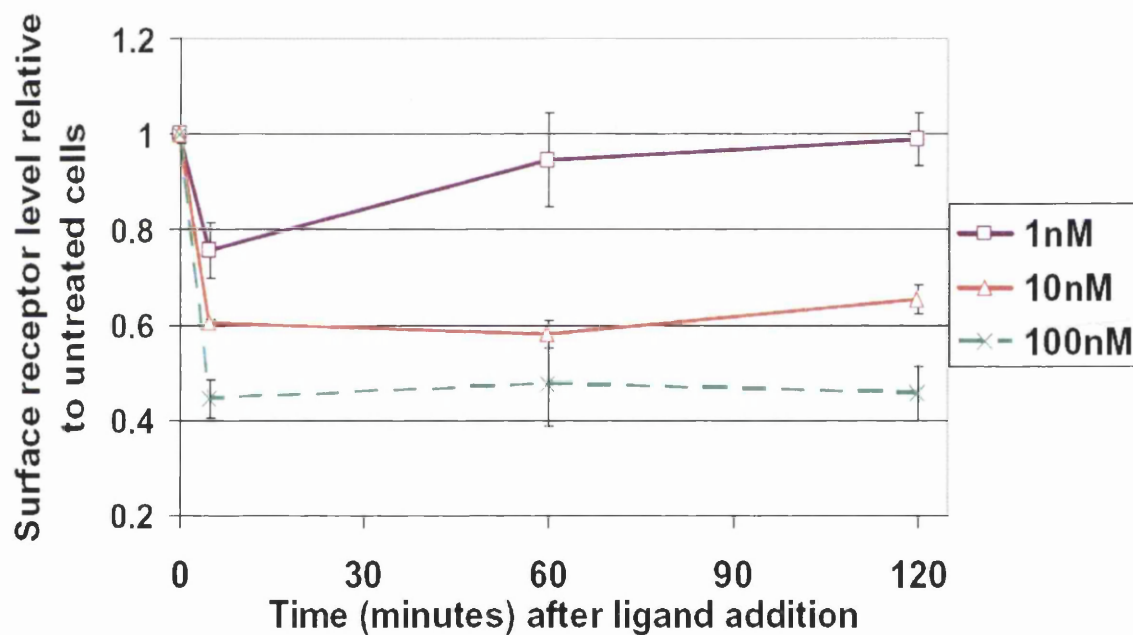


**Figure 3.1.22: CCL19 causes CCX-CKR Internalisation in a Dose Dependent Manner.**

Cells were treated in culture for 5-120min with 1-100nM CCL19 or left untreated. Cells were then cooled to 4°C before washing and harvesting. Harvested cells were incubated with anti-FLAG M1 antibody at 4°C which was then detected using anti-mouse IgG coupled to PE. Cells were then washed and analysed by flow cytometry. The relative amount of fluorescence of each sample, compared with untreated cells, is plotted. Each point shows the mean of a triplicate repeat and error bars are +/- the standard deviation. Repeat experiments showed similar trends (n=5).

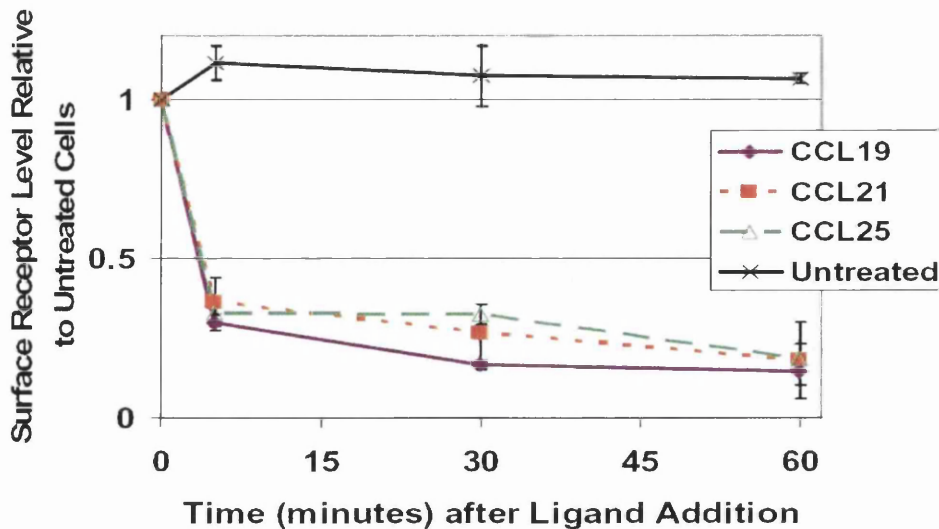


**Figure 3.1.23: CCL21 and CCL25 Induce Similar CCX-CKR Internalisation as CCL19.** Cells were harvested and then incubated at 37°C for 5-60min with 100nM of CCL19, CCL21, CCL25, or left untreated for the same length of time at 37°C. After washing, surface receptor assessments were made by staining with the anti-FLAG M1 antibody at 4°C followed by the anti-mouse IgG-PE antibody and analysed by flow cytometry. The relative amount of surface receptor compared to untreated cells (not incubated at 37°C) is plotted above. Each sample was included in triplicate and error bars represent +/- the standard deviation. A repeat experiment gave similar results (n=2).

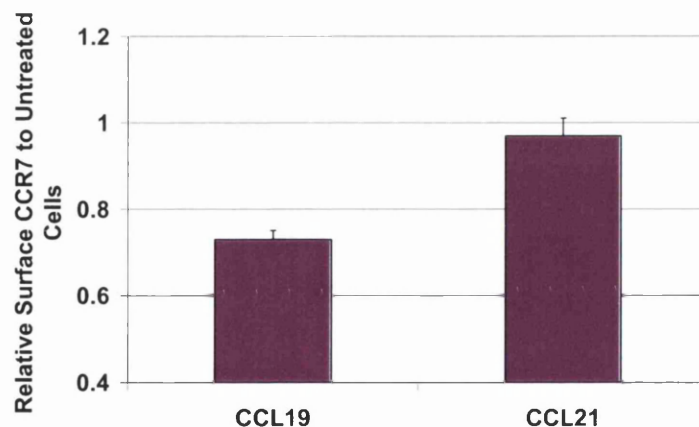


**Figure 3.1.24: Internalisation of CCR7 Following Ligand Stimulation.** HEK-hCCR7 cells were treated in culture for 1h with 10nM CCL19, 10nM CCL21 or left untreated. Cells were then washed, harvested, and surface CCR7 detected at 4°C using the anti-hCCR7 antibody followed by anti-mouse IgG-PE. Assessment of surface levels of CCR7 following chemokine treatment was made by flow cytometric analysis. The relative MFI of chemokine-treated cells was compared to that of untreated HEK-hCCR7 cells. Each sample was included in triplicate. Error bars represent +/- the standard deviation and statistical analysis was performed using a Student's t-test ( $p < 0.001$ ). Repeat experiments gave similar results (n=2).

From these experiments, it can be reasoned that i) the ligand-driven desensitisation of CCR7 can be explained, at least in part, through receptor internalisation, and ii) the greater degree of desensitisation induced by CCL19 is due to it more effectively causing CCR7 internalisation than CCL21. However, it is not the case that the ‘priming’ of CCX-CKR for CCL19 uptake is achieved through maintenance or increases in the levels of surface receptor. Instead, although less CCX-CKR is at the cell surface following ligand exposure, the behaviour of the receptor must have changed in a way that enables more rapid ligand internalisation (this is discussed further in chapter four). Detailed subsequent analysis of this was limited by the difficulties encountered with reliable antibody detection of CCX-CKR and the failure to successfully generate a CCX-CKR-GFP fusion protein, approaches that could help test this hypothesis. Finally, it is worthy of note that CCX-CKR appears to be behaving in a manner similar to typical signaling chemokine receptors, in that ligand-driven alterations in surface receptor levels are occurring. This in itself is likely to be controlled by ligand-induced receptor-derived signals, providing tentative evidence that CCX-CKR may not be a ‘silent’ receptor, and may couple to as yet uncharacterised signaling pathways.

## Summary

1. HEK-hCCX-CKR cells continue to accumulate CCL19 after chemokine exposure, while HEK-hCCR7 cells are less able to do this. Thus, CCX-CKR appears to avoid desensitisation.
2. Exposure to CCL19, CCL21 and CCL25 ‘primes’ CCX-CKR to more efficiently sequester CCL19.
3. Subsequent CCL19 accumulation through CCR7 is desensitised by prior exposure of the receptor to CCL19, and to a lesser extent, CCL21.

4. Ligand 'priming' of CCX-CKR increases the rate at which CCL19 is internalised by this receptor.
5. Priming of CCX-CKR cannot be explained by an increase in the amount of cell surface receptor following ligand exposure, as like CCR7, CCX-CKR surface receptor levels decrease following CCL19 stimulation.

These data suggest that CCX-CKR exhibits properties consistent with a 'decoy' receptor. The remainder of this thesis attempts to explain the molecular basis underpinning this behaviour, and explores the importance of CCX-CKR *in vivo* by generating and analysing CCX-CKR *null* mice.

### 3.1.4 Molecular Mechanisms of CCL19 Uptake

The data from the preceding sections clearly demonstrated that in the same cellular background, CCX-CKR behaves very differently to the related CCL19 receptor, CCR7. Dissecting the molecular mechanisms responsible for these differences is of considerable interest in understanding the biochemistry of these receptors. Thus, a comparative investigation of the molecular mechanisms of CCX-CKR and CCR7 internalisation was carried out aimed at determining how these receptors engage the endocytic machinery of the cell. The BioCCL19/PE uptake assay described in the previous section was particularly amenable to these investigations, as it allowed quantifiable assessment of levels of total chemokine uptake by live cells on a cell-to-cell basis. By exploiting this assay, and treating cells with well-characterised pharmacological or genetic inhibitors of various pathways of receptor internalisation or recycling, their importance in CCX-CKR- and CCR7-mediated CCL19 internalisation was revealed.

#### 3.1.4.1 Dynamin

The first molecule to be examined was dynamin, a large GTPase essential for most types of receptor-mediated endocytosis (but not pinocytosis), and which functions by ‘pinching’ vesicles from the plasma membrane (see section 1.3.5). To assess the impact of dynamin inhibition on CCL19 uptake, increasing quantities of a plasmid encoding a well-characterised dominant-negative version of this protein (dynamin K44A) were transiently transfected into HEK-hCCX-CKR cells. In parallel cultures, to give an indication of transfection efficiency, the same quantities of a plasmid encoding GFP were transfected into cells and the percentage of GFP+ cells assessed by flow cytometry, comparing GFP with mock-transfected cells. 24h after transfection, cells were harvested and assessed for their ability to accumulate BioCCL19/PE. In addition, cell lysates were made from transfected cells and dynamin expression visualised by Western blotting using a dynamin-

specific antibody. The data from these experiments are shown in figure 3.1.25. Increasing the quantity of transfected pEGFP-N2 plasmid led to a stepwise increase in GFP<sup>+</sup> cells. Concurrently, increasing the quantity of transfected dynamin K44A plasmid caused a stepwise increase in dynamin protein expression and a concurrent inhibition of the ability of HEK-hCCX-CKR cells to accumulate BioCCL19/PE. These data are consistent with the hypothesis that BioCCL19/PE is internalised by CCX-CKR via receptor-mediated endocytosis with dynamin playing an important role.

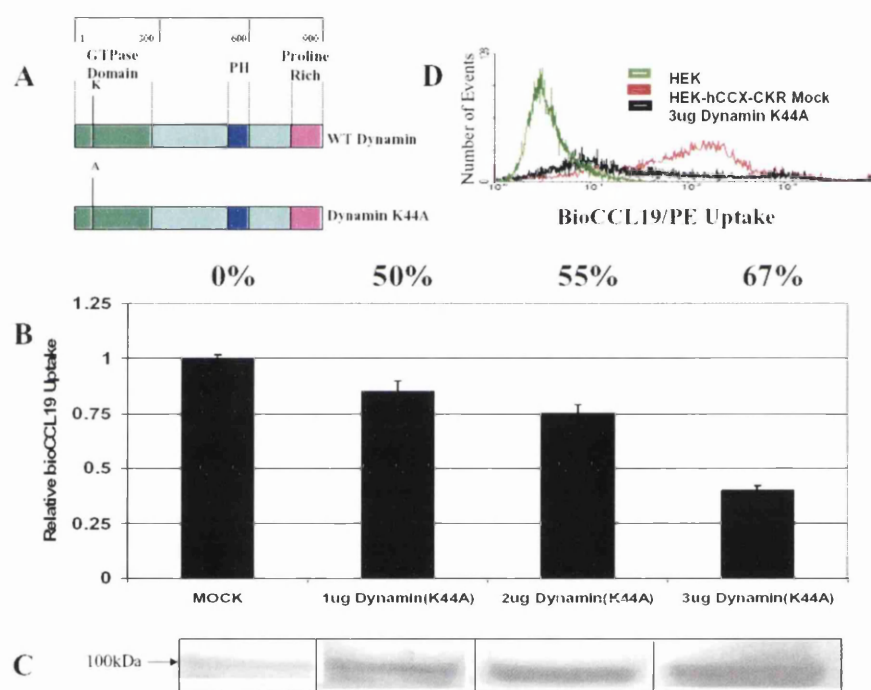


**Figure 3.1.25: Effect of Dynamin (K44A) on BioCCL19/PE Uptake by CCX-CKR.** (A) Dynamin (K44A) has a single amino acid substitution in the GTPase domain (1-900 are amino acid from N to C terminus; PH=Pleckstrin homology domain). HEK-hCCX-CKR cells transiently transfected with 1-3 $\mu$ g of dynamin (K44A), or 1-3 $\mu$ g of pEGFPN2, or mock-transfected were harvested 24h later. pEGFP-N2 transfectants were analysed by flow cytometry to estimate transfection efficiency relative to mock transfectants. (B) Transfection efficiency for each amount of plasmid is indicated above the graph. Dynamin (K44A) transfectants and mock transfectants were used in BioCCL19/PE uptake assays. The MFI relative of dynamin (K44A) transfectants to mock transfectants is plotted in the bar graph ( $p < 0.05$  between mocks and all transfected cells). Sample were included in triplicate, error bars are  $\pm$  the standard deviation and repeat experiments gave similar results ( $n=2$ ). (C) Increasing expression of the dynamin (K44A) with DNA quantity confirmed by cell lysates detecting dynamin by Western blotting, shown below the graph. Equal loading of these blots was ensured by careful lysis of  $1 \times 10^6$  cells in each case. (D) Representative histogram overlay showing maximal inhibition of uptake by dynamin (K44A).

### 3.1.4.2 $\beta$ -arrestins

Next, the potential role of  $\beta$ -arrestins in CCL19 uptake by CCX-CKR was explored. As discussed in section 1.3.5,  $\beta$ -arrestins are important in bringing about internalisation of a variety of GPCRs, including chemokine receptors. Two approaches were taken to investigate this. First, in a similar set of experiments to those carried out for dynamin, a well-characterised dominant-negative mutant of  $\beta$ -arrestin-1 (V53D) was transiently transfected into HEK-hCCX-CKR cells. Protein expression and transfection efficiency were determined by Western blotting and pEGFP-N2 transfection respectively, as described above for dynamin. As can be seen in figure 3.1.26, and in contrast to dynamin, increasing the expression of  $\beta$ -arrestin (V53D) in HEK-hCCX-CKR cells had no significant inhibitory effect upon BioCCL19/PE uptake, even when >50% of the cells were likely to have been transfected, and when robust protein expression could be confirmed by Western blotting. These data suggested that CCX-CKR internalisation of BioCCL19/PE was via a  $\beta$ -arrestin-independent route.

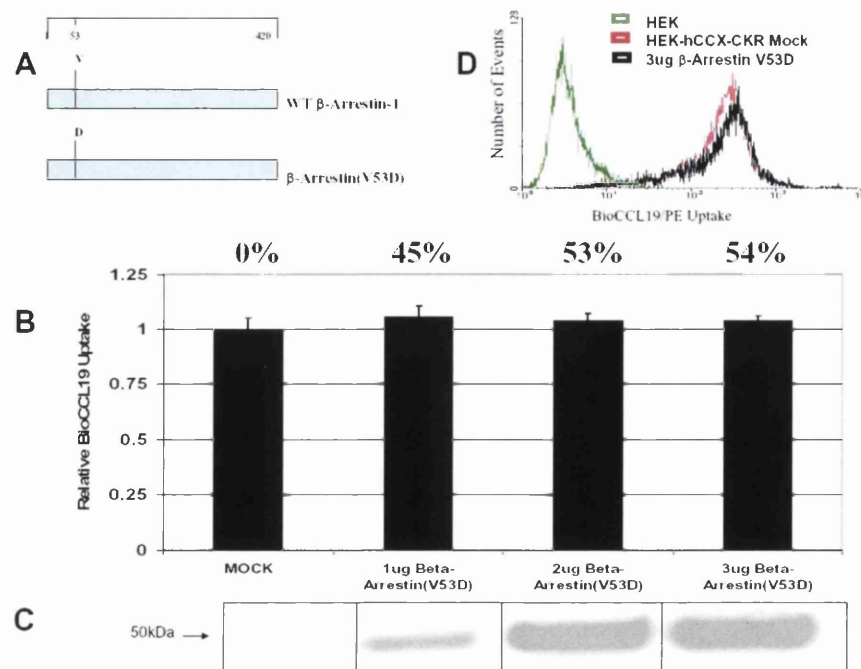


**Figure 3.1.26: Effect of  $\beta$ -arrestin-1 (V53D) on BioCCL19/PE Uptake by CCX-CKR. Legend Overleaf.**

**Figure 3.1.26: Effect of  $\beta$ -arrestin-1 (V53D) on BioCCL19/PE Uptake by CCX-CKR (from previous page).** (A)  $\beta$ -Arrestin-1 (V53D) has a single amino acid substitution at position 53 (Depicted schematically: 1-420 are amino acid number from N to C terminus). HEK-hCCX-CKR cells were transiently transfected with 1-3 $\mu$ g of  $\beta$ -arrestin-1 (V53D), or 1-3 $\mu$ g of pEGFPN2, or mock transfected. 24h later cells were harvested. pEGFP-N2 transfectants were analysed by flow cytometry to estimate transfection efficiency relative to mock transfectants. (B) The estimated transfection efficiency for each amount of plasmid used is indicated above the graph.  $\beta$ -arrestin-1 (V53D) transfectants and mock transfected cells were incubated with BioCCL19/PE for 1h and analysed by flow cytometry. The relative MFI of  $\beta$ -Arrestin-1 (V53D) transfectants compared to mock transfectants is plotted in the bar graph. Each sample was included in triplicate, error bars are +/- the standard deviation and repeat experiments gave similar results (n=3). (C) Increasing expression of the  $\beta$ -arrestin-1 (V53D) was confirmed by making cell lysates and detecting  $\beta$ -arrestin-1 by Western blotting, shown below the graph. Equal loading of these blots was ensured by careful lysis of exactly  $1 \times 10^6$  cells in each case. (D) A representative histogram overlay showing uptake of BioCCL19/PE uptake by cells maximally expressing  $\beta$ -arrestin-1 (V53D) is shown.

To more definitely address the role of  $\beta$ -arrestins, the ability of CCX-CKR and CCR7 to mediate CCL19 uptake into  $\beta$ -arrestin *null* and WT mouse embryonic fibroblasts (MEFs) was assessed. Ideally, constructs encoding GFP tagged receptors were to be used. However, as described in section 3.1.1.2, CCX-CKR GFP fusion proteins could not be generated. Thus, whilst CCR7-GFP was used, non-GFP tagged expression plasmids were used to express CCX-CKR, making careful comparisons with mock transfectants. Thus, MEFs were grown on fibronectin-coated coverslips and transiently transfected with either hCCX-CKR or hCCR7-GFP, or mock-transfected (Dr. Milasta in the laboratory of Prof G. Milligan in the Department of Biochemistry at the University of Glasgow carried out all MEF cell culture and performed these transfections). 24h after transfection, cells were washed and incubated with BioCCL19/Cy3 complexes at 37°C for 30min. Confocal microscopy was then used to assess ligand uptake and CCR7-GFP distribution (2.2.4.7 and 2.2.3.1). A number of observations were made. First, in MEFs which had been transfected with hCCR7-GFP there were clear differences observed between the  $\beta$ -arrestin WTs and *nulls*. In  $\beta$ -arrestin WT MEFs, those cells which expressed CCR7-GFP could clearly be

seen to have internalised BioCCL19/Cy3 with punctate intracellular red fluorescence, some of which appeared to co-localise with CCR7-GFP. BioCCL19/Cy3 uptake was specific to cells in which GFP could be visualised. The majority of the CCR7-GFP was located cytoplasmically in WT MEFs following BioCCL19/Cy3 incubation. In contrast, in  $\beta$ -arrestin *null* MEFs CCR7-GFP expressing cells did not contain any visible internalised BioCCL19/Cy3 and most of the CCR7-GFP remained at the cell surface after ligand application. This result, in agreement with previous studies (Kohout et al., 2004), strongly suggests that internalisation of CCR7 caused by CCL19 is dependent upon  $\beta$ -arrestins.

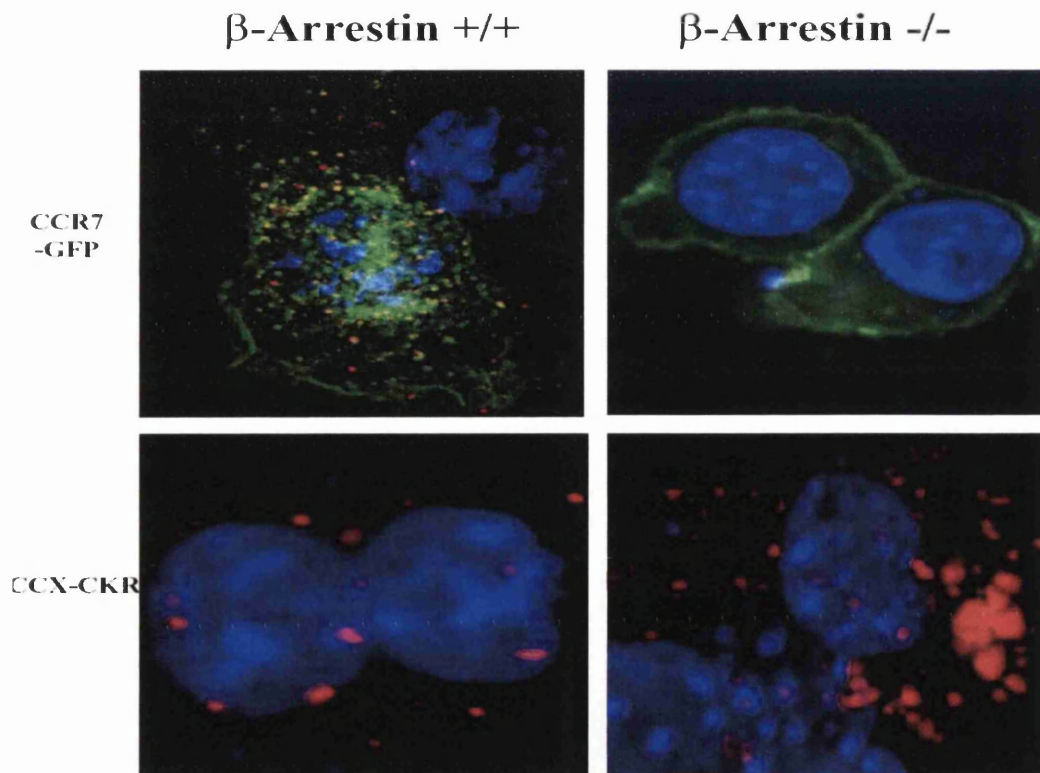


**Figure 3.1.27: Uptake of BioCCL19/Cy3 by MEFs (-/- or +/+ for  $\beta$ -arrestins).** WT and  $\beta$ -arrestin *null* MEFs were grown on fibronectin coated coverslips and transfected with either hCCR7-GFP, or FLAG-hCCX-CKR (see figure 3.1.1) plasmids or left mock transfected. 24h later cells were washed and BioCCL19/Cy3 added in fresh medium. Cells were then incubated in the dark at 37°C for 30min before being washed, fixed, and mounted on slides with Vectashield with DAPI. Slides were then analysed by confocal microscopy. Careful optical sections were taken to confirm intracellular location of BioCCL19/Cy3 (red). Cell nucleus appears blue in above pictures. Images shown are representative of cells observed in many fields. Repeat experiments gave similar results (n=2).

The second, and more significant, observation was that, in contrast to CCR7, no clear differences could be observed between  $\beta$ -arrestin WT and *null* MEFs which had been transfected with hCCX-CKR. Internalised punctate BioCCL19/Cy3 could be visualised in both  $\beta$ -arrestin WT and *null* cells, and careful optical dissection confirmed intracellular localisation. Mock-transfected cells did not display any uptake, indicating a dependence upon hCCX-CKR transfection. As a whole, these data, strongly suggest that CCX-CKR is capable of mediating CCL19 uptake independently of  $\beta$ -arrestins. As CCX-CKR is unlike all other described chemokine receptors in that it is 'primed' not desensitised by ligand, the fact that it is able to operate in a  $\beta$ -arrestin independent manner may be an important aspect of its biology.

### 3.1.4.3 EPS15

Many cell surface proteins are internalised via CCPs which invaginate from the plasma membrane forming intracellular vesicles. For many, but not all GPCRs, this is co-ordinated by  $\beta$ -arrestins that link activated receptors to the machinery of clathrin-mediated endocytosis. Therefore, to investigate the role of clathrin-mediated endocytosis in BioCCL19/PE uptake by CCX-CKR and CCR7, the potential involvement of the molecule EPS15 was examined. EPS15 has been demonstrated to play a critical role in the internalisation of several receptors by docking the AP-2 complex to the plasma membrane and CCPs (see section 1.3.5). Three well-characterised plasmids encoding forms of EPS15 were used in this study. These were two dominant negative forms of EPS15: E $\Delta$ 95/295 and DIII, and a non-inhibitory form, DIII $\Delta$ 2. All were produced fused to GFP (see figure 3.1.28) and have been successfully used in parallel studies with D6 to demonstrate the involvement of the clathrin pathway in receptor internalisation in a similar experimental system (Weber et al., 2004). The advantage of using GFP-tagged proteins is that they allow

a direct correlation between the levels of expression of the GFP-tagged protein and the amount of inhibition caused, allowing a quantifiable assessment of the effects of these plasmids on populations of transiently transfected cells.

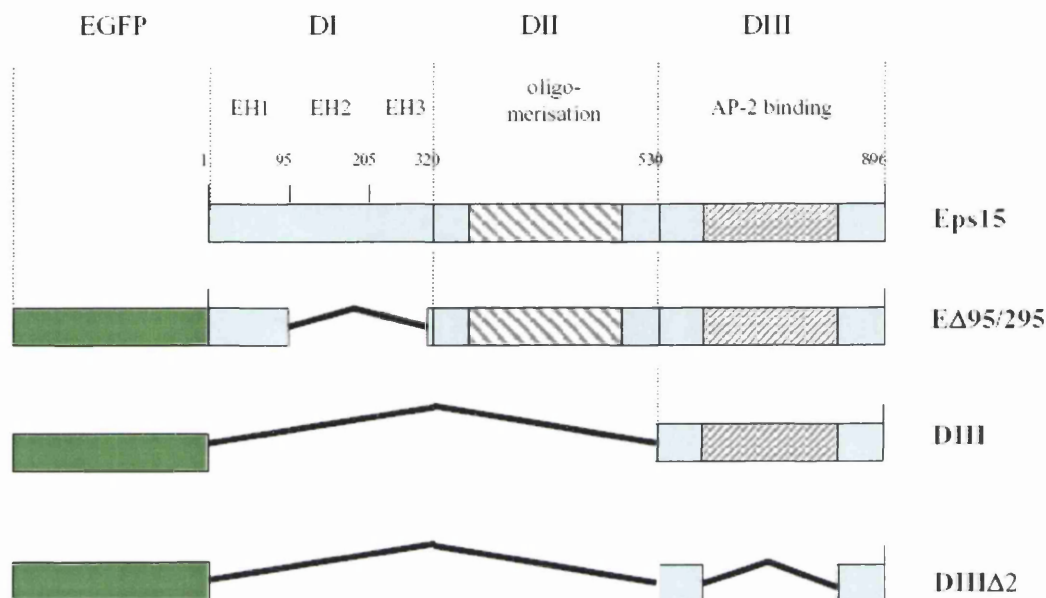


**Figure 3.1.28: Mutants of EPS15.** Three GFP tagged mutant of EPS15 which were used in this study. The three main domains of WT EPS15 (DI-DIII) are shown. Numbers represent the amino acid number from N-C terminus of the WT protein. The EPS15 homology domains (EH) are shown. The second and third of these is missing in the EΔ95/295 mutant. The DIII mutant contains only the AP-2 binding DIII domain fused to GFP. The DIIIΔ2 mutant contains only a GFP fused DIII domain with the AP-2 binding region removed.

Thus, HEK-hCCX-CKR and HEK-hCCR7 cells were transiently transfected with either one of these constructs or pEGFPN2, and 24h later fed BioCCL19/PE, and analysed by flow cytometry. Mock-transfected cells, and cells which had only been incubated with streptavidin-PE alone, were used as controls to set gates and compensation on the flow cytometer. As the amount of GFP-tagged protein in individual cells can be quantified on a cell-to-cell basis alongside the total amount of internalised BioCCL19/PE, the extent of uptake in cells expressing high levels of the GFP-tagged protein can be directly compared.

A comparison between cells expressing similar amounts of the GFP-tagged EPS15 mutants or GFP alone can then be made. As shown in figure 3.1.29 (page 169), both of the inhibitory EPS15 mutants, when expressed at high levels in HEK-hCCR7 cells caused significant inhibition of BioCCL19/PE uptake by these cells when compared with cells expressing high levels of GFP ( $p < 0.01$ ). HEK-hCCR7 cells with high expression of the non-inhibitory EPS15 mutant (DIII $\Delta$ 2) were indistinguishable from cells expressing high levels of GFP in terms of BioCCL19/PE uptake (see figure 3.1.29). In contrast, expression of these inhibitors of clathrin-mediated endocytosis has no significant effect on the ability HEK-hCCX-CKR cells to internalise BioCCL19/PE, even at high levels of expression. Taken together, these data provide evidence that hCCR7 internalisation is dependent, at least to some extent, on the formation of CCPs, whilst hCCX-CKR employs alternative routes of internalisation, not inhibited by dominant-negative forms of EPS15.

#### **3.1.4.4 Rab GTPases**

Next, the potential role of several RabGTPases in receptor-mediated endocytosis of CCL19 was studied. As discussed in the introduction, the Rab family of GTPases have important functions in regulating the intracellular trafficking and fusion of various endosomal compartments. To this end, we hypothesised that Rab5, a marker of the early endosomal compartment, may play an important role in the accumulation of BioCCL19/PE through hCCX-CKR and hCCR7, in a similar way as it does with CCL3 uptake by D6 (Weber et al., 2004). Furthermore, Rab4 and Rab11, which are involved in the function of the rapid and slow recycling endosomal compartments respectively, were also considered to possibly play a role in the continued intracellular accumulation of BioCCL19/PE through CCX-CKR. To this end, plasmids encoding dominant-negative GFP-tagged versions of each of these RabGTPases were obtained, and used in very similar assays to those described above using the EPS15 mutants.

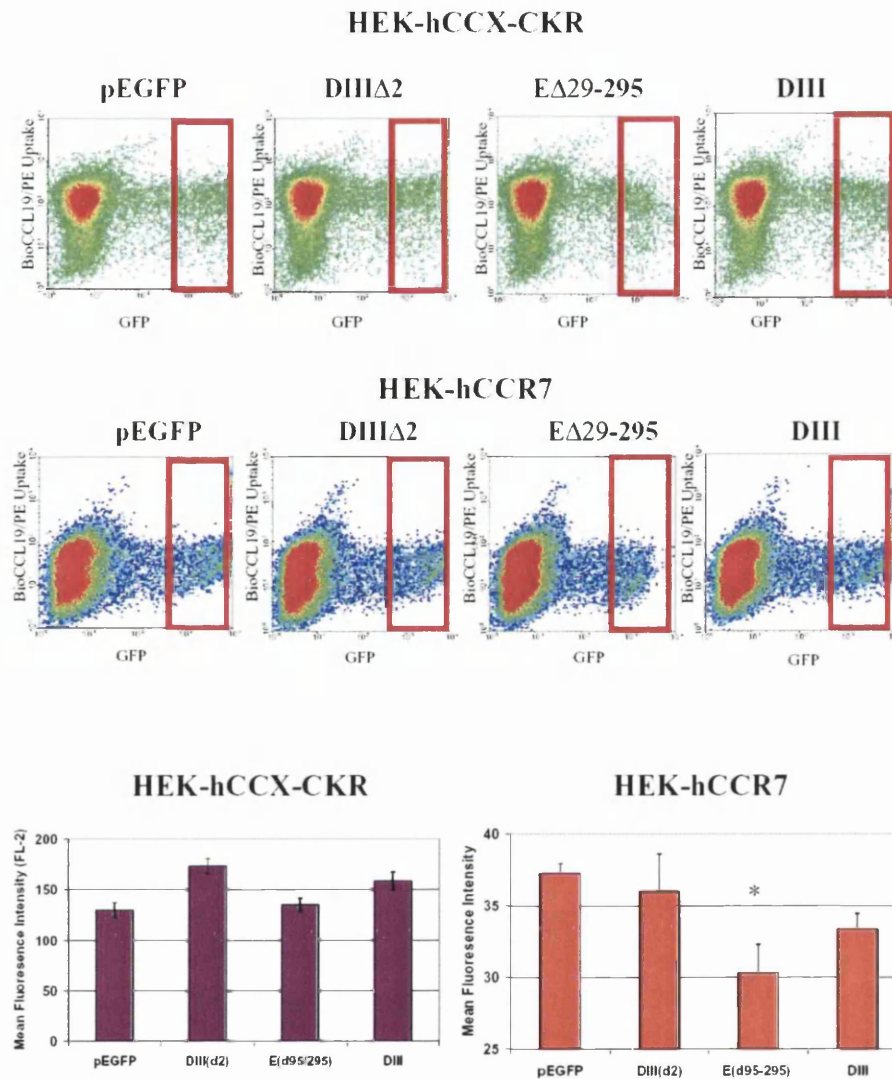


**Figure 3.1.29: Effect of Genetic Inhibition of EPS15 on BioCCL19/PE Uptake.** Cells were transfected with 1 $\mu$ g of each of one of the GFP tagged EPS15 mutants (figure 3.1.28) or pEGFPN2. 24h later, cells were harvested and incubated with BioCCL19/PE for 1h at 37°C. Cells were then washed and analysed by flow cytometry. The mean fluorescence intensity on the FL-2 channel was assessed for those cells which expressed high levels of GFP (red gates on density plots). Representative density plots for HEK-hCCX-CKR cells transfected with these plasmids are shown above with those for HEK-hCCR7 cells below. The MFI of gated cells is plotted below (\* indicates  $p < 0.05$  compared to pEGFP controls). Each sample was included in triplicate and error bars are +/- the standard deviation. Repeat experiments gave similar results ( $n=2$ ).

Analysis of BioCCL19/PE uptake in HEK-hCCR7 cells which express high levels of Rab5(S34N)GFP shows that expression of this protein significantly reduces the amount of internalisation through this receptor when compared with cells expressing similar levels of GFP (Figure 3.1.30). This is consistent with the hypothesis that CCR7 internalises through

CCPs which then fuse with Rab5 positive early endosomes. In contrast, HEK-hCCX-CKR cells which abundantly express Rab5(S34N)GFP are indistinguishable from 'high' GFP expressers in terms of BioCCL19/PE uptake (Figure 3.1.30). As with the EPS15 data, this suggests that alternative routes of internalisation are being employed by this receptor. High levels of dominant-negative Rab4(N121I) had no significant effect upon chemokine uptake by HEK-hCCR7 or HEK-CCX-CKR cells, while moderate inhibition of chemokine uptake was measured when Rab11(S25N) was abundant in HEK-CCX-CKR cells but not HEK-hCCR7 cells. This suggests that Rab11 may play a role in the accumulation of BioCCL19/PE by CCX-CKR through its role in the recycling endosomal compartment.

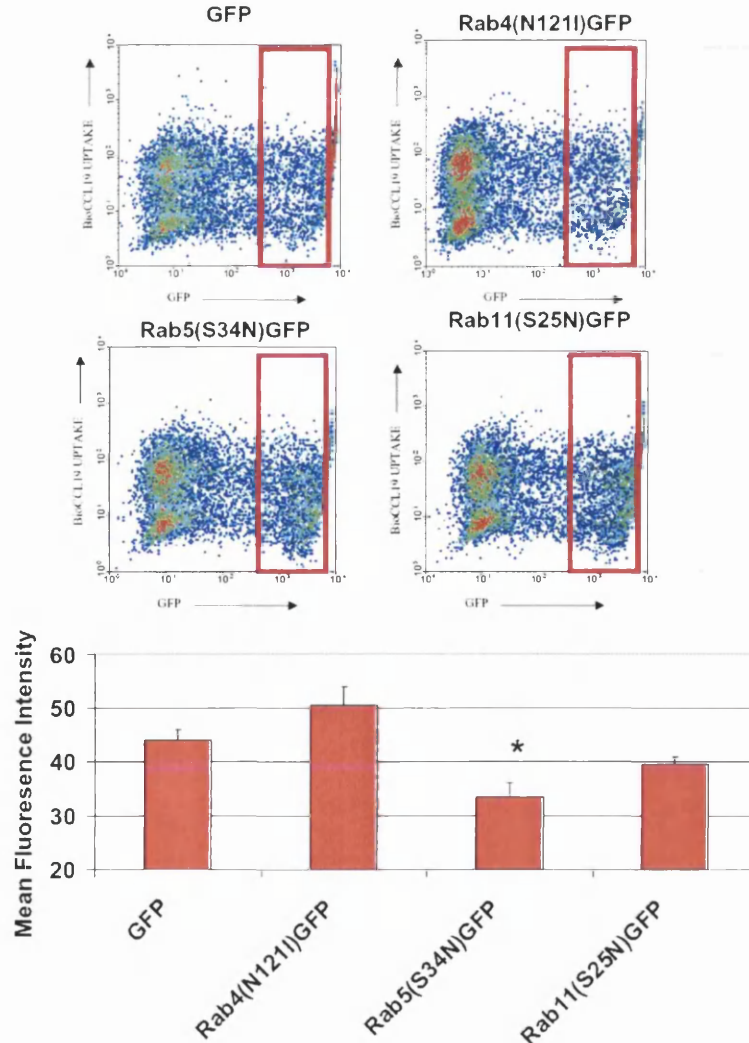


**Figure 3.1.30: Effect of Genetic Inhibition of RabGTPases on BioCCL19/PE Uptake.** Plots for HEK-hCCR7 cells shown. Legend and HEK-hCCX-CKR plots follow overleaf.

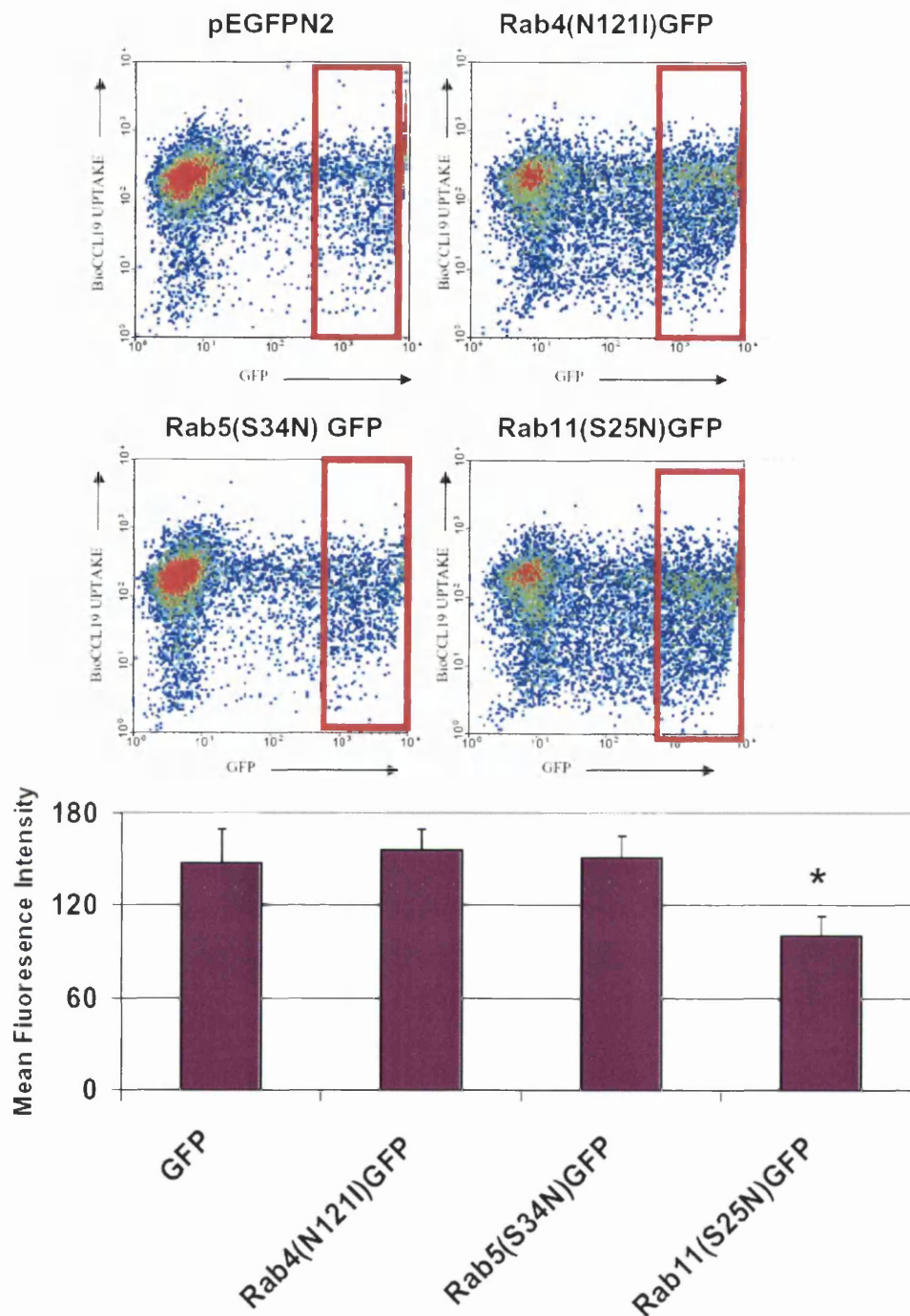


**Figure 3.1.30: Effect of Genetic Inhibition of RabGTPases on BioCCL19/PE Uptake.** Cells in culture were transfected with  $1\mu\text{g}$  of each of one of the GFP tagged RabGTPase mutants (described in text) or pEGFPN2. 24h later, cells were harvested and incubated with BioCCL19/PE for 1h at  $37^\circ\text{C}$ . Cells were then washed and analysed by flow cytometry. The mean fluorescence intensity on the FL-2 channel was assessed for those cells which expressed high levels of GFP (red gates on density plots). Representative density plots for HEK-hCCX-CKR cells transfected with these plasmids are shown here and for HEK-hCCR7 on the previous page. The MFI of gated cells is plotted below. Each sample was included in triplicate and error bars are  $\pm$  the standard deviation (\* indicates  $p < 0.05$  compared to GFP controls). Repeat experiments gave similar results ( $n=3$ ).

### 3.1.4.5 Caveolae and Lipid Rafts

The data above suggested that CCL19 uptake by CCX-CKR, in contrast to CCR7, was independent of  $\beta$ -arrestins, that interference with the formation of CCPs by genetic inhibition of EPS15 did not alter chemokine internalisation, and that uptake was not inhibited by blocking Rab5 function. Therefore, the involvement of alternative mechanisms of internalisation employed by CCX-CKR was investigated. The best-characterised clathrin-independent endocytic compartment is caveolae, a subset of cholesterol-rich plasma membrane-derived vesicles and invaginations which contain the membrane protein caveolin. The first approach taken to examine the possibility that these domains may be important in BioCCL19/PE internalisation was to use the cholesterol-depleting agent Methyl- $\beta$ -Cyclodextrin (Me $\beta$ CD), which is commonly used to prevent the formation of lipid raft structures. As previous work (Subtil et al., 1999) had demonstrated that cholesterol-depletion can affect clathrin-mediated endocytosis, Me $\beta$ CD treatment was at a concentration and duration previously shown not to disrupt transferrin uptake in HEK293 cells (V. Morrow and R.Nibbs, unpublished), a process dependent upon CCP formation. Figure 3.1.31 shows that pre-treatment of either HEK-hCCX-CKR or HEK-hCCR7 with Me $\beta$ CD effectively inhibits subsequent BioCCL19/PE uptake into these cells. While these data indicate that while both of these receptors require membrane cholesterol for optimal BioCCL19/PE uptake, this does not necessarily show that internalisation is via caveolae. Indeed, many receptors have a dependence on membrane cholesterol for proper function but do not endocytose via caveolae. Studies with CCR5 have recently shown that lipid rafts and cholesterol play a role in receptor activation and subsequent internalisation (which is via CCPs) (Signoret et al., 2005). The data here would suggest that CCR7 is like CCR5 in this regard.



To follow up this observation, cells were transiently transfected with a plasmid encoding either caveolin-1 with a C-terminal GFP tag (Cav-GFP: which behaves as the WT protein) or caveolin-1 with an N-terminal GFP tag (GFP-Cav: reported to act as a dominant-negative) (Pelkmans et al., 2001). Again, as in previous experiments, cells were harvested and assessed for their ability to accumulate BioCCL19/PE by flow cytometry. Although moderate to low expression of these proteins had minimal effect on uptake by HEK-hCCX-CKR cells, more abundant expression led to significant inhibition of BioCCL19/PE uptake (Figure 3.1.32). This was particularly evident for the Cav-GFP protein, in which high expressers were barely able to internalise any BioCCL19/PE. Because uptake in the HEK-hCCR7 cells is not significantly affected by high expression of these proteins (fig 3.1.33), the possibility that the inhibition is due to non-specific defects in cell viability, can be ruled out. Further supporting this contention, transfection of these plasmids had no impact on D6 mediated uptake of CCL3, or CCR5 internalisation (Nibbs, unpublished observation and Signoret et al., 2005).

Alongside the assessment of BioCCL19/PE uptake in these cells, levels of surface CCX-CKR were examined by staining with an anti-FLAG antibody at 4°C, with subsequent detection with a PE-conjugated anti-mouse IgG secondary antibody (2.2.4.8). When GFP+ cells were gated and analysed from these transfections, those transfected with Cav-GFP could be detected to have more than double the amount of receptor on their surface when compared with those which express GFP alone, and a more modest but significant increase was measured from cells expressing GFP-Cav (Figure 3.1.33).

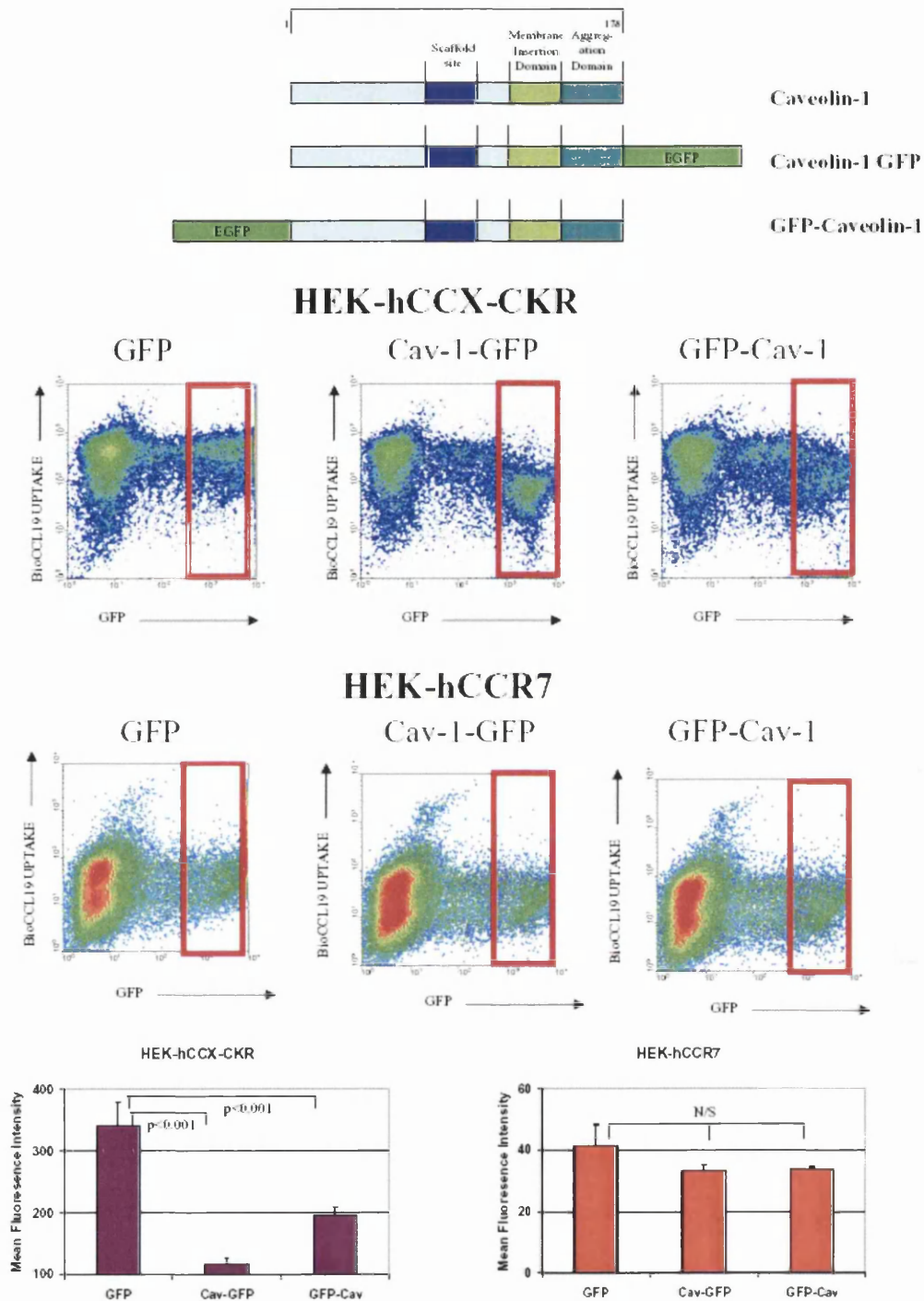


**Figure 3.132: Effect of Genetic Inhibition and Overexpression of Caveolin-1 on BioCCL19/PE Uptake.** Cells in culture were transfected with  $1\mu\text{g}$  of each of one of the GFP tagged versions of caveolin-1 (depicted at top of figure) or pEGFPN2. 24h later, cells were harvested and incubated with BioCCL19/PE for 1h at  $37^\circ\text{C}$ . Cells were then washed and analysed by flow cytometry. The mean fluorescence intensity on the FL-2 channel was assessed for those cells which expressed high levels of GFP (red gates on density plots). Representative density plots for HEK-hCCX-CKR cells transfected with these plasmids are shown above with those for HEK-hCCR7 cells below. The MFI of gated cells is plotted below. Each sample was included in triplicate and error bars are  $\pm$  the standard deviation. Repeat experiments gave similar results ( $n=3$ ).

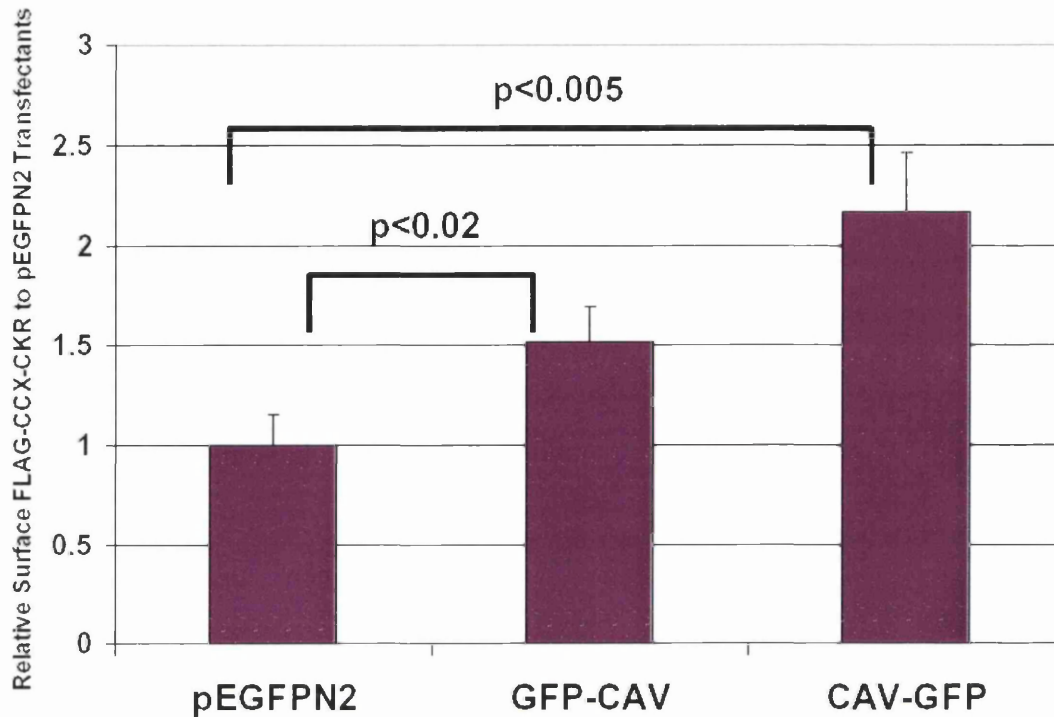


**Figure 3.1.33: Effect of Over-expression of Caveolin-1 on CCX-CKR Surface Receptor Levels.** Cells in culture were transfected with 1 $\mu$ g of each of one of the GFP tagged versions of Caveolin-1 (depicted at top of figure 3.1.33) or pEGFPN2. 24h later, cells were harvested and stained with anti-FLAG M1 followed by anti mouse IgG-PE at 4 $^{\circ}$ C to assess surface receptor levels. Cells were then analysed by flow cytometry. Cells which expressed GFP were gated upon and the MFI on FL-2 of these cells compared between pEGFPN2 transfectants and cell transfected with GFP-tagged Caveolin-1. The relative MFI of these cells compared to pEGFPN2 transfectants is shown above. Samples were performed in triplicate and error bars are +/- the standard deviation. Statistical analysis was performed using a Student's t-test.

The fact that overexpression of a protein with the same activity as endogenous caveolin (Cav-GFP) and a dominant negative inhibitor of caveolin (GFP-Cav) both have similar inhibitory effects on BioCCL19/PE uptake by HEK-hCCX-CKR cells is not necessarily contradictory. Caveolins reportedly function to stabilise caveolae at the cell surface, preventing their internalisation (Thomsen et al., 2002). Thus, if CCX-CKR internalises predominantly via caveolae, their stabilisation would limit CCL19 uptake and would concur with the increase in surface receptor measured. On the other hand, internalisation of caveolae can be induced by extracellular factors and this requires signals dependent upon

caveolin (Nabi and Le, 2003). A dominant-negative caveolin-1 would by its overexpression, reduce activation of endogenous caveolin-1 and thereby limit stimulated caveolae internalisation.

## Summary

1. CCL19 uptake by CCX-CKR is by receptor mediated endocytosis, dependent upon dynamin.
2. Unlike CCR7, CCL19 uptake by CCX-CKR does not require  $\beta$ -arrestins.
3. Genetic inhibition of endocytosis of CCPs inhibits CCL19 uptake by CCR7 but not CCX-CKR.
4. Inhibition of the early endosomal small GTPase Rab5 inhibits CCL19 uptake by CCR7 but not CCX-CKR.
5. Pharmacological depletion of membrane cholesterol inhibits CCL19 uptake by both CCX-CKR and CCR7, indicating that lipid rafts are likely to play a role in the biology of these receptors.
6. Overexpression of caveolin-1 strongly inhibits CCL19 uptake by CCX-CKR but not by CCR7. Expression of a dominant negative inhibitor of caveolin-1 also inhibits CCX-CKR driven CCL19 uptake. Overexpression of caveolin-1 leads to an increase in the levels of surface CCX-CKR.

Together, the data presented in this section demonstrate that CCX-CKR and CCR7 employ different routes of endocytosis. This may have important consequences for understanding the remarkably different behaviours these receptors have following exposure to ligand.

These issues, along with a more in-depth discussion of the possible implications of the data in this section are further debated in section 4.1. In parallel with the biochemical analyses described above, from the outset it was intended to study the *in vivo* significance of CCX-CKR through the generation and analysis of gene targeted mice. The remainder of this thesis focuses on this work.

## 3.2 Generation of Chemokine Receptor Knock-out mice

### 3.2.1 Strategy

The data presented in the previous sections show that clear differences in biochemical properties exist between CCX-CKR and a typical signaling chemokine receptor like CCR7. From this, it may be hypothesised that CCX-CKR plays a role in regulating the availability and/or the distribution of the chemokines CCL19, CCL21, and CCL25 *in vivo*. However, analysis of protein function by overexpression in heterologous transfectants is limited by the fact that conclusions can only be extended to encompass the experimental system used. A more robust approach to determining the essential functions of a particular gene is via the analysis of gene targeted animals in *in vivo* models. Therefore, mice were generated with a targeted ablation of CCX-CKR to enable an investigation of the indispensable function of CCX-CKR *in vivo*. As information regarding the different cell types which expressed CCX-CKR was not available, targeting constructs were designed to result in the insertion of a reporter gene in place of CCX-CKR under the control of endogenous CCX-CKR regulatory elements (a so called knock-in knock-out (KIKO) approach). There were several important considerations to take into account when deciding to generate KIKO mice. First of all, this is a more complicated process than the creation of a simple gene KO mouse. As reporter expression analysis is intended, the promoter from the selection cassette must be removed (in this case by Cre recombinase mediated deletion) to minimise interference with reporter expression. This adds extra steps to the process of generating the mice. However, there are many advantages to the KIKO approach. In the absence of suitable antibodies, these mice should provide a means of convenient analysis of CCX-CKR expression at the level of individual cells, and help provide a cellular basis for CCX-CKR *null* phenotypes that emerge.

Both to ensure that analysis of gene expression and studies of essential gene function were robust, two alternative reporter genes were employed, GFP and *lacZ*. There were two main reasons for this. First, the observed expression of a single reporter gene could be confirmed by the other, providing stronger evidence that the reporter expression accurately reflects that of the gene of interest. Second, methods of detection of GFP and *lacZ* are quite distinct, with *lacZ* detection more convenient on tissue sections and GFP easily detected in live cells by flow cytometry. Thus, the two different reporters would allow simple, convenient analysis of expression in a broad range of assays.

Alongside this process, it was intended to generate analogous mice for the chemokine receptor D6. Although D6 KO mice had already been generated elsewhere (in a collaboration between Prof. Graham and Dr. Nibbs at the Beatson Institute, and Dr. Cook and Dr. Lira at Schering Plough) (Jamieson et al., 2005), detailed information regarding the *in vivo* expression of D6 in the mouse was not available. Therefore, to enable analysis of D6 expression in the absence of a reliable anti-mouse D6 antibody, and to allow us to have D6 *null* mice to use in experiments of our choosing (without enforced Materiel Transfer Agreement restrictions), KIKO mice with a reporter gene under the control of the endogenous D6 promoter were also planned. From the outset, the CCX-CKR *null* mouse generation and analysis was to be the principal focus of the work for this thesis. Indeed, as time progressed the D6 project was transferred to post-doctoral colleagues.

This was a very ambitious project but, as described below, the availability of appropriate targeting constructs at the outset of the project, coupled to the expert assistance provided by the BITU, ensured success. All four planned KIKO strains were generated and phenotypes emerging in the CCX-CKR *null* mice are described in section 3.3.

### 3.2.2 Construction of CCX-CKR Targeting Vectors

A construct for targeting CCX-CKR containing the *lacZ* reporter had already been generated by Dr. Nibbs before this study commenced, using a genomic clone of the mouse CCX-CKR gene isolated and mapped in the lab (Townson and Nibbs, 2002). This construct is shown graphically in figure 3.2.1, and contains the following important features. Arms at either end of the construct are homologous to the genomic sequence flanking either side of the coding exon of CCX-CKR. Instead of the CCX-CKR open reading frame, a reporter cassette was inserted between these homology arms. Within this cassette, the *lacZ* gene was flanked upstream by an intra-ribosomal entry site (IRES) and downstream by a polyA tail. It was hoped that the IRES would ensure robust translation of the reporter transcripts. 3' of the polyA tail was a neomycin cassette, with the strong phosphoglycerine kinase (PGK) promoter driving expression of the neomycin resistance gene (*neo*), to allow selection for construct integration in ES cells. This portion of the construct was flanked by *loxP* sites to allow post-selection splicing of this region with Cre Recombinase, as open chromatin caused by the PGK promoter could influence the reporter gene expression.

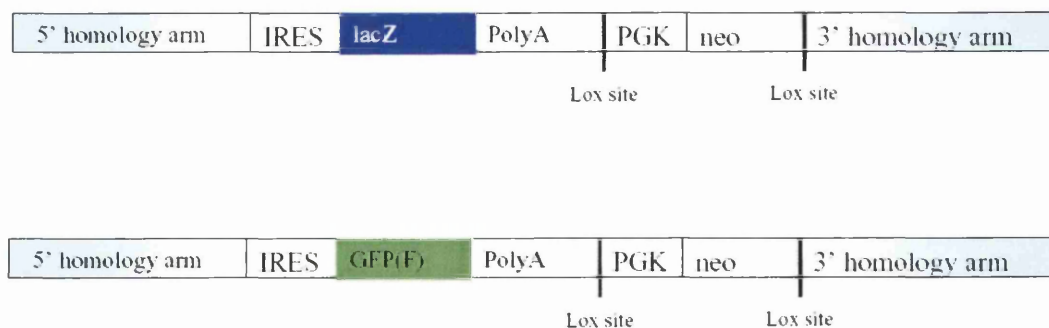


**Figure 3.2.1: Targeting constructs for CCX-CKR containing *lacZ* or GFP.** These constructs contained at each end a region homologous to the genomic sequence either side of CCX-CKR to allow targeted integration events. 5' of the reporter is an intra-ribosomal entry site (IRES). Downstream of the reporter is a poladenylation (PolyA) sequence to allow mRNA from the reporter to be translated efficiently. Then, flanked by *loxP* sites, is the sequence PGK which promotes the expression of the neomycin gene which confers resistance to G418, used for the purposes of ES cell selection.

A GFP reporter construct was generated from this plasmid by removing the *lacZ* coding sequence by restriction digestion and ligation of sequences encoding farnesylated GFP. Farnesylated GFP was used, as this should be expressed at the cell surface allowing convenient visualisation of positive cells. The resulting plasmid was verified by restriction mapping, and the coding sequence of GFP confirmed by sequencing. Both the *lacZ* and GFP KIKO plasmids were then linearised by restriction digestion, ready for transfection into murine embryonic stem (ES) cells. These transfections were performed by members of the BITU and while this was being done, a PCR screen for homologous recombination was developed. These plasmids are shown schematically in figure 3.2.1 and to scale with the CCX-CKR genomic clone in 3.2.2.

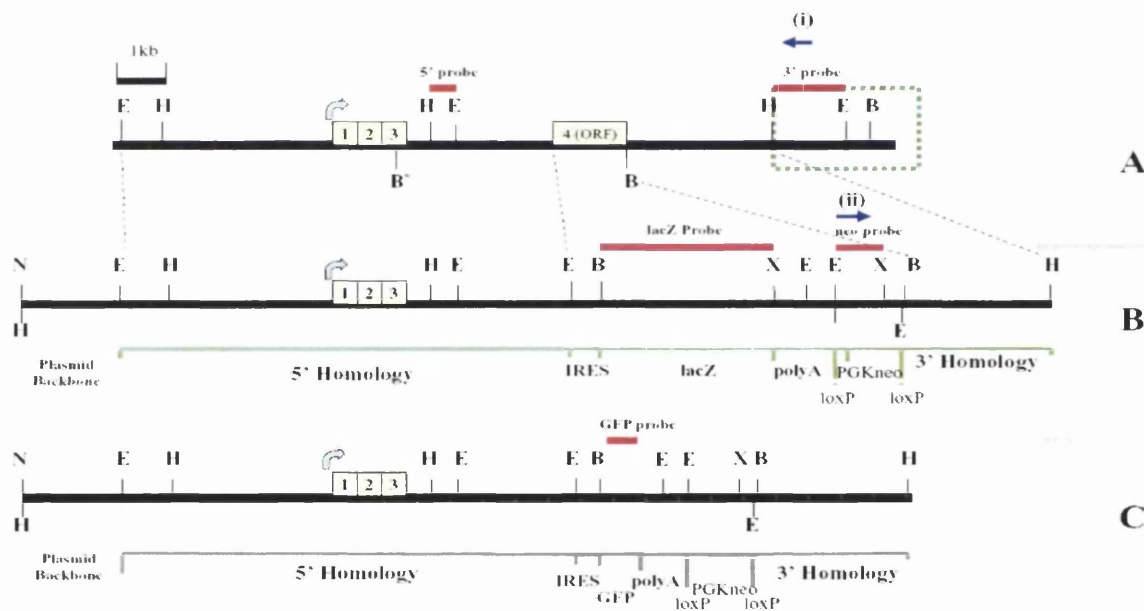


**Figure 3.2.2: Restriction Maps of the Mouse CCX-CKR Genomic Clone and Targeting Constructs.** (A) The mCCX-CKR genomic clone. Yellow hatched boxes=CCX-CKR exons, blue curved arrow=start codon. Portion of the genomic clone highlighted in the green dotted box is referred to again in figure 3.2.3. Fragments used as probes in subsequent Southern blots are shown in red. Positions of screening oligos are shown by blue arrows (i) and (ii). (B) CCX-CKR *lacZ* KIKO construct. Green line below shows position of various portions of the construct. Dotted lines show limits of areas of homology to genomic clone. (C) The CCX-CKR GFP KIKO construct. Grey line below shows position of various portions of the construct. Probes shown in diagram are restriction fragments between indicated sites. E=*EcoRI*, H=*HindIII*, B=*BamHI*, X=*XbaI*, N=*NotI*. (\*) indicates that site removed in targeting constructs. 1kb Scale bar shown above.

### 3.2.3 Targeting of CCX-CKR

To enable screening for targeted integrations, a PCR-based screen was designed and optimised. To help with this, a positive control plasmid was created by ligation of a fragment of the CCX-CKR genomic clone which lay downstream of the 3' homology arm present in the targeting construct into a vector containing PGKneo and the 3' homology arm (Figure 3.2.3). This plasmid was then diluted in murine genomic DNA such that it was present at the ratio 1 copy of plasmid: 1 copy of the genome. Then, to assess the sensitivity of the PCR, serial dilutions were made in water or genomic DNA. Various primer pairs were then assessed for their ability to detect this plasmid. These primers were designed from two specific regions. The 5' primers were from inside the neo cassette, whilst 3' primers were from the genomic DNA sequences just outside the 3' homology arm of the targeting construct, but within the region inserted into the positive control plasmid (Figure 3.2.3). This will allow for specific detection of insertion of exogenous DNA (the neo cassette) into the CCX-CKR locus. The predicted product size was ~3kb. One pair of primers ('mCCXout' and 'neoA') consistently gave sensitive detection of the positive control plasmid and this pair was selected to screen for a targeted integration event in DNA extracted from transfected mouse ES cells surviving selection in G418. Each clone was triplicate plated into 96-well plates by BITU members; two plates were cryopreserved and the other passed on for DNA extraction and screening. The lower panel of figure 3.2.3 shows a representative gel image of a small number of clones, including one positive.

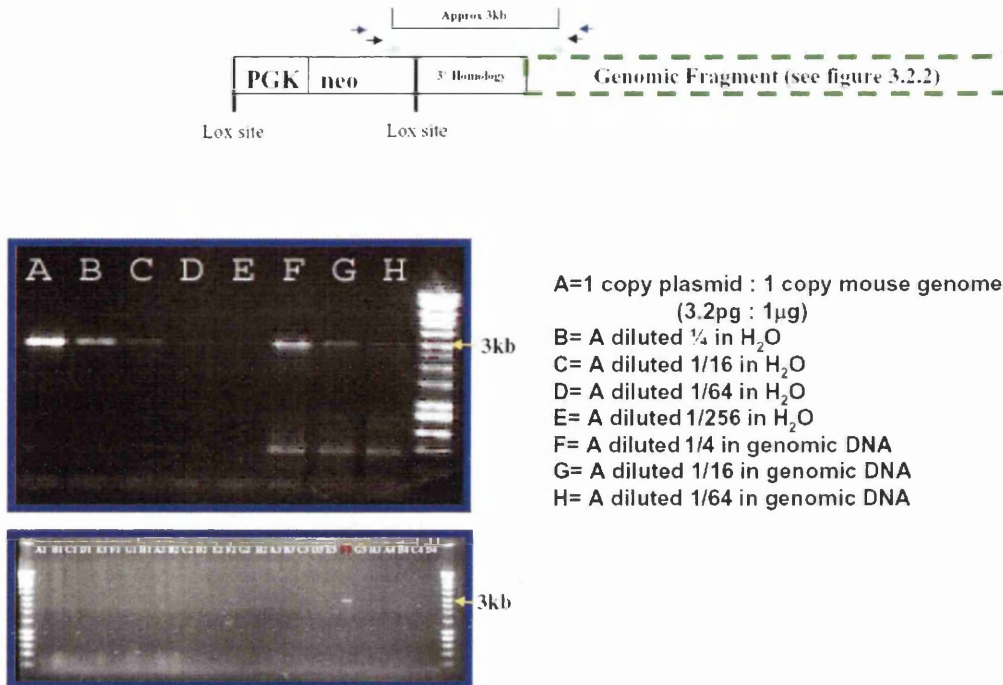


**Figure 3.2.3: PCR Screen for Targeted Integration of CCX-CKR KIKO Constructs.** Top: Schematic diagram of plasmid used as positive control for PCR identifying targeted integrations. Green dotted fragment is the same fragment in green box in figure 3.3.2. Various primer pairs used to optimise assay indicated by arrows. Below: Primer pair identified as suitably sensitive by amplification of 3kb band in lane 'H', shown as 'neo' and 'genomic' primer. This primer pair then used to screen many transfected ES cell clones (bottom panel). Clone 1F3 identified on this gel.

The positive clones identified were then expanded in culture and high quality genomic DNA prepared for Southern blotting, to confirm that a homologous recombination event had taken place, and that the only a single integration of the construct into the genome had occurred. To this end, DNA was completely digested with either *EcoRI* or *BamHI* then subjected to Southern blotting (as detailed in 2.2.1.10). Four different fragments from within and outwith the targeting constructs were then used to probe these blots. The position of the probes used is shown in figure 3.2.2. Representative Southern blots of all probes used for screening ES cell clones transfected with CCX-CKR-GFP-KIKO and CCX-CKR-*lacZ*-KIKO are shown in figure 3.2.4. Moreover, by using four distinct probes from within and outwith the targeting construct, the integrity of the integrated construct

could be validated at the level restriction DNA fragment sizes on a Southern blot. The use of this careful approach to screening the clones was vindicated as one clone, apparently containing a well-integrated targeted construct when analysed with three probes, revealed a shorter than predicted band with the fourth (not shown). The reason for this was unclear, but the exclusion of this clone from further study ensured that this anomaly did not interfere with subsequent work.

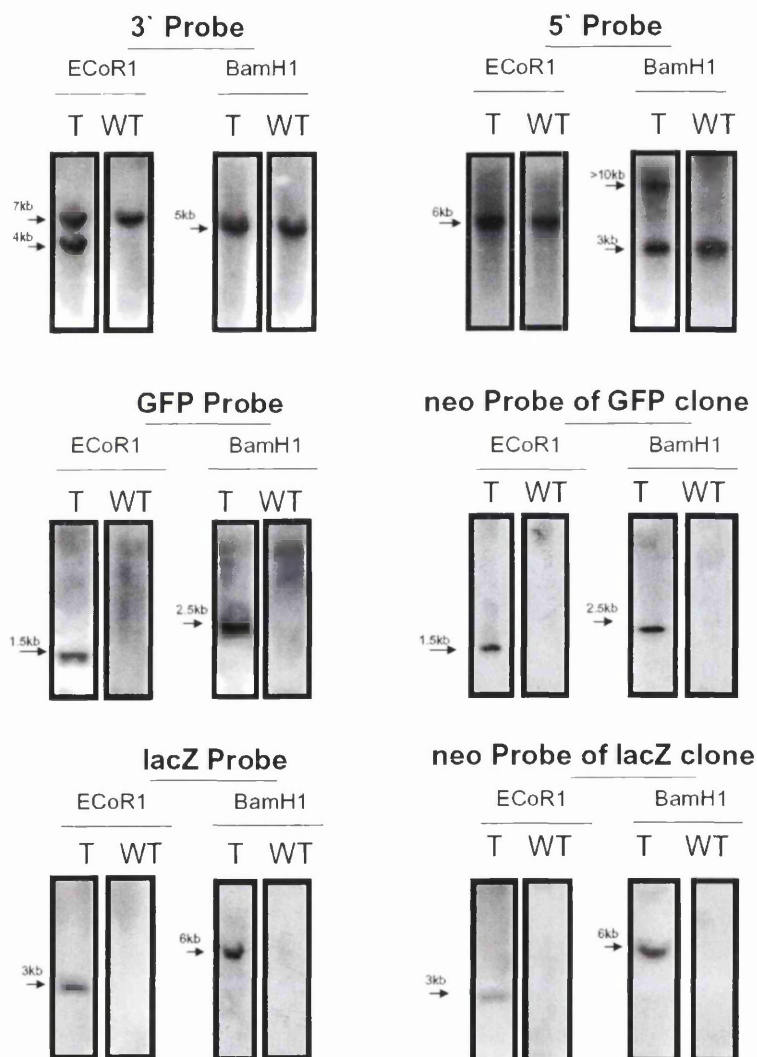


**Figure 3.2.4: Southern Blot Analysis of Targeted CCX-CKR KIKO ES Cell Clones.** Representative Southern blots showing the observed bands from targeted (T) and parental/ wild type (WT) ES cell clones when probed with the various probes shown in figure 3.2.1. Band sizes are indicated at side. Blots from the GFP probe and upper neo blot are from clones with a transfected with CCX-CKR GFP KIKO, while those from the *lacZ* probe and lower neo probe are from clones transfected with CCX-CKR *lacZ* KIKO. 5' and 3' probes gave the same bands for both these constructs. Refer to figure 3.2.2 for restriction maps and probe locations.

### 3.2.4 *In Vitro* Cre-Mediated Excision of Neomycin Resistance Cassette

Following identification of ES clones with a single targeted integration of the CCX-CKR-*lacZ*-KIKO or CCX-CKR-GFP-KIKO constructs, two approaches were taken to generate mice. As Cre recombination was required for the splicing out of the neomycin cassette, it was our intention to transfect ES cells with Cre Recombinase, and screen these clones by PCR and Southern blotting for successful splicing. However, conscious of potential difficulties in getting over-manipulated ES cells to contribute to the germline of chimeric animals, it was decided that we should use some of these ES cells for generation of transgenic animals which could then subsequently be crossed with animals expressing Cre Recombinase in the germline (ZP3-Cre) to drive neomycin cassette excision.

Therefore, ES cells clones containing targeted CCX-CKR-*lacZ*-KIKO integrations were transiently transfected with Cre Recombinase (performed by Dr. Forrow (BITU)), individual clones isolated, and DNA extracted. A PCR screen for Cre recombination was designed, and clones were assessed using this procedure (Figure 3.2.5). Clones positive for recombination were then further screened by Southern blotting to confirm that the correct recombination event had occurred (Figure 3.2.5). This led to the identification of ES clones in which the neomycin cassette had been successfully deleted *in vitro* which could then be used in blastocyst injections. On the other hand, ES cell clones transfected with CCX-CKR-GFP-KIKO which were identified by PCR and Southern blotting were used directly for blastocyst injection.

Table 3.1 and table 3.2 summarise the CCX-CKR-*lacZ*-KIKO clones which were identified by PCR screening and Southern blotting both before and after transient Cre-mediated neomycin cassette excision. These tables also indicate the clones that were used for blastocyst injections. Table 3.3 summarises the ES cell clones transfected with CCX-CKR-

GFP-KIKO which were identified by PCR screening and Southern blotting and which clones that were used for blastocyst injections.

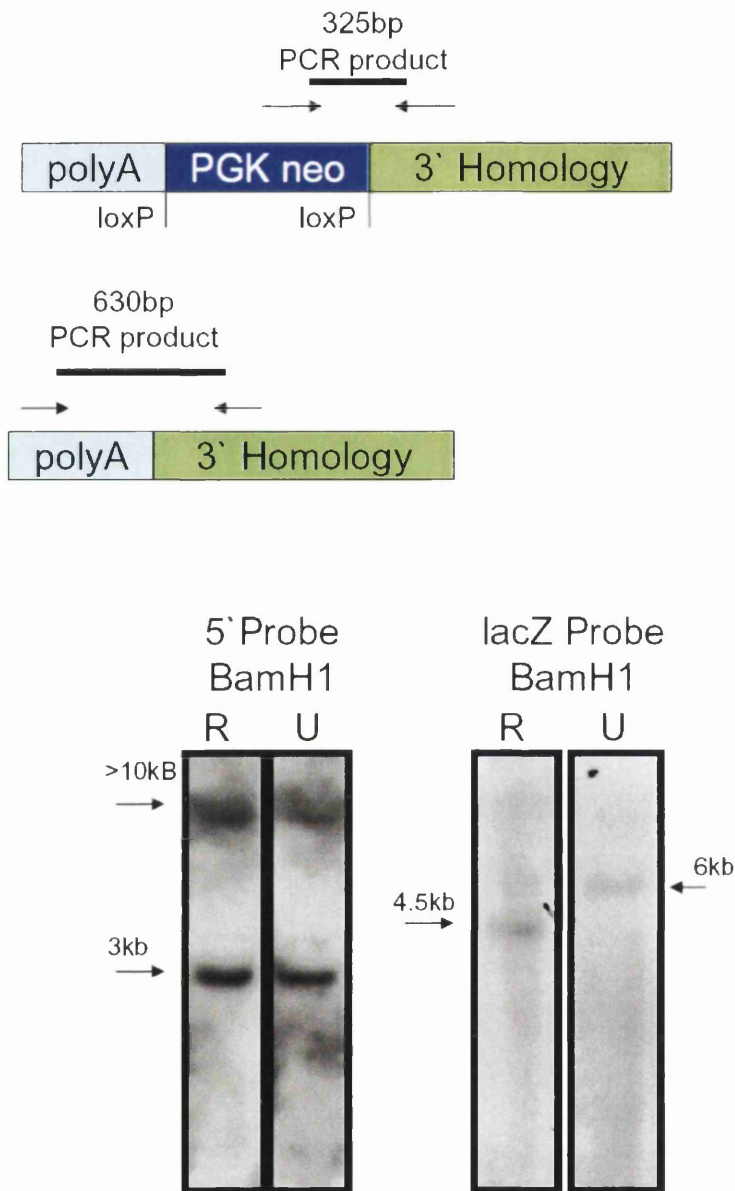


**Figure 3.2.5: PCR and Southern Blot Screen for *in vitro* Cre Recombination.** A PCR was designed to differentiate between clones which had recombined to splice out the PGKneo portion of the construct. Primers used were 'mCCXCKRwt', 'commonsreen' and 'target.neo' and PCR conditions were 'genotyping' (2.2.6.2). Positive clones identified by amplification of the indicated 630bp product were then screened by Southern blotting. The 5' probe was used to confirm that the CCX-CKR allele remained targeted and the *lacZ* probe used to show the splicing of PGKneo. R=recombined, U=unrecombined. Fragment sizes are indicated. Refer to figure 3.2.2 for restriction map and probe locations.

PCR +ve Clones	Southern Blot +ve	Used for <i>in vitro</i> Recombination
1A5	Yes	No
1C10	No	No
1C11	No	No
2A9	No	No
2D11	Yes	No
2E9	Yes	No
<b>2H4</b>	<b>Yes</b>	<b>Yes</b>
3B4	Yes	No
4C5	Yes	No
4D7	Yes	No
<b>4G8</b>	<b>Yes</b>	<b>Yes</b>

**Table 3.1: CCX-CKR *lacZ* KIKO ES Cell Clones Identified by PCR and Southern Blotting.** All ES cell clones identified as positive for a targeted integration of CCX-CKR *lacZ* KIKO (11 clones out of 384 screened) are listed along with the results obtained from Southern blots carried out subsequently on these. Two clones (highlighted in blue) were used for *in vitro* Cre Recombination.

PCR +ve Clones	Southern Blot +ve	Clone Injected	Germline Transmission
1A4 (2H4)	No	No	n/a
1C2 (2H4)	Yes	No	n/a
1C4 (2H4)	Yes	No	n/a
1D1 (2H4)	Yes	No	n/a
2A1 (2H4)	No	No	n/a
<b>2C1 (2H4)</b>	<b>Yes</b>	<b>Yes</b>	<b>Yes</b>
2D1 (2H4)	Yes	No	n/a
3D1 (2H4)	Yes	No	n/a
<b>1A3 (4G8)</b>	<b>Yes</b>	<b>Yes</b>	<b>Yes</b>
1B6 (4G8)	No	No	n/a
2B2 (4G8)	No	No	n/a
2B3 (4G8)	Yes	No	n/a
2B5 (4G8)	Yes	No	n/a
2C2 (4G8)	No	No	n/a
3A2 (4G8)	Yes	No	n/a
3B3 (4G8)	Yes	No	n/a
3C3 (4G8)	Yes	No	n/a

**Table 3.2: *In Vitro* Recombined CCX-CKR *lacZ* KIKO ES Cell Clones.** All clones of Cre Recombinase transfected ES cell clones from indicated targeted ES cell clones which were PCR +ve for recombination. Result of subsequent Southern blot analysis, whether this clone was used for blastocyst injections, and whether the clones gave germline transmission (highlighted in blue) is also indicated.

PCR +ve Clone	Southern Blot +ve	Clone Injected	Germline Transmission
1F3	No	No	n/a
2A2	Yes	No	na
2F12	No	No	n/a
3C3	No	No	n/a
3C7	Yes	Yes	No
3E3	Yes	No	n/a
4G4	Yes	No	n/a
5G6	Yes	No	n/a
5G10	Yes	No	n/a
6D12	No	No	n/a
7D6	Yes	Yes	No
7E6	No	No	n/a
7E12	Yes	No	n/a
A5 (W4)	Yes	Yes	Yes
G7 (W4)	Yes	No	n/a
C11 (W4)	Yes	No	n/a

**Table 3.3: CCX-CKR-GFP KIKO ES Cell Clones Identified by PCR and Southern Blotting.** All ES cell clones identified as positive for a targeted integration of CCX-CKR GFP KIKO by PCR (16 clones out of 768 screened) are listed along with the results obtained from Southern blots carried out subsequently on these. Clones which were then subsequently used in blastocyst injections are indicated and the clone which gave germline transmission highlighted in green.

### 3.2.5 Blastocyst Injections, Chimeras, and Test Breeds

Blastocyst injections and implantations were all performed by the BITU according to standard protocols. Chimeric offspring produced were then crossed with C57/Bl6 mice in test breeds to investigate whether transgenic ES cells were contributing to the germline of these mice. C57/Bl6 mice were used as the coat colour of this strain differs from, and is recessive to, the agouti coat colour of mice derived from 129/W4 ES cells. The presence of mice with agouti fur was therefore indicative of germline transmission. As shown in table 3.2 and table 3.3, all except two of the injected clones gave successful germline transmission.

Tailtip DNA was prepared from the offspring of chimeric mice and a triple-primer genotyping PCR (2.2.6.2) designed to determine which mice carried the CCX-CKR *null* allele (Figure 3.2.6). These triple-primer sets had one common primer from within either

the 3' or 5' homology arms of the targeting construct. The two other primers were specific either to the CCX-CKR open reading frame (ORF) or to the reporter cassette. Amplification products of the common primer and the two other primers were of different sizes. The advantage of screening at both ends of the construct were that not only did this allow verification of genotyping results, but also that if one band were to amplify preferentially this could be resolved by examining the result from the opposite end. Following optimisation of this PCR, all subsequent genotyping was carried out by members of the BITS.

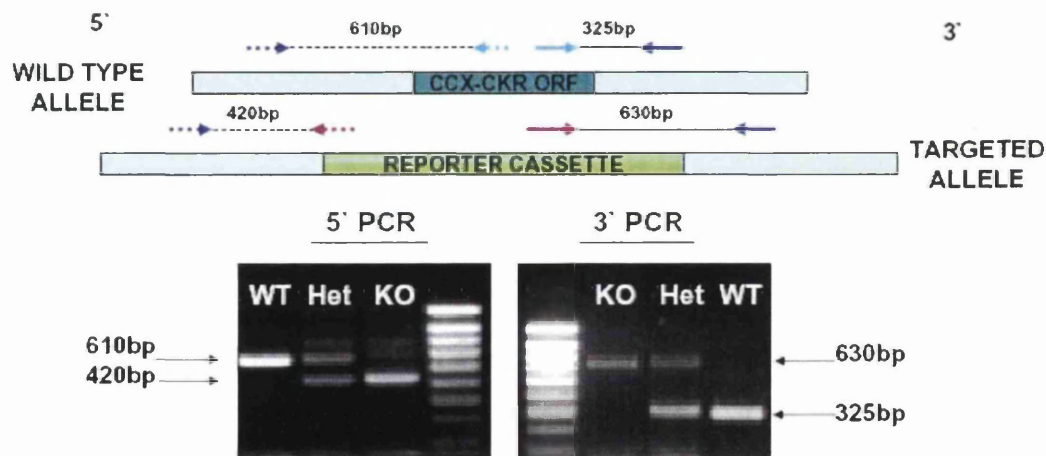


**Figure 3.2.6: Genotyping of Pups at CCX-CKR Locus.** A schematic of the targeted and WT alleles is shown with approximate positions of oligonucleotides used to screen. Primers common to both WT and targeted alleles are in blue. Primers hybridising only to the WT allele are coloured cyan and primers specific for the targeted allele are in purple. Those oligos used to screen the 5' end of the alleles are dotted. The ~size of fragments are indicated by dotted lines. The gel images show tailtip DNA from a mouse of each genotype at this locus screened by these two PCRs.

### 3.2.6 *In Vivo* Cre-Mediated Excision of Neomycin Resistance Gene

Chimeras heterozygous for CCX-CKR which were from non-*in vitro* recombined ES cells transfected with CCX-CKR-GFP-KIKO were then bred with ZP3-Cre transgenic FVB mice, and tailtip DNA prepared from the offspring. These pups were then genotyped by

PCR for the presence of the ZP3-Cre transgene and the CCX-CKR KIKO allele. ZP3-Cre is only expressed in the oocyte, so for recombination to take place, another mating was necessary. Therefore, female mice carrying both the ZP3-Cre and the CCX-CKR KIKO transgenes were then mated with WT FVB mice. FVB mice were used here as this was the strain carrying the ZP3-Cre, so this led to the derivation of FVB mice carrying the *null* allele. The offspring from these matings were then screened for the absence of the ZP3-Cre gene and presence of the CCX-CKR KIKO allele. The recombination of the CCX-CKR *null* locus was then confirmed by Southern blot analysis of tailtip DNA (representative blots shown in figure 3.2.7).

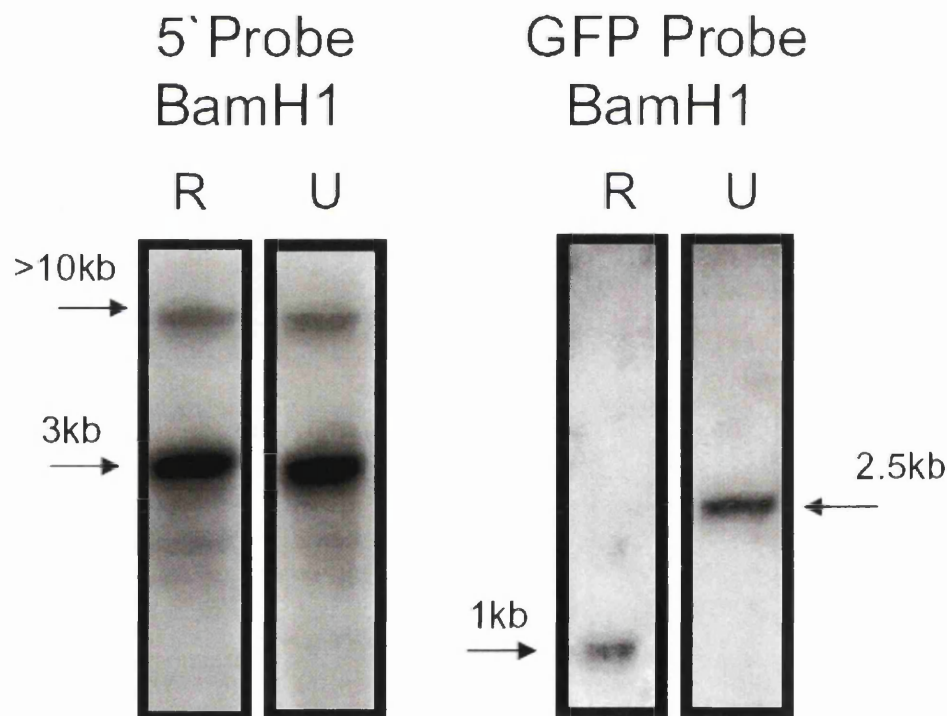


**Figure 3.2.7: Southern Blots of CCX-CKR GFP KIKO neo Recombination After ZP3/Cre Cross.** Pups from ZP3/Cre crosses were screened for PGKneo recombination by Southern blotting. The 5' probe was used to confirm that the CCX-CKR allele remained targeted and the GFP probe used to show the splicing of PGKneo. R=recombined, U=unrecombined. Fragment sizes are indicated. Refer to figure 3.2.2 for restriction map and probe locations.

Mice carrying successfully recombined CCX-CKR-GFP KIKO alleles were then backcrossed onto an FVB background until F5. These gave rise to the colony of mice known hereafter as CCX-CKRGFP-FVB. DNA extracted from the tailtip of the founder of this colony was extensively analysed by Southern blotting, to ensure that the targeted integration of the recombined allele was correct (figure 3.2.8).

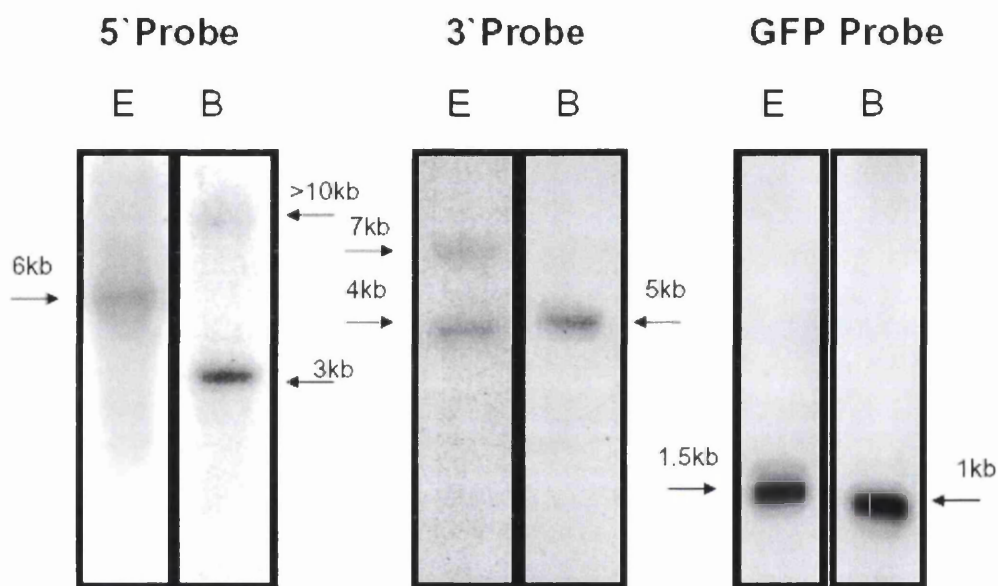


**Figure 3.2.8: Screening of Genomic DNA from CCX-CKR GFP KIKO Founder Mouse.** Tailtip DNA from the CCX-CKR GFP KIKO mouse which gave germline transmission of the targeted allele was screened by Southern blotting to ensure that the genetic structure of the locus was correct. E=*EcoRI* digested tailtip DNA, B=*BamHI* digested tailtip DNA. Fragment sizes are indicated. Refer to figure 3.2.2 for restriction map and probe locations.

### 3.2.7 Other CCX-CKR KIKO Strains

Chimeric mice derived from ES cells which had been recombined *in vitro* were also used to in test breeds as described above. However, chimeras which gave germline transmission of the manipulated ES cells and which carried the CCX-CKR *lacZ* KIKO allele were bred with 129/S6 females to give pure 129/S6 offspring. Although this allowed rapid derivation of a pure strain of mice carrying the *null* allele, 129/S6 mice have proved to be a poor

mating strain which led to difficulties in maintaining this colony. Therefore, chimeras which were capable of germline transmission of the targeted allele were also bred on to a C57/Bl6 background, currently at F7 (June 2005). This approach has led to the generation of CCX-CKR *null* mice on three different genetic backgrounds. In the future, this will enable detailed analysis of CCX-CKR function in different disease models where strain specificity plays a significant role. The overall strategy for the generation of these mice is summarised in figure 3.2.9.

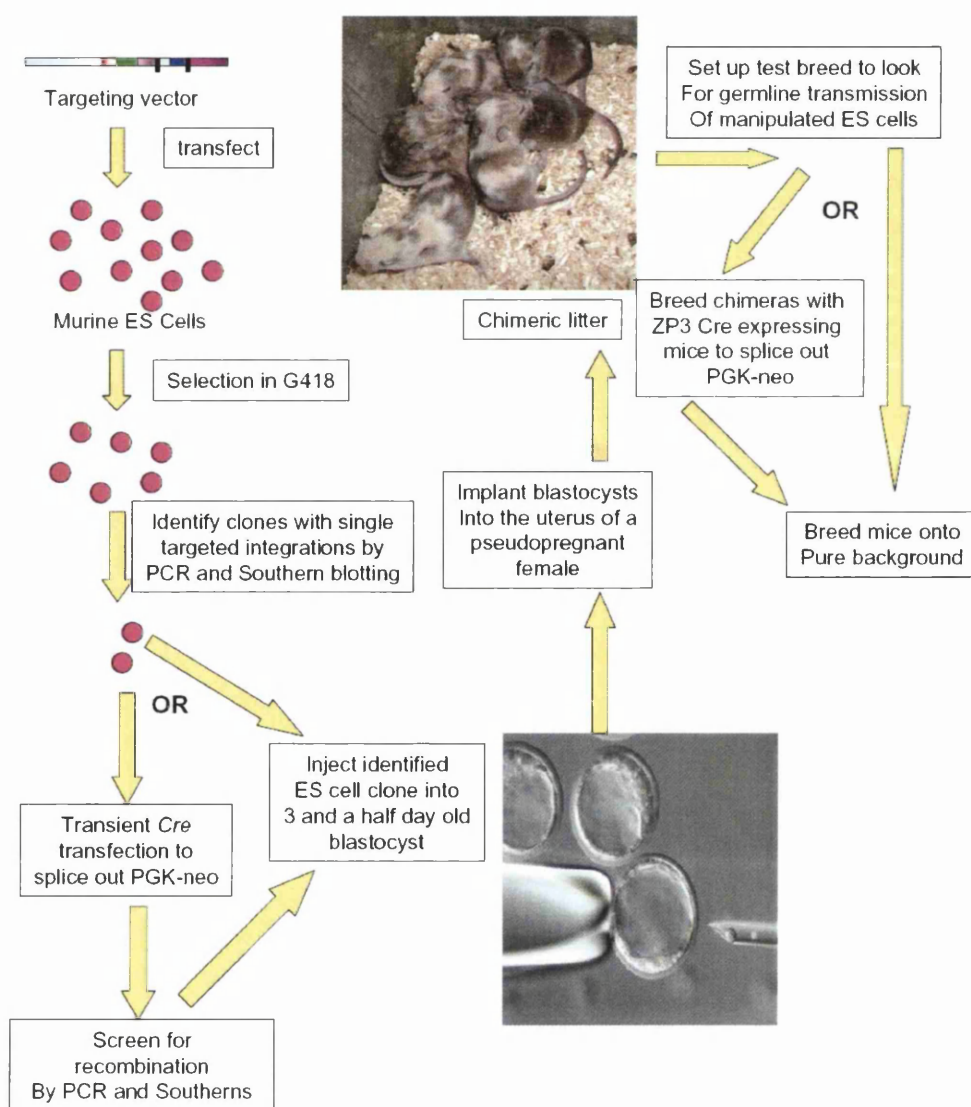


**Figure 3.2.9: Overall Strategy for Generation of CCX-CKR KIKO Mice.** A schematic diagram showing the basic overall strategy for the generation of CCX-CKR KIKO mice, as detailed in the text.

### 3.2.8 Targeting of D6

Alongside the generation of CCX-CKR KIKO mice, analogous mice at the D6 locus were also generated. This project involved contributions from several different people. As described above for CCX-CKR, a D6 *lacZ* KIKO construct was previously generated by Dr Nibbs. A D6-GFP KIKO construct was created by modification of the D6-*lacZ* KIKO plasmid (in a similar way to that described for CCX-CKR constructs in section 3.2.2). These were transfected into 129 W4 ES cells (by members of the BITU) and colonies surviving selection picked. I then prepared DNA from G418 resistant ES cell clones and these were screened by a PCR optimised by Dr. Nibbs. DNA from clones PCR positive for targeted integration of the construct was then digested for Southern blot analysis. These blots were then extensively probed with various probes from within and outside the construct to confirm that only a single correctly targeted recombination event had occurred (not shown).

ES cell clones identified in this way were then used for *in vitro* Cre recombination (as ES cells manipulated in this way had already been shown to be transmissible through the germline from previous experiments targeting CCX-CKR). At this point screening and subsequent analysis of D6 *null* mice was passed on to Dr. Morrow, to allow this project to focus more clearly upon CCX-CKR. D6 *null* mice, carrying an inserted GFP or *lacZ* reporter, were successfully generated by these techniques.

### 3.3 Analysis of CCX-CKR Knock-out mice

#### 3.3.1 Fertility and Viability

Fertility analysis, assessed by genotyping pups born from crosses set up between heterozygote males and heterozygote females, revealed that the absence of CCX-CKR does not lead to any disadvantage in the survival of these pups, with close to the expected genotyping frequencies observed (Figure 3.3.1). CCX-CKR *null* mice are viable and show no gross phenotypic abnormalities. Size, weight and appearance of CCX-CKR *null* mice, were normal.

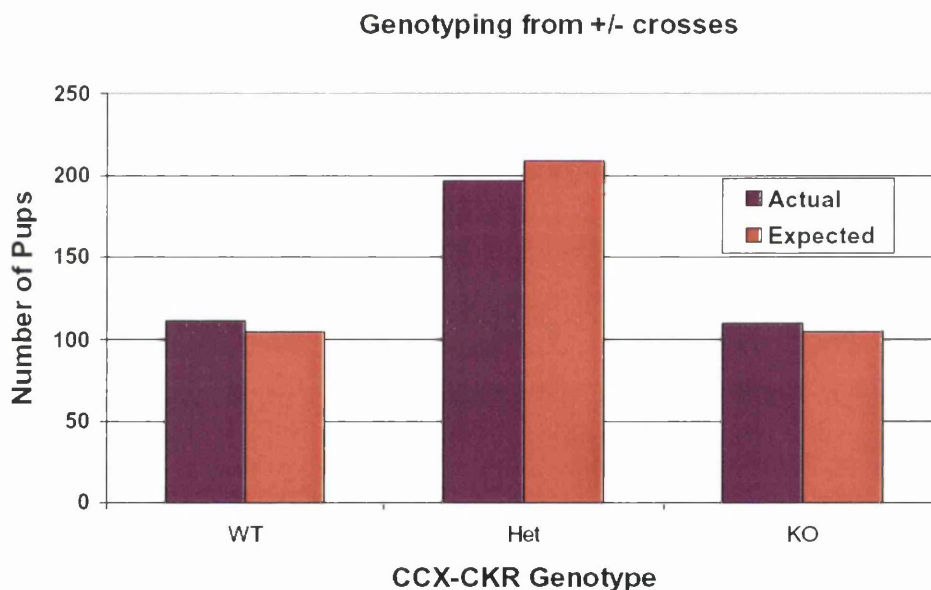


**Figure 3.3.1: Effect of CCX-CKR Ablation on Mouse Fertility.** The results of all genotyping performed on the offspring produced by male and female mice both heterozygote at the CCX-CKR locus. A total of 418 mice were screened. Expected numbers represent the numbers of mice expected of genotype given the normal ratio of 2:1:1 (Het: WT: KO).

#### 3.3.2 Histological Analysis

To further analyse these mice, the major organs from KO and WT littermates were removed, fixed, sectioned, and stained with H+E. Examination of these sections revealed no

gross differences between KO and WT mice (not shown). In these, and all subsequent experiments, animals were closely age and sex matched.

### 3.3.3 Secondary Lymphoid Organs

As discussed in detail in the introduction, two of the CCX-CKR ligands, CCL19 and CCL21 are intimately involved in cell homing to secondary lymphoid organs. Thus, a detailed analysis of these structures in CCX-CKR KO mice compared to WT counterparts was initiated. Because the ILNs drain the skin, and planned models of inflammation that were routinely used in the laboratory involved the topical route of delivery, analysis of LNs focused primarily upon these structures. Analysis of the spleen was also undertaken. This work was all performed on age and sex-matched mice from the CCX-CKR-GFP FVB F5 background. The principal focus of these studies was to assess the overall structure, size, and cellular composition of these organs, and then examine responses in ILN to inflammation, and immune challenge using cutaneous inflammatory models. This work was initiated late in the tenure of this studentship and while it has revealed a number of intriguing observations, these require further in-depth investigation.

#### 3.3.3.1 The Spleen

No abnormalities were apparent from initial analyses of spleens. H+E sections from CCX-CKR *null* mice revealed no gross phenotypic abnormalities with apparently normal red and white pulp development and T and B cell areas (not shown). Both the weight and number of recovered cells from WT and CCX-CKR *null* spleens were not significantly different (not shown).

More detailed analysis of the proportions of different cell populations in the spleen was also performed. Leukocytes were harvested from the spleen (see 2.2.6.6), and stained with a variety of fluorochrome-labelled antibodies against well-characterised surface markers of

various leukocyte populations (see 2.2.6.7). Antibodies against the following markers were chosen: CD3 (pan T cell marker), B220 (B cell specific CD45 isoform), CD4 (mainly found on helper T cells), CD8 (mainly found on cytotoxic T cells), I-A/I-E (a murine class II MHC haplotype), CD19 (a B cell-specific co-receptor), CD11c (an adhesion molecule commonly found on DCs) and F4/80 (a glycoprotein normally found on macrophages). Fluorochrome-labelled isotype control antibodies were used to set cytometer settings and single-stained cells were used to adjust cytometer compensation (see 2.2.3.2). Analysis using these antibodies allowed the characterisation of the main leukocytic subsets commonly found in secondary lymphoid organs.

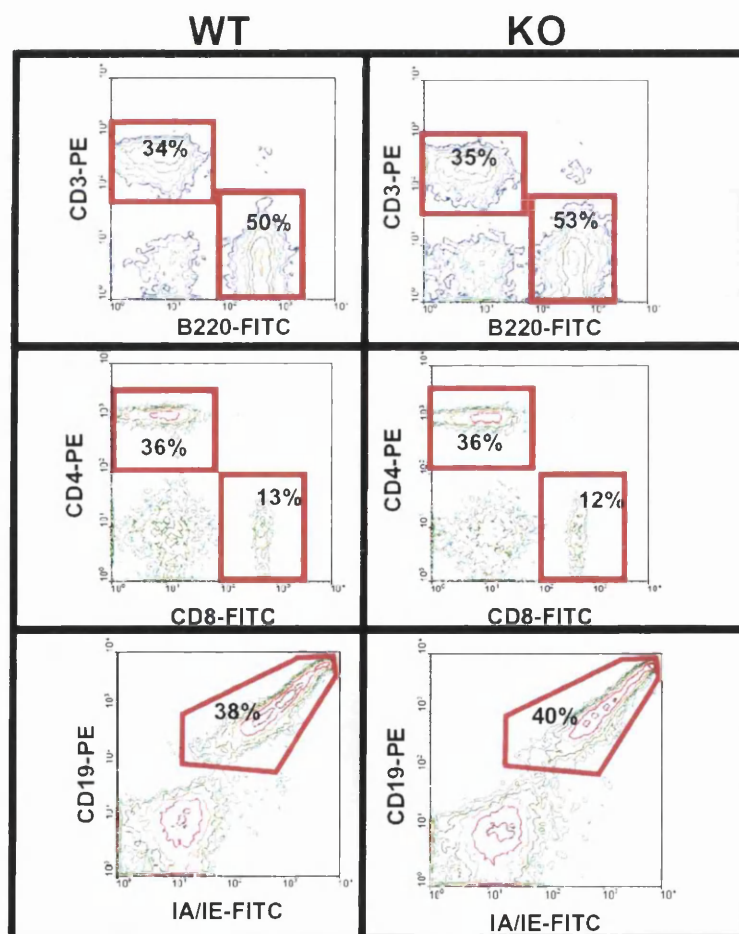


**Figure 3.3.2: Analysis of Leukocyte Populations in Spleens of CCX-CKR +/+ and -/-.** Part 1. Splenocytes were analysed by flow cytometry using well-characterised fluorochrome-labelled antibodies against leukocyte surface proteins. Isotype control antibodies were used to set cytometer settings and compensation (see section 2.2.3.2). Representative contour plots showing WT and KO cell populations are shown. Cells falling within the red gates were quantified (analysis in part 2 of figure over page).

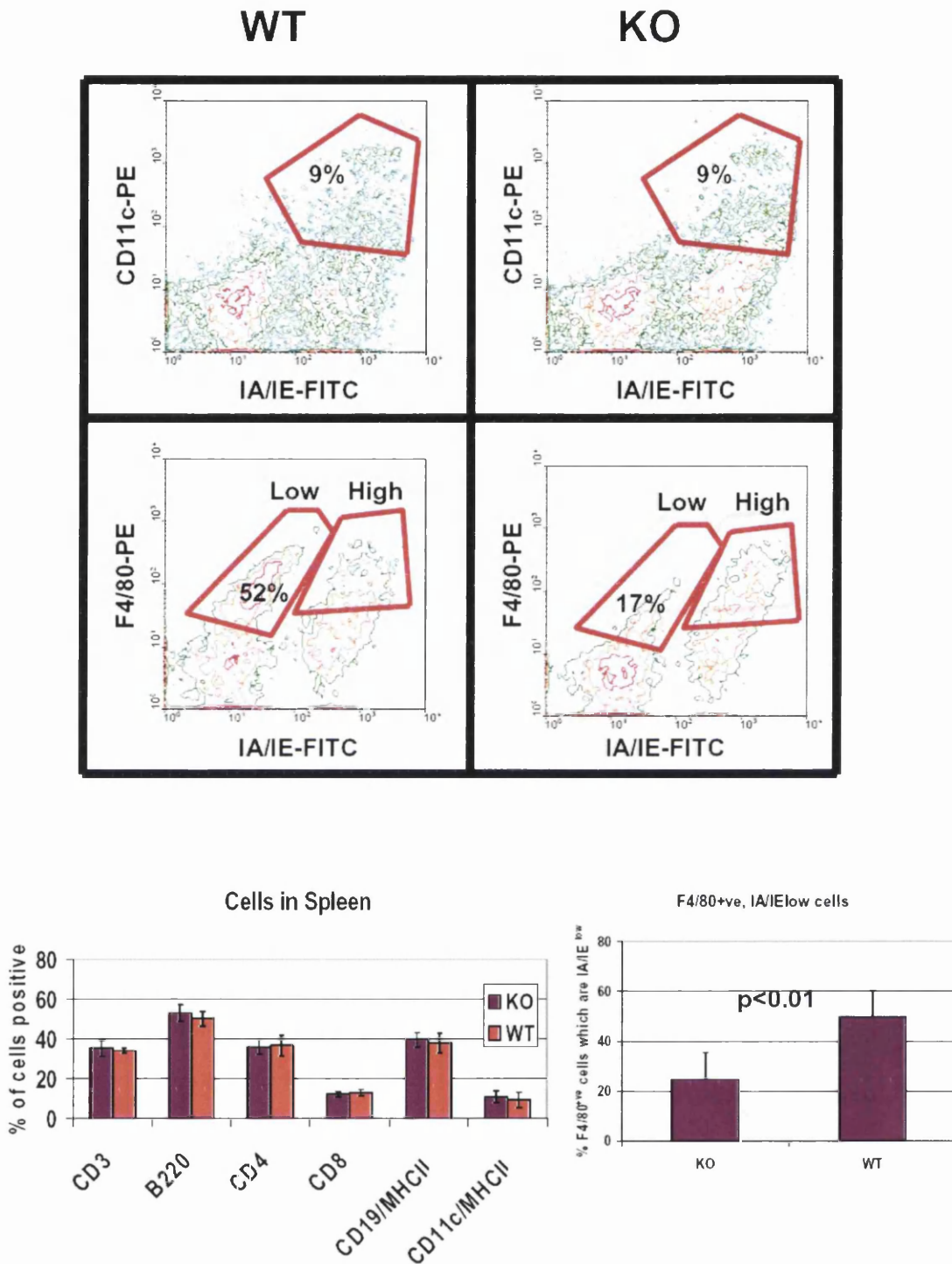


**Figure 3.3.2: Analysis of Leukocyte Populations in Spleens of CCX-CKR +/+ and -/-.** **Part 2.** Representative contour plots showing WT and KO cell populations are shown. Cells falling within the red gates were quantified. At least 5 mice in each group were analysed and error bars are +/- the standard deviation. Statistical analysis was performed using a Student's t-test. Repeat experiments gave very similar results (n=3).

As can be seen in figure 3.3.2, the proportions of all cell types examined in the spleens of CCX-CKR KO animals was largely similar to the WT animals. There were no significant differences in the relative proportions of T cells (CD4+ or CD8+), B cells (determined both by B220+ or CD19+/classII MHC+), macrophages (F4/80+) or DCs (CD11c+). However, close analysis revealed subtle differences in splenic macrophages. CCX-CKR KO animals expressed higher levels of MHC classII (I-A/I-E staining) on F4/80+ cells than WT mice. On average F4/80+ cells from CCX-CKR KO mice were more positive for class II MHC and fewer F4/80 cells were in the I-A/I-E low population than those isolated from WT FVB mice (figure 3.3.2). Recent work has shown that splenic macrophages express CCR7 and require this receptor for appropriate localisation in the spleen (Ato et al., 2004). In addition it has been shown that stimulation of APCs with CCL19 or CCL21 can induce their activation, including up-regulation of class II MHC (Marsland et al., 2005). Therefore the possibility that the lack of CCX-CKR is leading to excessive available CCR7 ligands, which in turn causes hyper-activation of splenic macrophages, is worthy of further investigation and is discussed in at greater length in the section 4.3. It should be noted however, that no significant increase in class II MHC levels was measurable between CCX-CKR *null* and WT CD11c+ DCs, indicating that this phenomenon is not universal for splenic APCs.

### 3.3.3.2 Inguinal Lymph Nodes

Similar analysis to that conducted on the spleen was initiated with ILNs. Analysis of H+E stained sections of ILNs revealed no gross abnormalities between CCX-CKR KO and WT animals (Figure 3.3.3). ILNs from CCX-CKR *null* animals retained major structural features such as the cortex, medulla, T cell areas and B cell follicles. However, in contrast to the spleen, ILNs from CCX-CKR KO mice were consistently smaller and weighed significantly less than those from WT counterparts (figure 3.3.4). Moreover, further

analysis of ILNs revealed that the total number of recovered cells from KO ILNs was consistently less than the number recovered from WT ILNs (figure 3.3.4). The reasons for this could be manifold and are discussed in detail in section 4.3.

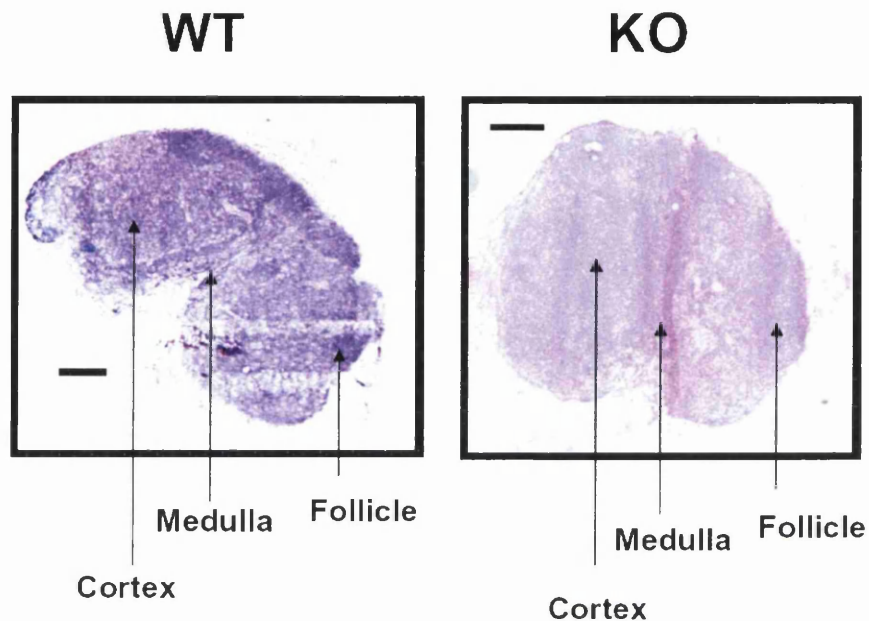


**Figure 3.3.3: Analysis of H+E Sections of ILNs from CCX-CKR +/+ and -/-.** ILNs were removed from age and sex matched CCX-CKR KO and WT mice and were fixed in formalin, paraffin embedded and sectioned. Sections were then stained H+E. Slides were then visualized by light microscopy and images obtained using the Axvision digital camera. The three main areas of the LN are highlighted with arrows. Representative images of 6 sections of ILNs of each genotype are shown. The black scale bars indicate 200 $\mu$ m.

The question of whether this difference in cellularity of CCX-CKR KO ILNs could be explained by the absence or reduction of a particular cell population from these LNs was addressed next. ILN cells were stained with a variety of antibodies against well-characterised markers of various leukocyte populations (2.2.6.7), in a similar manner to that described above for the spleen. The differences in ILN cellular composition observed between CCX-CKR KO and WT ILNs were subtle, but intriguing. No gross differences in the proportions T or B cells (assessed by CD3, CD4, CD8, B220, CD19, and class II MHC staining) were apparent between KO and WT ILNs (Figure 3.3.5). However, when a population of CD4-, CD8<sup>low</sup> cells were compared between CCX-CKR KO and WT ILNs,

there was a significant reduction in the proportion of these cells in KO ILNs. Further investigation is merited to identify the precise phenotype and function of this population, to understand the biological significance of this observation and the impact on CCX-CKR *null* mice.

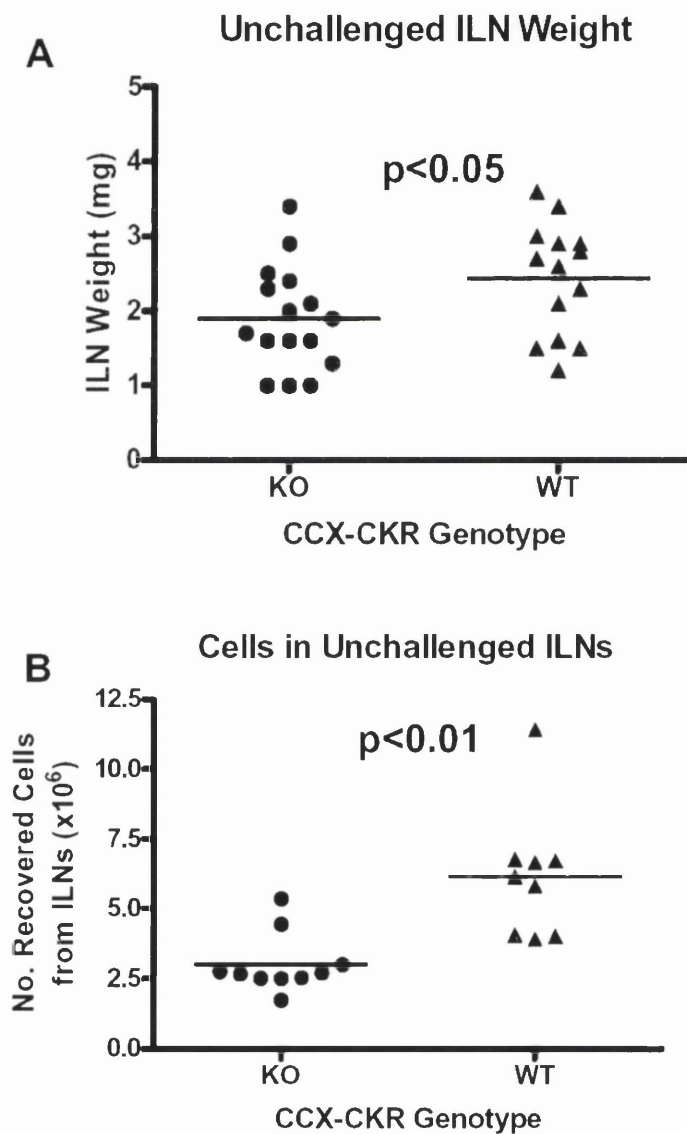


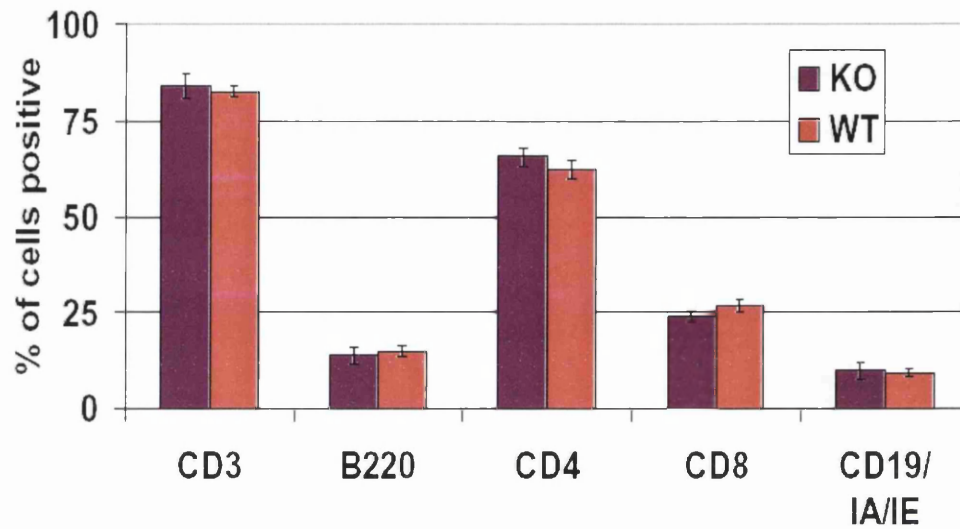
**Figure 3.3.4: Weight and Cell Number from ILNs of CCX-CKR  $+/+$  and  $-/-$ .** ILNs were removed from age and sex matched CCX-CKR KO and WT mice and trimmed under the dissection microscope. They were then carefully weighed on a microbalance. The weight in milligrams of ILNs from KO and WT mice is shown in (A). Cells were isolated from pooled ILNs (2 from each animal) by mashing through nitex membrane. Recovered cells were counted in a haemocytometer. The number of cells recovered from pooled ILNs from each animal is shown in (B). Statistical analysis was performed using a Student's t-test.

Technical difficulties were encountered when attempting to quantify the composition of APCs in ILNs. Recovered ILN cells did not stain with either CD11c or F4/80 antibodies (for DCs and macrophages respectively) any more than isotype control antibodies. This is most likely due to the method of cell separation used. In future, collagenase treatment should be employed to recover and assess these cell types.



**Figure 3.3.5: Analysis of Leukocytes in ILNs from CCX-CKR +/+ and -/-. Contour plots from FACS analysis shown. The rest of the figure and legend are shown overleaf.**

### Cells in Inguinal Lymph Nodes



### % of CD4<sup>-ve</sup> CD8<sup>low</sup> cells in ILN

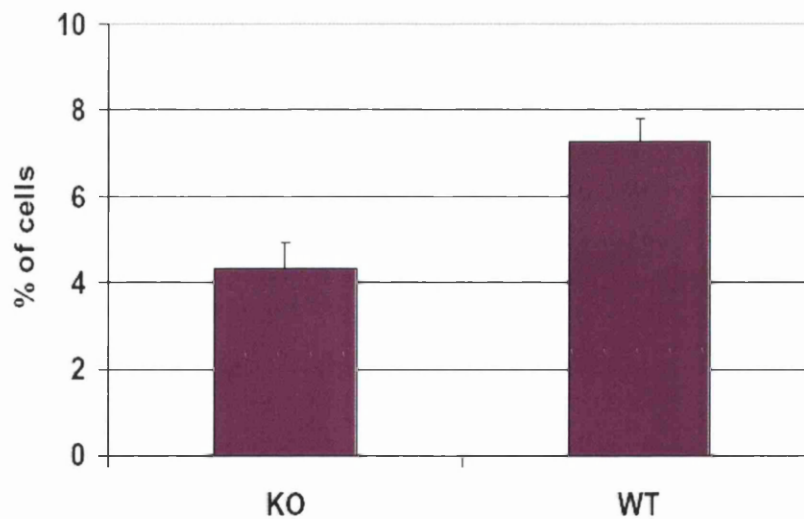


**Figure 3.3.5: Analysis of Leukocytes in ILNs from CCX-CKR  $+/+$  and  $-/-$ .** Representative contour plots showing WT and KO cell populations are shown on the previous page. Cells falling within the coloured gates were quantified. At least 5 mice in each group were analysed and error bars are  $\pm$  the standard deviation of the mean. Statistical analysis was performed using a Student's t-test (differences are not significant in upper graph and  $p < 0.05$  in lower graph). Repeat experiments gave similar results ( $n=3$ ).

## Summary

1. CCX-CKR ablation has no apparent consequences for mouse fertility, health, or viability.
2. CCX-CKR *null* mice develop normally, with no obvious abnormalities in size, weight, appearance or major organ development.
3. CCX-CKR is not required for the development of secondary lymphoid organs. Spleen, mesenteric and peripheral LNs, and Peyers patches are all found in *null* mice. Gross architecture of these structures appears to be normal.
4. Analysis of the leukocytes which populate the spleens of CCX-CKR *null* mice reveals that similar frequencies of T cells, B cells, DCs, and macrophages are found in both WT and KO animals.
5. F4/80+ cells from the spleens of CCX-CKR KO animals are more strongly positive for class II MHC, indicating that splenic macrophages may be more mature in these animals.
6. ILNs from CCX-CKR *null* mice are significantly smaller than those found in their WT counterparts, explained by the fact that fewer cells are contained within these LNs in KO animals.
7. There are no differences in T cell / B cell ratios or CD4<sup>high</sup> / CD8<sup>high</sup> ratios in cells recovered from ILNs from CCX-CKR KO and WT mice. However, in ILNs of CCX-CKR *null* mice a CD4<sup>-</sup>, CD8<sup>low</sup> population of cells is significantly reduced compared to WT counterparts.

### 3.3.4 Inguinal Lymph Node and Skin Responses to Topical Application of Phorbol Ester Irritant

To further examine the regulation of ILN cellularity in CCX-CKR *null* mice, a model of inflammation known to induce Langerhans cell (LC) migration and subsequent ILN hypertrophy was utilised. Specifically, the topical application of the phorbol ester 12-O-tetradecanoylphorbol-13-acetate (PMA) was employed (Jamieson et al., 2005; Ragg et al., 1994). The proposed mechanism of ILN hypertrophy in this model is that the cutaneous application of PMA causes the induction of inflammation, cytokine production and LC maturation. Mature LCs upregulate CCR7, and migrate to the ILN where they promote lymphocyte recruitment and induce lymphocyte proliferation, causing subsequent ILN expansion. In addition, inflammatory cytokine and chemokine production caused by PMA application inhibits lymphocyte egress from the ILNs, which may also contribute to the ILN hypertrophy. To provide further rationale for doing these experiments with CCX-CKR *null* mice, information regarding CCX-CKR expression in the skin was collected. Available cDNA from the skins of WT mice (Jamieson et al., 2005) was analysed by RT-PCR for expression of CCX-CKR, using  $\beta$ -actin as a control. Both CCX-CKR and  $\beta$ -actin transcripts were detectable from all skin samples. The possibility that genomic DNA may have contaminated this assay was excluded by the inclusion of control samples treated identically, with the exception that reverse transcriptase was not included in reactions (Figure 3.3.6). More detailed investigations revealed that this expression is maintained after PMA painting, though it may decrease at later timepoints (data not shown). This result provided the rationale to compare not only ILNs of CCX-CKR KO and WT mice, but also to compare the phenotype of the skin itself. The painting procedure followed was one which had recently been used extensively in parallel experiments with D6 *null* mice, involving 3 consecutive PMA (or vehicle control) paints on the back skin on 3 consecutive days (2.2.6.10). On day 3, 5 and 7 following the third application of PMA, animals were

sacrificed and the back skin removed for histological analysis. ILNs were also removed and weighed to assess expansion relative to those from mice painted with vehicle only.

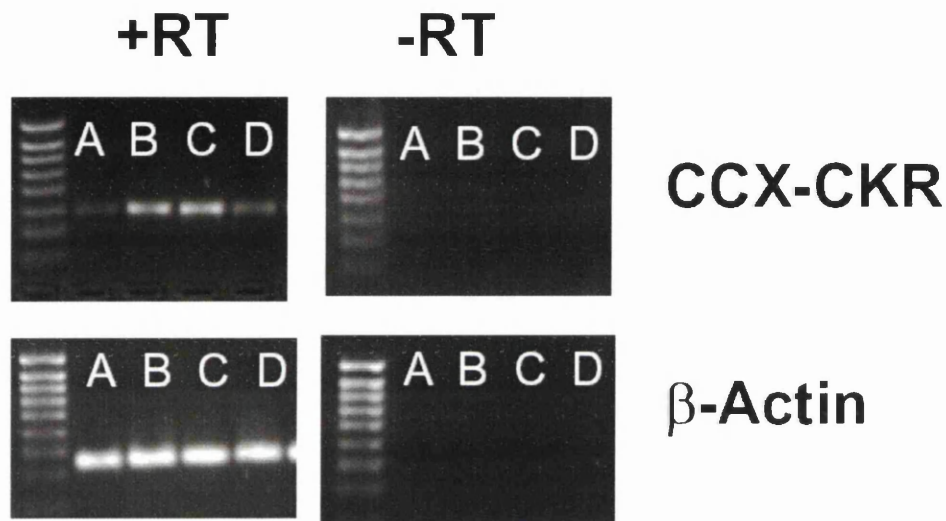


**Figure 3.3.6: Expression of CCX-CKR in Normal Mouse Skin.** RNA from skins of WT mice was prepared, DNAase treated and reverse transcribed into cDNA (+/-reverse transcriptase enzyme). cDNA was then amplified using PCR cycle 'cDNA amplification' (2.2.1.3) with primers specific for either CCX-CKR or  $\beta$ -Actin (mCCXU/mCCXD and  $\beta$ -actinU/ $\beta$ -actinD respectively) and the resulting products run on a 1.5% agarose gel with ethidium bromide.

Examination of the skin H+E sections revealed that, at a gross level, the cutaneous inflammation in CCX-CKR KO and WT mice was broadly similar. Evidence of inflammation (epidermal thickening and leukocyte infiltration) was apparent by day 3 in both the WT and KO's, and remained at day 5. By day 7 post third PMA application, inflammation in the back skin from both KO and WT had begun to resolve (Figure 3.3.7). Analysis of ILN weights from these mice revealed that on day 3 and day 5 the ILNs from CCX-CKR KO mice were significantly smaller than WT counterparts (Figure 3.3.8). On day 7, there was no significant difference in ILN weight between KO and WT. However,

this can in part be explained by the fact that WT ILNs have reduced in size between day 5 and day 7.

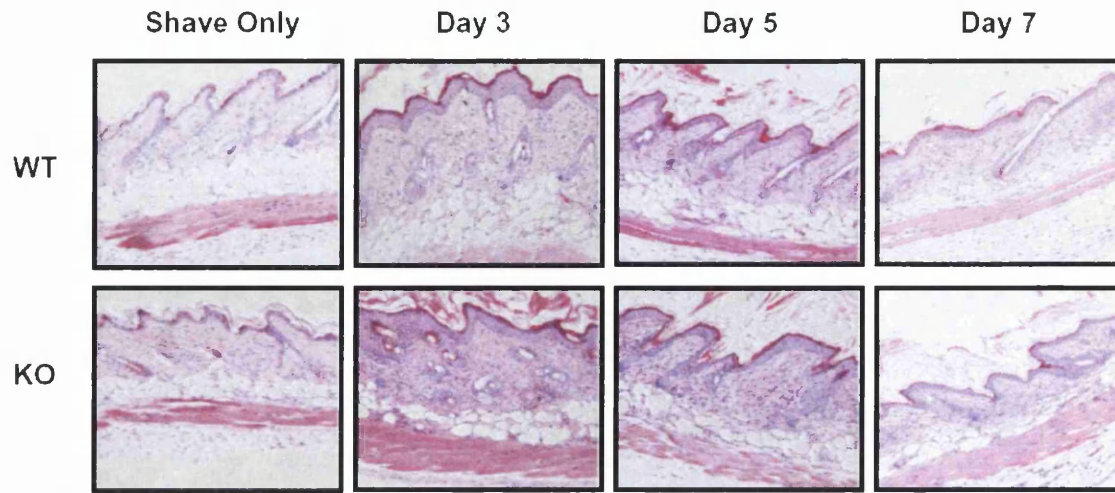


**Figure 3.3.7: Histological Analysis of Mouse Skin Following 3xPMA Paint.** The back skin from age and sex matched CCX-CKR KO and WT mice which had been either shaved then painted with PMA for three consecutive days (or shaved only) was removed on day 3, day 5, and day 7 after the third PMA application. Skins were formalin fixed, paraffin embedded and sectioned. Sections were then stained with H+E, analysed by light microscopy and photographs taken using an Axiom digital camera. Images shown are representative of many fields of view from sections from 6 mice in each group.

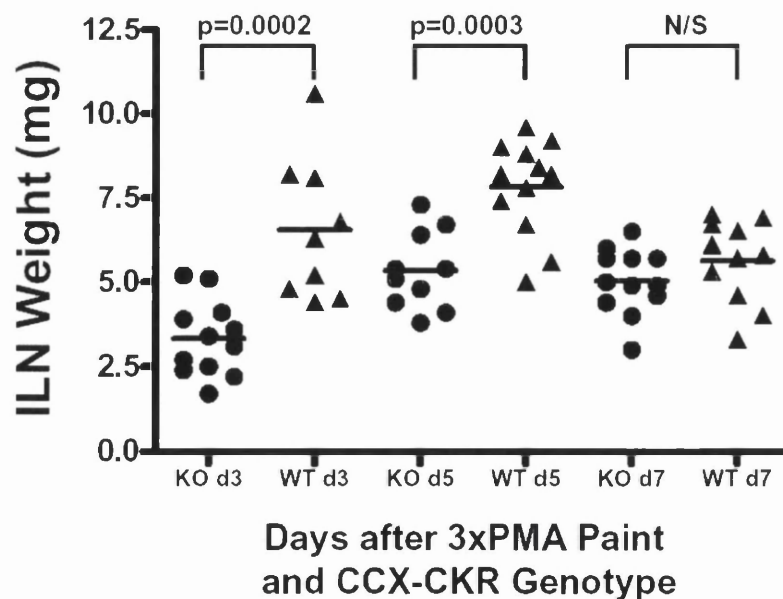


**Figure 3.3.8: Analysis of Inguinal Lymph Node Weight Following 3xPMA Paint.** Age and sex matched CCX-CKR KO and WT mice were shaved then painted with PMA on three consecutive days. On day 3, day 5, and day 7 after the third PMA application, ILNs were removed, trimmed, and weighed on a microbalance. Statistical analysis was performed using a Student's t-test (N/S= not significant).

Next, to assess whether this difference in weight between KO and WT ILNs is due to the presence of fewer cells in CCX-CKR KO ILNs, cell counts were performed from ILNs which were harvested from mice on day 3 after triple PMA application. ILNs from CCX-CKR KO mice had significantly fewer cells than their WT counterparts (Figure 3.3.9).

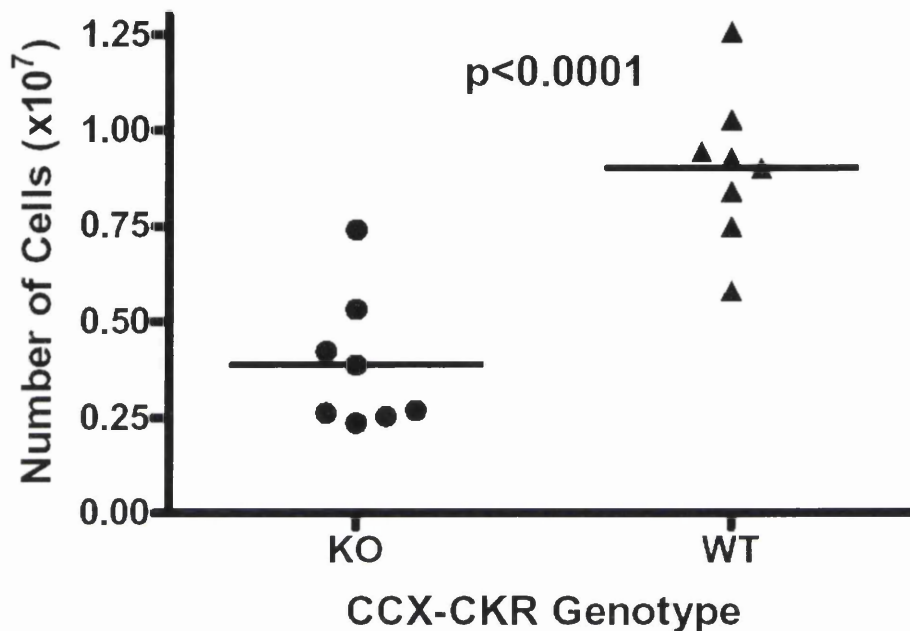


**Figure 3.3.9: Analysis of Cellularity of ILNs 3 Days After 3xPMA Paint.** Age and sex matched CCX-CKR KO and WT mice were shaved then painted with PMA on three consecutive days. On day 3 after the third PMA application, ILNs from each animal were removed, pooled, and mashed through nitex membrane to give a single cell suspension. Recovered cells were then counted in a haemocytometer. Statistical analysis was performed using a Student's t-test.

Next, to investigate whether a particular cell population was absent from CCX-CKR KO ILNs on day 3 after PMA painting, immunostaining and flow cytometric analysis was carried out as previously. The relative proportions of all major cells types analysed were largely similar between KO and WT animals (figure 3.3.10). However, similarly to that found in unchallenged mice, the small population of CD4<sup>-</sup>, CD8<sup>low</sup> cells was significantly reduced in KO compared with WT mice.

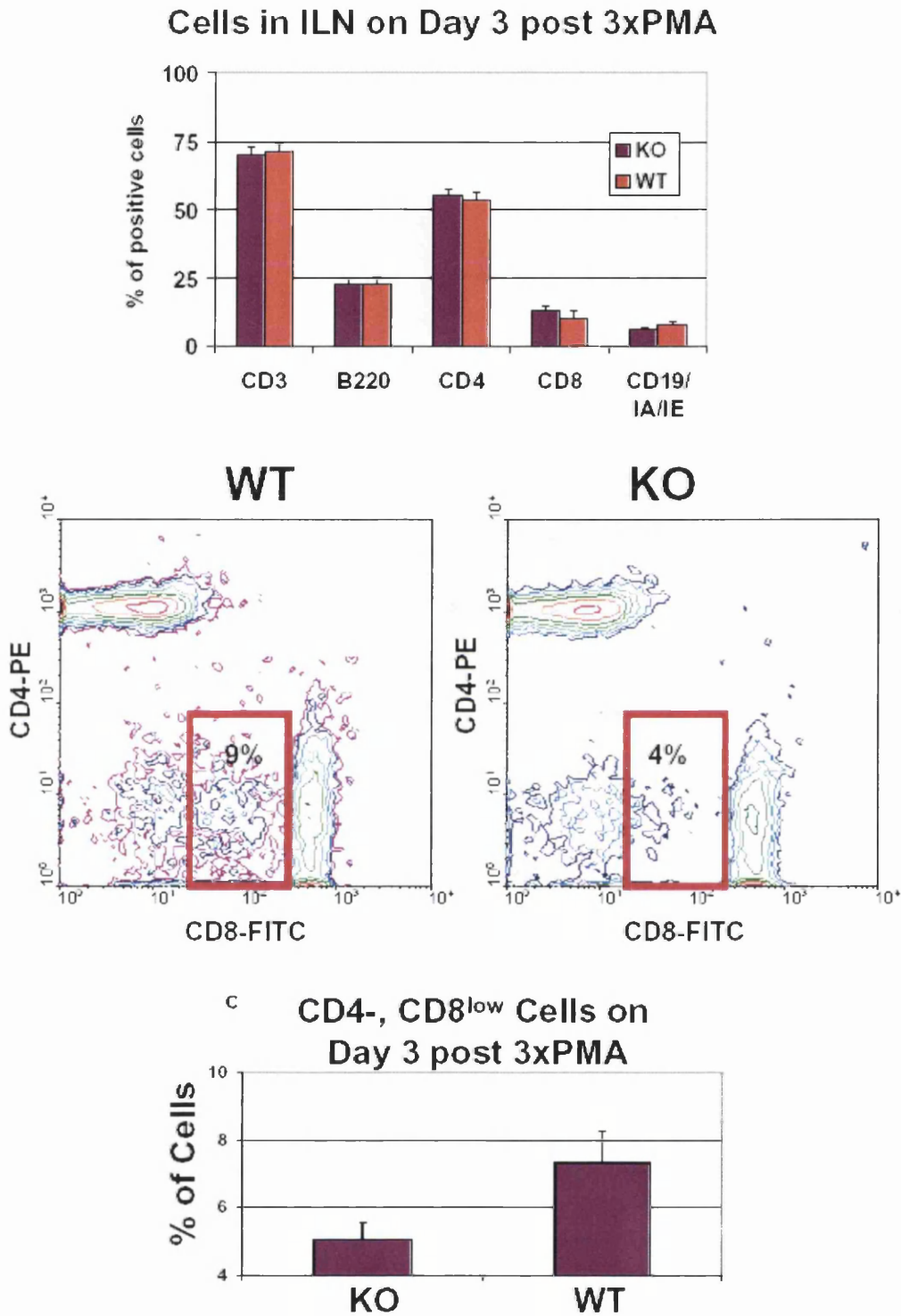


**Figure 3.3.10: Analysis of Leukocytes in ILNs 3 Days After 3xPMA Paint.** Representative contour plots showing WT and KO cell populations are shown for CD4 vs CD8 staining. Cells falling within the coloured gates were quantified. At least 5 mice in each group were analysed and error bars are +/- the standard deviation. Statistical analysis was performed using a Student's t-test ( $p < 0.001$  in lower graph). Repeat experiments gave very similar results ( $n=2$ ). Analysis of plots for other staining gave the results shown in the bar graph at the top of figure (not significant).

## Summary

1. CCX-CKR is constitutively expressed in mouse skin.
2. Topical application of PMA causes epidermal thickening and apparent cutaneous inflammation similarly in both CCX-CKR KO and WT mice.
3. Inflammation in the skins of both WT and CCX-CKR *null* mice appears to resolve with similar kinetics.
4. ILNs of WT mice become significantly enlarged by day 3 and day 5 following PMA application. This ILN enlargement is not apparent in CCX-CKR *null* mice.
5. Three days after PMA application has ceased, significantly fewer cells are found in ILNs of CCX-CKR *null* mice compared with WT mice.
6. All cell populations examined in the ILNs of PMA painted mice were similarly represented in CCX-CKR KO and WT mice. However CD4<sup>-</sup>, CD8<sup>low</sup> cells were significantly reduced in proportion in KO animals, results similar to those observed in untreated animals.

### 3.4.5 Primary Immune Responses to Subcutaneous Antigen

The hypotrophic ILNs which had been observed both in resting and PMA-treated CCX-CKR *null* mice led next to an investigation into whether CCX-CKR KO FVB mice were capable of mounting normal immune responses in ILNs. To answer this, a model of immunity was used whereby OVA emulsified in CFA is injected subcutaneously (see 2.2.6.10). As previous experiments had shown a phenotype in the ILNs, the injections were into each flank of the mice to encourage drainage of Ag to this site. All injections were performed with the expert assistance of experienced animal technician Tom Hamilton of the Beatson animal facility to ensure consistency between injections. On day 3 after immunisation, some animals were sacrificed and cells from the ILNs counted and analysed by flow cytometry. Both KO and WT mice showed significant enlargement of ILNs at this timepoint but unlike the PMA model, there was no significant difference between the weight or total cellularity of ILNs from KO versus WT (Figure 3.3.11). Immunostaining revealed no differences in the proportion of any cell type within these ILNs (figure 3.3.12). Interestingly, no differences were apparent between KO and WT mice when the proportions of CD4<sup>-</sup>, CD8<sup>low</sup> cells were analysed at this time (not shown).

Next immune response parameters were measured, examining the generation of OVA-specific IgG and T cells. On day 10, mice were bled from the tail-vein to assess the levels of OVA-specific IgG antibody in the serum. Mice were then sacrificed on either day 17 or day 24. Peripheral blood was removed by cardiac puncture and the serum separated for analysis of anti-OVA IgG antibody titres (see 2.2.6.11). ILNs were also removed, the number of recovered cells counted, and these cells then cultured with medium alone (to assess background proliferation), with OVA (to assess Ag-specific proliferation), or with Concanavalin-A (ConA) (to assess non-specific proliferative capability). Supernatants were taken from these cultures after 48h for analysis of cytokine production. After 96h, cells

were pulsed with tritiated thymidine to assess levels of cell proliferation (2.2.6.12). The results from these experiments are shown in figures 3.1.13 to 3.1.19.

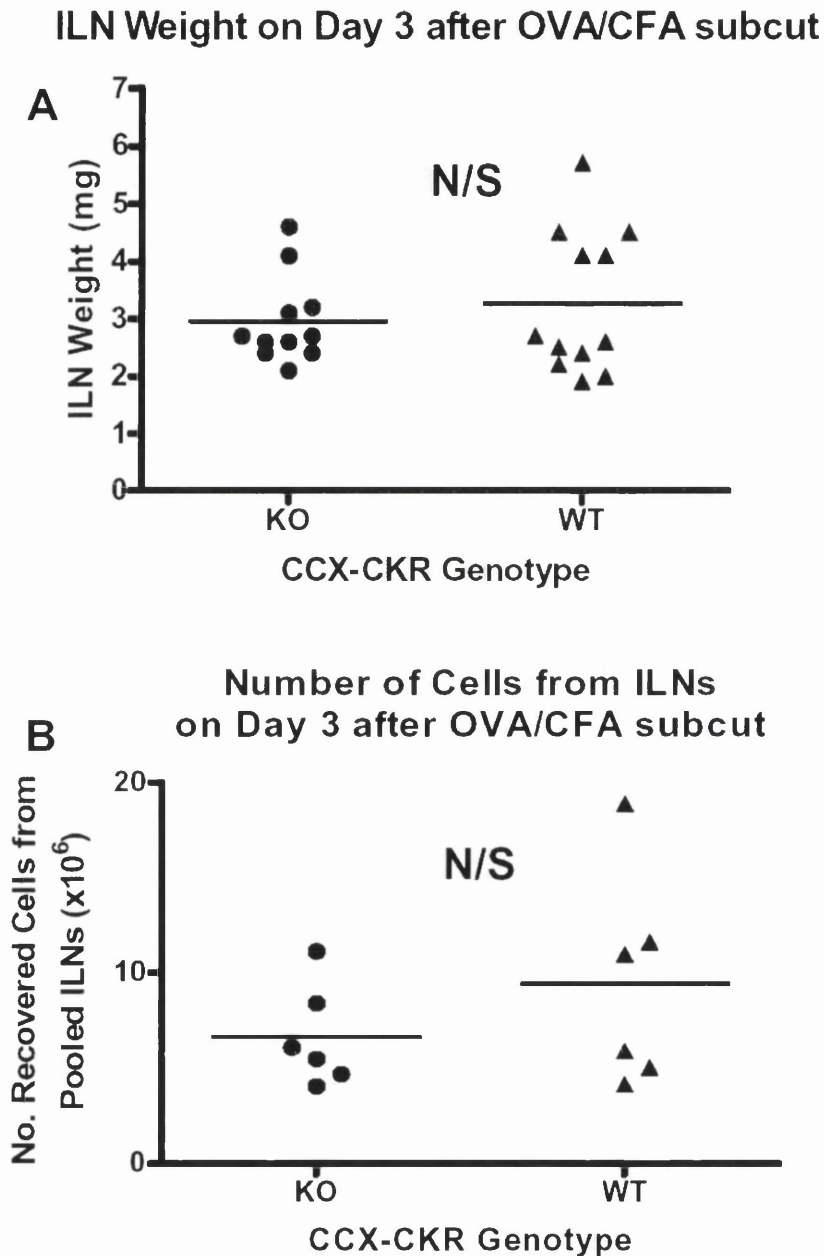


**Figure 3.3.11: Analysis of ILN Weight and Cellularity 3 Days After OVA/CFA.** ILNs were removed from age and sex matched CCX-CKR KO and WT mice on day 3 following subcutaneous OVA/CFA immunisation. These were then and trimmed under the dissection microscope. They were then carefully weighed on a microbalance. The weight in milligrams of ILNs from KO and WT mice is shown in (A). Cells were isolated from pooled ILNs (2 from each animal) by mashing through nitex membrane. Recovered cells were counted in a haemocytometer. The number of cells recovered from pooled ILNs from each animal is shown in (B). Statistical analysis was performed using a Student's t-test. (N/S= not significant)

First of all, it is of note that throughout the course of the experiment, WT ILNs consistently had more cells in them than CCX-CKR KO ILNs, although the differences were not significant, except in unimmunised control animals (Figure 3.1.13). Second, levels of anti-OVA serum IgG antibody were not measurably different between KOs and WTs at any timepoint (Figure 3.3.14), indicating that humoral immune responses in CCX-CKR deficient animals are still intact. ILN cells from both CCX-CKR KO and WT ILNs were capable of proliferation *in vitro* when cultured with OVA (Figure 3.1.15), indicating that cellular immunity has also been induced. At day 17, ILN cells from both KO and WT were highly proliferative *in vitro* to OVA, indicating that many OVA-specific lymphocytes were present. Interestingly however, cells taken from KO ILNs 24 days post-immunisation were still capable of proliferation to OVA while cells from WT animals were not. At this timepoint, responses to medium alone or ConA were not significantly different between KO and WT (Figure 3.3.15).

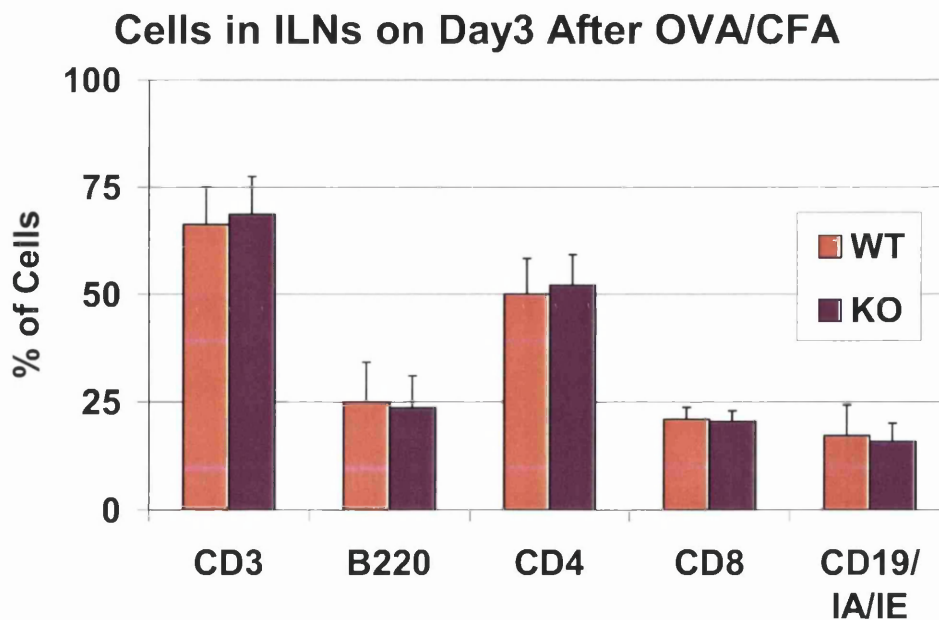


**Figure 3.3.12: Analysis of Leukocytes in ILNs on Day 3 After OVA/CFA.** Graph shows the proportions of cells positive for the markers shown from ILNs taken from mice 3 days after OVA/CFA immunization. Refer to figure 3.3.5 for details of gates used for quantification of staining. 6 mice were included in each group and error bars are +/- the standard deviation.

### Total Cell Number in pooled ILNs

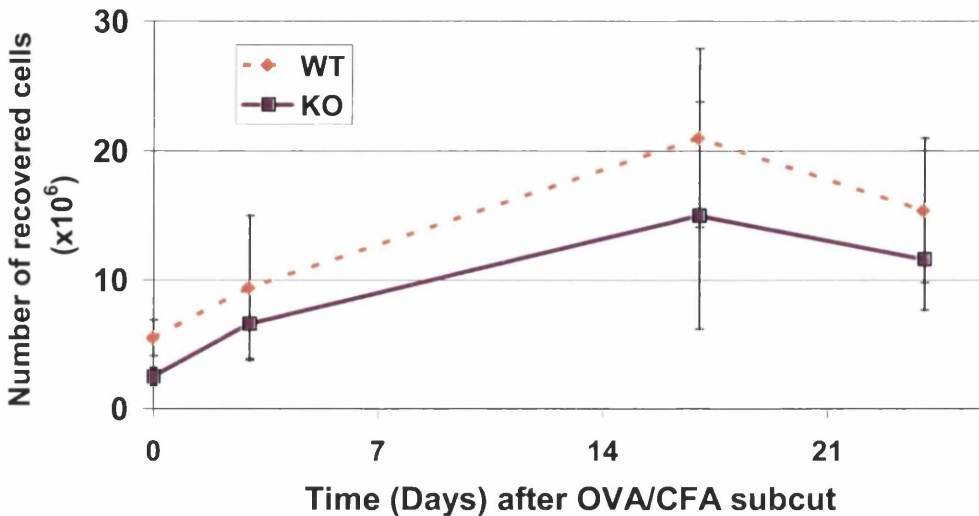


**Figure 3.3.13: Cellularity of ILNs Following OVA/CFA Immunisation.** On the indicated day following OVA/CFA immunisation, mice were sacrificed and ILNs removed. ILNs from each animal were pooled and single cell suspension prepared from these. These were then counted in a haemocytometer. 6 mice were in each group at each timepoint. Error bars are +/- the standard deviation.

### Anti-OVA IgG Antibody in Serum

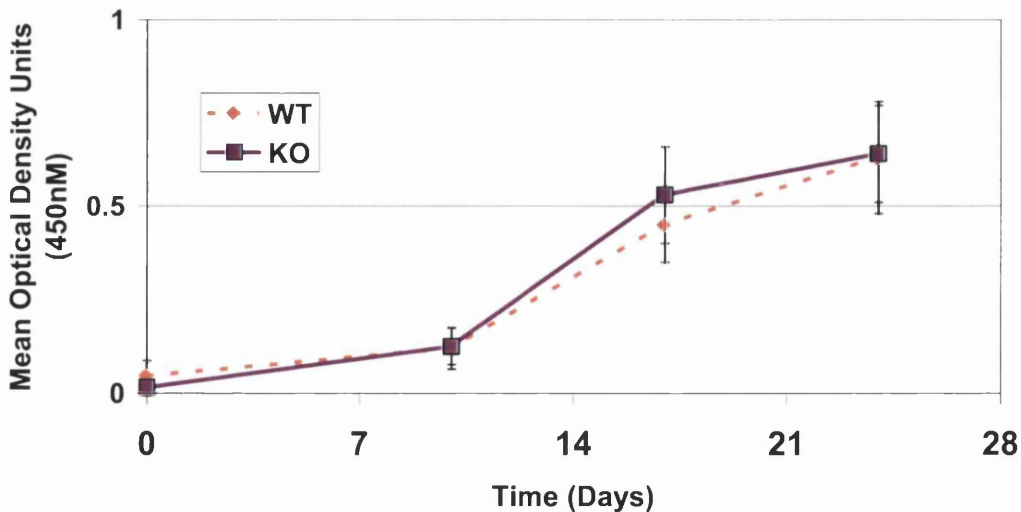


**Figure 3.3.14: Analysis of OVA-Specific IgG in Mouse Serum After OVA/CFA.** 50  $\mu$ l of serum taken from animals over timecourse of assay was analysed by ELISA for anti-OVA IgG. 6 mice were in each group and zero represents unimmunised controls. In the absence of standards, actual concentrations cannot be calculated but relative optical densities can be compared. The error bars are +/- the standard deviation.

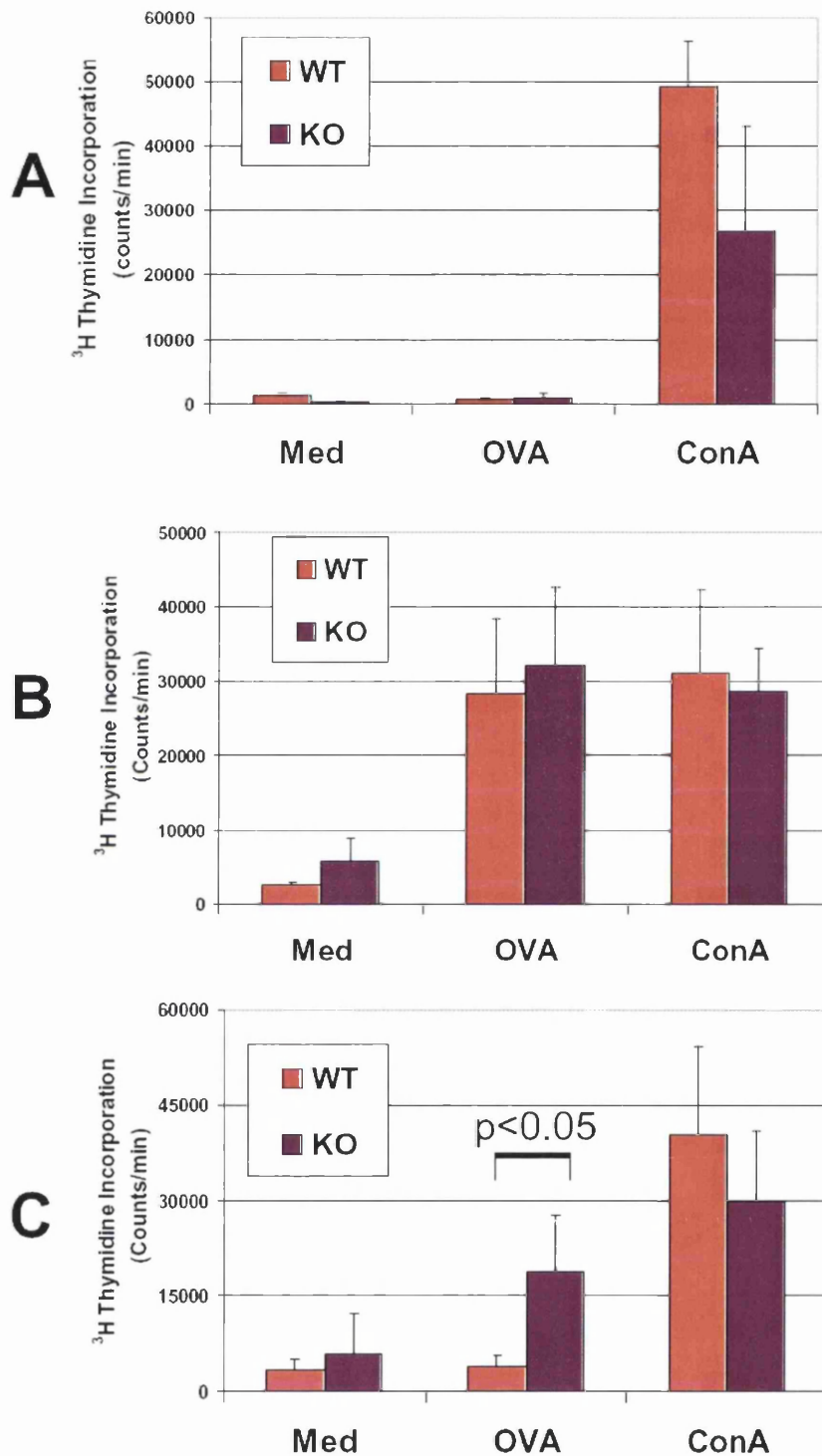


**Figure 3.3.15: Analysis of OVA-Specific Proliferation in ILN Cell Culture.** ILN cells were isolated on the days indicated following OVA/CFA immunisation. These were then cultured for 96h in either medium alone (MED), with Ovalbumin (OVA) or with Concanavilin A (ConA).  $^3\text{H}$ -thymidine was then added and the cells cultured for an additional 24h. Cells were then harvested and the level of proliferation assessed by  $^3\text{H}$  Thymidine incorporation. **A:** unimmunised mice **B:** mice 17 days after immunisation. **C:** mice 24 days after immunisation. 6 mice included / group. Error bars are +/- the standard deviation. Statistically significant differences are indicated.

Supernatants taken from ILN cell cultures were then analysed for the presence of various cytokines. As the FVB mouse is relatively poorly-characterised compared with other strains of mice in this type of model, the assessment of multiple cytokines was desirable. To this end, the Luminex™ *Six plex* Th1/Th2 ELISA kit was utilised (see 2.2.6.13). This was performed with the assistance of Dr. Gracie (Glasgow Royal Infirmary) and attempted to measure the levels of the following cytokines. These were IL-2, IL-4, IL-5, IL-10, IL-12, IL-13 and IFN $\gamma$ . No significant levels of any cytokine were detected in supernatants from cells cultured in medium alone, or cells from unimmunised mice which had been cultured in OVA (Figure 3.3.16 and data not shown). However, cells taken from both KO and WT immunised mice on day 17 had detectable levels of the Th2 cytokines IL-5, IL-10, and IL-13, and low levels of the Th1 cytokine IFN- $\gamma$  when cultured with OVA (Figure 3.3.16), although no significant differences in the levels of these could be quantified between KO and WT. IL-2, IL-4 and IL-12 could not be detected in any of the supernatants (not shown). Interestingly, by day 24, significantly greater levels of IL-5 and IL-13, but not IL-10 or IFN- $\gamma$ , could be detected in supernatants from CCX-CKR KO compared to WT cells when cultured in OVA. Supernatants from cells from WT ILNs on day 24 contained very low levels all cytokines tested. The data from day 24 are consistent with the prolonged presence of OVA-responsive T cells in CCX-CKR *null* ILN revealed by the proliferation assays (Figure 3.3.15). With the exception of IL-4, all cytokines were detectably produced by cells cultured in the presence of ConA (Figure 3.3.16 and data not shown). The FVB mouse is particularly prone to Th2 type immune responses (Choi et al., 2003; Christie et al., 1999; Whitehead et al., 2003), and this was reflected the cytokines secreted by cells from these mice in response to OVA and ConA, although the inability to detect IL-4 was something of a surprise.

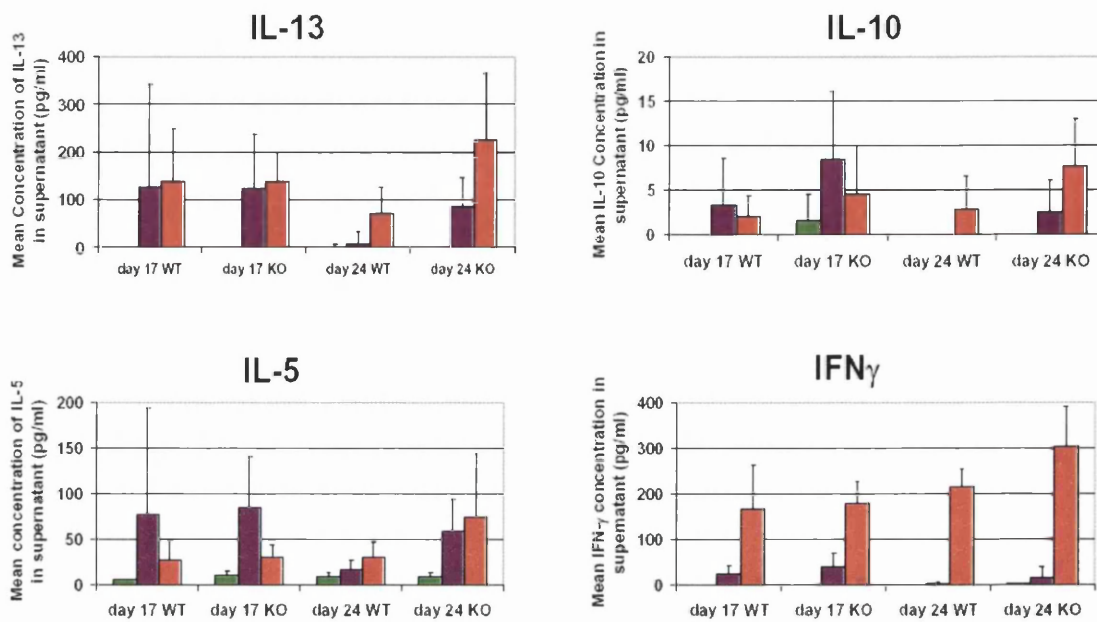


**Figure 3.3.16: Analysis of Cytokine Levels in Supernatants from ILN Cell Culture.** Results from Luminex ELISA for IL-5, IL-10, IL-13 and IFN- $\gamma$  from supernatants taken from ILN cells cultured for 48h in either medium alone (green fill), OVA (purple fill), or ConA (orange fill). Concentrations were calculated from standard curves generated using known quantities of each cytokine (see 2.2.6.13). Supernatants from cells from ILNs of at least 4 mice in each group were analysed. Statistical analysis was performed using a Student's t-test and error bars are +/- standard deviation.

## Summary

1. Subcutaneous injection of OVA/CFA caused significant ILN hypertrophy post-immunisation in both CCX-CKR KO and WT animals. No proportional differences were apparent between KO and WT mice in any cell types examined in the ILNs.
2. Serum levels of anti-OVA IgG were indistinguishable between CCX-CKR KO and WT mice at all time points measured post-immunisation.
3. ILN cells taken from KO and WT mice on day 17 after OVA/CFA immunisation were, in response to OVA, similarly capable of *in vitro* proliferation and produced similar levels of IL-5, IL-10, IL-13 and IFN- $\gamma$ .

4. By day 24 after immunisation, WT ILN cells no longer proliferated or produced cytokines in response to OVA. However, OVA-responsive cells persisted in KO ILNs, proliferating and produced detectable levels of IL-5 and IL-13 after OVA stimulation.

A tentative conclusion from these data is that the absence of CCX-CKR encourages the persistence of Ag-specific T cells in ILNs after challenge. The interpretation and limitations of these results is discussed in greater depth in section 4.3.

### 3.5.6 Contact Hypersensitivity Responses to the Hapten DNFB

From the previous experiment, it is clear that whilst the absence of CCX-CKR may influence the precise kinetics of an immune response, it is dispensable for the induction of Ab and responsive T cells after subcutaneous injection of soluble Ag. However, it is notable that the LN phenotype apparent in the PMA model was not observed after subcutaneous OVA/CFA immunisation. Thus, this model does not directly examine the impact of LN hypotrophy on immune responses. This clear difference between the PMA and OVA/CFA challenges may be related to the anatomical site challenged in these models. PMA will principally stimulate the epidermis and lead to LC migration to the ILN. Subcutaneous OVA/CFA challenge, on the other hand, will not be so dependent on these cells. Thus, to test whether responses to Ag delivered via the epidermis are defective in CCX-CKR *null* mice, a model of immunity using the hapten di-Nitro-Fluoro-Benzene (DNFB) was employed. In this model, the topically-applied hapten covalently couples to proteins in the skin, these haptened proteins are ingested and processed by LCs, which then migrate to the draining LN where they prime hapten-specific T cells (Engeman et al., 2000; Streilein and Bergstresser, 1981). It was hoped that, in this way, it would be possible to examine the impact of ILN hypotrophy on immune responses.

DNFB was applied topically to the back skin of mice on two consecutive days (see 2.2.6.14). 24h later, ILNs were removed from some mice, weighed, and the cell number counted. 7 days later, with the remainder of the mice, ear thickness was measured and then the left ear was challenged with DNFB and vehicle alone was applied to the right. Ear swelling was then measured 24 and 48h later, and after 48h, the ears were removed for sectioning and H+E staining.

Similarly to the PMA painting, ILNs from CCX-CKR KO mice were significantly smaller than WT ILNs 24h after two applications of DNFB on the back skin (figure 3.3.17). This was quantified both in terms of ILN weight and the number of cells recovered. These data suggest that topical delivery of Ag is less effective at inducing ILN hypertrophy in CCX-CKR KO animals than subcutaneous delivery.

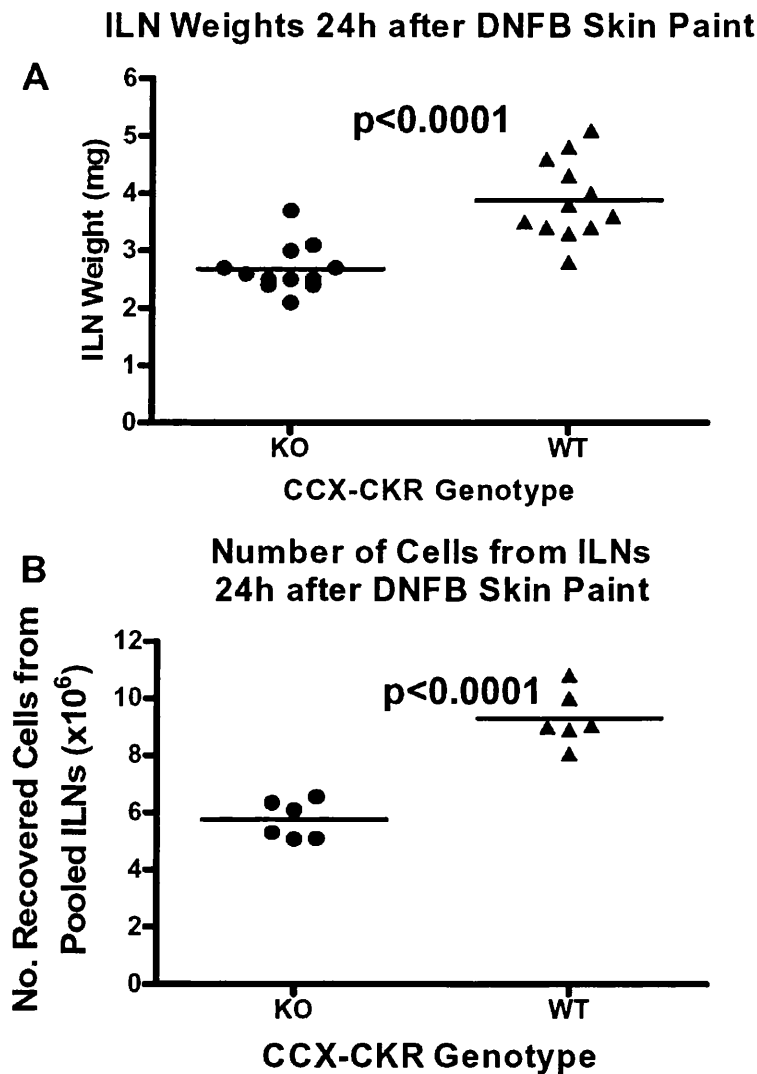


**Figure 3.3.17: Analysis of ILN Weight and Cellularity on Day 3 After DNFB Paint.** ILNs were removed from age and sex matched CCX-CKR KO and WT mice 24h after DNFB painting for 2 consecutive days on the back skin. ILNs were trimmed under the dissection microscope and carefully weighed on a microbalance. The weight in milligrams of ILNs from KO and WT mice is shown in (A). Cells were isolated from pooled ILNs (2 from each animal) by mashing through nitex membrane. Recovered cells were counted in a haemocytometer. The number of cells recovered from pooled ILNs from each animal is shown in (B). Statistical analysis was performed using a Student's t-test.

The left ears of mice painted with DNFB were measurably thicker than the right ears by 24h after ear challenge (Figure 3.3.18) in both CCX-CKR KO and WT animals. By 48h after ear challenge, the difference in ear thickness between left and right was more pronounced. Despite the clear differences in ILN cellularity after DNFB painting, no differences were apparent in either the extent or timing of the left ear swelling between KO and WT animals (Figure 3.3.18). Histological analysis of ears 48h after DNFB challenged showed a robust inflammation in both KO and WT animals with epidermal thickening and leukocyte infiltration. No clear differences in the nature or extent of this response were observed (Figure 3.3.19).

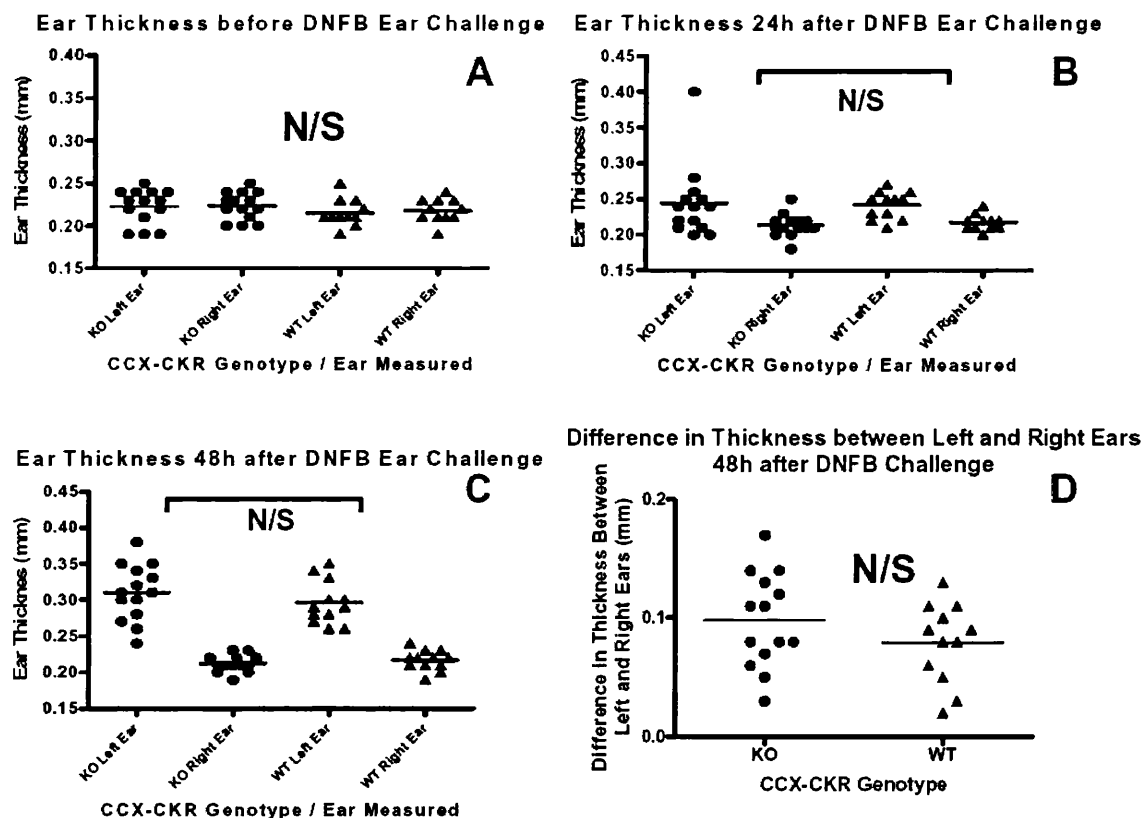


**Figure 3.3.18: Measurements of Ear Thickness in Mice Following DNFB Challenge.** Ear thickness of mice before (A) and 24h (B) and 48h (C) after challenge with DNFB on the left ear and vehicle control on the right ear. (D) Shows the difference in thickness between left and right ears 48h after challenge. Thickness was measured using electronic callipers. Statistical analysis was performed using a Student's-t test.

Together these data suggest that, in this model, although less pronounced ILN hypertrophy is induced by DNFB painting on the back skin in CCX-CKR KO than WT animals, CCX-CKR is not required for the induction of cutaneous immunity. Although an examination of factors such as Ag dose and timing may reveal more subtle phenotypes in this model, CCX-CKR appears to be dispensable for the generation of immune responses. Discussion of this point, along with other issues arising from the results described in this section and suggested future experiments, can be found in section 4.3. Although not completely resolved, the studies of the CCX-CKR *null* mice generated in this thesis are clearly revealing exciting phenotypic consequences of CCX-CKR deletion which will aid our understanding of the indispensable role played by this receptor *in vivo*.

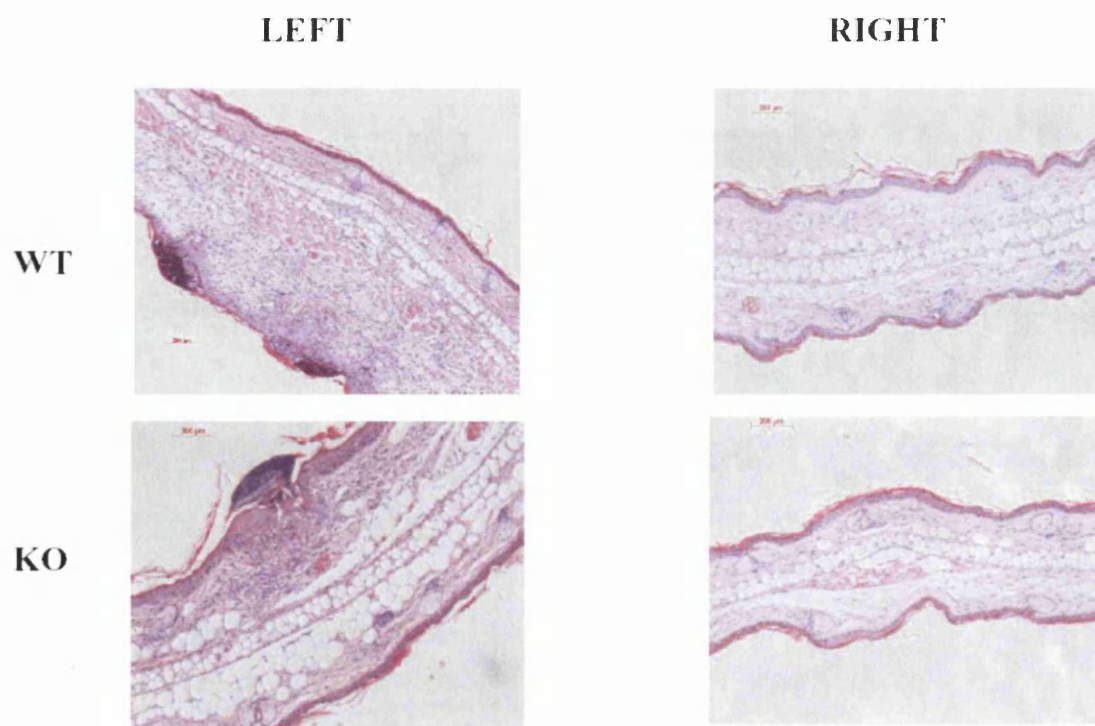


**Figure 3.3.19: Analysis of H+E Sections of Ears Either Painted or Unpainted with DNFB.** Left and right ears from mice which had been challenged with DNFB on the left ear and vehicle control on the right ear were removed 48h after challenge. These were formalin fixed, paraffin embedded and sectioned. Sections were then stained with H+E and analysed by light microscopy. Images were captured using the Axiom digital camera. Scale bar=200 $\mu$ m.

### 3.4 Reporter Expression in CCX-CKR KIKO Animals

Alongside the phenotypic analysis of the CCX-CKR *null* mice, parallel investigations to reveal the domains of expression of the inserted reporter genes were planned to help identify CCX-CKR-expressing cells, and provide a cellular basis for emerging phenotypes. Therefore, various approaches were taken to examine expression of GFP and *lacZ* in targeted mice. First, the transcription of reporter gene was assessed by RT-PCR to ensure that this mirrored the observed pattern of CCX-CKR transcription. As the first CCX-CKR KIKO mice available were CCX-CKR-GFP, RT-PCR looking for GFP expression and CCX-CKR expression from a range of tissues from these mice was performed. RNA was extracted from various CCX-CKR-GFP heterozygote (het) and WT mouse tissues RT-PCR used to detect GFP, CCX-CKR, and  $\beta$ -actin (see 2.2.1.7 and 2.2.1.3). To ensure that the GFP signal was specific to the introduced reporter, the 5' oligo was designed to hybridise within the IRES. The oligonucleotides used to amplify these products were as follows: i) for GFP: 5'TRES and GFPD1 ii) for CCX-CKR: mCCXU, mCCXD iii)  $\beta$ -actinU,  $\beta$ -actinD. Strong PCR signals for both CCX-CKR and GFP were detected in all tissues tested from het mice. This CCX-CKR expression pattern was detected similarly in WT mice, which had no GFP expression with only weak background bands of the incorrect size observed (Figure 3.4.1).

## CCX-CKR PCR

## GFP PCR

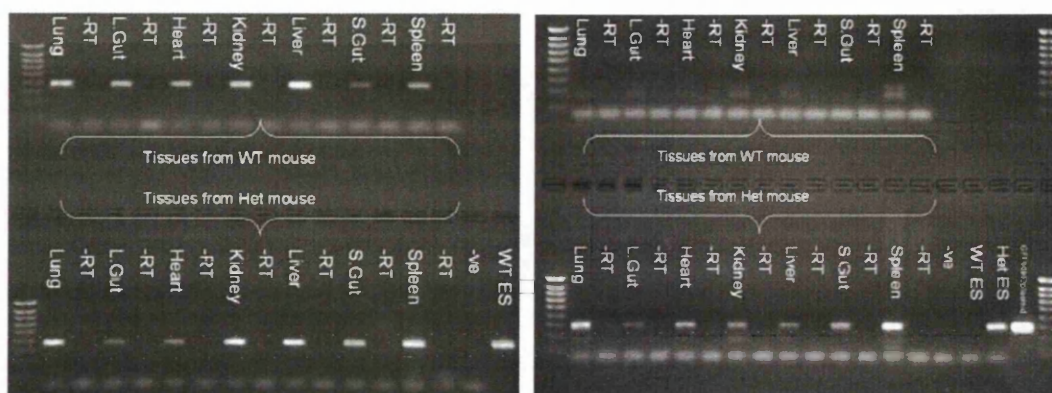


**Figure 3.4.1: Analysis of CCX-CKR and GFP Expression in +/+ and +/- CCX-CKR GFP KIKO Mice.** cDNA was prepared from various tissues of WT and CCX-CKR GFP KIKO heterozygote mice (+/-RT). This was then amplified by PCR with primers specific for CCX-CKR and GFP. Products were run on a 1.5% gel stained with ethidium bromide.

This result encouraged attempts to directly visualise GFP in these heterozygote animals. Several approaches were taken to do this. First, cells from peripheral blood, spleen and ILNs were isolated and analysed by flow cytometry. By gating on different fractions of cells based upon their size and granularity, it was hoped that populations of cells could be identified that were GFP, and by inference CCX-CKR, positive. However, no green cells were detected from any of these tissues by this method. There are many possible explanations for this. For example, the CCX-CKR promoter may not be particularly active in blood cells, the amount of GFP expressed in these cells may be below the levels of detection of this assay, or the GFP transcript may not be efficiently translated.

Next, to try to visualise GFP reporter expression by a different method, tissue sections from a range of organs from CCX-CKR-GFP mice were prepared, and analysed by confocal microscopy. As previous reports had indicated that sites of high endogenous CCX-CKR expression were the heart and gut, these organs were examined in the most detail. Unfortunately, fluorescent emissions corresponding to that of GFP could not be specifically detected from het mice on any of the sections analysed, and a large amount of background auto-fluorescence may have prevented detection of low level GFP expression.

When CCX-CKR-*lacZ* mice became available, staining of embryos and sections of various tissues using standard X-gal staining techniques was carried out. This was done both by staining sections directly and staining pieces of tissue which were then sectioned. Analysis of the stained embryos revealed no blue staining specific to mice which had the reporter. Likewise staining of adult tissue sections did not reveal any blue staining which could not also be observed in WT animals.

Without appropriate positive controls, detection of the GFP and *lacZ* reporters by methods which were available to me was likely to prove difficult. Careful optimisation of reporter detection was therefore deemed likely, and with limited time remaining for my project, I was unable to pursue this any further. However, in the future these mice may be an extremely valuable tool for continued studies of the expression, regulation, and function of CCX-CKR.

## CHAPTER FOUR

### DISCUSSION

#### 4.1 Comparative Biochemistry of CCX-CKR and CCR7

CCX-CKR has been previously classified as a 'silent' receptor for the chemokines CCL19, CCL21 and CCL25. Similar to D6 and DARC, chemokine decoy and transport functions have been hypothesised for this receptor. Therefore, investigations were undertaken to study the biochemistry of this receptor to answer the following important questions. Can CCX-CKR internalise chemokines? If so, what is the fate of internalised chemokine? Can functional consequences of CCX-CKR activity be measured? And what are the molecular mechanisms controlling the biochemical behaviour of CCX-CKR? Throughout these investigations, the biochemistry of CCX-CKR was compared to that of CCR7. Both are receptors for CCL19 and CCL21, but CCR7 is the only known signaling receptor for these chemokines, and all the biological functions currently assigned to CCL19 and CCL21 can be explained by interactions with CCR7. Therefore, it seemed possible that despite sharing high affinity binding for CCL19 and CCL21, these receptors mediate completely different outcomes following ligation. The data presented clearly show that CCX-CKR exhibits biochemical properties distinct from CCR7, and provide evidence that support its proposed role as a decoy receptor. However, as shall be discussed, the results do not exclude transport functions or alternative signaling roles for CCX-CKR. Indeed, it is important to remember that all three of these possibilities are not mutually exclusive.

The first simple question addressed in this thesis was whether CCX-CKR and CCR7 could internalise CCL19. Using radiolabelled or biotinylated CCL19, the results clearly demonstrate that both receptors, when expressed in HEK-293 cells, induce the rapid

internalisation of this chemokine at 37°C. Thus, similar to D6 (Bonecchi et al., 2004; Fra et al., 2003; Weber et al., 2004), CCX-CKR is able to internalise chemokine in the apparent absence of typical ligand-induced signaling. Moreover, although previous studies had shown that CCR7 can be internalised following exposure to CCL19 (Bardi et al., 2001; Breitfeld et al., 2000), chemokine internalisation via CCR7, although likely, had not been previously demonstrated. Notably, differences in the precise kinetics of CCL19 internalisation were observed between the two receptors, with CCX-CKR able to internalise CCL19 more rapidly, hinting that different mechanisms of internalisation were being employed by the two receptors.

Next, the fate of internalised radiolabelled CCL19 was studied in pulse-chase experiments. CCL19, internalised via CCX-CKR, was more rapidly degraded than that internalised via CCR7. Furthermore, internalised CCL19 was released intact from CCR7 transfectants, but not cells expressing CCX-CKR. A potential explanation for this was provided by the demonstration that CCL19 rapidly dissociates from CCX-CKR at the acidic pHs found in endosomes, while CCR7 retains ligand binding at these pHs. Together, this data suggested that, as previously shown for D6 and CCR5 (Weber et al., 2004), CCX-CKR would release its internalised cargo in acidic endosomes, while CCR7-associated chemokine would be less inclined to do so. However, surprisingly, CCL19 internalised by CCX-CKR could re-emerge intact when competitor was added following internalisation. Thus, prior to being targeted for degradation, a proportion of CCL19 internalised by CCX-CKR remains associated with a compartment which recycles back to the cell surface. In the absence of extracellular CCL19, this is presumably re-internalised and degraded. The significance of this observation is not clear.

The differences between CCX-CKR and CCR7 when tracking pulsed, internalised radioligand were fairly subtle and did not indicate any particular specialisation of CCX-CKR for chemokine sequestration. However, when chemokine degradation was measured in continuous culture fundamental differences were observed. Specifically, CCX-CKR mediated the rapid degradation of large quantities of CCL19 ( $\sim 10^5$  molecules/cell/h) while CCR7 simply did not. These results are unlikely to be due to differences in the levels of receptors on HEK-hCCR7 and HEK-hCCX-CKR cells as HEK-hCCR7 cells consistently bound 2-3x more CCL19 than HEK-CCX-CKR cells in radioligand binding assays at 4°C. Although differences in affinity rather than receptor number could account for this (Scatchard analysis of CCX-CKR was precluded by the low levels of radioligand binding), it is nonetheless clear that the cell lines used in this study do not express dramatically different numbers of cell surface receptors.

As a result of this impressive ability to degrade CCL19, CCX-CKR could modify an environment high in chemokines such that chemotactic responses through CCR7 were partially abolished. This is exactly the functional outcome which one would predict if a decoy receptor hypothesis were correct and it is tempting to speculate that *in vivo*, CCX-CKR sequesters and destroys its ligands to modify responses exerted through CCR7 and CCR9. Indeed, similar *in vitro* observations have been made with D6, which abolishes CCR4-driven chemotaxis towards CCL22 (Bonicchi et al., 2004), and subsequent analysis of D6 *null* mice demonstrate that this receptor limits pro-inflammatory chemokines *in vivo* (Jamieson et al., 2005), and thereby limits cutaneous inflammation.

So why is CCX-CKR able to mediate such significant chemokine sequestration? Interestingly, the answer to this appears to lie in its inability to undergo desensitisation following exposure to ligand. Although both CCR7 and CCX-CKR are able to degrade the

CCL19 they internalise, CCR7 becomes much less able to internalise CCL19 after it has been exposed to this chemokine. This may be explained by reduced surface CCR7 following CCL19 treatment, but is also likely to be influenced by the inability of remaining surface receptor to undergo ligand-driven internalisation. These results are in agreement with previous data showing desensitisation and internalisation of CCR7 in response to CCL19 (Bardi et al., 2001; Kohout et al., 2004). Again, consistent with these published studies, exposure of CCR7 to CCL21 did not induce surface receptor downregulation, or desensitise the receptor to subsequently internalise CCL19. This is likely to be due to CCR7 coupling to distinct signaling pathways depending upon whether it is ligated with CCL19 or CCL21 (Kohout et al., 2004).

Contrary to CCR7, it is apparent that CCX-CKR is not only resistant to desensitisation when exposed to its ligands, but that its ability to internalise chemokine is actually enhanced: a so-called 'priming' effect. Perhaps counterintuitively, surface receptor levels of CCX-CKR, as detected by the anti-FLAG antibody, are reduced following exposure to its ligands. Ligand-induced surface receptor downregulation is most commonly associated with receptor desensitisation. However, in the case of CCX-CKR, cells with low levels of surface receptor are able to internalise chemokine more rapidly than those with higher levels. How is this achieved? The rapidity of CCX-CKR trafficking may provide an answer. Antibody detection of surface receptor levels provides only a 'snapshot' of the amount of receptor on the cell surface at any one time. Thus, it is feasible that after initial CCL19 exposure, CCX-CKR is trafficking more rapidly to and from the cell surface to achieve increase CCL19 uptake. This would mean that although less CCX-CKR is on the surface of the cells at a given moment, over time more CCX-CKR will have been to the cell surface and thus, the potential exists to internalise more chemokines. The problems encountered with the generation of GFP-tagged CCX-CKR and the fact that the FLAG epitope was not

readily detectable in many assays, unfortunately precluded investigations of receptor localisation and trafficking. Thus, alternative means of detecting CCX-CKR need to be sought in future, such as the development of reliable antibodies or the use of alternative epitope or fluorescent tags, before this hypothesis can be tested. In addition to changes in receptor trafficking kinetics, as discussed below increased ligand affinity may contribute to enhanced CCL19 uptake by CCX-CKR after CCL19 exposure, and this also needs to be examined in more depth in the future.

Several other key questions arise from these data. First, what are the molecular mechanisms underpinning CCX-CKR 'priming' for enhanced CCL19 uptake? Second, how is the apparent ligand-driven reduction in surface receptor achieved? It is very likely that both of these phenomena require ligand-driven signaling, suggesting that CCX-CKR is not as 'silent' as initially thought. Some investigation into the nature of these signals was initiated during the course of this thesis, although this work requires future resolution. As CCX-CKR resembles a GPCR, preliminary investigations into the involvement of G-protein signaling were undertaken. Intriguingly, priming of CCX-CKR by CCL21 (but not by CCL19 or CCL25) was inhibited by pre-treatment of CCX-CKR transfectants with the  $G_{\alpha i}$  inhibitor, pertussis toxin (PTX) (data not shown). Although this result needs to be confirmed, it suggests that CCL21 uses  $G_{\alpha i}$ -dependent signaling to induce priming of CCX-CKR, while CCL19 and CCL25 do not. The use of other pharmacological and genetic inhibitors should also be employed to dissect out the essential signaling components of CCX-CKR 'priming'. For example, PI3K involvement could be examined using wortmannin and the small molecule inhibitor LY294002, the role of PKC could be investigated with the inhibitor RO-32-0432, and PKB inhibitors could be employed as well. Dominant-negative versions of signaling molecules could also be introduced to assess the relative contributions of specific signalling pathways. Indeed, in several of the assays

exploiting dominant negative inhibitors of the endocytic machinery, their effect on CCX-CKR 'priming' was also assessed. However, inhibitors of dynamin,  $\beta$ -arrestins, RabGTPases or EPS15 did not attenuate the ligand-driven enhancement of CCX-CKR function (not shown).

Alongside the use of inhibitors, mutagenesis of CCX-CKR could be employed to identify key residues or domains essential for its behaviour. To this end, plasmids encoding CCX-CKR C-terminal truncation mutants, and mutants with neutralised DRY motifs were successfully generated towards the end of this study. However, due to time constraints, stable cell lines expressing these proteins were not generated. Nonetheless, in transient assays, CCX-CKR DRY mutants were able to internalise BioCCL19/PE, but had reduced ligand-driven priming responses (data not shown). Again, this suggests that G-protein coupling may be important in the priming response. Another key question must be whether CCX-CKR becomes phosphorylated following ligation, or whether, like D6 and US28 it is constitutively phosphorylated, presumably to allow continuous trafficking to and from the cell surface (Blackburn et al., 2004; Casarosa et al., 2001). Phospholabelling, followed by immunoprecipitation of CCX-CKR would address this issue.

As well as being differentially 'primed' or desensitised, CCX-CKR and CCR7 employ different routes of endocytosis described graphically in figure 4.1.1. Indeed, this may contribute to their profoundly different responses following ligand exposure. The molecules shown to be involved in CCR7 internalisation are typical of those known to be involved in the endocytosis of other chemokine receptors (Signoret et al., 2005; Yang et al., 1999), and GPCRs in general (Gaborik et al., 2001; Zhang et al., 1997). It was demonstrated in a recently published study that  $\beta$ -arrestins are recruited to CCR7 following ligation with CCL19 (Kohout et al., 2004). My work confirms and extends this by demonstrating that  $\beta$ -

arrestins are critically involved in CCL19-driven CCR7 internalisation. As outlined in section 1.3.5,  $\beta$ -arrestins bound to a GPCR normally act as adaptors, linking phosphorylated receptor complexes to AP-2 and clathrin for internalisation via CCPs. Indeed, genetic inhibition of CCP formation, using EPS15 inhibitors, prevented CCL19 uptake through CCR7. As EPS15 is an essential component of the clathrin endocytic machinery (Benmerah et al., 1999; Carbone et al., 1997), this indicates that CCR7 internalisation is likely to be dependent, at least to some extent, on the formation of CCPs. The reason why inhibition was not more marked in these assays could be that CCR7 is also able to internalise via clathrin-independent mechanisms, or simply that the EPS15 dominant negative mutants do not completely block clathrin-mediated endocytosis. Interestingly, chemokine uptake by CCR7 was also inhibited by depletion of membrane cholesterol using M $\beta$ CD. This indicates that cholesterol rich lipid rafts are likely to play some role in CCR7 internalisation. In this respect, CCR7 may be behaving in a similar fashion to CCR5 which also requires membrane cholesterol for optimal ligand binding, but the internalisation of which takes place via CCPs (Nguyen and Taub, 2002; Signoret et al., 2005). Once internalised, it is likely that CCVs containing CCR7 fuse with the early endosomal compartment, a process dependent upon the small GTPase Rab5. Inhibition of Rab5 function significantly reduced the amount of chemokine uptake through CCR7. Therefore, from all these investigations, it seems likely that CCR7 employs a 'typical' route of chemokine driven endocytosis and trafficking (Figure 4.1.1). CCX-CKR, on the other hand, appears to use a completely distinct route of internalisation.

In contrast to CCR7, chemokine uptake was not prevented when CCX-CKR was transfected into  $\beta$ -arrestin *null* cells and overexpression of a dominant negative inhibitor of  $\beta$ -arrestins had no effect on chemokine uptake by CCX-CKR. This strongly suggests that CCX-CKR internalisation is not dependent on  $\beta$ -arrestins and may explain the ability of the

receptor to avoid ligand-driven desensitisation. The viral chemokine receptor US28 has also been reported to internalise independently of  $\beta$ -arrestins (Fraile-Ramos et al., 2003), and the role of  $\beta$ -arrestins in D6 internalisation has yet to be resolved (Galliera et al., 2004; Weber et al., 2004). However, both of these receptors undergo constitutive internalisation via CCPs (Fraile-Ramos et al., 2001; Fraile-Ramos et al., 2003; Weber et al., 2004). It was of some surprise therefore that inhibition of clathrin-mediated endocytosis, using the dominant negative inhibitors of EPS15, had no effect on chemokine uptake by CCX-CKR. Instead, my data strongly suggest that CCX-CKR endocytosis is dependent upon caveolae. Impressive inhibition of CCX-CKR-mediated chemokine uptake was observed using both the dominant-negative inhibitor of caveolin-1 and WT caveolin-1, and this occurred with concomitant increases in the level of surface CCX-CKR. These effects were specific to CCX-CKR, as the caveolin plasmids used left internalisation via CCR7 and D6 untouched.

There are several puzzling aspects to the results obtained with the caveolin-1 plasmids, although reasonable explanations can be provided. The fact that both dominant-negative inhibitor and WT versions of caveolin-1 inhibit internalisation may at first seem counterintuitive. However, caveolin-1 can stabilise caveolae at the cell surface (Minshall et al., 2000; Nabi and Le, 2003; Nichols, 2003) with the endocytosis of these domains being regulated by signals dependent upon caveolin-1 (Pelkmans et al., 2001). Therefore, in my experiments, it can be envisaged that caveolae are being stabilised at the plasma membrane by the overexpression of the WT caveolin-1, whilst expression of the dominant-negative inhibitor is preventing the transduction of signals (presumably originating from CCX-CKR) through caveolin, thereby preventing caveolar endocytosis. The fact that surface CCX-CKR levels are increased in cells over-expressing caveolin-1 proteins may be further evidence that receptor internalisation is being blocked by these proteins. It is notable that cells with high levels of surface receptor have less potential to internalise ligand, while 'primed'

HEK-hCCX-CKR cells (which have lower surface receptor levels than untreated cells) show increased CCL19 uptake. It is also of note that overexpression of WT caveolin-1 causes greater inhibition of uptake than dominant-negative caveolin-1, and also causes more significant increases to the level of receptor at the cell surface. Again, these data indicate that it may be the rate of trafficking of CCX-CKR that determines uptake, rather than absolute surface levels at a given time.

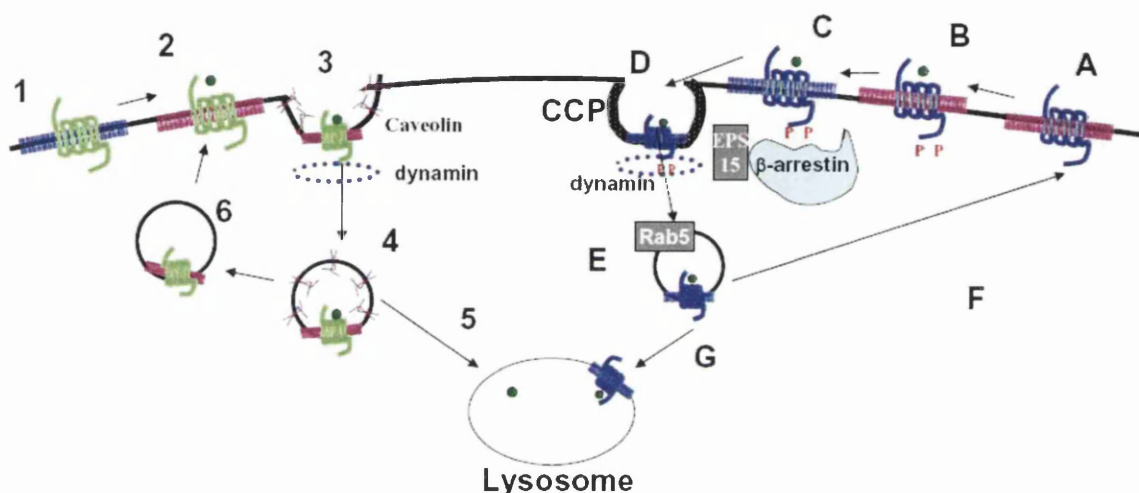


**Figure 4.1.1: Proposed Model of CCL19 Uptake by CCX-CKR and CCR7.** A schematic showing potential routes of endocytosis employed by CCX-CKR and CCR7. (1) CCX-CKR is outside of cholesterol rich membrane domains but localise to these regions after CCL19 stimulation (2). (3) CCL19 driven signals from CCX-CKR through caveolin-1 drive endocytosis of caveolae, dependent on dynamin (4). Chemokine internalised is then released intracellularly and degraded (5) while CCX-CKR recycles (6) back to cholesterol rich plasma membrane domains where it can rapidly undergo caveolin regulated endocytosis. CCR7 (A) may constitutively localise to cholesterol rich domains which are important for ligand binding and receptor activation (B). Phosphorylation of CCR7 recruits  $\beta$ -arrestins (C) which links the receptor complex to CCPs which endocytose dependent on dynamin and EPS15 (D). CCPVs fuse with Rab5+ early endosomes and the receptor and CCL19 either recycle back to the cell surface (F) or are targeted for degradation (G). Key: Green receptor=CCX-CKR, blue receptor=CCR7, blue plasma membrane=outside lipid rafts, purple plasma membrane=lipid raft, dark green circles=CCL19.

These observations present the following working model for CCX-CKR internalisation, summarised in figure 4.1.1. Initially localised outside caveolae, CCX-CKR is envisaged to require relocation to caveolae for internalisation. This could be ligand-driven. Once in caveolae, CCX-CKR may transduce signals causing caveolar endocytosis and subsequent

rapid trafficking of CCX-CKR to and from the cell surface. The presence of cholesterol in membrane microdomains has been shown to alter the ligand affinities of several GPCRs (Gimpl et al., 1997), including the chemokine receptor CCR5 (Nguyen and Taub, 2002). Therefore, it is possible that CCX-CKR in caveolae has an increased affinity for ligand. This could contribute to the 'priming' phenomenon observed, with relocalisation of CCX-CKR, induced by prior exposure to ligand, into this high affinity, internalising state resulting in more effective subsequent uptake.

Clearly this hypothesis requires testing. To begin to do this, one would first want to examine whether there is a change in receptor affinity following ligand exposure. Preliminary data suggest that this is indeed the case (not shown), but careful Scatchard analysis should be able to confirm this. Next, if such an affinity change is dependent on localisation to cholesterol-rich domains, it should be inhibitable with cholesterol-depleting agents, such as M $\beta$ CD. Alternatively, the addition of free cholesterol may be able to mimic this change to enhance ligand binding affinity. If relocalisation into caveolae following receptor activation does occur, this can also be tested. First, it would be expected that CCX-CKR would be found outside of Triton-X-100 insoluble membrane fractions (indicative of lipid raft localisation) before ligand addition, and within these fractions after exposure to chemokine. Ligand-induced co-localisation of CCX-CKR and caveolin-1 GFP could be analysed. With the aid of a reliable antibody to CCX-CKR (or an epitope tag), localisation of the receptor to caveolae could be assessed by electron microscopy. Furthermore, fluorescence resonance energy transfer technology could potentially be used to show interactions between CCX-CKR and caveolin. Alternatively, BioCCL19/Cy3 complexes could be exploited to examine its localisation with caveolin-GFP during internalisation, an association which one might anticipate would be enhanced following priming. Finally, it would be predicted that in cells with non-endocytosing caveolae, such as those highly

overexpressing the WT protein, ligand-induced priming would not occur. This is readily testable with existing technology.

If CCX-CKR does localise to caveolae, how does it get there? Other GPCRs found in these domains use one of several mechanisms, including cholesterol binding, fatty acylation, or protein-protein interactions (Chini and Parenti, 2004). Indeed, it has been shown that CCR5 localises to plasma membrane lipid rafts via palmitoylation of cysteine residues in its C-terminus, and that this is responsible for the slow rate of endocytosis of this receptor (Venkatesan et al., 2003). Notably the C-terminus of CCX-CKR is completely lacking in cysteine residues. Interestingly however, CCX-CKR exhibits a putative caveolin binding site ( $\phi XX\phi XXXX\phi$  or  $\phi XXXX\phi X\phi$  where  $\phi$ =Tyr, Phe, or Trp and X=any amino acid) towards the end of the final transmembrane region going into the C-terminus. These sequences are present in all proteins that have been shown to directly interact with caveolins (Couet et al., 1997). This is conserved in CCX-CKR homologs between humans, chimpanzees, mice, cows, and even *Xenopus laevis* (Figure 4.1.2). Whether this sequence mediates interactions with caveolins remains to be determined. Caveolin binding motifs are not particularly unusual sequences, and do not necessarily result in interaction with caveolins. Indeed, other closely-related chemokine receptors to CCX-CKR, such as CCR9, also display this motif. Nonetheless, mutagenesis of this motif and subsequent analysis of receptor behaviour and association with caveolin would be worthy experiments to consider for the future.

To my knowledge, CCX-CKR is the first chemokine receptor to show such tight regulation by caveolins over internalisation. As outlined in section 1.3.5, ECs are rich in caveolae, and these structures are commonly thought to mediate transcytosis of nutrients and macromolecules across these barriers. This is of obvious interest when the in vivo function

of CCX-CKR is considered. Although, the data presented here suggest that CCX-CKR may be specialised to mediate the continuous sequestration and degradation of chemokines, a chemokine transport function cannot be ruled out. In fact, some CCL19 internalised by CCX-CKR is able to recycle intact back to the cell surface. Therefore, the possibility exists that CCX-CKR may mediate the transport (and perhaps even presentation) of at least some of its chemokine cargo. It would be of interest to determine if this occurs in a directional manner, and in a more significant cell type, such as ECs. With this in mind, defining the cell types expressing CCX-CKR *in vivo* arises as a key future objective.

There is clearly much to be learned about endocytosis via caveolae. The molecular mechanisms controlling this process and regulating the fate of caveosome cargo have not yet been fully elucidated. Therefore, the full implications of CCX-CKR regulation by caveolin and caveolae cannot yet be fully understood. Moreover, while the results discussed in this section demonstrate clear differences between CCX-CKR and CCR7 in the experimental systems used, care must be taken when drawing conclusions from over-expression of proteins in cell lines. Ideally, experiments should be performed using cells which endogenously express these receptors. Thus, whilst *in vitro* experimentation on transfected cell lines provides clues to receptor functions in their endogenous settings, more robust evidence ideally from *in vivo* studies must be forthcoming before protein functions can be reliably assigned. The generation and analysis of animals lacking CCX-CKR are clearly an important step towards achieving this aim.

## **4.2 The *In Vivo* Expression of CCX-CKR**

The CCX-CKR null mice successfully generated in this study provide an invaluable tool for characterising the essential functions of this receptor. Several intriguing observations have

already been made in experiments with these mice and the implications of these shall be discussed in more detail in section 4.3. However, to understand the functions of CCX-CKR in the mouse, it is of key importance to generate information regarding the cell types which express this receptor, and understand how this expression is regulated. In this regard, the reporter genes inserted in place of the CCX-CKR open-reading frame should be of use in providing these valuable insights. Precedents for the successful use of this approach for studying chemokine receptor expression and function have been set by the CX3CR1, CCR6, and CCR9 GFP KIKO mice (Benz et al., 2004; Jung et al., 2000; Kucharzik et al., 2002; Niess et al., 2005).

Although preliminary investigations of reporter expression were disappointing and did not result in the detection of GFP or lacZ gene products, the suitability of this approach for identifying CCX-CKR-expressing cells should not yet be rejected. It may be that cells positive for the reporters were present in these animals, but were so rare, or expressed the reporters at such low levels, that detection was not possible. Although neither GFP fluorescence nor lacZ activity were consistently observed, this could not be properly interpreted without using reliable positive controls. A priority for the future is the optimisation of staining and detection procedures using animals which express these reporters in a known pattern, and then applying these techniques to tissues from CCX-CKR KIKO mice. If it is the case that the reporters are not being expressed at high enough levels to be directly detected, the use of antibodies to these reporters in immunohistochemical approaches may help amplify signals.

However, it is possible that despite transcripts for the reporter genes being readily detectable, these transcripts are not being successfully translated into protein. Given the importance of determining the cell types which express CCX-CKR, it may be necessary to

consider alternative means of CCX-CKR detection. There are various ways this could be achieved. *In situ* hybridisation could be used to detect cells expressing CCX-CKR transcripts. The development of a reliable antibody against mouse CCX-CKR would represent an important advance enabling detection of the receptor on tissue sections by immunohistochemistry. Finally, to detect functional expression of CCX-CKR at the level of single cells, *in situ* radioligand binding assays, similar to those used to characterise DARC and D6 expression (Hub and Rot, 1998; Nibbs et al., 2001), could be performed. In all approaches, the comparison of CCX-CKR KO and WT tissue sections will prove to be very useful to validate results.

Once the expression profile of CCX-CKR has been confirmed, various key experiments can be performed. For example, if the reporter genes can be shown to work, the cells positive for the reporter can be purified and used in *in vitro* assays similar to those performed here using transfected HEK293 cells. This will provide a more physiological cell background to study CCX-CKR function and can be used to confirm the validity of the findings presented here. In addition, KO vs WT cells can be purified and used in *in vitro* assays to define the indispensable functions of CCX-CKR in various cell types. The nature of experiments performed would clearly depend upon the types of cell, and circumstances under which CCX-CKR was expressed. The development of technologies to help answer the questions above, are eagerly anticipated.

### **4.3 The *In Vivo* Function of CCX-CKR**

The investigations of CCX-CKR null mice initiated in this study have not yet been completed in sufficient detail to precisely determine the indispensable functions of CCX-CKR in the mouse. Clearly, information regarding the cells and circumstances under which

CCX-CKR is expressed will inform and direct analysis of these mice in the future. However, some basic characterisation of CCX-CKR null mice has been performed and this has revealed several extremely interesting phenotypes worthy of discussion.

Perhaps unsurprisingly, CCX-CKR null mice are viable, develop normally, and are fertile. So far, among chemokine receptors, only the CXCR4 null mouse has displayed defects which lead to failure of embryogenesis (Tachibana et al., 1998; Zou et al., 1998). It is only upon more detailed investigation, often in disease models, that defects in other chemokine receptor null mice have become apparent (Power, 2003). The biochemical analysis (discussed above) prompted consideration that, *in vivo*, CCX-CKR may play a regulatory role in the biology of CCR7 and CCR9 through controlling availability of their agonist ligands CCL19, CCL21, and CCL25. Based on this, it is in the thymus, secondary lymphoid organs, and small-intestinal immune system where one may expect to see an effect of dysregulation of these chemokines. This study has focussed primarily on the secondary lymphoid organs, examining their cellularity at steady state, and their response during inflammatory and immune challenge. The main observations made were as follows. First, ILNs in CCX-CKR null mice were significantly smaller than those from WT mice, and contained fewer cells. Normal proportions of T and B cells were present in CCX-CKR null ILNs, though there was a subtle change in a small population of CD4<sup>-</sup>, CD8<sup>low</sup> cells. Specifically, these were significantly reduced in ILNs from animals lacking CCX-CKR. Second, in the spleen, normal proportions of cells were observed, but F4/80<sup>+</sup> cells expressed higher levels of MHC classII. Third, in response to the topical application of PMA, draining ILNs of CCX-CKR null mice did not undergo the same degree of LN hypertrophy, although the inflammatory response in the skin appeared similar. A similar phenotype in the ILN was apparent when mice were sensitised topically with DNFB, however subsequent DTH responses in the ear were intact. Fourth, subcutaneous

immunisation with OVA/CFA revealed that CCX-CKR null mice apparently develop normal antibody responses, and ILNs expanded in a fashion similar to WT during the response. However, the cellular immune response within the ILN appeared to be prolonged.

#### 4.2.1 Steady State Analysis

The first phenomenon to consider is the reduction in resting ILN cellularity. In some respects, this has similarities to phenotypes reported in CCR7 null and *plt* mice (Forster et al., 1999); (Nakano et al., 1997), which display reduced numbers of cells in LNs. However, in both of these strains, it is T cells which are specifically lacking. In contrast, only a small population of CD4<sup>-</sup>,CD8<sup>low</sup> cells appears to be specifically lacking in CCX-CKR nulls, with the cellular reduction reflecting a general deficit of T and B cells within ILNs. The exact phenotype of the CD4<sup>-</sup>,CD8<sup>low</sup> cells is clearly worthy of further investigation. It is possible that they represent a population of DCs. So-called 'lymphoid' DCs express CD8, and are present in resting mouse LNs (Salomon et al., 1998). They preferentially stimulate a Th1 type cytokine profile in CD4<sup>+</sup> T cells (Maldonado-Lopez et al., 1999) and have also been implicated in the resolution and regulation of CD4 and CD8 T cell responses (Kronin et al., 2001; Kronin et al., 1996; Suss and Shortman, 1996). Intriguingly, these cells are likely to represent a mobile population of DCs and have been shown to be responsive to both CCL19 and CCL21 (but not CCL25) *in vitro* (Colvin et al., 2004). Alternatively, these cells could be CD8<sup>low</sup> T cells, a poorly-characterised sub-population of T cells, shown to originate from CD8 T cells following activation in the presence of IL-4 (Kienzle et al., 2005). These cells are only weakly cytolytic, but still capable of cytokine production (Kienzle et al., 2004). Further immunophenotyping is merited to properly characterise this cell population. For example, analysis of whether these cells express CD3 or CD11c and MHC classII should give an indication of the phenotype of these cells. Once this has been clarified, investigation

is important to determine the reasons for the lack of this population and the functional impact of this defect in CCX-CKR null mice.

When the decoy receptor hypothesis for CCX-CKR is considered, a reduced total cellularity in the LNs perhaps seems counter-intuitive. Excess CCL19 and CCL21, caused by a lack of post-translational regulation of their availability (normally exerted by CCX-CKR), may be expected to lead to increased levels of these chemokines within LNs and hence a greater influx of CCR7<sup>+</sup> cells. However, there are several reasons why this may not be the case. First, it is possible that CCX-CKR expressed in the peripheral tissues, helps prevent CCR7<sup>+</sup> cells entering these sites by sequestering CCL21 produced by lymphatic ECs. The loss of this regulation in the knock-out may therefore cause lymphocytes to aberrantly traffic to peripheral tissues, rather than secondary lymphoid organs, leading to the observed reduction in total ILN cellularity. Second, CCX-CKR may be normally expressed on CCR7<sup>+</sup> cells themselves, as a mechanism to regulate the responsiveness of CCR7. The absence of CCX-CKR could then conceivably lead to excessive activation of CCR7, leading to its desensitisation, and preventing entry into LNs. Third, while the presumption is that more chemokines equals more chemotaxis, this may not be the case. As mentioned in the introduction, in the thymus CCR7<sup>+</sup> DN thymocytes migrate outwards away from the medulla, an area dense in CCR7 ligands. A chemorepulsive effect has been suggested to drive this (Witt and Robey, 2004). Indeed, chemorepulsion has been proposed to occur elsewhere in the chemokine system, such as when high levels of CXCL12 are encountered by CXCR4<sup>+</sup> cells in some circumstances (Poznansky et al., 2002; Poznansky et al., 2000). Therefore it should be considered that if CCX-CKR normally regulates CCL19 and CCL21 levels in secondary lymphoid organs, then overabundance of these proteins may start to exert a chemorepulsive effect on CCR7<sup>+</sup> cells, inhibiting their entry into the LNs.

The above discussion is conjecture, and whilst the biochemical data presented in this thesis support a decoy function for CCX-CKR, there are, as yet, no robust *in vivo* data to suggest that CCX-CKR does indeed play such a role. Therefore, alternative hypotheses of CCX-CKR function should be considered. Prominent amongst these is the chemokine transport hypothesis. If CCX-CKR is involved in endothelial transcytosis and/or presentation of its ligands, its absence may lead to reduced levels of CCL19 or CCL21 available for CCR7<sup>+</sup> cells on HEVs or lymphatic vessels. This in turn could result in the observed reduction in the number of cells in ILNs. One problem with this hypothesis however, is that one might expect that the phenotype of ILNs would be more similar to that reported in *CCR7*<sup>-/-</sup> or *plt* mice, and show a T cell-specific deficiency. As B cells are still able to enter LNs in these mice, through CXCR4/CXCL12 and possibly CXCR5/CXCL13 interactions, a similar scenario would be imagined to occur in mice deficient in EC presentation of CCR7 ligands.

The modified phenotype of macrophages in the spleens of CCX-CKR mice is also intriguing and requires further investigation. An increase in MHC class II<sup>high</sup> macrophages, with a concomitant reduction in MHC class II<sup>low</sup> populations, may indicate that macrophages in CCX-CKR<sup>-/-</sup> spleens are of a more activated phenotype. Again, this could be explained by dysregulation of the protein levels of CCL19 and CCL21 in the spleens of these animals. A recent report showed that CCL19 and CCL21 can act as terminal differentiation factors for APCs, inducing their maturation including the upregulation of MHC class II (Marsland et al., 2005). Although this phenotype was not apparent in CD11c<sup>+</sup> DCs from CCX-CKR null spleens, it is nonetheless conceivable that CCR7 ligation contributes to macrophage activation. Alternatively, as F4/80 expression is highest in red pulp macrophages and largely absent from MZ macrophages (Taylor et al., 2005), and as CCL19 and CCL21 are normally restricted to the PALS of the spleen, it is possible that deficiency in CCX-CKR is allowing access of these chemokines into the red pulp where it

is causing this observed upregulation of MHC classII on resident macrophages. Further immunophenotyping of the macrophage populations in the spleens of these animals is clearly required. Furthermore, as CCL19 and CCL21 have recently been shown to be necessary for the localisation of macrophages within the splenic MZ (Ato et al., 2004), immunohistochemistry should be performed to study the localisation of these cells in the spleen.

Thus, in summary, there is much still to be done to fully characterise the steady-state phenotypes emerging in the secondary lymphoid organs of CCX-CKR<sup>-/-</sup> mice. Principally, detailed histological analysis is required to examine the localisation of different cell types within these organs. Although H+E sections of spleen and LNs were examined and revealed no obvious abnormalities, thorough immunohistochemistry examining the location of all the various leukocyte populations is required. Furthermore, detailed analysis of PPs, tonsils, adenoids and other LNs should be undertaken. Of course, a key aim in future work is to determine how CCX-CKR is acting at the molecular level such that its loss causes these defects. Are the decoy or transport hypotheses justified, or does CCX-CKR control some other aspect of the biology of its chemokine ligands? In this regard, it will be very interesting to examine the protein levels of the various chemokine ligands of CCX-CKR in these organs. If CCX-CKR exerts a decoy function, then levels of CCL19, CCL21 and CCL25 might be elevated. This should be fairly straightforward to examine by making lysates from the tissue of interest and examining chemokine levels by ELISA. Analysis of CCX-CKR ligand localisation may also be possible via immunohistochemistry. Finally, as discussed above, determining which cell types express CCX-CKR will clearly aid in the interpretation of these homeostatic defects in CCX-CKR null mice. It is imperative that attempts are made to examine if the chemokine sequestration properties observed in transfected cells, also apply to CCX-CKR *in vivo*.

### 4.2.2 Function of CCX-CKR in Immunity and Inflammation

Topical application of PMA or DNFB fails to induce ILN hypertrophy in CCX-CKR null mice. Although ILNs from CCX-CKR null animals are smaller than their WT counterparts prior to challenge, the relative increase in ILN weight and cellularity is much greater in WT than in KO animals. This phenomenon could be caused by a number of aberrations in KO mice. First, DCs from the skin may not be migrating as efficiently to ILNs. Published work has shown that DC migration from the periphery to LNs is sufficient to cause LN hypertrophy and the extent of this is proportional to the number of DCs which reach the node. In this instance, hypertrophy was observed before the induction of cell proliferation within the LN, and was maximal at around 3-5 days after the injection of DCs (Martín-Fontecha et al., 2003). There are various ways in which aberrant DC migration could be occurring in CCX-CKR<sup>-/-</sup> animals. CCR7 plays a clear role in controlling LC migration from the epidermis into the lymphatic vessels and then into LNs (Forster et al., 1999; Ohl et al., 2004). CCX-CKR may play a role at any number of stages along this migration pathway. For example, LC responsiveness to CCR7 ligands may be regulated by CCX-CKR expression on the LCs themselves. Alternatively, CCX-CKR may be involved in the presentation of CCL21 on skin lymphatic vessels or control the positioning or retention of LCs upon arrival at LNs.

Defects in LC migration are not the only possible explanation. CCX-CKR may be required for the retention of lymphocytes within ILNs, perhaps by regulating peripheral levels of CCL21 and CCL19. Alternatively, cells within the ILN may not be as proliferative in CCX-CKR<sup>-/-</sup> mice, or LC maturation may be affected preventing appropriate lymphocyte expansion within the LN. Clearly, many of these ideas are testable experimentally. For example, to assess LC migration, various well-established approaches could be taken. The topical application of FITC, followed by analysis of green cells arriving in the draining LN

should answer whether there is a general defect in LC migration from the skin. Furthermore, epidermal sheets could be prepared and LCs enumerated, both with and without the prior application of a topical irritant. This would allow assessment of whether there is a steady state defect in LCs and whether these cells are able to begin their exodus from the epidermis in CCX-CKR<sup>-/-</sup> mice.

Despite these alterations in draining LN expansion in response to the epicutaneous Ag delivery, immune responses in CCX-CKR<sup>-/-</sup> mice still develop in response to DNFB challenge. Indeed, no differences in the DTH response in terms of ear thickness were observed. This does not necessarily contradict hypotheses which predict aberrant LC migration in these mice. Although development of normal contact hypersensitivity responses to topically applied Ag requires LC migration (Del Prete et al., 2004; Streilein et al., 1980; Toews et al., 1980), the high Ag dose used in the experiments here may mask an effect on subsequent responses. Perhaps at lower doses of DNFB, partial aberrations in LC function present in CCX-CKR<sup>-/-</sup> mice, may result in the emergence of defects in the subsequent induction of contact hypersensitivity responses.

The immune response to the subcutaneously delivered OVA/CFA also revealed several interesting observations, not least the fact that the cellularity of draining LNs of CCX-CKR KO and WT animals was indistinguishable following administration of Ag by this route. This suggests that the route of Ag delivery is important and, as lymphatic drainage probably accounts for the main route of delivery in this model, may provide supporting evidence that the defect in the cutaneous applied models is indeed due to aberrant LC migration. Although relatively normal primary immune response were measured to OVA, the cellular response appears to last longer in CCX-CKR KO animals. This may represent a delay in the kinetics of the immune response. More detailed timecourse analysis of the cellular immune

response is merited to investigate this. Interestingly, *plt* mice have been shown to mount delayed, yet enhanced immune responses in a similar model (Mori et al., 2001). It remains to be seen if the CCX-CKR<sup>-/-</sup> mouse is behaving in a similar way. Alternatively, there may be a failure of regulation of T cell responses. Indeed, CD8<sup>+</sup> DCs have been shown to contribute to T cell regulation (Kronin et al., 2001; Kronin et al., 1996; Suss and Shortman, 1996), and as it is possible that there is a steady state defect in this population in CCX-CKR null mice, this is certainly worthy of further investigation. A third possibility is that T cells may be primed more efficiently in CCX-CKR null mice. Again, if CCL19 and CCL21 levels are enhanced in the LN then one may predict that APCs will be more activated and potentially able to induce more robust T cell responses. Finally, defects in T cell apoptosis or LN egress could also potentially explain the prolongation of Ag-specific proliferation and cytokine production.

Immunological studies in CCX-CKR null mice should be extended. The experiments described here should be repeated, perhaps with variations in Ag dosage or routes of delivery, and more detailed analysis of the kinetics of the responses undertaken. Furthermore, analysis of immune responses could be taken further to examine the production of various different Ig isotypes, the production of other cytokines, and to assess the phenotype of DCs, macrophages, and lymphocytes in KO and WT LN. As with future studies of the steady-state defects in these mice, detailed analysis of cell localisation during immune responses should also be studied by immunohistochemistry. It will also be of interest to do these experiments with mice on a better-characterised genetic background, such as C57Bl/6 or BALB/c, to investigate whether the phenotypes observed in FVB mice are observed in other strains. In addition, models of immunopathology should be examined in these mice, such as experimental autoimmune encephalomyelitis, collagen induced arthritis, or allograft rejection. In particular, inflammation and immunity in the small

intestine, such as salmonella infection or colitis, will be of interest to study, as the other CCX-CKR ligand (CCL25) is of importance in homing to this site. Finally, as discussed above, considerable efforts need to be expended to determine, at the molecular level, exactly how CCX-CKR deletion influences the chemokine network to see if models describing CCX-CKR as a chemokine transport or decoy receptor are truly justified.

#### **4.4 Overall Conclusions and Future Perspectives**

This study has begun to unravel the biochemistry of CCX-CKR *in vitro*, and generated the tools which have provided the first insights into the *in vivo* function of this receptor. In HEK293 cells, CCX-CKR utilises mechanisms of endocytosis distinct from those typically engaged by chemokine receptors, to ensure that it is capable of the continued internalisation of CCL19. By continually sequestering and degrading CCL19, CCX-CKR is capable of modifying chemotactic responses to this chemokine *in vitro*. These biochemical properties make CCX-CKR ideally suited to its proposed *in vivo* role as a decoy receptor for CCL19, 21 and 25, chemokines which play a major role in the primary and secondary lymphoid microenvironments. Consistent with this, analysis of CCX-CKR null mice demonstrated that this receptor plays a role in regulating the cellularity and phenotype of cells in the secondary lymphoid organs at steady-state and during cutaneous inflammation. CCX-CKR null mice are capable of mounting humoral and cellular primary immune responses, but the kinetics or regulation of the cellular response appear to be altered. More thorough analysis of CCX-CKR null mice should provide the insights required to determine its *in vivo* function. In addition, the reporter mice generated in this study should provide a valuable means of determining the *in vivo* expression of CCX-CKR, which will provide vital clues as to the function of this intriguing receptor.

Our understanding of the function of CCX-CKR is still at a very early stage. However, if as has been hypothesised, CCX-CKR does indeed act as decoy or transport receptor for its chemokine ligands then not only will studies of this receptor give us a deeper knowledge of in vivo chemokine networks, but there are also potential therapeutic applications to be considered. CCX-CKR ligands play important roles in the induction of immunity, and represent potential targets for the pharmaceutical industry in the treatment of autoimmune disease, allograft rejection, allergy, infectious disease, and cancer. That CCX-CKR may be able to regulate these chemokines means that by controlling its expression with pharmaceuticals or gene therapy, we may be able to use this receptor to therapeutically modify immune responses in human disease.

## CHAPTER FIVE

### REFERENCES

- Abbas, A. K., and Lichtman, A. H. (2005). Cellular and molecular immunology, 5th edn (Philadelphia, PA, Elsevier/Saunders).
- Agenes, F., Bosco, N., Mascarell, L., Fritah, S., and Ceredig, R. (2005). Differential expression of regulator of G-protein signalling transcripts and in vivo migration of CD4+ naive and regulatory T cells. *Immunology* *115*, 179-188.
- Aichele, P., Zinke, J., Grode, L., Schwendener, R. A., Kaufmann, S. H., and Seiler, P. (2003). Macrophages of the splenic marginal zone are essential for trapping of blood-borne particulate antigen but dispensable for induction of specific T cell responses. *J Immunol* *171*, 1148-1155.
- Alcami, A. (2003). Viral mimicry of cytokines, chemokines and their receptors. *Nat Rev Immunol* *3*, 36-50.
- Alcami, A., Symons, J. A., Collins, P. D., Williams, T. J., and Smith, G. L. (1998). Blockade of chemokine activity by a soluble chemokine binding protein from vaccinia virus. *J Immunol* *160*, 624-633.
- Allen, C. D., Ansel, K. M., Low, C., Lesley, R., Tamamura, H., Fujii, N., and Cyster, J. G. (2004). Germinal center dark and light zone organization is mediated by CXCR4 and CXCR5. *Nat Immunol* *5*, 943-952.
- Andjelkovic, A. V., Song, L., Dzenko, K. A., Cong, H., and Pachter, J. S. (2002). Functional expression of CCR2 by human fetal astrocytes. *J Neurosci Res* *70*, 219-231.
- Annunziato, F., Romagnani, P., Cosmi, L., Lazzeri, E., and Romagnani, S. (2001). Chemokines and lymphopoiesis in human thymus. *Trends Immunol* *22*, 277-281.
- Ansel, K. M., McHeyzer-Williams, L. J., Ngo, V. N., McHeyzer-Williams, M. G., and Cyster, J. G. (1999). In vivo-activated CD4 T cells upregulate CXC chemokine receptor 5 and reprogram their response to lymphoid chemokines. *J Exp Med* *190*, 1123-1134.
- Ansel, K. M., Ngo, V. N., Hyman, P. L., Luther, S. A., Forster, R., Sedgwick, J. D., Browning, J. L., Lipp, M., and Cyster, J. G. (2000). A chemokine-driven positive feedback loop organizes lymphoid follicles. *Nature* *406*, 309-314.
- Ato, M., Nakano, H., Kakiuchi, T., and Kaye, P. M. (2004). Localization of marginal zone macrophages is regulated by C-C chemokine ligands 21/19. *J Immunol* *173*, 4815-4820.
- Bacon, K. B., and Camp, R. D. (1990). Interleukin (IL)-8-induced in vitro human lymphocyte migration is inhibited by cholera and pertussis toxins and inhibitors of protein kinase C. *Biochem Biophys Res Commun* *169*, 1099-1104.

- Baekkevold, E. S., Yamanaka, T., Palframan, R. T., Carlsen, H. S., Reinholt, F. P., von Andrian, U. H., Brandtzaeg, P., and Haraldsen, G. (2001). The CCR7 ligand elc (CCL19) is transcytosed in high endothelial venules and mediates T cell recruitment. *J Exp Med* *193*, 1105-1112.
- Baggiolini, M. (1998). Chemokines and leukocyte traffic. *Nature* *392*, 565-568.
- Baggiolini, M., Dewald, B., and Moser, B. (1997). Human chemokines: an update. *Annu Rev Immunol* *15*, 675-705.
- Bais, C., Santomasso, B., Coso, O., Arvanitakis, L., Raaka, E. G., Gutkind, J. S., Asch, A. S., Cesarman, E., Gershengorn, M. C., Mesri, E. A., and Gerhengorn, M. C. (1998). G-protein-coupled receptor of Kaposi's sarcoma-associated herpesvirus is a viral oncogene and angiogenesis activator. *Nature* *391*, 86-89.
- Bais, C., Van Geelen, A., Eroles, P., Mutlu, A., Chiozzini, C., Dias, S., Silverstein, R. L., Rafii, S., and Mesri, E. A. (2003). Kaposi's sarcoma associated herpesvirus G protein-coupled receptor immortalizes human endothelial cells by activation of the VEGF receptor-2/ KDR. *Cancer Cell* *3*, 131-143.
- Baldwin, E. T., Weber, I. T., St Charles, R., Xuan, J. C., Appella, E., Yamada, M., Matsushima, K., Edwards, B. F., Clore, G. M., Gronenborn, A. M., and et al. (1991). Crystal structure of interleukin 8: symbiosis of NMR and crystallography. *Proc Natl Acad Sci U S A* *88*, 502-506.
- Banchereau, J., and Steinman, R. M. (1998). Dendritic cells and the control of immunity. *Nature* *392*, 245-252.
- Bandeira-Melo, C., Sugiyama, K., Woods, L. J., Phoofolo, M., Center, D. M., Cruikshank, W. W., and Weller, P. F. (2002). IL-16 promotes leukotriene C(4) and IL-4 release from human eosinophils via CD4- and autocrine CCR3-chemokine-mediated signaling. *J Immunol* *168*, 4756-4763.
- Bardi, G., Lipp, M., Baggiolini, M., and Loetscher, P. (2001). The T cell chemokine receptor CCR7 is internalized on stimulation with ELC, but not with SLC. *Eur J Immunol* *31*, 3291-3297.
- Barone, F., Bombardieri, M., Manzo, A., Blades, M. C., Morgan, P. R., Challacombe, S. J., Valesini, G., and Pitzalis, C. (2005). Association of CXCL13 and CCL21 expression with the progressive organization of lymphoid-like structures in Sjogren's syndrome. *Arthritis Rheum* *52*, 1773-1784.
- Beckmann, J. H., Yan, S., Luhrs, H., Heid, B., Skubich, S., Forster, R., and Hoffmann, M. W. (2004). Prolongation of allograft survival in *ccr7*-deficient mice. *Transplantation* *77*, 1809-1814.
- Belleudi, F., Visco, V., Ceridono, M., Leone, L., Muraro, R., Frati, L., and Torrisi, M. R. (2003). Ligand-induced clathrin-mediated endocytosis of the keratinocyte growth factor receptor occurs independently of either phosphorylation or recruitment of eps15. *FEBS Lett* *553*, 262-270.

- Benlimame, N., Le, P. U., and Nabi, I. R. (1998). Localization of autocrine motility factor receptor to caveolae and clathrin-independent internalization of its ligand to smooth endoplasmic reticulum. *Mol Biol Cell* *9*, 1773-1786.
- Benmerah, A., Bayrou, M., Cerf-Bensussan, N., and Dautry-Varsat, A. (1999). Inhibition of clathrin-coated pit assembly by an Eps15 mutant. *J Cell Sci* *112 (Pt 9)*, 1303-1311.
- Benmerah, A., Lamaze, C., Begue, B., Schmid, S. L., Dautry-Varsat, A., and Cerf-Bensussan, N. (1998). AP-2/Eps15 interaction is required for receptor-mediated endocytosis. *J Cell Biol* *140*, 1055-1062.
- Benz, C., Heinzl, K., and Bleul, C. C. (2004). Homing of immature thymocytes to the subcapsular microenvironment within the thymus is not an absolute requirement for T cell development. *Eur J Immunol* *34*, 3652-3663.
- Berahovich, R. D., Miao, Z., Wang, Y., Premack, B., Howard, M. C., and Schall, T. J. (2005). Proteolytic Activation of Alternative CCR1 Ligands in Inflammation. *J Immunol* *174*, 7341-7351.
- Berek, C., and Ziegner, M. (1993). The maturation of the immune response. *Immunol Today* *14*, 400-404.
- Billstrom, M. A., Johnson, G. L., Avdi, N. J., and Worthen, G. S. (1998). Intracellular signaling by the chemokine receptor US28 during human cytomegalovirus infection. *J Virol* *72*, 5535-5544.
- Birkenbach, M., Josefsen, K., Yalamanchili, R., Lenoir, G., and Kieff, E. (1993). Epstein-Barr virus-induced genes: first lymphocyte-specific G protein-coupled peptide receptors. *J Virol* *67*, 2209-2220.
- Blackburn, P. E., Simpson, C. V., Nibbs, R. J., M, O. H., Booth, R., Poulos, J., Isaacs, N. W., and Graham, G. J. (2004). Purification and biochemical characterisation of the D6 chemokine receptor. *Biochem J* *379*, 263-272.
- Bodaghi, B., Jones, T. R., Zipeto, D., Vita, C., Sun, L., Laurent, L., Arenzana-Seisdedos, F., Virelizier, J. L., and Michelson, S. (1998). Chemokine sequestration by viral chemoreceptors as a novel viral escape strategy: withdrawal of chemokines from the environment of cytomegalovirus-infected cells. *J Exp Med* *188*, 855-866.
- Bonacchi, A., Petrai, I., Defranco, R. M., Lazzeri, E., Annunziato, F., Efsen, E., Cosmi, L., Romagnani, P., Milani, S., Failli, P., *et al.* (2003). The chemokine CCL21 modulates lymphocyte recruitment and fibrosis in chronic hepatitis C. *Gastroenterology* *125*, 1060-1076.
- Bonecchi, R., Locati, M., Galliera, E., Vulcano, M., Sironi, M., Fra, A. M., Gobbi, M., Vecchi, A., Sozzani, S., Haribabu, B., *et al.* (2004). Differential recognition and scavenging of native and truncated macrophage-derived chemokine (macrophage-derived chemokine/CC chemokine ligand 22) by the D6 decoy receptor. *J Immunol* *172*, 4972-4976.

Bowman, E. P., Campbell, J. J., Soler, D., Dong, Z., Manlongat, N., Picarella, D., Hardy, R. R., and Butcher, E. C. (2000). Developmental switches in chemokine response profiles during B cell differentiation and maturation. *J Exp Med* *191*, 1303-1318.

Bowman, E. P., Kuklin, N. A., Youngman, K. R., Lazarus, N. H., Kunkel, E. J., Pan, J., Greenberg, H. B., and Butcher, E. C. (2002). The intestinal chemokine thymus-expressed chemokine (CCL25) attracts IgA antibody-secreting cells. *J Exp Med* *195*, 269-275.

Braun, M., Wunderlin, M., Spieth, K., Knochel, W., Gierschik, P., and Moepps, B. (2002). *Xenopus laevis* Stromal cell-derived factor 1: conservation of structure and function during vertebrate development. *J Immunol* *168*, 2340-2347.

Breitfeld, D., Ohl, L., Kremmer, E., Ellwart, J., Sallusto, F., Lipp, M., and Forster, R. (2000). Follicular B helper T cells express CXC chemokine receptor 5, localize to B cell follicles, and support immunoglobulin production. *J Exp Med* *192*, 1545-1552.

Brint, E. K., Xu, D., Liu, H., Dunne, A., McKenzie, A. N., O'Neill, L. A., and Liew, F. Y. (2004). ST2 is an inhibitor of interleukin 1 receptor and Toll-like receptor 4 signaling and maintains endotoxin tolerance. *Nat Immunol* *5*, 373-379.

Campbell, D. J., and Butcher, E. C. (2002). Intestinal attraction: CCL25 functions in effector lymphocyte recruitment to the small intestine. *Journal of Clinical Investigation* *110*, 1079-1081.

Campbell, D. J., Kim, C. H., and Butcher, E. C. (2003). Chemokines in the systemic organization of immunity. *Immunol Rev* *195*, 58-71.

Campbell, J. J., Hedrick, J., Zlotnik, A., Siani, M. A., Thompson, D. A., and Butcher, E. C. (1998). Chemokines and the arrest of lymphocytes rolling under flow conditions. *Science* *279*, 381-384.

Cannon, D. C., and Wissler, R. W. (1965). Migration of spleen cells into the blood stream following antigen stimulation of the rat. *Nature* *207*, 654-655.

Carbone, R., Fre, S., Iannolo, G., Belleudi, F., Mancini, P., Pelicci, P. G., Torrisci, M. R., and Di Fiore, P. P. (1997). eps15 and eps15R are essential components of the endocytic pathway. *Cancer Res* *57*, 5498-5504.

Carlsen, H. S., Haraldsen, G., Brandtzaeg, P., and Baekkevold, E. S. (2005). Disparate lymphoid chemokine expression in mice and men: no evidence of CCL21 synthesis by human high endothelial venules. *Blood* *106*, 444-446

Casarosa, P., Bakker, R. A., Verzijl, D., Navis, M., Timmerman, H., Leurs, R., and Smit, M. J. (2001). Constitutive signaling of the human cytomegalovirus-encoded chemokine receptor US28. *J Biol Chem* *276*, 1133-1137.

Catalfamo, M., Karpova, T., McNally, J., Costes, S. V., Lockett, S. J., Bos, E., Peters, P. J., and Henkart, P. A. (2004). Human CD8<sup>+</sup> T cells store RANTES in a unique secretory compartment and release it rapidly after TcR stimulation. *Immunity* *20*, 219-230.

- Chaudhuri, A., Nielsen, S., Elkjaer, M. L., Zbrzezna, V., Fang, F., and Pogo, A. O. (1997). Detection of Duffy antigen in the plasma membranes and caveolae of vascular endothelial and epithelial cells of nonerythroid organs. *Blood* *89*, 701-712.
- Chaudhuri, A., Polyakova, J., Zbrzezna, V., Williams, K., Gulati, S., and Pogo, A. O. (1993). Cloning of glycoprotein D cDNA, which encodes the major subunit of the Duffy blood group system and the receptor for the *Plasmodium vivax* malaria parasite. *Proc Natl Acad Sci U S A* *90*, 10793-10797.
- Chen, S. C., Vassileva, G., Kinsley, D., Holzmann, S., Manfra, D., Wiekowski, M. T., Romani, N., and Lira, S. A. (2002). Ectopic expression of the murine chemokines CCL21a and CCL21b induces the formation of lymph node-like structures in pancreas, but not skin, of transgenic mice. *J Immunol* *168*, 1001-1008.
- Chini, B., and Parenti, M. (2004). G-protein coupled receptors in lipid rafts and caveolae: how, when and why do they go there? *J Mol Endocrinol* *32*, 325-338.
- Chintalacheruvu, S. R., Wang, J. X., Giaconia, J. M., and Venkataraman, C. (2005). An essential role for CCL3 in the development of collagen antibody-induced arthritis. *Immunol Lett* *100*, 202-204.
- Choi, Y. K., Yoon, B. I., Won, Y. S., Lee, C. H., Hyun, B. H., Kim, H. C., Oh, G. T., and Kim, D. Y. (2003). Cytokine responses in mice infected with *Clonorchis sinensis*. *Parasitol Res* *91*, 87-93.
- Christe, M., Rutti, B., and Brossard, M. (1999). Influence of the genetic background and parasite load of mice on the immune response developed against nymphs of *Ixodes ricinus*. *Parasitol Res* *85*, 557-561.
- Christopherson, K. W., Hood, A. F., Travers, J. B., Ramsey, H., and Hromas, R. A. (2003). Endothelial induction of the T-cell chemokine CCL21 in T-cell autoimmune diseases. *Blood* *101*, 801-806.
- Chung, C. W., Cooke, R. M., Proudfoot, A. E., and Wells, T. N. (1995). The three-dimensional solution structure of RANTES. *Biochemistry* *34*, 9307-9314.
- Cinamon, G., Matloubian, M., Lesneski, M. J., Xu, Y., Low, C., Lu, T., Proia, R. L., and Cyster, J. G. (2004). Sphingosine 1-phosphate receptor 1 promotes B cell localization in the splenic marginal zone. *Nat Immunol* *5*, 713-720.
- Clark-Lewis, I., Kim, K. S., Rajarathnam, K., Gong, J. H., Dewald, B., Moser, B., Baggiolini, M., and Sykes, B. D. (1995). Structure-activity relationships of chemokines. *J Leukoc Biol* *57*, 703-711.
- Clore, G. M., Appella, E., Yamada, M., Matsushima, K., and Gronenborn, A. M. (1990). Three-dimensional structure of interleukin 8 in solution. *Biochemistry* *29*, 1689-1696.
- Columba-Cabezas, S., Serafini, B., Ambrosini, E., and Aloisi, F. (2003). Lymphoid chemokines CCL19 and CCL21 are expressed in the central nervous system during experimental autoimmune encephalomyelitis: implications for the maintenance of chronic neuroinflammation. *Brain Pathol* *13*, 38-51.

- Colvin, B. L., Morelli, A. E., Logar, A. J., Lau, A. H., and Thomson, A. W. (2004). Comparative evaluation of CC chemokine-induced migration of murine CD8 $\alpha$ <sup>+</sup> and CD8 $\alpha$ <sup>-</sup> dendritic cells and their in vivo trafficking. *J Leukoc Biol* 75, 275-285.
- Combadiere, C., Ahuja, S. K., and Murphy, P. M. (1995). Cloning and functional expression of a human eosinophil CC chemokine receptor. *J Biol Chem* 270, 16491-16494.
- Comerford, I., and Nibbs, R. J. (2005). Post-translational control of chemokines: a role for decoy receptors? *Immunol Lett* 96, 163-174.
- Constantin, G., Majeed, M., Giagulli, C., Piccio, L., Kim, J. Y., Butcher, E. C., and Laudanna, C. (2000). Chemokines trigger immediate beta2 integrin affinity and mobility changes: differential regulation and roles in lymphocyte arrest under flow. *Immunity* 13, 759-769.
- Cook, D. N. (1996). The role of MIP-1 alpha in inflammation and hematopoiesis. *J Leukoc Biol* 59, 61-66.
- Corry, D. B., Rishi, K., Kanellis, J., Kiss, A., Song Lz, L. Z., Xu, J., Feng, L., Werb, Z., and Kheradmand, F. (2002). Decreased allergic lung inflammatory cell egression and increased susceptibility to asphyxiation in MMP2-deficiency. *Nat Immunol* 3, 347-353.
- Couet, J., Sargiacomo, M., and Lisanti, M. P. (1997). Interaction of a receptor tyrosine kinase, EGF-R, with caveolins. Caveolin binding negatively regulates tyrosine and serine/threonine kinase activities. *J Biol Chem* 272, 30429-30438.
- Cronshaw, D. G., Owen, C., Brown, Z., and Ward, S. G. (2004). Activation of phosphoinositide 3-kinases by the CCR4 ligand macrophage-derived chemokine is a dispensable signal for T lymphocyte chemotaxis. *J Immunol* 172, 7761-7770.
- Crump, M. P., Gong, J. H., Loetscher, P., Rajarathnam, K., Amara, A., Arenzana-Seisdedos, F., Virelizier, J. L., Baggiolini, M., Sykes, B. D., and Clark-Lewis, I. (1997). Solution structure and basis for functional activity of stromal cell-derived factor-1; dissociation of CXCR4 activation from binding and inhibition of HIV-1. *Embo J* 16, 6996-7007.
- Cyster, J. G., and Goodnow, C. C. (1995). Pertussis toxin inhibits migration of B and T lymphocytes into splenic white pulp cords. *J Exp Med* 182, 581-586.
- D'Apuzzo, M., Rolink, A., Loetscher, M., Hoxie, J. A., Clark-Lewis, I., Melchers, F., Baggiolini, M., and Moser, B. (1997). The chemokine SDF-1, stromal cell-derived factor 1, attracts early stage B cell precursors via the chemokine receptor CXCR4. *Eur J Immunol* 27, 1788-1793.
- Darbonne, W. C., Rice, G. C., Mohler, M. A., Apple, T., Hebert, C. A., Valente, A. J., and Baker, J. B. (1991). Red blood cells are a sink for interleukin 8, a leukocyte chemotaxin. *J Clin Invest* 88, 1362-1369.
- Davatelis, G., Tekamp-Olson, P., Wolpe, S. D., Hermsen, K., Luedke, C., Gallegos, C., Coit, D., Merryweather, J., and Cerami, A. (1988). Cloning and characterization of a cDNA for murine macrophage inflammatory protein (MIP), a novel monokine with inflammatory and chemokinetic properties. *J Exp Med* 167, 1939-1944.

- Dawson, T. C., Lentsch, A. B., Wang, Z., Cowhig, J. E., Rot, A., Maeda, N., and Peiper, S. C. (2000). Exaggerated response to endotoxin in mice lacking the Duffy antigen/receptor for chemokines (DARC). *Blood* *96*, 1681-1684.
- de la Torre, Y. M., Locati, M., Buracchi, C., Dupor, J., Cook, D. N., Bonecchi, R., Nebuloni, M., Rukavina, D., Vago, L., Vecchi, A., *et al.* (2005). Increased inflammation in mice deficient for the chemokine decoy receptor D6. *Eur J Immunol* *35*, 1342-1346.
- Del Prete, A., Vermi, W., Dander, E., Otero, K., Barberis, L., Luini, W., Bernasconi, S., Sironi, M., Santoro, A., Garlanda, C., *et al.* (2004). Defective dendritic cell migration and activation of adaptive immunity in PI3Kgamma-deficient mice. *Embo J* *23*, 3505-3515.
- Dorf, M. E., Berman, M. A., Tanabe, S., Heesen, M., and Luo, Y. (2000). Astrocytes express functional chemokine receptors. *Journal of Neuroimmunology* *111*, 109-121.
- Droese, J., Mokros, T., Hermosilla, R., Schulein, R., Lipp, M., Hopken, U. E., and Rehm, A. (2004). HCMV-encoded chemokine receptor US28 employs multiple routes for internalization. *Biochem Biophys Res Commun* *322*, 42-49.
- Du, J., Luan, J., Liu, H., Daniel, T. O., Peiper, S., Chen, T. S., Yu, Y., Horton, L. W., Nanney, L. B., Strieter, R. M., and Richmond, A. (2002). Potential role for Duffy antigen chemokine-binding protein in angiogenesis and maintenance of homeostasis in response to stress. *J Leukoc Biol* *71*, 141-153.
- Dzenko, K. A., Andjelkovic, A. V., Kuziel, W. A., and Pachter, J. S. (2001). The chemokine receptor CCR2 mediates the binding and internalization of monocyte chemoattractant protein-1 along brain microvessels. *J Neurosci* *21*, 9214-9223.
- Ebert, L. M., Schaerli, P., and Moser, B. (2005). Chemokine-mediated control of T cell traffic in lymphoid and peripheral tissues. *Mol Immunol* *42*, 799-809.
- Ebisuno, Y., Tanaka, T., Kanemitsu, N., Kanda, H., Yamaguchi, K., Kaisho, T., Akira, S., and Miyasaka, M. (2003). Cutting edge: the B cell chemokine CXC chemokine ligand 13/B lymphocyte chemoattractant is expressed in the high endothelial venules of lymph nodes and Peyer's patches and affects B cell trafficking across high endothelial venules. *J Immunol* *171*, 1642-1646.
- Ellyard, J. I., Avery, D. T., Mackay, C. R., and Tangye, S. G. (2005). Contribution of stromal cells to the migration, function and retention of plasma cells in human spleen: potential roles of CXCL12, IL-6 and CD54. *Eur J Immunol* *35*, 699-708.
- Elves, M. W. (1970). Migration of small lymphocytes from the skin to the regional lymph nodes. *Nature* *227*, 725-727.
- Endres, M. J., Garlisi, C. G., Xiao, H., Shan, L., and Hedrick, J. A. (1999). The Kaposi's sarcoma-related herpesvirus (KSHV)-encoded chemokine vMIP-I is a specific agonist for the CC chemokine receptor (CCR)8. *J Exp Med* *189*, 1993-1998.
- Engeman, T. M., Gorbachev, A. V., Gladue, R. P., Heeger, P. S., and Fairchild, R. L. (2000). Inhibition of functional T cell priming and contact hypersensitivity responses by treatment with anti-secondary lymphoid chemokine antibody during hapten sensitization. *J Immunol* *164*, 5207-5214.

- Escrive, M., Burgueno, J., Ciruela, F., Canela, E. I., Mallol, J., Enrich, C., Lluís, C., and Franco, R. (2003). Ligand-induced caveolae-mediated internalization of A1 adenosine receptors: morphological evidence of endosomal sorting and receptor recycling. *Exp Cell Res* 285, 72-90.
- Fan, G. H., Lapierre, L. A., Goldenring, J. R., and Richmond, A. (2003). Differential regulation of CXCR2 trafficking by Rab GTPases. *Blood* 101, 2115-2124.
- Flanagan, K., Moroziewicz, D., Kwak, H., Horig, H., and Kaufman, H. L. (2004). The lymphoid chemokine CCL21 costimulates naive T cell expansion and Th1 polarization of non-regulatory CD4(+) T cells. *Cell Immunol* 231, 75-84.
- Fleischer, B. (1994). CD26: a surface protease involved in T-cell activation. *Immunol Today* 15, 180-184.
- Forster, R., Mattis, A. E., Kremmer, E., Wolf, E., Brem, G., and Lipp, M. (1996). A putative chemokine receptor, BLR1, directs B cell migration to defined lymphoid organs and specific anatomic compartments of the spleen. *Cell* 87, 1037-1047.
- Forster, R., Schubel, A., Breitfeld, D., Kremmer, E., Renner-Müller, I., Wolf, E., and Lipp, M. (1999). CCR7 coordinates the primary immune response by establishing functional microenvironments in secondary lymphoid organs. *Cell* 99, 23-33.
- Fra, A. M., Locati, M., Otero, K., Sironi, M., Signorelli, P., Massardi, M. L., Gobbi, M., Vecchi, A., Sozzani, S., and Mantovani, A. (2003). Cutting edge: scavenging of inflammatory CC chemokines by the promiscuous putatively silent chemokine receptor D6. *J Immunol* 170, 2279-2282.
- Fraile-Ramos, A., Kledal, T. N., Pelchen-Matthews, A., Bowers, K., Schwartz, T. W., and Marsh, M. (2001). The human cytomegalovirus US28 protein is located in endocytic vesicles and undergoes constitutive endocytosis and recycling. *Mol Biol Cell* 12, 1737-1749.
- Fraile-Ramos, A., Kohout, T. A., Waldhoer, M., and Marsh, M. (2003). Endocytosis of the viral chemokine receptor US28 does not require beta-arrestins but is dependent on the clathrin-mediated pathway. *Traffic* 4, 243-253.
- Fukuma, N., Akimitsu, N., Hamamoto, H., Kusuhara, H., Sugiyama, Y., and Sekimizu, K. (2003). A role of the Duffy antigen for the maintenance of plasma chemokine concentrations. *Biochem Biophys Res Commun* 303, 137-139.
- Fulkerson, P. C., Zimmermann, N., Brandt, E. B., Muntel, E. E., Doepker, M. P., Kavanaugh, J. L., Mishra, A., Witte, D. P., Zhang, H., Farber, J. M., *et al.* (2004). Negative regulation of eosinophil recruitment to the lung by the chemokine monokine induced by IFN-gamma (Mig, CXCL9). *Proc Natl Acad Sci U S A* 101, 1987-1992.
- Gaborik, Z., Szaszak, M., Szidonya, L., Balla, B., Paku, S., Catt, K. J., Clark, A. J., and Hunyady, L. (2001). Beta-arrestin- and dynamin-dependent endocytosis of the AT1 angiotensin receptor. *Mol Pharmacol* 59, 239-247.
- Galliera, E., Jala, V. R., Trent, J. O., Bonocchi, R., Signorelli, P., Lefkowitz, R. J., Mantovani, A., Locati, M., and Haribabu, B. (2004). beta -arrestin dependent constitutive

internalization of the human chemokine decoy receptor D6. *J Biol Chem* 279, 25590-25597.

Gao, J. L., Kuhns, D. B., Tiffany, H. L., McDermott, D., Li, X., Francke, U., and Murphy, P. M. (1993). Structure and functional expression of the human macrophage inflammatory protein 1 alpha/RANTES receptor. *J Exp Med* 177, 1421-1427.

Garside, P., Ingulli, E., Merica, R. R., Johnson, J. G., Noelle, R. J., and Jenkins, M. K. (1998). Visualization of specific B and T lymphocyte interactions in the lymph node. *Science* 281, 96-99.

Ge, S., and Pachter, J. S. (2004). Caveolin-1 knockdown by small interfering RNA suppresses responses to the chemokine monocyte chemoattractant protein-1 by human astrocytes. *J Biol Chem* 279, 6688-6695.

Gerard, C. (2005). Inflammatory chemokines: tuned in, turned on, dropped out. *Nat Immunol* 6, 366-368.

Giagulli, C., Scarpini, E., Ottoboni, L., Narumiya, S., Butcher, E. C., Constantin, G., and Laudanna, C. (2004). RhoA and zeta PKC control distinct modalities of LFA-1 activation by chemokines: critical role of LFA-1 affinity triggering in lymphocyte in vivo homing. *Immunity* 20, 25-35.

Gimpl, G., Burger, K., and Fahrenholz, F. (1997). Cholesterol as modulator of receptor function. *Biochemistry* 36, 10959-10974.

Gines, S., Ciruela, F., Burgueno, J., Casado, V., Canela, E. I., Mallol, J., Lluís, C., and Franco, R. (2001). Involvement of caveolin in ligand-induced recruitment and internalization of A(1) adenosine receptor and adenosine deaminase in an epithelial cell line. *Mol Pharmacol* 59, 1314-1323.

Girard, J. P., Baekkevold, E. S., Yamanaka, T., Haraldsen, G., Brandtzaeg, P., and Amalric, F. (1999). Heterogeneity of endothelial cells: the specialized phenotype of human high endothelial venules characterized by suppression subtractive hybridization. *Am J Pathol* 155, 2043-2055.

Goldsby, R. A. (2003). *Immunology*, 5th edn (New York, W.H. Freeman).

Gonzalez, E., Kulkarni, H., Bolivar, H., Mangano, A., Sanchez, R., Catano, G., Nibbs, R. J., Freedman, B. I., Quinones, M. P., Bamshad, M. J., *et al.* (2005). The Influence of CCL3L1 Gene-Containing Segmental Duplications on HIV-1/AIDS Susceptibility. *Science* 307, 1434-1440.

Goodman, O. B., Jr., Krupnick, J. G., Santini, F., Gurevich, V. V., Penn, R. B., Gagnon, A. W., Keen, J. H., and Benovic, J. L. (1996). Beta-arrestin acts as a clathrin adaptor in endocytosis of the beta2-adrenergic receptor. *Nature* 383, 447-450.

Gortz, A., Nibbs, R. J. B., McLean, P., Jarmin, D., Lambie, W., Baird, J. W., and Graham, G. J. (2002). The chemokine ESkin/CCL27 displays novel modes of intracrine and paracrine function. *Journal of Immunology* 169, 1387-1394.

- Gosling, J., Dairaghi, D. J., Wang, Y., Hanley, M., Talbot, D., Miao, Z., and Schall, T. J. (2000). Cutting edge: identification of a novel chemokine receptor that binds dendritic cell- and T cell-active chemokines including ELC, SLC, and TECK. *Journal of Immunology* *164*, 2851-2856.
- Gough, P. J., Garton, K. J., Wille, P. T., Rychlewski, M., Dempsey, P. J., and Raines, E. W. (2004). A disintegrin and metalloproteinase 10-mediated cleavage and shedding regulates the cell surface expression of CXC chemokine ligand 16. *J Immunol* *172*, 3678-3685.
- Gowans, J. L. (1959). The recirculation of lymphocytes from blood to lymph in the rat. *J Physiol* *146*, 54-69.
- Grady, E. F., Bohm, S. K., and Bunnett, N. W. (1997). Turning off the signal: mechanisms that attenuate signaling by G protein-coupled receptors. *Am J Physiol* *273*, G586-601.
- Grant, A. J., Goddard, S., Ahmed-Choudhury, J., Reynolds, G., Jackson, D. G., Briskin, M., Wu, L., Hubscher, S. G., and Adams, D. H. (2002). Hepatic expression of secondary lymphoid chemokine (CCL21) promotes the development of portal-associated lymphoid tissue in chronic inflammatory liver disease. *Am J Pathol* *160*, 1445-1455.
- Gretz, J. E., Anderson, A. O., and Shaw, S. (1997). Cords, channels, corridors and conduits: critical architectural elements facilitating cell interactions in the lymph node cortex. *Immunol Rev* *156*, 11-24.
- Guan, E., Wang, J., and Norcross, M. A. (2004). Amino-terminal processing of MIP-1beta/CCL4 by CD26/dipeptidyl-peptidase IV. *J Cell Biochem* *92*, 53-64.
- Guan, E., Wang, J., Roderiquez, G., and Norcross, M. A. (2002). Natural truncation of the chemokine MIP-1 beta /CCL4 affects receptor specificity but not anti-HIV-1 activity. *J Biol Chem* *277*, 32348-32352.
- Gunn, M. D., Kyuwa, S., Tam, C., Kakiuchi, T., Matsuzawa, A., Williams, L. T., and Nakano, H. (1999). Mice lacking expression of secondary lymphoid organ chemokine have defects in lymphocyte homing and dendritic cell localization. *J Exp Med* *189*, 451-460.
- Hadley, T. J., Lu, Z. H., Wasniowska, K., Martin, A. W., Peiper, S. C., Hesselgesser, J., and Horuk, R. (1994). Postcapillary venule endothelial cells in kidney express a multispecific chemokine receptor that is structurally and functionally identical to the erythroid isoform, which is the Duffy blood group antigen. *J Clin Invest* *94*, 985-991.
- Haffner, C., Takei, K., Chen, H., Ringstad, N., Hudson, A., Butler, M. H., Salcini, A. E., Di Fiore, P. P., and De Camilli, P. (1997). Synaptotagmin 1: localization on coated endocytic intermediates in nerve terminals and interaction of its 170 kDa isoform with Eps15. *FEBS Lett* *419*, 175-180.
- Hardy, R. R., and Hayakawa, K. (2001). B cell development pathways. *Annu Rev Immunol* *19*, 595-621.
- Hargreaves, D. C., Hyman, P. L., Lu, T. T., Ngo, V. N., Bidgol, A., Suzuki, G., Zou, Y. R., Littman, D. R., and Cyster, J. G. (2001). A coordinated change in chemokine responsiveness guides plasma cell movements. *J Exp Med* *194*, 45-56.

- Henley, J. R., Krueger, E. W., Oswald, B. J., and McNiven, M. A. (1998). Dynamically mediated internalization of caveolae. *J Cell Biol* *141*, 85-99.
- Hernandez-Lopez, C., Varas, A., Sacedon, R., Jimenez, E., Munoz, J. J., Zapata, A. G., and Vicente, A. (2002). Stromal cell-derived factor 1/CXCR4 signaling is critical for early human T-cell development. *Blood* *99*, 546-554.
- Hess, C., Means, T. K., Autissier, P., Woodberry, T., Altfeld, M., Addo, M. M., Frahm, N., Brander, C., Walker, B. D., and Luster, A. D. (2004). IL-8 responsiveness defines a subset of CD8 T cells poised to kill. *Blood* *104*, 3463-3471.
- Hjelmstrom, P. (2001). Lymphoid neogenesis: de novo formation of lymphoid tissue in chronic inflammation through expression of homing chemokines. *J Leukoc Biol* *69*, 331-339.
- Holmes, W. E., Lee, J., Kuang, W. J., Rice, G. C., and Wood, W. I. (1991). Structure and functional expression of a human interleukin-8 receptor. *Science* *253*, 1278-1280.
- Homey, B., Alenius, H., Muller, A., Soto, H., Bowman, E. P., Yuan, W., McEvoy, L., Lauerma, A. I., Assmann, T., Bunemann, E., *et al.* (2002). CCL27-CCR10 interactions regulate T cell-mediated skin inflammation. *Nat Med* *8*, 157-165.
- Honda, K., Nakano, H., Yoshida, H., Nishikawa, S., Rennert, P., Ikuta, K., Tamechika, M., Yamaguchi, K., Fukumoto, T., Chiba, T., and Nishikawa, S. I. (2001). Molecular basis for hematopoietic/mesenchymal interaction during initiation of Peyer's patch organogenesis. *J Exp Med* *193*, 621-630.
- Hoover, D. M., Mizoue, L. S., Handel, T. M., and Lubkowski, J. (2000). The crystal structure of the chemokine domain of fractalkine shows a novel quaternary arrangement. *J Biol Chem* *275*, 23187-23193.
- Horuk, R. (1994). Molecular properties of the chemokine receptor family. *Trends Pharmacol Sci* *15*, 159-165.
- Horuk, R., Chitnis, C. E., Darbonne, W. C., Colby, T. J., Rybicki, A., Hadley, T. J., and Miller, L. H. (1993). A receptor for the malarial parasite *Plasmodium vivax*: the erythrocyte chemokine receptor. *Science* *261*, 1182-1184.
- Hosoe, N., Miura, S., Watanabe, C., Tsuzuki, Y., Hokari, R., Oyama, T., Fujiyama, Y., Nagata, H., and Ishii, H. (2004). Demonstration of functional role of TECK/CCL25 in T lymphocyte-endothelium interaction in inflamed and uninfamed intestinal mucosa. *Am J Physiol Gastrointest Liver Physiol* *286*, G458-466.
- Huang, D. R., Wang, J., Kivisakk, P., Rollins, B. J., and Ransohoff, R. M. (2001). Absence of monocyte chemoattractant protein 1 in mice leads to decreased local macrophage recruitment and antigen-specific T helper cell type 1 immune response in experimental autoimmune encephalomyelitis. *J Exp Med* *193*, 713-726.
- Hub, E., and Rot, A. (1998). Binding of RANTES, MCP-1, MCP-3, and MIP-1 alpha to cells in human skin. *Am J Pathol* *152*, 749-757.

- Huising, M. O., Stet, R. J., Kruiswijk, C. P., Savelkoul, H. F., and Lidy Verburg-van Kemenade, B. M. (2003). Molecular evolution of CXC chemokines: extant CXC chemokines originate from the CNS. *Trends Immunol* 24, 307-313.
- Huising, M. O., van der Meulen, T., Flik, G., and Verburg-van Kemenade, B. M. (2004). Three novel carp CXC chemokines are expressed early in ontogeny and at nonimmune sites. *Eur J Biochem* 271, 4094-4106.
- Hundhausen, C., Misztela, D., Berkhout, T. A., Broadway, N., Saftig, P., Reiss, K., Hartmann, D., Fahrenholz, F., Postina, R., Matthews, V., *et al.* (2003). The disintegrin-like metalloproteinase ADAM10 is involved in constitutive cleavage of CX3CL1 (fractalkine) and regulates CX3CL1-mediated cell-cell adhesion. *Blood* 102, 1186-1195.
- Imai, T., Chantry, D., Raport, C. J., Wood, C. L., Nishimura, M., Godiska, R., Yoshie, O., and Gray, P. W. (1998). Macrophage-derived chemokine is a functional ligand for the CC chemokine receptor 4. *J Biol Chem* 273, 1764-1768.
- James, M. J., Belaramani, L., Prodromidou, K., Datta, A., Nourshargh, S., Lombardi, G., Dyson, J., Scott, D., Simpson, E., Cardozo, L., *et al.* (2003). Anergic T cells exert antigen-independent inhibition of cell-cell interactions via chemokine metabolism. *Blood* 102, 2173-2179.
- Jamieson, T., Cook, D. N., Nibbs, R. J., Rot, A., Nixon, C., McLean, P., Alcami, A., Lira, S. A., Wiekowski, M., and Graham, G. J. (2005). The chemokine receptor D6 limits the inflammatory response in vivo. *Nat Immunol* 6, 403-411
- Janeway, C., and Travers, P. (1997). *Immunobiology : the immune system in health and disease*, 3rd edn (London ; San Francisco; New York, Current Biology ; Garland Pub.).
- Jilma-Stohlawetz, P., Homoncik, M., Drucker, C., Marsik, C., Rot, A., Mayr, W. R., Seibold, B., and Jilma, B. (2001). Fy phenotype and gender determine plasma levels of monocyte chemotactic protein. *Transfusion* 41, 378-381.
- Johansson-Lindbom, B., Svensson, M., Wurbel, M. A., Malissen, B., Marquez, G., and Agace, W. (2003). Selective generation of gut tropic T cells in gut-associated lymphoid tissue (GALT): requirement for GALT dendritic cells and adjuvant. *J Exp Med* 198, 963-969.
- Jung, S., Aliberti, J., Graemmel, P., Sunshine, M. J., Kreutzberg, G. W., Sher, A., and Littman, D. R. (2000). Analysis of fractalkine receptor CX(3)CR1 function by targeted deletion and green fluorescent protein reporter gene insertion. *Mol Cell Biol* 20, 4106-4114.
- Junt, T., Scandella, E., Forster, R., Krebs, P., Krautwald, S., Lipp, M., Hengartner, H., and Ludewig, B. (2004). Impact of CCR7 on priming and distribution of antiviral effector and memory CTL. *J Immunol* 173, 6684-6693.
- Karlsson, M. C., Guinamard, R., Bolland, S., Sankala, M., Steinman, R. M., and Ravetch, J. V. (2003). Macrophages control the retention and trafficking of B lymphocytes in the splenic marginal zone. *J Exp Med* 198, 333-340.

- Khoja, H., Wang, G., Ng, C. T., Tucker, J., Brown, T., and Shyamala, V. (2000). Cloning of CCRL1, an orphan seven transmembrane receptor related to chemokine receptors, expressed abundantly in the heart. *Gene* 246, 229-238.
- Kienzle, N., Baz, A., and Kelso, A. (2004). Profiling the CD8<sup>low</sup> phenotype, an alternative career choice for CD8 T cells during primary differentiation. *Immunol Cell Biol* 82, 75-83.
- Kienzle, N., Olver, S., Buttigieg, K., Groves, P., Janas, M. L., Baz, A., and Kelso, A. (2005). Progressive differentiation and commitment of CD8<sup>+</sup> T cells to a poorly cytolytic CD8<sup>low</sup> phenotype in the presence of IL-4. *J Immunol* 174, 2021-2029.
- Kim, C. H., Pelus, L. M., Appelbaum, E., Johanson, K., Anzai, N., and Broxmeyer, H. E. (1999). CCR7 ligands, SLC/6CKine/Exodus2/TCA4 and CKbeta-11/MIP-3beta/ELC, are chemoattractants for CD56(+)CD16(-) NK cells and late stage lymphoid progenitors. *Cell Immunol* 193, 226-235.
- Kim, C. H., Pelus, L. M., White, J. R., and Broxmeyer, H. E. (1998). Macrophage-inflammatory protein-3 beta/EBI1-ligand chemokine/CK beta-11, a CC chemokine, is a chemoattractant with a specificity for macrophage progenitors among myeloid progenitor cells. *J Immunol* 161, 2580-2585.
- Kledal, T. N., Rosenkilde, M. M., Coulin, F., Simmons, G., Johnsen, A. H., Alouani, S., Power, C. A., Lutichau, H. R., Gerstoft, J., Clapham, P. R., *et al.* (1997). A broad-spectrum chemokine antagonist encoded by Kaposi's sarcoma-associated herpesvirus. *Science* 277, 1656-1659.
- Koch, A. E., Volin, M. V., Woods, J. M., Kunkel, S. L., Connors, M. A., Harlow, L. A., Woodruff, D. C., Burdick, M. D., and Strieter, R. M. (2001). Regulation of angiogenesis by the C-X-C chemokines interleukin-8 and epithelial neutrophil activating peptide 78 in the rheumatoid joint. *Arthritis Rheum* 44, 31-40.
- Kohout, T. A., Nicholas, S. L., Perry, S. J., Reinhart, G., Junger, S., and Struthers, R. S. (2004). Differential desensitization, receptor phosphorylation, beta-arrestin recruitment, and ERK1/2 activation by the two endogenous ligands for the CC chemokine receptor 7. *J Biol Chem* 279, 23214-23222.
- Kronin, V., Fitzmaurice, C. J., Caminschi, I., Shortman, K., Jackson, D. C., and Brown, L. E. (2001). Differential effect of CD8(+) and CD8(-) dendritic cells in the stimulation of secondary CD4(+) T cells. *Int Immunol* 13, 465-473.
- Kronin, V., Winkel, K., Suss, G., Kelso, A., Heath, W., Kirberg, J., von Boehmer, H., and Shortman, K. (1996). A subclass of dendritic cells regulates the response of naive CD8 T cells by limiting their IL-2 production. *J Immunol* 157, 3819-3827.
- Kryczek, I., Lange, A., Mottram, P., Alvarez, X., Cheng, P., Hogan, M., Moons, L., Wei, S., Zou, L., Machelon, V., *et al.* (2005). CXCL12 and vascular endothelial growth factor synergistically induce neoangiogenesis in human ovarian cancers. *Cancer Res* 65, 465-472.
- Kucharzik, T., Hudson, J. T., 3rd, Waikel, R. L., Martin, W. D., and Williams, I. R. (2002). CCR6 expression distinguishes mouse myeloid and lymphoid dendritic cell subsets: demonstration using a CCR6 EGFP knock-in mouse. *Eur J Immunol* 32, 104-112.

- Kunkel, E. J., and Butcher, E. C. (2002). Chemokines and the tissue-specific migration of lymphocytes. *Immunity* *16*, 1-4.
- Kunkel, E. J., Campbell, J. J., Haraldsen, G., Pan, J., Boisvert, J., Roberts, A. I., Ebert, E. C., Vierra, M. A., Goodman, S. B., Genovese, M. C., *et al.* (2000). Lymphocyte CC chemokine receptor 9 and epithelial thymus-expressed chemokine (TECK) expression distinguish the small intestinal immune compartment: Epithelial expression of tissue-specific chemokines as an organizing principle in regional immunity. *J Exp Med* *192*, 761-768.
- Kunkel, E. J., Kim, C. H., Lazarus, N. H., Vierra, M. A., Soler, D., Bowman, E. P., and Butcher, E. C. (2003). CCR10 expression is a common feature of circulating and mucosal epithelial tissue IgA Ab-secreting cells. *J Clin Invest* *111*, 1001-1010.
- Kuschert, G. S., Coulin, F., Power, C. A., Proudfoot, A. E., Hubbard, R. E., Hoogewerf, A. J., and Wells, T. N. (1999). Glycosaminoglycans interact selectively with chemokines and modulate receptor binding and cellular responses. *Biochemistry* *38*, 12959-12968.
- Ladant, D., and Ullmann, A. (1999). Bordetella pertussis adenylate cyclase: a toxin with multiple talents. *Trends Microbiol* *7*, 172-176.
- Lakkis, F. G., Arakelov, A., Konieczny, B. T., and Inoue, Y. (2000). Immunologic 'ignorance' of vascularized organ transplants in the absence of secondary lymphoid tissue. *Nat Med* *6*, 686-688.
- Lalani, A. S., Graham, K., Mossman, K., Rajarathnam, K., Clark-Lewis, I., Kelvin, D., and McFadden, G. (1997). The purified myxoma virus gamma interferon receptor homolog M-T7 interacts with the heparin-binding domains of chemokines. *J Virol* *71*, 4356-4363.
- Lambeir, A. M., Proost, P., Durinx, C., Bal, G., Senten, K., Augustyns, K., Scharpe, S., Van Damme, J., and De Meester, I. (2001). Kinetic investigation of chemokine truncation by CD26/dipeptidyl peptidase IV reveals a striking selectivity within the chemokine family. *J Biol Chem* *276*, 29839-29845.
- Lance, E. M., and Taub, R. N. (1969). Segregation of lymphocyte populations through differential migration. *Nature* *221*, 841-843.
- Laporte, S. A., Oakley, R. H., Zhang, J., Holt, J. A., Ferguson, S. S., Caron, M. G., and Barak, L. S. (1999). The beta2-adrenergic receptor/betaarrestin complex recruits the clathrin adaptor AP-2 during endocytosis. *Proc Natl Acad Sci U S A* *96*, 3712-3717.
- Le, P. U., Guay, G., Altschuler, Y., and Nabi, I. R. (2002). Caveolin-1 is a negative regulator of caveolae-mediated endocytosis to the endoplasmic reticulum. *J Biol Chem* *277*, 3371-3379.
- Le, Y., Honczarenko, M., Glodek, A. M., Ho, D. K., and Silberstein, L. E. (2005). CXC chemokine ligand 12-induced focal adhesion kinase activation and segregation into membrane domains is modulated by regulator of G protein signaling 1 in pro-B cells. *J Immunol* *174*, 2582-2590.
- Lee, J. S., Frevert, C. W., Thorning, D. R., Segerer, S., Alpers, C. E., Cartron, J. P., Colin, Y., Wong, V. A., Martin, T. R., and Goodman, R. B. (2003a). Enhanced expression of

- Duffy antigen in the lungs during suppurative pneumonia. *J Histochem Cytochem* 51, 159-166.
- Lee, J. S., Frevert, C. W., Wurfel, M. M., Peiper, S. C., Wong, V. A., Ballman, K. K., Ruzinski, J. T., Rhim, J. S., Martin, T. R., and Goodman, R. B. (2003b). Duffy antigen facilitates movement of chemokine across the endothelium in vitro and promotes neutrophil transmigration in vitro and in vivo. *J Immunol* 170, 5244-5251.
- Lefkowitz, R. J., and Shenoy, S. K. (2005). Transduction of receptor signals by beta-arrestins. *Science* 308, 512-517.
- Li, Q., Park, P. W., Wilson, C. L., and Parks, W. C. (2002). Matrilysin shedding of syndecan-1 regulates chemokine mobilization and transepithelial efflux of neutrophils in acute lung injury. *Cell* 111, 635-646.
- Liston, A., and McColl, S. (2003). Subversion of the chemokine world by microbial pathogens. *Bioessays* 25, 478-488.
- Liu, C., Ueno, T., Kuse, S., Saito, F., Nitta, T., Piali, L., Nakano, H., Kakiuchi, T., Lipp, M., Hollander, G. A., and Takahama, Y. (2005). The role of CCL21 in recruitment of T-precursor cells to fetal thymi. *Blood* 105, 31-39.
- Loetscher, P., Pellegrino, A., Gong, J. H., Mattioli, I., Loetscher, M., Bardi, G., Baggiolini, M., and Clark-Lewis, I. (2001). The ligands of CXC chemokine receptor 3, I-TAC, Mig, and IP10, are natural antagonists for CCR3. *J Biol Chem* 276, 2986-2991.
- Lu, T. T., and Cyster, J. G. (2002). Integrin-mediated long-term B cell retention in the splenic marginal zone. *Science* 297, 409-412.
- Lubkowski, J., Bujacz, G., Boque, L., Domaille, P. J., Handel, T. M., and Wlodawer, A. (1997). The structure of MCP-1 in two crystal forms provides a rare example of variable quaternary interactions. *Nat Struct Biol* 4, 64-69.
- Ludwig, A., Schiemann, F., Mentlein, R., Lindner, B., and Brandt, E. (2002). Dipeptidyl peptidase IV (CD26) on T cells cleaves the CXC chemokine CXCL11 (I-TAC) and abolishes the stimulating but not the desensitizing potential of the chemokine. *J Leukoc Biol* 72, 183-191.
- Luo, H., Chaudhuri, A., Zbrzezna, V., He, Y., and Pogo, A. O. (2000). Deletion of the murine Duffy gene (*Dfy*) reveals that the Duffy receptor is functionally redundant. *Mol Cell Biol* 20, 3097-3101.
- Luther, S. A., Ansel, K. M., and Cyster, J. G. (2003). Overlapping roles of CXCL13, interleukin 7 receptor alpha, and CCR7 ligands in lymph node development. *J Exp Med* 197, 1191-1198.
- Luther, S. A., Bidgol, A., Hargreaves, D. C., Schmidt, A., Xu, Y., Paniyadi, J., Matloubian, M., and Cyster, J. G. (2002). Differing activities of homeostatic chemokines CCL19, CCL21, and CXCL12 in lymphocyte and dendritic cell recruitment and lymphoid neogenesis. *J Immunol* 169, 424-433.

- Luther, S. A., and Cyster, J. G. (2001). Chemokines as regulators of T cell differentiation. *Nature Immunology* 2, 102-107.
- Ma, Q., Jones, D., Borghesani, P. R., Segal, R. A., Nagasawa, T., Kishimoto, T., Bronson, R. T., and Springer, T. A. (1998). Impaired B-lymphopoiesis, myelopoiesis, and derailed cerebellar neuron migration in CXCR4- and SDF-1-deficient mice. *Proc Natl Acad Sci U S A* 95, 9448-9453.
- Ma, Q., Jones, D., and Springer, T. A. (1999). The chemokine receptor CXCR4 is required for the retention of B lineage and granulocytic precursors within the bone marrow microenvironment. *Immunity* 10, 463-471.
- Maldonado-Lopez, R., De Smedt, T., Pajak, B., Heirman, C., Thielemans, K., Leo, O., Urbain, J., Maliszewski, C. R., and Moser, M. (1999). Role of CD8alpha+ and CD8alpha-dendritic cells in the induction of primary immune responses in vivo. *J Leukoc Biol* 66, 242-246.
- Mandala, S., Hajdu, R., Bergstrom, J., Quackenbush, E., Xie, J., Milligan, J., Thornton, R., Shei, G. J., Card, D., Keohane, C., *et al.* (2002). Alteration of lymphocyte trafficking by sphingosine-1-phosphate receptor agonists. *Science* 296, 346-349.
- Mantovani, A. (1999). The chemokine system: redundancy for robust outputs. *Immunol Today* 20, 254-257.
- Mantovani, A., Locati, M., Polentarutti, N., Vecchi, A., and Garlanda, C. (2004). Extracellular and intracellular decoys in the tuning of inflammatory cytokines and Toll-like receptors: the new entry TIR8/SIGIRR. *J Leukoc Biol* 75, 738-742.
- Mantovani, A., Locati, M., Vecchi, A., Sozzani, S., and Allavena, P. (2001). Decoy receptors: a strategy to regulate inflammatory cytokines and chemokines. *Trends Immunol* 22, 328-336.
- Marsal, J., Svensson, M., Ericsson, A., Iranpour, A. H., Carramolino, L., Marquez, G., and Agace, W. W. (2002). Involvement of CCL25 (TECK) in the generation of the murine small-intestinal CD8alpha alpha+CD3+ intraepithelial lymphocyte compartment. *Eur J Immunol* 32, 3488-3497.
- Marsland, B. J., Battig, P., Bauer, M., Ruedl, C., Lassing, U., Beerli, R. R., Dietmeier, K., Ivanova, L., Pfister, T., Vogt, L., *et al.* (2005). CCL19 and CCL21 Induce a Potent Proinflammatory Differentiation Program in Licensed Dendritic Cells. *Immunity* 22, 493-505.
- Martin, S. P., and Chaudhuri, S. N. (1952). Effect of bacteria and their products on migration of leukocytes. *Proc Soc Exp Biol Med* 81, 286-288.
- Martin-Fontecha, A., Sebastiani, S., Hopken, U. E., Ugucioni, M., Lipp, M., Lanzavecchia, A., and Sallusto, F. (2003). Regulation of dendritic cell migration to the draining lymph node: impact on T lymphocyte traffic and priming. *J Exp Med* 198, 615-621.

- Matloubian, M., David, A., Engel, S., Ryan, J. E., and Cyster, J. G. (2000). A transmembrane CXC chemokine is a ligand for HIV-coreceptor Bonzo. *Nat Immunol* *1*, 298-304.
- Matloubian, M., Lo, C. G., Cinamon, G., Lesneski, M. J., Xu, Y., Brinkmann, V., Allende, M. L., Proia, R. L., and Cyster, J. G. (2004). Lymphocyte egress from thymus and peripheral lymphoid organs is dependent on S1P receptor 1. *Nature* *427*, 355-360.
- McLachlan, J. B., Hart, J. P., Pizzo, S. V., Shelburne, C. P., Staats, H. F., Gunn, M. D., and Abraham, S. N. (2003). Mast cell-derived tumor necrosis factor induces hypertrophy of draining lymph nodes during infection. *Nat Immunol* *4*, 1199-1205.
- McMillan, S. J., Kearley, J., Campbell, J. D., Zhu, X. W., Larbi, K. Y., Shipley, J. M., Senior, R. M., Nourshargh, S., and Lloyd, C. M. (2004). Matrix metalloproteinase-9 deficiency results in enhanced allergen-induced airway inflammation. *J Immunol* *172*, 2586-2594.
- McQuibban, G. A., Butler, G. S., Gong, J. H., Bendall, L., Power, C., Clark-Lewis, I., and Overall, C. M. (2001). Matrix metalloproteinase activity inactivates the CXC chemokine stromal cell-derived factor-1. *J Biol Chem* *276*, 43503-43508.
- McQuibban, G. A., Gong, J. H., Tam, E. M., McCulloch, C. A., Clark-Lewis, I., and Overall, C. M. (2000). Inflammation dampened by gelatinase A cleavage of monocyte chemoattractant protein-3. *Science* *289*, 1202-1206.
- McQuibban, G. A., Gong, J. H., Wong, J. P., Wallace, J. L., Clark-Lewis, I., and Overall, C. M. (2002). Matrix metalloproteinase processing of monocyte chemoattractant proteins generates CC chemokine receptor antagonists with anti-inflammatory properties in vivo. *Blood* *100*, 1160-1167.
- Mebius, R. E. (2003). Organogenesis of lymphoid tissues. *Nat Rev Immunol* *3*, 292-303.
- Mebius, R. E., Rennert, P., and Weissman, I. L. (1997). Developing lymph nodes collect CD4<sup>+</sup>CD3<sup>-</sup>LTβ<sup>+</sup> cells that can differentiate to APC, NK cells, and follicular cells but not T or B cells. *Immunity* *7*, 493-504.
- Middleton, J., Neil, S., Wintle, J., Clark-Lewis, I., Moore, H., Lam, C., Auer, M., Hub, E., and Rot, A. (1997). Transcytosis and surface presentation of IL-8 by venular endothelial cells. *Cell* *91*, 385-395.
- Miller, L. H., Mason, S. J., Dvorak, J. A., McGinniss, M. H., and Rothman, I. K. (1975). Erythrocyte receptors for (*Plasmodium knowlesi*) malaria: Duffy blood group determinants. *Science* *189*, 561-563.
- Minshall, R. D., Tirupathi, C., Vogel, S. M., Niles, W. D., Gilchrist, A., Hamm, H. E., and Malik, A. B. (2000). Endothelial cell-surface gp60 activates vesicle formation and trafficking via G(i)-coupled Src kinase signaling pathway. *J Cell Biol* *150*, 1057-1070.
- Misslitz, A., Pabst, O., Hintzen, G., Ohl, L., Kremmer, E., Petrie, H. T., and Forster, R. (2004). Thymic T cell development and progenitor localization depend on CCR7. *J Exp Med* *200*, 481-491.

- Miyawaki, S., Nakamura, Y., Suzuka, H., Koba, M., Yasumizu, R., Ikehara, S., and Shibata, Y. (1994). A new mutation, *aly*, that induces a generalized lack of lymph nodes accompanied by immunodeficiency in mice. *Eur J Immunol* *24*, 429-434.
- Mokros, T., Rehm, A., Droese, J., Oppermann, M., Lipp, M., and Hopken, U. E. (2002). Surface expression and endocytosis of the human cytomegalovirus-encoded chemokine receptor US28 is regulated by agonist-independent phosphorylation. *J Biol Chem* *277*, 45122-45128.
- Moratz, C., Harrison, K., and Kehrl, J. H. (2004). Regulation of chemokine-induced lymphocyte migration by RGS proteins. *Methods Enzymol* *389*, 15-32.
- Moratz, C., Kang, V. H., Druet, K. M., Shi, C. S., Scheschonka, A., Murphy, P. M., Kozasa, T., and Kehrl, J. H. (2000). Regulator of G protein signaling 1 (RGS1) markedly impairs Gi alpha signaling responses of B lymphocytes. *J Immunol* *164*, 1829-1838.
- Mori, S., Nakano, H., Aritomi, K., Wang, C. R., Gunn, M. D., and Kakiuchi, T. (2001). Mice lacking expression of the chemokines CCL21-ser and CCL19 (plt mice) demonstrate delayed but enhanced T cell immune responses. *J Exp Med* *193*, 207-218.
- Moriguchi, M., Hissong, B. D., Gadina, M., Yamaoka, K., Tiffany, H. L., Murphy, P. M., Candotti, F., and O'Shea, J. J. (2005). CXCL12 signaling is independent of Jak2 and Jak3. *J Biol Chem* *280*, 17408-17414.
- Moser, B., and Loetscher, P. (2001). Lymphocyte traffic control by chemokines. *Nature Immunology* *2*, 123-128.
- Mowat, A. M. (2003). Anatomical basis of tolerance and immunity to intestinal antigens. *Nat Rev Immunol* *3*, 331-341.
- Mueller, A., and Strange, P. G. (2004). CCL3, acting via the chemokine receptor CCR5, leads to independent activation of Janus kinase 2 (JAK2) and Gi proteins. *FEBS Lett* *570*, 126-132.
- Muller, G., Hopken, U. E., and Lipp, M. (2003). The impact of CCR7 and CXCR5 on lymphoid organ development and systemic immunity. *Immunol Rev* *195*, 117-135.
- Mummidi, S., Ahuja, S. S., Gonzalez, E., Anderson, S. A., Santiago, E. N., Stephan, K. T., Craig, F. E., O'Connell, P., Tryon, V., Clark, R. A., *et al.* (1998). Genealogy of the CCR5 locus and chemokine system gene variants associated with altered rates of HIV-1 disease progression. *Nat Med* *4*, 786-793.
- Murphy, P. M. (2002). International Union of Pharmacology. XXX. Update on chemokine receptor nomenclature. *Pharmacological Reviews* *54*, 227-229.
- Murphy, P. M., Baggiolini, M., Charo, I. F., Hebert, C. A., Horuk, R., Matsushima, K., Miller, L. H., Oppenheim, J. J., and Power, C. A. (2000). International union of pharmacology. XXII. Nomenclature for chemokine receptors. *Pharmacol Rev* *52*, 145-176.
- Murphy, P. M., and Tiffany, H. L. (1991). Cloning of complementary DNA encoding a functional human interleukin-8 receptor. *Science* *253*, 1280-1283.

- Nabi, I. R., and Le, P. U. (2003). Caveolae/raft-dependent endocytosis. *J Cell Biol* *161*, 673-677.
- Nagasawa, T., Hirota, S., Tachibana, K., Takakura, N., Nishikawa, S., Kitamura, Y., Yoshida, N., Kikutani, H., and Kishimoto, T. (1996). Defects of B-cell lymphopoiesis and bone-marrow myelopoiesis in mice lacking the CXC chemokine PBSF/SDF-1. *Nature* *382*, 635-638.
- Nakano, H., and Gunn, M. D. (2001). Gene duplications at the chemokine locus on mouse chromosome 4: multiple strain-specific haplotypes and the deletion of secondary lymphoid-organ chemokine and EBI-1 ligand chemokine genes in the *plt* mutation. *J Immunol* *166*, 361-369.
- Nakano, H., Tamura, T., Yoshimoto, T., Yagita, H., Miyasaka, M., Butcher, E. C., Nariuchi, H., Kakiuchi, T., and Matsuzawa, A. (1997). Genetic defect in T lymphocyte-specific homing into peripheral lymph nodes. *Eur J Immunol* *27*, 215-221.
- Nakayama, T., Fujisawa, R., Yamada, H., Horikawa, T., Kawasaki, H., Hieshima, K., Izawa, D., Fujiie, S., Tezuka, T., and Yoshie, O. (2001). Inducible expression of a CC chemokine liver- and activation-regulated chemokine (LARC)/macrophage inflammatory protein (MIP)-3 alpha/CCL20 by epidermal keratinocytes and its role in atopic dermatitis. *Int Immunol* *13*, 95-103.
- Neote, K., Darbonne, W., Ogez, J., Horuk, R., and Schall, T. J. (1993). Identification of a promiscuous inflammatory peptide receptor on the surface of red blood cells. *J Biol Chem* *268*, 12247-12249.
- Neote, K., Mak, J. Y., Kolakowski, L. F., Jr., and Schall, T. J. (1994). Functional and biochemical analysis of the cloned Duffy antigen: identity with the red blood cell chemokine receptor. *Blood* *84*, 44-52.
- Nguyen, D. H., and Taub, D. (2002). Cholesterol is essential for macrophage inflammatory protein 1 beta binding and conformational integrity of CC chemokine receptor 5. *Blood* *99*, 4298-4306.
- Nibbs, R., Graham, G., and Rot, A. (2003). Chemokines on the move: control by the chemokine "interceptors" Duffy blood group antigen and D6. *Seminars in Immunology* *15*, 287-294.
- Nibbs, R. J., Kriehuber, E., Ponath, P. D., Parent, D., Qin, S., Campbell, J. D., Henderson, A., Kerjaschki, D., Maurer, D., Graham, G. J., and Rot, A. (2001). The beta-chemokine receptor D6 is expressed by lymphatic endothelium and a subset of vascular tumors. *American Journal of Pathology* *158*, 867-877.
- Nibbs, R. J., Wylie, S. M., Yang, J., Landau, N. R., and Graham, G. J. (1997). Cloning and characterization of a novel promiscuous human beta-chemokine receptor D6. *Journal of Biological Chemistry* *272*, 32078-32083.
- Nibbs, R. J. B., Salcedo, T. W., Campbell, J. D. M., Yao, X. T., Li, Y. L., Nardelli, B., Olsen, H. S., Morris, T. S., Proudfoot, A. E. I., Patel, V. P., and Graham, G. J. (2000). C-C chemokine receptor 3 antagonism by the beta-chemokine macrophage inflammatory protein

- 4, a property strongly enhanced by an amino-terminal alanine-methionine swap. *Journal of Immunology* *164*, 1488-1497.
- Nichols, B. (2003). Caveosomes and endocytosis of lipid rafts. *J Cell Sci* *116*, 4707-4714.
- Niess, J. H., Brand, S., Gu, X., Landsman, L., Jung, S., McCormick, B. A., Vyas, J. M., Boes, M., Ploegh, H. L., Fox, J. G., *et al.* (2005). CX3CR1-mediated dendritic cell access to the intestinal lumen and bacterial clearance. *Science* *307*, 254-258.
- Nomiyama, H., Mera, A., Ohneda, O., Miura, R., Suda, T., and Yoshie, O. (2001). Organization of the chemokine genes in the human and mouse major clusters of CC and CXC chemokines: diversification between the two species. *Genes Immun* *2*, 110-113.
- Nomura, H., Nielsen, B. W., and Matsushima, K. (1993). Molecular cloning of cDNAs encoding a LD78 receptor and putative leukocyte chemotactic peptide receptors. *Int Immunol* *5*, 1239-1249.
- O'Garra, A., and Vieira, P. (2004). Regulatory T cells and mechanisms of immune system control. *Nat Med* *10*, 801-805.
- Ogilvie, P., Paoletti, S., Clark-Lewis, I., and Uguccioni, M. (2003). Eotaxin-3 is a natural antagonist for CCR2 and exerts a repulsive effect on human monocytes. *Blood* *102*, 789-794.
- Ogilvie, P., Thelen, S., Moepps, B., Gierschik, P., da Silva Campos, A. C., Baggiolini, M., and Thelen, M. (2004). Unusual chemokine receptor antagonism involving a mitogen-activated protein kinase pathway. *J Immunol* *172*, 6715-6722.
- Ohl, L., Henning, G., Krautwald, S., Lipp, M., Hardtke, S., Bernhardt, G., Pabst, O., and Forster, R. (2003). Cooperating mechanisms of CXCR5 and CCR7 in development and organization of secondary lymphoid organs. *J Exp Med* *197*, 1199-1204.
- Ohl, L., Mohaupt, M., Czeloth, N., Hintzen, G., Kiafard, Z., Zwirner, J., Blankenstein, T., Henning, G., and Forster, R. (2004). CCR7 governs skin dendritic cell migration under inflammatory and steady-state conditions. *Immunity* *21*, 279-288.
- Ohmori, Y., and Hamilton, T. A. (1990). A macrophage LPS-inducible early gene encodes the murine homologue of IP-10. *Biochem Biophys Res Commun* *168*, 1261-1267.
- Okada, T., Ngo, V. N., Ekland, E. H., Forster, R., Lipp, M., Littman, D. R., and Cyster, J. G. (2002). Chemokine requirements for B cell entry to lymph nodes and Peyer's patches. *J Exp Med* *196*, 65-75.
- Opdenakker, G., Van den Steen, P. E., Dubois, B., Nelissen, I., Van Coillie, E., Masure, S., Proost, P., and Van Damme, J. (2001). Gelatinase B functions as regulator and effector in leukocyte biology. *J Leukoc Biol* *69*, 851-859.
- Oynebraten, I., Bakke, O., Brandtzaeg, P., Johansen, F. E., and Haraldsen, G. (2004). Rapid chemokine secretion from endothelial cells originates from 2 distinct compartments. *Blood* *104*, 314-320.

- Palframan, R. T., Jung, S., Cheng, G., Weninger, W., Luo, Y., Dorf, M., Littman, D. R., Rollins, B. J., Zweerink, H., Rot, A., and von Andrian, U. H. (2001). Inflammatory chemokine transport and presentation in HEV: a remote control mechanism for monocyte recruitment to lymph nodes in inflamed tissues. *J Exp Med* *194*, 1361-1373.
- Parent, C. A. (2004). Making all the right moves: chemotaxis in neutrophils and Dictyostelium. *Curr Opin Cell Biol* *16*, 4-13.
- Parry, C. M., Simas, J. P., Smith, V. P., Stewart, C. A., Minson, A. C., Efstathiou, S., and Alcami, A. (2000). A broad spectrum secreted chemokine binding protein encoded by a herpesvirus. *J Exp Med* *191*, 573-578.
- Patterson, A. M., Siddall, H., Chamberlain, G., Gardner, L., and Middleton, J. (2002). Expression of the duffy antigen/receptor for chemokines (DARC) by the inflamed synovial endothelium. *J Pathol* *197*, 108-116.
- Pelkmans, L., Burli, T., Zerial, M., and Helenius, A. (2004). Caveolin-stabilized membrane domains as multifunctional transport and sorting devices in endocytic membrane traffic. *Cell* *118*, 767-780.
- Pelkmans, L., and Helenius, A. (2002). Endocytosis via caveolae. *Traffic* *3*, 311-320.
- Pelkmans, L., Kartenbeck, J., and Helenius, A. (2001). Caveolar endocytosis of simian virus 40 reveals a new two-step vesicular-transport pathway to the ER. *Nat Cell Biol* *3*, 473-483.
- Pelletier, A. J., van der Laan, L. J., Hildbrand, P., Siani, M. A., Thompson, D. A., Dawson, P. E., Torbett, B. E., and Salomon, D. R. (2000). Presentation of chemokine SDF-1 alpha by fibronectin mediates directed migration of T cells. *Blood* *96*, 2682-2690.
- Petit, I., Szyper-Kravitz, M., Nagler, A., Lahav, M., Peled, A., Habler, L., Ponomaryov, T., Taichman, R. S., Arenzana-Seisdedos, F., Fujii, N., *et al.* (2002). G-CSF induces stem cell mobilization by decreasing bone marrow SDF-1 and up-regulating CXCR4. *Nature Immunology* *3*, 687-694.
- Pilkington, K. R., Clark-Lewis, I., and McColl, S. R. (2004). Inhibition of generation of cytotoxic T lymphocyte activity by a CCL19/macrophage inflammatory protein (MIP)-3beta antagonist. *J Biol Chem* *279*, 40276-40282.
- Power, C. A. (2003). Knock out models to dissect chemokine receptor function in vivo. *J Immunol Methods* *273*, 73-82.
- Poznansky, M. C., Olszak, I. T., Evans, R. H., Wang, Z., Foxall, R. B., Olson, D. P., Weibrecht, K., Luster, A. D., and Scadden, D. T. (2002). Thymocyte emigration is mediated by active movement away from stroma-derived factors. *J Clin Invest* *109*, 1101-1110.
- Poznansky, M. C., Olszak, I. T., Foxall, R., Evans, R. H., Luster, A. D., and Scadden, D. T. (2000). Active movement of T cells away from a chemokine. *Nat Med* *6*, 543-548.
- Procko, E., and McColl, S. R. (2005). Leukocytes on the move with phosphoinositide 3-kinase and its downstream effectors. *Bioessays* *27*, 153-163.

- Proost, P., De Meester, I., Schols, D., Struyf, S., Lambeir, A. M., Wuyts, A., Opdenakker, G., De Clercq, E., Scharpe, S., and Van Damme, J. (1998). Amino-terminal truncation of chemokines by CD26/dipeptidyl-peptidase IV. Conversion of RANTES into a potent inhibitor of monocyte chemotaxis and HIV-1-infection. *J Biol Chem* 273, 7222-7227.
- Proost, P., Menten, P., Struyf, S., Schutyser, E., De Meester, I., and Van Damme, J. (2000). Cleavage by CD26/dipeptidyl peptidase IV converts the chemokine LD78beta into a most efficient monocyte attractant and CCR1 agonist. *Blood* 96, 1674-1680.
- Proost, P., Schutyser, E., Menten, P., Struyf, S., Wuyts, A., Opdenakker, G., Detheux, M., Parmentier, M., Durinx, C., Lambeir, A. M., *et al.* (2001). Amino-terminal truncation of CXCR3 agonists impairs receptor signaling and lymphocyte chemotaxis, while preserving antiangiogenic properties. *Blood* 98, 3554-3561.
- Proudfoot, A. E., Handel, T. M., Johnson, Z., Lau, E. K., LiWang, P., Clark-Lewis, I., Borlat, F., Wells, T. N., and Kosco-Vilbois, M. H. (2003). Glycosaminoglycan binding and oligomerization are essential for the in vivo activity of certain chemokines. *Proc Natl Acad Sci U S A* 100, 1885-1890.
- Qin, X., Wan, Y., and Wang, X. (2005). CCL2 and CXCL1 trigger calcitonin gene-related peptide release by exciting primary nociceptive neurons. *J Neurosci Res* 81, 51-62.
- Ragg, S. J., Dandie, G. W., Woods, G. M., O'Connell, P. J., and Muller, H. K. (1994). Langerhans cell migration patterns from sheep skin following topical application of carcinogens. *Int J Exp Pathol* 75, 23-28.
- Ramjeesingh, R., Leung, R., and Siu, C. H. (2003). Interleukin-8 secreted by endothelial cells induces chemotaxis of melanoma cells through the chemokine receptor CXCR1. *Faseb J* 17, 1292-1294.
- Randolph, G. J., Beaulieu, S., Lebecque, S., Steinman, R. M., and Muller, W. A. (1998). Differentiation of monocytes into dendritic cells in a model of transendothelial trafficking. *Science* 282, 480-483.
- Rapacciuolo, A., Suvarna, S., Barki-Harrington, L., Luttrell, L. M., Cong, M., Lefkowitz, R. J., and Rockman, H. A. (2003). Protein kinase A and G protein-coupled receptor kinase phosphorylation mediates beta-1 adrenergic receptor endocytosis through different pathways. *J Biol Chem* 278, 35403-35411.
- Reif, K., Ekland, E. H., Ohl, L., Nakano, H., Lipp, M., Forster, R., and Cyster, J. G. (2002). Balanced responsiveness to chemoattractants from adjacent zones determines B-cell position. *Nature* 416, 94-99.
- Reif, K., Okkenhaug, K., Sasaki, T., Penninger, J. M., Vanhaesebroeck, B., and Cyster, J. G. (2004). Cutting edge: differential roles for phosphoinositide 3-kinases, p110gamma and p110delta, in lymphocyte chemotaxis and homing. *J Immunol* 173, 2236-2240.
- Rennert, P. D., Hochman, P. S., Flavell, R. A., Chaplin, D. D., Jayaraman, S., Browning, J. L., and Fu, Y. X. (2001). Essential role of lymph nodes in contact hypersensitivity revealed in lymphotoxin-alpha-deficient mice. *J Exp Med* 193, 1227-1238.

- Salcedo, R., and Oppenheim, J. J. (2003). Role of chemokines in angiogenesis: CXCL12/SDF-1 and CXCR4 interaction, a key regulator of endothelial cell responses. *Microcirculation* *10*, 359-370.
- Salcedo, R., Resau, J. H., Halverson, D., Hudson, E. A., Dambach, M., Powell, D., Wasserman, K., and Oppenheim, J. J. (2000). Differential expression and responsiveness of chemokine receptors (CXCR1-3) by human microvascular endothelial cells and umbilical vein endothelial cells. *Faseb J* *14*, 2055-2064.
- Salcini, A. E., Chen, H., Iannolo, G., De Camilli, P., and Di Fiore, P. P. (1999). Epidermal growth factor pathway substrate 15, Eps15. *Int J Biochem Cell Biol* *31*, 805-809.
- Sallusto, F., and Lanzavecchia, A. (2000). Understanding dendritic cell and T-lymphocyte traffic through the analysis of chemokine receptor expression. *Immunol Rev* *177*, 134-140.
- Sallusto, F., Lenig, D., Forster, R., Lipp, M., and Lanzavecchia, A. (1999). Two subsets of memory T lymphocytes with distinct homing potentials and effector functions. *Nature* *401*, 708-712.
- Sallusto, F., Mackay, C. R., and Lanzavecchia, A. (2000). The role of chemokine receptors in primary, effector, and memory immune responses. *Annu Rev Immunol* *18*, 593-620.
- Salomon, B., Cohen, J. L., Masurier, C., and Klatzmann, D. (1998). Three populations of mouse lymph node dendritic cells with different origins and dynamics. *J Immunol* *160*, 708-717.
- Sasaki, T., Irie-Sasaki, J., Jones, R. G., Oliveira-dos-Santos, A. J., Stanford, W. L., Bolon, B., Wakeham, A., Itie, A., Bouchard, D., Kozieradzki, I., *et al.* (2000). Function of PI3Kgamma in thymocyte development, T cell activation, and neutrophil migration. *Science* *287*, 1040-1046.
- Schaerli, P., Loetscher, P., and Moser, B. (2001). Cutting edge: induction of follicular homing precedes effector Th cell development. *J Immunol* *167*, 6082-6086.
- Schall, T. J., Jongstra, J., Dyer, B. J., Jorgensen, J., Clayberger, C., Davis, M. M., and Krensky, A. M. (1988). A human T cell-specific molecule is a member of a new gene family. *J Immunol* *141*, 1018-1025.
- Schweickart, V. L., Epp, A., Raport, C. J., and Gray, P. W. (2000). CCR11 is a functional receptor for the monocyte chemoattractant protein family of chemokines. *Journal of Biological Chemistry* *275*, 9550-9556.
- Schweickart, V. L., Raport, C. J., Godiska, R., Byers, M. G., Eddy, R. L., Jr., Shows, T. B., and Gray, P. W. (1994). Cloning of human and mouse EB11, a lymphoid-specific G-protein-coupled receptor encoded on human chromosome 17q12-q21.2. *Genomics* *23*, 643-650.
- Seachrist, J. L., Anborgh, P. H., and Ferguson, S. S. (2000). beta 2-adrenergic receptor internalization, endosomal sorting, and plasma membrane recycling are regulated by rab GTPases. *J Biol Chem* *275*, 27221-27228.

- Seachrist, J. L., and Ferguson, S. S. (2003). Regulation of G protein-coupled receptor endocytosis and trafficking by Rab GTPases. *Life Sci* 74, 225-235.
- Serra, H. M., Eberhard, Y., Martin, A. P., Gallino, N., Gagliardi, J., Baena-Cagnani, C. E., Lascano, A. R., Ortiz, S., Mariani, A. L., and Ugucioni, M. (2004). Secondary lymphoid tissue chemokine (CCL21) is upregulated in allergic contact dermatitis. *Int Arch Allergy Immunol* 133, 64-71.
- Sever, S. (2002). Dynamin and endocytosis. *Curr Opin Cell Biol* 14, 463-467.
- Shirozu, M., Nakano, T., Inazawa, J., Tashiro, K., Tada, H., Shinohara, T., and Honjo, T. (1995). Structure and chromosomal localization of the human stromal cell-derived factor 1 (SDF1) gene. *Genomics* 28, 495-500.
- Signoret, N., Hewlett, L., Wavre, S., Pelchen-Matthews, A., Oppermann, M., and Marsh, M. (2005). Agonist-induced endocytosis of CC chemokine receptor 5 is clathrin dependent. *Mol Biol Cell* 16, 902-917.
- Simmons, G., Reeves, J. D., Hibbitts, S., Stine, J. T., Gray, P. W., Proudfoot, A. E., and Clapham, P. R. (2000). Co-receptor use by HIV and inhibition of HIV infection by chemokine receptor ligands. *Immunol Rev* 177, 112-126.
- Sixt, M., Kanazawa, N., Selg, M., Samson, T., Roos, G., Reinhardt, D. P., Pabst, R., Lutz, M. B., and Sorokin, L. (2005). The conduit system transports soluble antigens from the afferent lymph to resident dendritic cells in the T cell area of the lymph node. *Immunity* 22, 19-29.
- Soldevila, G., Licona, I., Salgado, A., Ramirez, M., Chavez, R., and Garcia-Zepeda, E. (2004). Impaired chemokine-induced migration during T-cell development in the absence of Jak 3. *Immunology* 112, 191-200.
- Sozzani, S., Sallusto, F., Luini, W., Zhou, D., Piemonti, L., Allavena, P., Van Damme, J., Valitutti, S., Lanzavecchia, A., and Mantovani, A. (1995). Migration of dendritic cells in response to formyl peptides, C5a, and a distinct set of chemokines. *J Immunol* 155, 3292-3295.
- Stein, J. V., Rot, A., Luo, Y., Narasimhaswamy, M., Nakano, H., Gunn, M. D., Matsuzawa, A., Quackenbush, E. J., Dorf, M. E., and von Andrian, U. H. (2000). The CC chemokine thymus-derived chemotactic agent 4 (TCA-4, secondary lymphoid tissue chemokine, 6Ckine, exodus-2) triggers lymphocyte function-associated antigen 1-mediated arrest of rolling T lymphocytes in peripheral lymph node high endothelial venules. *J Exp Med* 191, 61-76.
- Stine, J. T., Wood, C., Hill, M., Epp, A., Raport, C. J., Schweickart, V. L., Endo, Y., Sasaki, T., Simmons, G., Boshoff, C., *et al.* (2000). KSHV-encoded CC chemokine vMIP-III is a CCR4 agonist, stimulates angiogenesis, and selectively chemoattracts TH2 cells. *Blood* 95, 1151-1157.
- Streilein, J. W., and Bergstresser, P. R. (1981). Langerhans cell function dictates induction of contact hypersensitivity or unresponsiveness to DNFB in Syrian hamsters. *J Invest Dermatol* 77, 272-277.

- Streilein, J. W., Toews, G. T., Gilliam, J. N., and Bergstresser, P. R. (1980). Tolerance or hypersensitivity to 2,4-dinitro-1-fluorobenzene: the role of Langerhans cell density within epidermis. *J Invest Dermatol* 74, 319-322.
- Strieter, R. M., Polverini, P. J., Kunkel, S. L., Arenberg, D. A., Burdick, M. D., Kasper, J., Dzuiba, J., Van Damme, J., Walz, A., Marriott, D., and et al. (1995). The functional role of the ELR motif in CXC chemokine-mediated angiogenesis. *J Biol Chem* 270, 27348-27357.
- Subtil, A., Gaidarov, I., Kobylarz, K., Lampson, M. A., Keen, J. H., and McGraw, T. E. (1999). Acute cholesterol depletion inhibits clathrin-coated pit budding. *Proc Natl Acad Sci U S A* 96, 6775-6780.
- Suss, G., and Shortman, K. (1996). A subclass of dendritic cells kills CD4 T cells via Fas/Fas-ligand-induced apoptosis. *J Exp Med* 183, 1789-1796.
- Tachibana, K., Hirota, S., Iizasa, H., Yoshida, H., Kawabata, K., Kataoka, Y., Kitamura, Y., Matsushima, K., Yoshida, N., Nishikawa, S., et al. (1998). The chemokine receptor CXCR4 is essential for vascularization of the gastrointestinal tract. *Nature* 393, 591-594.
- Takata, H., Tomiyama, H., Fujiwara, M., Kobayashi, N., and Takiguchi, M. (2004). Cutting edge: expression of chemokine receptor CXCR1 on human effector CD8+ T cells. *J Immunol* 173, 2231-2235.
- Tang, H. L., and Cyster, J. G. (1999). Chemokine Up-regulation and activated T cell attraction by maturing dendritic cells. *Science* 284, 819-822.
- Taylor, P. R., Martinez-Pomares, L., Stacey, M., Lin, H. H., Brown, G. D., and Gordon, S. (2005). Macrophage receptors and immune recognition. *Annu Rev Immunol* 23, 901-944.
- Thelen, M. (2001). Dancing to the tune of chemokines. *Nature Immunology* 2, 129-134.
- Thomsen, P., Roepstorff, K., Stahlhut, M., and van Deurs, B. (2002). Caveolae are highly immobile plasma membrane microdomains, which are not involved in constitutive endocytic trafficking. *Mol Biol Cell* 13, 238-250.
- Tian, Y., New, D. C., Yung, L. Y., Allen, R. A., Slocombe, P. M., Twomey, B. M., Lee, M. M., and Wong, Y. H. (2004). Differential chemokine activation of CC chemokine receptor 1-regulated pathways: ligand selective activation of Galpha 14-coupled pathways. *Eur J Immunol* 34, 785-795.
- Toews, G. B., Bergstresser, P. R., and Streilein, J. W. (1980). Epidermal Langerhans cell density determines whether contact hypersensitivity or unresponsiveness follows skin painting with DNFB. *J Immunol* 124, 445-453.
- Townson, J. R., and Nibbs, R. J. (2002). Characterization of mouse CCX-CKR, a receptor for the lymphocyte-attracting chemokines TECK/mCCL25, SLC/mCCL21 and MIP-3beta/mCCL19: comparison to human CCX-CKR. *European Journal of Immunology* 32, 1230-1241.
- Tuvim, M. J., Adachi, R., Hoffenberg, S., and Dickey, B. F. (2001). Traffic control: Rab GTPases and the regulation of interorganellar transport. *News Physiol Sci* 16, 56-61.

- Uehara, S., Grinberg, A., Farber, J. M., and Love, P. E. (2002a). A role for CCR9 in T lymphocyte development and migration. *J Immunol* *168*, 2811-2819.
- Uehara, S., Song, K., Farber, J. M., and Love, P. E. (2002b). Characterization of CCR9 expression and CCL25/thymus-expressed chemokine responsiveness during T cell development: CD3(high)CD69+ thymocytes and gammadeltaTCR+ thymocytes preferentially respond to CCL25. *J Immunol* *168*, 134-142.
- Ueno, T., Hara, K., Willis, M. S., Malin, M. A., Hopken, U. E., Gray, D. H., Matsushima, K., Lipp, M., Springer, T. A., Boyd, R. L., *et al.* (2002). Role for CCR7 ligands in the emigration of newly generated T lymphocytes from the neonatal thymus. *Immunity* *16*, 205-218.
- Ueno, T., Saito, F., Gray, D. H., Kuse, S., Hieshima, K., Nakano, H., Kakiuchi, T., Lipp, M., Boyd, R. L., and Takahama, Y. (2004). CCR7 signals are essential for cortex-medulla migration of developing thymocytes. *J Exp Med* *200*, 493-505.
- Utgaard, J. O., Jahnsen, F. L., Bakka, A., Brandtzaeg, P., and Haraldsen, G. (1998). Rapid secretion of prestored interleukin 8 from Weibel-Palade bodies of microvascular endothelial cells. *J Exp Med* *188*, 1751-1756.
- Van Damme, J., Struyf, S., Wuyts, A., Van Coillie, E., Menten, P., Schols, D., Sozzani, S., De Meester, I., and Proost, P. (1999). The role of CD26/DPP IV in chemokine processing. *Chem Immunol* *72*, 42-56.
- Vanguri, P., and Farber, J. M. (1990). Identification of CRG-2. An interferon-inducible mRNA predicted to encode a murine monokine. *J Biol Chem* *265*, 15049-15057.
- Venkatesan, S., Rose, J. J., Lodge, R., Murphy, P. M., and Foley, J. F. (2003). Distinct mechanisms of agonist-induced endocytosis for human chemokine receptors CCR5 and CXCR4. *Mol Biol Cell* *14*, 3305-3324.
- Vielkind, S., Gallagher-Gambarelli, M., Gomez, M., Hinton, H. J., and Cantrell, D. A. (2005). Integrin Regulation by RhoA in Thymocytes. *J Immunol* *175*, 350-357.
- Vila-Coro, A. J., Rodriguez-Frade, J. M., Martin De Ana, A., Moreno-Ortiz, M. C., Martinez, A. C., and Mellado, M. (1999). The chemokine SDF-1alpha triggers CXCR4 receptor dimerization and activates the JAK/STAT pathway. *Faseb J* *13*, 1699-1710.
- Voigt, I., Camacho, S. A., de Boer, B. A., Lipp, M., Forster, R., and Berek, C. (2000). CXCR5-deficient mice develop functional germinal centers in the splenic T cell zone. *Eur J Immunol* *30*, 560-567.
- von Andrian, U. H., and Mempel, T. R. (2003). Homing and cellular traffic in lymph nodes. *Nat Rev Immunol* *3*, 867-878.
- von Boehmer, H., Aifantis, I., Gounari, F., Azogui, O., Haughn, L., Apostolou, I., Jaeckel, E., Grassi, F., and Klein, L. (2003). Thymic selection revisited: how essential is it? *Immunol Rev* *191*, 62-78.

- Wagner, L., Yang, O. O., Garcia-Zepeda, E. A., Ge, Y., Kalams, S. A., Walker, B. D., Pasternack, M. S., and Luster, A. D. (1998). Beta-chemokines are released from HIV-1-specific cytolytic T-cell granules complexed to proteoglycans. *Nature* *391*, 908-911.
- Waldhoer, M., Casarosa, P., Rosenkilde, M. M., Smit, M. J., Leurs, R., Whistler, J. L., and Schwartz, T. W. (2003). The carboxyl terminus of human cytomegalovirus-encoded 7 transmembrane receptor US28 camouflages agonism by mediating constitutive endocytosis. *J Biol Chem* *278*, 19473-19482.
- Walz, A., Peveri, P., Aschauer, H., and Baggiolini, M. (1987). Purification and amino acid sequencing of NAF, a novel neutrophil-activating factor produced by monocytes. *Biochem Biophys Res Commun* *149*, 755-761.
- Walz, D. A., Wu, V. Y., de Lamo, R., Dene, H., and McCoy, L. E. (1977). Primary structure of human platelet factor 4. *Thromb Res* *11*, 893-898.
- Ward, S. G. (2004). Do phosphoinositide 3-kinases direct lymphocyte navigation? *Trends Immunol* *25*, 67-74.
- Warnock, R. A., Campbell, J. J., Dorf, M. E., Matsuzawa, A., McEvoy, L. M., and Butcher, E. C. (2000). The role of chemokines in the microenvironmental control of T versus B cell arrest in Peyer's patch high endothelial venules. *J Exp Med* *191*, 77-88.
- Webb, L. M., Ehrenguber, M. U., Clark-Lewis, I., Baggiolini, M., and Rot, A. (1993). Binding to heparan sulfate or heparin enhances neutrophil responses to interleukin 8. *Proc Natl Acad Sci U S A* *90*, 7158-7162.
- Weber, M., Blair, E., Simpson, C. V., O'Hara, M., Blackburn, P. E., Rot, A., Graham, G. J., and Nibbs, R. J. (2004). The chemokine receptor d6 constitutively traffics to and from the cell surface to internalize and degrade chemokines. *Mol Biol Cell* *15*, 2492-2508.
- Wells, T. N., and Peitsch, M. C. (1997). The chemokine information source: identification and characterization of novel chemokines using the WorldWideWeb and expressed sequence tag databases. *J Leukoc Biol* *61*, 545-550.
- Weninger, W., Carlsen, H. S., Goodarzi, M., Moazed, F., Crowley, M. A., Baekkevold, E. S., Cavanagh, L. L., and von Andrian, U. H. (2003). Naive T cell recruitment to nonlymphoid tissues: a role for endothelium-expressed CC chemokine ligand 21 in autoimmune disease and lymphoid neogenesis. *J Immunol* *170*, 4638-4648.
- Weninger, W., and von Andrian, U. H. (2003). Chemokine regulation of naive T cell traffic in health and disease. *Semin Immunol* *15*, 257-270.
- Whitehead, G. S., Walker, J. K., Berman, K. G., Foster, W. M., and Schwartz, D. A. (2003). Allergen-induced airway disease is mouse strain dependent. *Am J Physiol Lung Cell Mol Physiol* *285*, L32-42.
- Wilson, N. S., El-Sukkari, D., Belz, G. T., Smith, C. M., Steptoe, R. J., Heath, W. R., Shortman, K., and Villadangos, J. A. (2003). Most lymphoid organ dendritic cell types are phenotypically and functionally immature. *Blood* *102*, 2187-2194.

- Witt, C. M., and Robey, E. A. (2004). The ins and outs of CCR7 in the thymus. *J Exp Med* 200, 405-409.
- Wolff, B., Burns, A. R., Middleton, J., and Rot, A. (1998). Endothelial cell "memory" of inflammatory stimulation: human venular endothelial cells store interleukin 8 in Weibel-Palade bodies. *J Exp Med* 188, 1757-1762.
- Wolpe, S. D., Davatelis, G., Sherry, B., Beutler, B., Hesse, D. G., Nguyen, H. T., Moldawer, L. L., Nathan, C. F., Lowry, S. F., and Cerami, A. (1988). Macrophages secrete a novel heparin-binding protein with inflammatory and neutrophil chemokinetic properties. *J Exp Med* 167, 570-581.
- Wu, V. Y., Walz, D. A., and McCoy, L. E. (1977). Purification and characterization of human and bovine platelet factor 4. *Prep Biochem* 7, 479-493.
- Wurbel, M. A., Malissen, M., Guy-Grand, D., Meffre, E., Nussenzweig, M. C., Richelme, M., Carrier, A., and Malissen, B. (2001). Mice lacking the CCR9 CC-chemokine receptor show a mild impairment of early T- and B-cell development and a reduction in T-cell receptor gamma delta(+) gut intraepithelial lymphocytes. *Blood* 98, 2626-2632.
- Xanthou, G., Duchesnes, C. E., Williams, T. J., and Pease, J. E. (2003). CCR3 functional responses are regulated by both CXCR3 and its ligands CXCL9, CXCL10 and CXCL11. *Eur J Immunol* 33, 2241-2250.
- Yamagami, S., Tokuda, Y., Ishii, K., Tanaka, H., and Endo, N. (1994). cDNA cloning and functional expression of a human monocyte chemoattractant protein 1 receptor. *Biochem Biophys Res Commun* 202, 1156-1162.
- Yanagawa, Y., and Onoe, K. (2002). CCL19 induces rapid dendritic extension of murine dendritic cells. *Blood* 100, 1948-1956.
- Yang, W., Wang, D., and Richmond, A. (1999). Role of clathrin-mediated endocytosis in CXCR2 sequestration, resensitization, and signal transduction. *J Biol Chem* 274, 11328-11333.
- Yoshida, R., Imai, T., Hieshima, K., Kusuda, J., Baba, M., Kitaura, M., Nishimura, M., Kakizaki, M., Nomiyama, H., and Yoshie, O. (1997). Molecular cloning of a novel human CC chemokine EBI1-ligand chemokine that is a specific functional ligand for EBI1, CCR7. *J Biol Chem* 272, 13803-13809.
- Yoshida, R., Nagira, M., Kitaura, M., Imagawa, N., Imai, T., and Yoshie, O. (1998). Secondary lymphoid-tissue chemokine is a functional ligand for the CC chemokine receptor CCR7. *J Biol Chem* 273, 7118-7122.
- Yoshie, O., Imai, T., and Nomiyama, H. (1997). Novel lymphocyte-specific CC chemokines and their receptors. *J Leukoc Biol* 62, 634-644.
- Yoshimura, T., Matsushima, K., Oppenheim, J. J., and Leonard, E. J. (1987). Neutrophil chemotactic factor produced by lipopolysaccharide (LPS)-stimulated human blood mononuclear leukocytes: partial characterization and separation from interleukin 1 (IL 1). *J Immunol* 139, 788-793.

- Yoshimura, T., Yuhki, N., Moore, S. K., Appella, E., Lerman, M. I., and Leonard, E. J. (1989). Human monocyte chemoattractant protein-1 (MCP-1). Full-length cDNA cloning, expression in mitogen-stimulated blood mononuclear leukocytes, and sequence similarity to mouse competence gene JE. *FEBS Lett* 244, 487-493.
- Zhang, J., Barak, L. S., Winkler, K. E., Caron, M. G., and Ferguson, S. S. (1997). A central role for beta-arrestins and clathrin-coated vesicle-mediated endocytosis in beta2-adrenergic receptor resensitization. Differential regulation of receptor resensitization in two distinct cell types. *J Biol Chem* 272, 27005-27014.
- Zhang, K., McQuibban, G. A., Silva, C., Butler, G. S., Johnston, J. B., Holden, J., Clark-Lewis, I., Overall, C. M., and Power, C. (2003). HIV-induced metalloproteinase processing of the chemokine stromal cell derived factor-1 causes neurodegeneration. *Nat Neurosci* 6, 1064-1071.
- Zhang, X. F., Wang, J. F., Matczak, E., Proper, J. A., and Groopman, J. E. (2001). Janus kinase 2 is involved in stromal cell-derived factor-1alpha-induced tyrosine phosphorylation of focal adhesion proteins and migration of hematopoietic progenitor cells. *Blood* 97, 3342-3348.
- Zlotnik, A., and Yoshie, O. (2000). Chemokines: a new classification system and their role in immunity. *Immunity* 12, 121-127.
- Zou, Y. R., Kottmann, A. H., Kuroda, M., Taniuchi, I., and Littman, D. R. (1998). Function of the chemokine receptor CXCR4 in haematopoiesis and in cerebellar development. *Nature* 393, 595-599.

## CHAPTER SIX

### APPENDICES

#### 6.1 The Genetic Code

<b>TTT-Phe</b>	<b>TCT-Ser</b>	<b>TAT-Tyr</b>	<b>TGT-Cys</b>
<b>TTC-Phe</b>	<b>TCC-Ser</b>	<b>TAC-Tyr</b>	<b>TGC-Cys</b>
<b>TTA-Leu</b>	<b>TCA-Ser</b>	<b>TAA-STOP</b>	<b>TGA-STOP</b>
<b>TTG-Leu</b>	<b>TCG-Ser</b>	<b>TAG-STOP</b>	<b>TGG-Trp</b>
<b>CTT-Leu</b>	<b>CCT-Pro</b>	<b>CAT-His</b>	<b>CGT-Arg</b>
<b>CTC-Leu</b>	<b>CCC-Pro</b>	<b>CAC-His</b>	<b>CGC-Arg</b>
<b>CTA-Leu</b>	<b>CCA-Pro</b>	<b>CAA-Gln</b>	<b>CGA-Arg</b>
<b>CTG-Leu</b>	<b>CCG-Pro</b>	<b>CAG-Gln</b>	<b>CGG-Arg</b>
<b>ATT-Ile</b>	<b>ACT-Thr</b>	<b>AAT-Asn</b>	<b>AGT-Ser</b>
<b>ATC-Ile</b>	<b>ACC-Thr</b>	<b>AAC-Asn</b>	<b>AGC-Ser</b>
<b>ATA-Ile</b>	<b>ACA-Thr</b>	<b>AAA-Lys</b>	<b>AGA-Arg</b>
<b>ATG-Met</b>	<b>ACG-Thr</b>	<b>AAG-Lys</b>	<b>AGG-Arg</b>
<b>GTT-Val</b>	<b>GCT-Ala</b>	<b>GAT-Asp</b>	<b>GGT-Gly</b>
<b>GTC-Val</b>	<b>GCC-Ala</b>	<b>GAC-Asp</b>	<b>GGC-Gly</b>
<b>GTA-Val</b>	<b>GCA-Ala</b>	<b>GAA-Glu</b>	<b>GGA-Gly</b>
<b>GTG-Val</b>	<b>GCG-Ala</b>	<b>GAG-Glu</b>	<b>GGG-Gly</b>

## 6.2 The Amino Acids

Amino Acid	3 Letter Code	1 Letter Code	MW (Da)	Properties
Alanine	Ala	A	89	Hydrophobic
Arginine	Arg	R	174	Hydrophilic
Asparagine	Asn	N	132	Hydrophilic
Aspartic Acid	Asp	D	133	Hydrophilic
Cysteine	Cys	C	121	Hydrophilic
Glutamine	Gln	Q	146	Hydrophilic
Glutamic Acid	Glu	E	147	Hydrophilic
Glycine	Gly	G	75	Hydrophilic
Histidine	His	H	155	Hydrophilic
Isoleucine	Ile	I	131	Hydrophobic
Leucine	Leu	L	131	Hydrophobic
Lysine	Lys	K	146	Hydrophilic
Methionine	Met	M	149	Hydrophobic
Phenylalanine	Phe	F	165	Hydrophobic
Proline	Pro	P	115	Hydrophobic
Serine	Ser	S	105	Hydrophilic
Threonine	Thr	T	119	Hydrophilic
Tryptophan	Trp	W	204	Hydrophobic
Tyrosine	Tyr	Y	181	Hydrophobic
Valine	Val	V	117	Hydrophobic

Acidic amino acids are shown in red, basic amino acids are shown in purple. Uncharged hydrophobic amino acids are in green and residues with non-charged polar side chains are highlighted in grey.

## 6.3 The Greek Alphabet

A	α	Alpha
B	β	Beta
Γ	γ	Gamma
Δ	δ	Delta
E	ε	Epsilon
Z	ζ	Zeta
H	η	Eta
Θ	θ	Theta
I	ι	Iota
K	κ	Kappa
Λ	λ	Lambda
M	μ	Mu
N	ν	Nu
Ξ	ξ	Xi
O	ο	Omicron
Π	π	Pi
P	ρ	Rho
Σ	σ	Sigma
T	τ	Tau
Υ	υ	Upsilon
Φ	φ	Phi
X	χ	Chi
Ψ	ψ	Psi
Ω	ω	Omega

## 6.4 Primary Sequence Line-up of CCX-CKR Across Species

```

1
human  ~~~~maleqn  qstdyyyeen  emngtydysq  yelicoikedv  refakvflpv  fltativigl  agnsmvvaig
chimp  ~~~~maleqn  qstdyyyeen  emngtydysq  yelicoikedv  refakvflpv  fltiafvigl  agnsmvvaig
cow    ~~~~maveyn  qstdyyyeen  emndthdysq  yevicoikeev  rkfakvflpa  fftiafiigl  agnsmvvaig
mouse  ~~~~maleln  qsaeyyyeen  emnythdysq  yevicoikeev  rqfakvflpa  fftvafvtgl  agnsmvvaig
xeno   meekinttir  attenydeyg  dt..tfdygn  yeelockkeev  rqfaqiflpa  fyavafvigv  agnslvvaig
tetra  ~~~~~mdas  eeggyyylen  .isftfsyed  yplcokeev   rsfaalfpv  myavolvwgl  agntvvvavv

71
human  ayykkqrktk  dvyilnlava  dllllftlpf  wavnvhwgw  lgkimckits  alytlnfvsg  mqflacisid
chimp  ayykkqrktk  dvyilnlava  dllllftlpf  wavnvhwgw  lgkimckits  alytlnfvsg  mqflacisid
cow    ayykkrrktk  dvyilnlava  dlfillftlpf  wavnvhwgw  lgkimckvts  alytvnfvsg  mqflacisid
mouse  ayykkqrktk  dvyilnlava  dllllftlpf  wavnvhwgw  lgkimckvts  alytvnfvsg  mqflacisid
xeno   ayykkmkskt  dvyilnlava  dllllftlpf  watdaavgw  fgimckits  alytlnfvsg  mqflacisid
tetra  ayikrirtmt  dvmfthlava  dllllftlpf  waadaagwv  lgtatckmvs  smyvtvftoc  nmilacisvd

141
human  ryvavtkvps  qsgvg.....  ....kpcwii  ofcvwmaail  lsipqlvfyt  v...ndnarc  ipifprylgt
chimp  ryvavtkvps  qsgvg.....  ....kpcwii  ofcvwmaail  lsipqlvfyt  v...ndnarc  ipifprylgt
cow    ryvavtkvps  qsgvg.....  ....kpcwvi  ofcvwmaail  lsipqlvfyt  v...nhkarc  vpiifpyhigt
mouse  ryvavtkvps  qsgvg.....  ....kpcwii  ofcvwmaail  lsipqlvfyt  v...nqnarc  tpiifphhigt
xeno   ryvavtkvps  qsgvg.....  ....kpcwvi  ofcvwmaail  lsipqlvfyt  v...nqnarc  tpiifphhigt
tetra  rrlalaaarg  e.grgrilqr  vftkkhchwkv  ofavwalaif  lglpdlvise  vrwlsnrsvc  lvvypgsavv

211
human  smkaligml  icigfvvpfl  imgvcyfita  rtlmkmp...  niklsrplkv  lltvvivfiv  tqlpynivkf
chimp  smkaligml  icigfvvpfl  imgvcyfita  rtlmkmp...  niklsrplkv  lltvvivfiv  tqlpynivkf
cow    smkasigml  icigfvvpfl  imgvcyfita  rtlmkmp...  niklsrplkv  lltvvivfiv  tqlpynivkf
mouse  slkasigml  icigfvvpfl  imgvcyasta  ralikmp...  nikksrplkv  llavvvfiv  tqlpynivkf
xeno   qttvliqile  ivfcflpfl  vmvfcyasma  kivlktp...  nikrsrplkv  llavvvfiv  tqlpynivkf
tetra  gkgaglemme  vllgflpl  vmvfcyasma  qalkglpves  zsrkwralrv  lltvvavfvv  tqlpynivkv

281
human  craidiiysl  itsodmskrm  diaiqvtesi  alfhaclnpi  lyvfmgasfk  nyvmkvakky  gswrrqr.qs
chimp  craidiiysl  itsodmskrm  diaiqvtesi  alfhaclnpi  lyvfmgasfk  nyvmkvakky  gswrrqr.qs
cow    cqaidiiysl  itsodmskrm  dvaigvtesi  alfhaclnpy  lyvfmgtstfk  nyimkvakky  gswrrqr.qn
mouse  cqaidaiyll  itsodmskrm  dvaigvtesi  alfhaclnpi  lyvfmgasfk  nyimkvakky  gswrrqr.qn
xeno   wraidiiyal  itsodmsrtd  dimiqvtesl  alfhaclnpy  lyafmgstfk  cyisklakrc  gslrrqrihs
tetra  yravdsvytl  vthcasskal  draaqvtesl  alchoclnpy  lyafvgstfk  qhmvklakqf  gqkrrkrpnp

351
human  ve.....efp  fdsegptept  stfsi
chimp  ve.....efp  fdsegptept  stfsi
cow    ve.....eip  fosedatept  stfsi
mouse  ve.....eip  fdsegptept  ssfti
xeno   te.....efs  mhshnhveet  ssfsi
tetra  paeeggmems  fnshdaaget  ntfsv

```

The amino acid sequence from amino to carboxy terminus of CCX-CKR in humans, chimpanzees, cows, mice, *Xenopus laevis* (xeno) and zebrafish (tetra). The modified DRY motif is highlighted in green and the potential caveolin binding site highlighted in red.